# Investigating the heterogeneity of T Stem Cell Memory cell (Tscm) and their role in maintenance of long-term immunity following vaccination in humans

Charandeep Kaur

Department of Infectious Disease
Faculty of Medicine
Imperial College London

January 2024

Submitted for the Degree of Doctor of Philosophy

# Abstract

Memory T cells, with their critical role in immune responses, have become a central focus of research in the field of immunology. Among these memory T cells, Tscm (memory stem cells) has gathered significant attention due to their stem-like characteristics, including self-renewal and multipotency, suggesting a role in maintaining long-term immunity. Building upon prior research conducted by our laboratory, we have uncovered the existence of kinetic heterogeneity within the Tscm compartment, leading to the identification of two distinct subpopulations based on CD95 expression: CD95hi and CD95int.

This thesis investigates the characteristics of these Tscm subpopulations and their role in the maintenance of long-term immunity. Our study begins by validating kinetic heterogeneity within the Tscm compartment, involving the examination of proliferation markers, cell division history, age-related trends, and their tissue distributions. Additionally, by investigating the dynamics of HIV specific-Tscm subsets following HIV vaccination in healthy volunteers we concluded that CD95hi and CD95int have distinct identities and both subsets play essential roles in memory maintenance.

CD95int cells exhibit a quiescent profile characterized by low proliferation rates, relative stability with aging, prevalence in human lymph nodes, and the persistent low expression of activation and co-stimulatory molecules. In contrast, the CD95hi subset presents an activated phenotype with higher proliferation rates, increased activation molecule expression and accumulates with age. In HIV trial vaccination studies, both subsets display unique dynamics post-vaccination, with CD95int being less prominent while CD95hi demonstrates a high frequency at all the timepoints

post-boost and exhibits a significant correlation with the rate of decay of HIV-specific CD8+T memory.

In conclusion, our findings highlight that CD95 expression can distinguish the two proposed subpopulations within the Tscm compartment. Despite different dynamics, both subsets contribute significantly to memory maintenance.

# Declaration of Originality

I declare that the work presented in this thesis is original work undertaken and written by myself unless stated otherwise. All other work is appropriately referenced.

# Copyright Declaration

The copyright of this thesis rests with the author. Unless otherwise indicated, its contents are licensed under a Creative Commons Attribution-NonCommercial 4.0 International Licence (CC BY-NC).

Under this licence, you may copy and redistribute the material in any medium or format. You may also create and distribute modified versions of the work. This is on the condition that: you credit the author and do not use it, or any derivative works, for a commercial purpose.

When reusing or sharing this work, ensure you make the licence terms clear to others by naming the licence and linking to the licence text. Where a work has been adapted, you should indicate that the work has been changed and describe those changes.

Please seek permission from the copyright holder for uses of this work that are not included in this licence or permitted under UK Copyright Law.

# Acknowledgements

First and foremost, I would like to express my deepest gratitude to the Almighty for granting me the intellectual capacity and blessings that enabled me to undertake and complete this work.

I have been exceptionally fortunate to have the guidance and unwavering support of remarkable supervisors who have been helpful throughout my Ph.D. I extend my heartfelt appreciation to my primary supervisor, Prof. Becca Asquith, for her invaluable advice and mentorship. Her guidance has played a pivotal role in enhancing my learning, technical expertise, and critical thinking abilities, which I am confident will greatly benefit my future career. I am profoundly grateful for her patience and support during the challenging moments of my Ph.D., as well as for her encouragement that motivated me to take initiatives that not only advanced my research project but also contributed to my overall professional development. Her dedication, perseverance, and intellect are truly inspiring, and I aspire to emulate these qualities in my future endeavors. It has been an absolute pleasure to work under her guidance.

I would also like to extend my thanks to my co-supervisor, Dr. Katrina Pollock, whose continuous support and enthusiasm for vaccination studies significantly contributed to my doctoral journey and helped me clarify my future aspirations. Her mentorship was instrumental in achieving many of my PhD goals.

A special note of appreciation goes to my additional co-supervisor, Dr. Catherine Kibirige, who joined my journey during a time of challenges in my ddPCR experiments. Her advice and unwavering motivation were critical in the successful

completion of this project.

I wish to express my gratitude to our collaborators, Dr. Hannah M Cheeseman, Dr. Julia Makinde, and Dr. Peter Hayes, for their invaluable assistance in obtaining samples from the HIV trial vaccination studies. Their guidance, advice, and suggestions have been instrumental to my research.

I would like to thank the fellow members of our research group, namely, Dr. Danai A. Koftori, Dr. Jonas Mackerodt, Laura Mora-Britria, and Dr. Ada Yan. Working with all of you has been an absolute pleasure. Your collective support throughout my Ph.D., and particularly Laura's critical assessment of my work and writing, Danai's assistance with experimental setup plans, and Jonas and Ada's advice and input during lab meetings on my data, have been invaluable.

Furthermore, I am grateful to all the individuals within the department with whom I had the privilege of working during this period. Special thanks to Dominic Smith, our exceptional lab manager, and to Allison Maher, Dr. Aris Aristodemou, and Dr. Claudia Selck for consistently offering their assistance whenever needed.

I would also like to express my appreciation to all the members of the QuanTII group, from whom I have learned a great deal during our interactions.

A heartfelt thank you to my friends from India, Dr. Rajendra Mandage, Akshay Munjal, Atreyi Pramanik, and Deepak Rathi. Your unwavering support, your willingness to be there when I needed it most, and your patience in listening to my successes and failures have been invaluable during the challenging times of my PhD.

I would be remiss not to mention my daughter-like niece, Amrit Kaur, whose trust in me and my work served as a constant source of motivation. Her presence and her affectionate hugs, which could dispel any stress, have been a true blessing.

I extend my sincere thanks to my dear father for the confidence and independence he has given me. To my dearest mother, thank you for the abundant love and pride you showered on my past achievements. Mum, this accomplishment is the result of your continued prayers. I hope you are in a better place, and I miss you every day. My heartfelt thanks to my sister and brother, who have consistently supported me.

Above all, I wish to convey my deepest gratitude to my in-law family, whose unwavering support was a cornerstone of my PhD journey. Your presence alleviated any stress I may have faced, and I appreciate it greatly.

Finally, and most importantly, my PhD journey would not have been possible without the unwavering support of my incredible husband, Mr. Gurpreet Singh. Your continuous support and encouragement have been my driving force, pushing me across the finish line. I owe you all of this and so much more.

# Contents

**1 Introduction** **18**

1.1 Immune System . . . . . 18

1.2 Adaptive immune response . . . . . 19

1.3 T cell memory: generation and heterogeneity . . . . . 21

1.3.1 Generation of memory . . . . . 21

1.3.2 Memory CD8+ T cell heterogeneity . . . . . 23

1.3.3 Factors affecting the heterogeneity of memory T cell pool . . . 29

1.4 Models of CD8+ T-Cell Memory . . . . . 33

1.5 Stem-like memory T cells . . . . . 35

1.5.1 Characteristics and Discovery . . . . . 35

1.5.2 Longevity and persistence . . . . . 36

1.5.3 Tscm cells in vaccination . . . . . 40

1.5.4 Heterogeneity of Tscm cells in humans . . . . . 43

1.6 Study Overview and Roadmap . . . . . 44

1.6.1 Aim . . . . . 44

1.6.2 Hypothesis . . . . . 45

1.6.3 Research approach . . . . . 45

1.7 Thesis outline . . . . . 47

**2 Materials and Methods** **49**

2.1 Immunophenotyping of memory T cells . . . . . 49

2.1.1 Donor information . . . . . 49

2.1.2 Peripheral Blood Mononuclear Cell (PBMC) isolation . . . . . 49
2.1.3 Flow cytometry and cell sorting . . . . . 50
2.1.4 Data analysis . . . . . 51
2.2 Droplet Digital Polymerase Chain Reaction . . . . . 51
2.2.1 DNA Extraction . . . . . 51
2.2.2 Cell lysate preparation . . . . . 51
2.2.3 Cell lysate viscosity breakdown step . . . . . 52
2.2.4 ddPCR reaction mixture preparation . . . . . 52
2.2.5 ddPCR droplet generation and thermocycler protocol . . . . . 53
2.2.6 Assay accuracy . . . . . 53
2.2.7 Limit of Blank . . . . . 54
2.2.8 Limit of Detection, and Limit of Quantification . . . . . 54
2.2.9 Repeatability of the crude lysate ddPCR assay . . . . . 54
2.2.10 Droplet volume size estimated by optical microscopy . . . . . 55
2.2.11 Data analysis . . . . . 55
2.3 Antigen specific CD8+ T cell . . . . . 56
2.3.1 Donor information . . . . . 56
2.3.2 Stimulation with peptide . . . . . 56
2.3.3 Inhibition of TCRs and pMHC complexes . . . . . 56
2.3.4 Flow cytometry . . . . . 56
2.3.5 Data analysis . . . . . 58
2.4 Tissue distribution of memory subpopulations . . . . . 58
2.4.1 Donor information and study design . . . . . 58
2.4.2 Blood and lymph node samples . . . . . 58
2.4.3 Study Immunogen . . . . . 59
2.4.4 Cellular subset phenotyping . . . . . 59
2.4.5 Detection of antigen-specific CD8+T cells - CD137IRF4 assay 60
2.4.6 Data analysis . . . . . 61
2.5 HIV clinical trial vaccination studies . . . . . 62

2.5.1 Donor information and Study design . . . . . 62
2.5.2 Detection of antigen-specific T cells . . . . . 63
2.5.3 Data analysis . . . . . 63
2.6 RNAseq experiment . . . . . 63
2.6.1 Cell sorting . . . . . 63
2.6.2 RNA isolation . . . . . 63
2.6.3 RNAseq experiment and analysis . . . . . 64

**3 Optimizing the Crude Lysate ddPCR protocol for rare gene targets in rare cells 65**

3.1 Introduction . . . . . 65
3.2 Results . . . . . 67
3.2.1 Standardisation and validation of standard ddPCR . . . . . 67
3.2.2 Standardisation and Validation of Crude lysate ddPCR . . . . 69
3.2.3 Discussion . . . . . 84

**4 Characterizing the heterogeneity of the TSCM subset 89**

4.1 Introduction . . . . . 89
4.2 Results . . . . . 91
4.2.1 CD95 as a marker for Tscm heterogeneity . . . . . 91
4.2.2 Age-related variations in Tscm frequencies and memory populations . . . . . 95
4.2.3 Tscm subsets have different division histories . . . . . 97
4.2.4 Tissue specific distribution . . . . . 99
4.2.5 Transcriptional analysis of sorted memory subpopulation . . . 101
4.3 Discussion . . . . . 103
4.4 Supplementary Figures . . . . . 109

**5 Comparison of activation-induced markers to detect antigen-specific CD8+T cells 111**

5.1 Introduction . . . . . 111

5.1.1 OX40-CD25 combination . . . 113
5.1.2 HLADR-CD38 combination . . . 114
5.1.3 CD137 and its combinations . . . 116
5.2 Results . . . 118
5.2.1 Dynamic of AIM marker combinations on Flu-specific CD8+T cells over time . . . 118
5.2.2 Performance assessment of AIM markers: Sensitivity Specificity 119
5.2.3 Background levels for AIM marker combinations . . . 122
5.2.4 Bystander responses to different AIM marker combinations . . 123
5.2.5 Evaluation of marker expression consistency across memory subtypes . . . 125
5.2.6 Co-expression of different AIM markers . . . 127
5.3 Discussion . . . 128
5.3.1 Supplementary . . . 131

**6 Antigen-specific CD8+Tscm and their role in sustaining memory post-vaccination 132**

6.1 Introduction . . . 132
6.2 Results . . . 135
6.2.1 Assessment of HIV-specific CD8+T cell responses . . . 135
6.2.2 HIV-specific memory CD8+ T subpopulations across trial studies . . . 137
6.2.3 Comparative analysis of early immune responses generated by the vaccinations . . . 139
6.2.4 Understanding the interplay between Tscm and long-term memory maintenance . . . 140
6.2.5 Discussion . . . 143
6.2.6 Supplementary Figures . . . 149

**7 Immune cell profiles in blood and lymph nodes post intramuscular**

**HIV envelope immunization** **151**

7.1 Introduction . . . . . 151

7.2 Results . . . . . 153

7.2.1 Tolerability and yield of US-guided FNA procedure . . . . . 153

7.2.2 Cellular landscape of blood and LN is divergent . . . . . 154

7.2.3 Memory T subset distribution is tissue specific . . . . . 156

7.2.4 Naive CD8+ T cells in the LN are heterogenous . . . . . 157

7.2.5 Tfh with a germinal center (GC)-like phenotype are exclusive to the LN . . . . . 158

7.2.6 Induction of HIV-specific T cell response in LN . . . . . 162

7.3 Discussion . . . . . 166

7.4 Publication . . . . . 168

**8 Discussion** **169**

8.1 Summary and Outlook . . . . . 169

8.2 Limitations . . . . . 175

8.3 Future work . . . . . 177

8.4 Final words . . . . . 180

# List of Figures


1.1 Generation and maintenance of CD8+ T cell memory . . . . . 22

1.2 Diagram depicting the differentiation and various subsets of CD8+ T cells . . . . . 25

1.3 Phenotypic identity of different CD8+ T memory subpopulations with functional and metabolic attributes . . . . . 27

1.4 Regulatory Factors Influencing Effector and Memory Cell Fate . . . . 32

1.5 Proposed models to explain CD8+ T-cell memory heterogeneity . . . 34

1.6 Tscm generation based on spatial T cell position . . . . . 39

3.1 Standardisation and validation of standard ddPCR . . . . . 68

3.2 Evaluation of different methods for preparing the crude lysate . . . . 71

3.3 Linearity and accuracy assessment of crude lysate ddPCR using lysis buffer 1 and 2. . . . . 72

3.4 Importance of viscosity breakdown step in crude lysate ddPCR . . . . 74

3.5 Limit of Blank (LOB) of crude lysate ddPCR . . . . . 76

3.6 Limit of Detection (LOD) and Limit of Quantification (LOQ) of crude lysate ddPCR . . . . . 77

3.7 Optical microscopy to measure droplet volume . . . . . 78

3.8 Direct comparison of crude lysate ddPCR with the standard ddPCR . 80

3.9 Crude lysate ddPCR on fixed and permeabilized (FP) cells . . . . . 82

3.10 Troubleshooting the crude lysate ddPCR . . . . . 83

4.1 Ki67+ memory CD8+ T cells exhibit increased CD95 expression . . . 92

4.2 CD95hi subset exhibits higher frequency of Ki67+ cells . . . . . 93
4.3 Frequencies of different memory subpopulations in healthy individuals 94
4.4 Tscm accumulates with age . . . . . 96
4.5 CD95hi population has lower TREC count than CD95int . . . . . 98
4.6 Frequency of Tscm and its subsets in lymph node cells . . . . . 100
4.7 Effect of SEB stimulation on Tscm subsets . . . . . 101
4.8 Differential expression of activation and co-stimulatory markers on CD95hi and CD95int Tscm . . . . . 102

5.1 Gating strategy used to gate Flu-specific CD8+ T cells and its comparison with AIM combinations . . . . . 119
5.2 Frequencies of various AIM Marker Combinations from CD8+ Pentamer+ T Cells at 12hr, 18hr, and 24hr Timepoints . . . . . 120
5.3 Sensitivity of different AIM marker combinations to detect antigen-specific CD8+ T cells . . . . . 121
5.4 Specificity of different AIM marker combinations to detect antigen-specific CD8+ T cells . . . . . 123
5.5 Comparison of background levels in different AIM marker combinations 124
5.6 IRF4CD137 expression is MHC-TCR dependent . . . . . 125
5.7 IRF4 is uniformly expressed by all CD8+ T memory subpopulations . 126
5.8 IRF4CD137+ CD8+ T cells co-express CD69CD137 markers . . . . . 127
5.9 IRF4CD137 expression is MHC-TCR dependent in HIV vaccinated individuals . . . . . 131

6.1 Timepoints for sample collection and analysis post vaccinations . . . 135
6.2 Frequency of HIV-specific CD8+ T cell post-boost across HIV trial vaccination studies . . . . . 136
6.3 Dynamics of HIV-specific CD8+T memory subpopulation post-boost 138
6.4 Comparison of memory profile two weeks post-boost among HIV trial vaccine studies . . . . . 140

6.5 Relation between frequency of HIV-specific CD8+ Tscm at 2 weeks post-boost with the rate of decay of memory . . . . . 141
6.6 Relation between frequency of HIV-specific CD8+ Tscm at 2 weeks post-boost with the rate of decay of Tem in B001 study . . . . . 142
6.7 Relation between frequency of HIV-specific CD8+ Tscm at 2 week post-boost with rate of decay of Tcm and Temra in B001 study . . . 143

7.1 Cellular diversity in PBMCs and LNCs . . . . . 155
7.2 Comparative analysis of frequencies of different memory population in PBMCs and LNCs . . . . . 156
7.3 Comparison of phenotypic features in CD8+ T Cells between LN and Blood . . . . . 158
7.4 HIV-specific CD8+ T cell responses in donors following vaccination . 159
7.5 Different CD8+ T naïve phenotype in LNC and Peripheral Blood Mononuclear Cells (PBMC) . . . . . 160
7.6 LN-resident Tfh (Tfh) and Circulating Tfh (cTfh) in Blood and Lymph nodes (LNs) . . . . . 161
7.7 t-SNE and FlowSOM analysis of paired LN and blood samples on Live CD4+ T Cells . . . . . 162
7.8 Phenotypic differences in Tfh and ctfh cells . . . . . 163
7.9 Induction of HIV-Specific CD4+ T Cells in LN and suppression of superantigen response compared to blood . . . . . 164
7.10 Representative gating strategy for SEB stimulated LNC CD8+T memory subpopulation for IRF4CD137 assay . . . . . 165
7.11 Comparison of activation status of T memory subpopulations in PBMC and LNC after stimulation with SEB . . . . . 166

# List of Tables

2.1 Antibodies used for flow cytometry and cell sorting . . . . . 50
2.2 Proportion of T cell DNA and macrophage DNA used to make different dilutions . . . . . 54
2.3 Antibodies used for the experiment aimed to detect antigen-specific CD8+ T cells . . . . . 57
2.4 Antibody cocktail 1 for phenotyping different immune cells from LNC and PBMC . . . . . 59
2.5 Antibody cocktail 2 for detection of activated CD8+ and CD4+ T cells following 18hr stimulation . . . . . 60
2.6 Antibodies used for the IRF4-CD137 experiment aimed to detect antigen-specific CD8+ T cells . . . . . 61

3.1 Intra-assay variability (Crude lysate ddPCR) . . . . . 79

# Chapter 1

# Introduction

## 1.1 Immune System

The immune system, an extraordinary defense network, plays a pivotal role in protecting the host against a wide variety of pathogens and foreign substances, while also targeting aberrant host cells to defend against diseases like cancer. It mounts a coordinated response with the help of different immune cells, tissues and molecules to maintain homeostasis and preserve the overall health of the host. Impaired functionality of the immune system can result in the development of autoimmunity, life-threatening infections, cancer and various other critical health implications. Throughout history, understanding of the immune system's crucial significance in various fields such as medicine, immunology, infectious diseases, cancer research, immunotherapies and transplantation has led to advancements in diagnostics, therapeutics, vaccinology and disease prevention. For instance, during the COVID-19 pandemic, understanding the pathogen's immunogenicity and developing effective vaccines were crucial steps in managing the pandemic. Thus, the immune system acts as a vital shield by ensuring our well-being and understanding the immune system holds immense potential for improving human health and combating diseases.

The immune system is generally composed of two interconnected components (i) Innate immune system, and (ii) Adaptive immune system. The innate immune system is the first line of defense against invading pathogens. This response is rapid and non-specific while also recruiting the adaptive immune system for a more

specific response. Typical components of the innate immune system include physical barriers (e.g. skin, mucous membrane), phagocytes and natural killer cells. The adaptive immune system complements the innate system by generating pathogen-specific responses to destroy the pathogens that escape from the innate system. It may take a few days to develop but confers long-term immunity by generating antigen-specific memory cells. The key components of the adaptive immune system are B and T lymphocytes. Together these two systems form a comprehensive and dynamic defense network that provides a quick response upon pathogen recognition (by the innate system) followed by a slow and specialised response (by the adaptive system).

In this thesis, we are focusing on the adaptive immune system only.

## 1.2 Adaptive immune response

B and T lymphocytes (cells) mediate the core functions of adaptive immune responses. Before coming across any antigen, both B and T cells are referred as naive and circulate between blood and lymphoid tissue until they recognize and respond to the pathogen; after which they are classified as memory cells.

B cells initiate antibody-mediated immune responses by recognizing extracellular antigens such as bacterial toxins (Alberts et al. 2002, Hoffman et al. 2016). These cells possess specialised antigen-binding receptors called B cell receptors (BCRs) on their surface, enabling them to identify antigens to become activated. Once activated, B cells differentiate into plasma cells and memory cells. Plasma cells produce antibodies that target pathogen elimination, while memory B cells help to maintain long-term immunity (Hoffman et al. 2016). However, B cells require assistance from T cells to produce antibodies.

T cells elicit cell-mediated immune responses by identifying specific antigens presented by antigen presenting cell (APC) (typically dendritic cells, but also B cells or macrophages) via their T cell receptors (TCRs) (Butcher & Picker 1996). APCs process the antigen and display it on major histocompatibility complex (MHC) class I (for intracellular antigen) (Yewdell et al. 1999) or II molecules (for extracellular antigen) (Chicz et al. 1992) present on their surface. The MHC-antigen complex

activates naive T cells, causing them to differentiate into either T-helper (Th cells) (CD4+ cells) or cytotoxic T cells (CD8+ cells) (Alberts et al. 2002). CD4+Th cells recognise antigens bound on MHC classII molecules and, once activated, secrete cytokines to help and regulate other immune cells. However, they do not possess the ability to kill the infected cells/pathogens directly (Janeway Jr et al. 1988). Hence, they play an essential role in coordinating and enhancing immune response. On the other hand, CD8+ T cells identify the antigen presented on MHC class I molecules (Golstein et al. 1972). Upon activation, CD8+ T cells enter the expansion phase, leading to clonal expansion and the production of effector cells that migrate to the site of infection and induce apoptosis of the target cells. Once the infection is resolved, the response enters the contraction phase, during which most of the effector cells die, while a few remain as memory cells (Zhang & Bevan 2011). These memory cells provide a rapid and vigorous response upon subsequent encounters with the same antigen. This ability to remember and respond faster upon re-encountering with the same pathogen is known as immunological memory.

**Immunological memory** - is the hallmark of adaptive immune responses. The evidence of immunological memory can be seen in human history as follows:

> "For this disease never took any man the second time so as to be mortal."
>
> Thucydides, The History of the Peloponnesian War
>
> (translation by Thomas Hobbes)

However, how this immunological memory is maintained over a long period is still a matter of debate (Pace 2021). In this thesis, the CD8+ T-cell response is assessed to define its role in the generation and maintenance of immunological memory. The subsequent sections provide detailed information on the current understanding of T memory cell development, subtypes, lineage, and their role in maintaining long-term immunity.

## 1.3 T cell memory: generation and heterogeneity

### 1.3.1 Generation of memory

The kinetics of memory generation in an acute infection can be characterized by three distinguishable phases: expansion and fate commitment, contraction and death, memory formation and maintenance (Figure 1.1) (Ahmed & Gray 1996, Williams & Bevan 2007).

During the expansion phase, 100-200 naive antigen-specific precursors cells expand up to $10^4$-fold to $10^5$-fold within a mere 8 days after the infection, marking the peak of the immune response (Arstila et al. 1999, Blattman et al. 2002). This extensive proliferation of T cells plays a crucial role in establishing long-term immunity as the magnitude of the initial clonal burst usually determines the number of memory T cells formed (Hou et al. 1994, Murali-Krishna et al. 1998).

Most of the cells in the expansion phase are antigen-specific "effector T cells". This effector T cell population is heterogeneous and made up of antigen-specific short-lived effector cells (SLECs) and memory precursor effector cells (MPECs) (Figure 1.1). SLECs migrate to various tissues and employ multiple mechanisms, such as cytotoxic activity (via perforin and granzymes), cytokine release (interferon(IFN)-$\gamma$, tumor necrosis factor(TNF)$\alpha$) and chemokine production to recruit other leukocytes and effectively eradicate the pathogen (Kaech et al. 2002, Wherry & Ahmed 2004, Williams & Bevan 2007). A major fraction of the antigen-specific SLECs (80-95%) from the expansion phase die over the next several weeks during the contraction phase response. Leaving behind a small fraction (5-20%) of MPECs. These MPECs are heterogeneous and long-lived (Muroyama & Wherry 2021). These two SLECs and MPECs populations can be differentiated on the basis of expression of IL-7 receptor $\alpha$ chain (IL7-R$\alpha$) and Killer cell lectin-like receptor subfamily G member 1 (KLRG1), as MPECs express IL7-R$\alpha$, but not KLRG1 (IL7-R$\alpha$+ KLRG1-) while SLECs which express KLRG1, but not IL7-R$\alpha$ (IL7-R$\alpha$- KLRG1+). (Obar & Lefrançois 2010, Remmerswaal et al. 2019). Further, these MPECs are capable of persisting long-term in an antigen-independent, but cytokine-dependent (namely interleukin-15 [IL-15] and IL-7) manner with slow homeostatic turnover (Surh et al. 2006). Apart from SLECs and MPEC, there are additional variants of effector CD8+

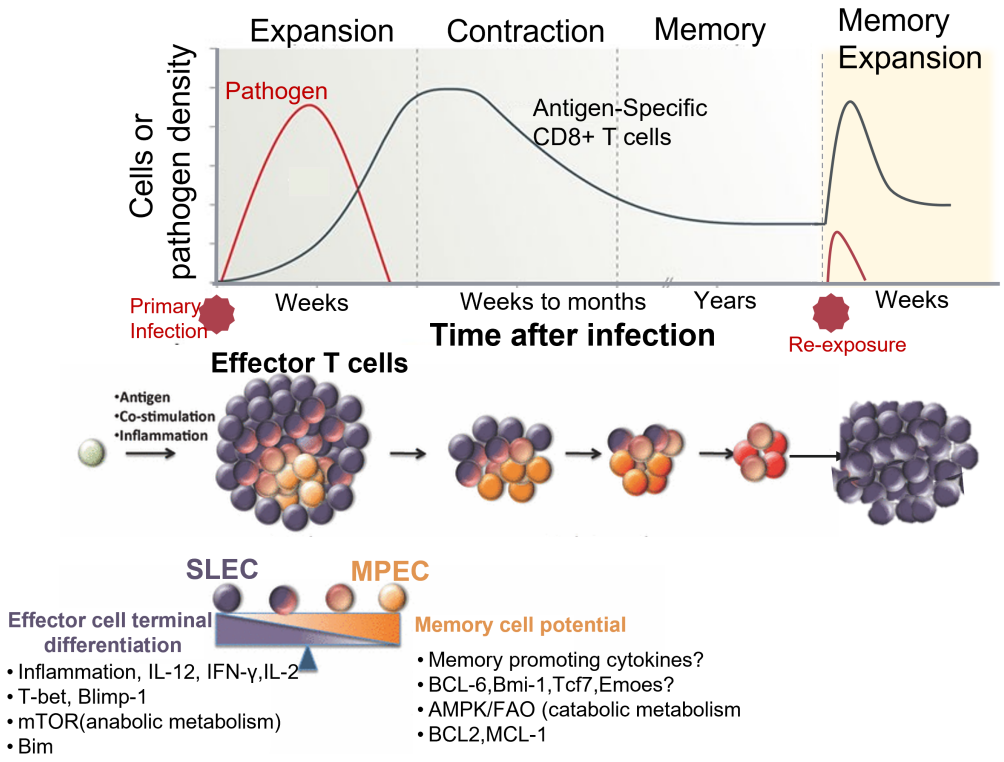



**Figure 1.1**: **Generation and maintenance of CD8+ T cell memory.** Figure adapted from Kaech & Cui (2012) and Cui & Kaech (2010). Primary infection with a pathogen leads to expansion of the pathogen during the first few days until the adaptive response is activated and clears the infection in the expansion phase. Most of the cells in the expansion phase are effector T cells including SLECs (Short-lived effector cells) in Purple and MPECs (Memory precursor effector cells) in Orange. There are additional variants of effector CD8+ T cells that exhibit a combination of characteristics, including properties associated with both terminally differentiated cells and memory precursor cells. In the contraction phase, most of the effector cells die, leaving behind a small fraction of MPECs. These MPECs give rise to diverse subsets of memory T cells which are maintained over time without antigenic stimulation. During a secondary exposure, memory cells expand and control the pathogen. IL, interleukin; IFN-$\gamma$, interferon-$\gamma$; mTOR, mammalian target of rapamycin; AMPK, 5-adenosine monophosphate-activated protein kinase; FAO, fatty acid oxidation; SLEC, short-lived effector cell; MPEC, memory precursor effector cell.

T cells, exhibiting a combination of characteristics, including properties associated with both terminally differentiated cells and memory precursor cells (Figure 1.1). Upon encountering the same antigen during secondary infection, the MPECs undergo rapid clonal expansion and differentiate into effector T cells (Figure 1.1). This process allows them to respond much more quickly and efficiently to control the infection compared to the primary immune response.

Several studies have shown that MPECs generate various long-lived memory CD8+ T cells (Kaech & Cui 2012, Kaech & Wherry 2007, Joshi et al. 2007, Mackay et al. 2013, Sheridan et al. 2014). The formation of memory CD8+ T cell pool is regulated by various factors, including the initial strength of activation, starting number of naive CD8+ T-cells (Moon et al. 2007, van Heijst et al. 2009), the dose of antigen (Wherry et al. 2003) and the duration of antigen presentation, along with stimuli from the environment such as cytokines, chemokines and stress signals, metabolic changes (Pace 2021) and co-stimulatory signals during activation (Pace 2021). All these factors shape the heterogeneity of the memory T cell compartment (Pace 2021). Understanding the heterogeneity of the memory T compartment is essential for investigating the maintenance of immunological memory.

### 1.3.2 Memory CD8+ T cell heterogeneity

Heterogeneity of memory T cell population refers to the diversity and variability observed among memory T cells in terms of their phenotype, function and transcriptional characteristics.

Initially, memory T cells were categorised into subsets based on their homing and migration markers, along with effector functions (Hamann et al. 1997, Sallusto et al. 1999). However, advancements in technology have allowed the detailed identification of numerous T memory subsets (Figure 1.2)(Newell et al. 2012), but the question of whether these subsets represent unique T-cell identities or merely different phenotypic states of a smaller number of T cell fates remain unresolved (Muroyama & Wherry 2021).

Nevertheless, the major CD8+ T cell subsets that can be defined by their phenotype, behavior and function are presented below.

**Central memory T cell (Tcm)** represent a quiescent population of memory T cells that express Lymph node (LN) homing receptors like CD62L and CCR7 (Figure 1.3). They exhibit a high capacity of proliferation while demonstrating a low level of cytotoxic activity (Wherry et al. 2003). Upon stimulation, these cells produce cytokines such as IL-2 and IFN-$\gamma$ (Wherry et al. 2003, Muroyama & Wherry 2021). These cells have a unique capacity to self-renew in response to IL-7 and IL-15 (Wherry et al. 2003). Furthermore, Tcm cells can give rise to

effector progeny upon antigen restimulation (Wherry et al. 2003). In humans, Tcm cells are typically identified as CD45RA-CD45R0+CCR7+CD27+CD28+ (Hamann et al. 1997, Mahnke et al. 2013). Anatomically, Tcm can be found in blood and lymphoid tissues such as the spleen and lymph nodes and can circulate among the compartments. In much lower frequencies they are found in lungs too (Thome et al. 2014, Farber et al. 2014). Transcription factors such as Eomes, TCF1, BCL-6, ID3, and STAT3 play a crucial role in promoting the development and function of Tcm (Banerjee et al. 2010, Joshi et al. 2007, Rutishauser et al. 2009, Yang et al. 2011, Intlekofer et al. 2005). Moreover, several studies strongly support the hypothesis that the centralized location of Tcm cells allows them to effectively manage systemic infections compared to other memory subsets (Bachmann et al. 2005, Wherry et al. 2003).

**Effector memory T cells (Tem)** lack LN homing receptors (CD62L and CCR7) but express molecules allowing homing to nonlymphoid tissues or inflammatory site, hence circulate between blood and peripheral tissues surveying for reinfection (Muroyama & Wherry 2021). Tem were, originally, described as memory cells capable of rapidly producing effector functions against reinfection. However, recent understanding suggests that the Tem population is complex and heterogeneous, containing more than one subset such as tissue-resident memory (Trm) cells (discussed below) (Schenkel et al. 2014). Interestingly, a subset of Tem can differentiate to Tcm cells in the absence of antigen stimulation, indicating lineage flexibility (Wherry et al. 2003, Muroyama & Wherry 2021). Tem cells are phenotypically characterised as CD45RA-CD45RO+CCR7-CD27- in humans (Figure 1.3) (Hamann et al. 1997, Mahnke et al. 2013). Transcription factors associated with Tem cells development are T-bet, Blimp1, ID2, and STAT4 (Joshi et al. 2007, Rutishauser et al. 2009, Cannarile et al. 2006, Yang et al. 2011). Tem cells play a crucial role in handling infections arising within peripheral organs due to their cytotoxicity and ability to localize to tissues (Martin & Badovinac 2018).

**Effector memory RA+ T cells (Temra)** constitute a terminally differentiated subset of human CD8+ T cells that reexpress CD45RA while lacking CD27 (i.e. CD27-CD45RA+) (Figure 1.3) (Hamann et al. 1997, Mahnke et al. 2013). Additionally, Temra cells do not express CCR7, CD62L or CD28 (CCR7-CD62L-CD28-)

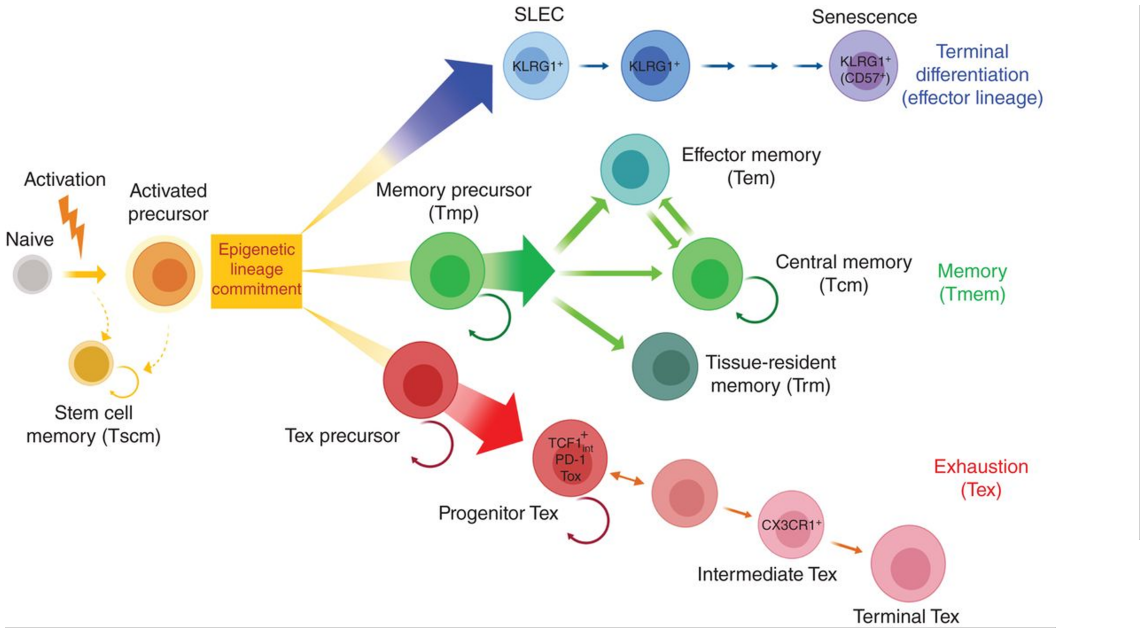



**Figure 1.2**: **Diagram depicting the differentiation and various subsets of CD8+ T cells**. Figure taken from Muroyama & Wherry (2021). The diagram illustrates the differentiation of CD8+ T cells into various subsets. The blue cells represent terminally differentiated effector (Teff) cell lineage, which is often associated with immediate responses to infections. The green cells represent the memory (Tmem) cell lineage, which includes long-lasting memory cells that help provide immunity against future infections. The red cells represent the exhausted (Tex) cell lineage, which may exhibit impaired function due to prolonged exposure to antigens or infections.

(Lugli et al. 2010). These cells secrete high levels of cytotoxic molecules and are capable of producing proinflammatory cytokines. They are considered terminally differentiated as they express markers associated with terminal differentiation, such as KLRG1 and/or CD57 (Brenchley et al. 2003, Henson & Akbar n.d.). Moreover, they exhibit the shortest telomeres among human T cells (Romero et al. 2007).

However, conflicting studies suggest that Temra cells might not be definitively terminally differentiated but could require specific costimulatory signals for proliferation (Waller et al. 2007, Chong et al. 2008). Notably, deuterium labelling studies indicate contradictory results regarding CD57 expression, commonly viewed as a marker of immune senescence (Chong et al. 2008, Ahmed et al. 2020). These studies propose that CD57+ cells proliferate at a similar rate as CD57- cells (Chong et al. 2008, Ahmed et al. 2020). These findings challenge the notion that CD8+CD57+ Temra cells should be categorically considered as terminally differentiated effector T cells.

Approximately 30% of Temra cells are found in blood and blood-rich tissues such as spleen, bone marrow, and lung (Thome et al. 2014). Notably, these cells tend to accumulate with repetitive stimulation, which is evident during chronic infections such as cytomegalovirus (CMV) (Weekes et al. 1999, Patin et al. 2018) and Human immunodeficiency viruses (HIV) (Meraviglia et al. 2019) in humans. Moreover, the frequency of CD8+ Temra cells increases with age (Ligotti et al. 2023) and in autoimmune diseases (Perl & Morel 2023). A recent study showed that higher levels of Temra cells in the blood of kidney transplant patients are associated with a greater risk of graft failure (Jacquemont et al. 2020). These findings suggest a potential link between these cells and immune dysregulation, which may contribute the transplanted organ rejection.

**Memory stem T cells (Tscm)** are recently categorised subset of memory T cells. Tscm are antigen-experienced cells that exhibit a phenotype resembling naive T cells with markers CD45RA+CCR7+CD27+CD28+CD62L+(Figure 1.3) (Figure 1.3). They can be distinguished from naive T cells by the expression of CD95, CD122 and CXCR3 (Gattinoni et al. 2011). Tscm are known for their longevity and possess stem cell-like properties, such as self-renewal capacity and multipotency to differentiate into various memory and effector CD8+ T cells (Gattinoni et al. 2017). In comparison to Tcm cells, Tscm are relatively rare and less differentiated. While the exact ontogeny of Tscm cells is yet to be fully understood, further details about Tscm cells are provided in section 1.5.

**Tissue-resident memory cells (Trm)** are a specialised subset of memory T cells that reside in non-lymphiod tissues, such as skin, mucosal surfaces, and organs, rather than circulating in the bloodstream, serving as a frontline defense against reinfection (Klonowski et al. 2004, Steinert et al. 2015, Jiang et al. 2012, Masopust et al. 2006, Szabo et al. 2019). Initially, it was identified in the intestinal mucosa and considered to be a subset of Tem cells (Masopust et al. 2001). However, subsequent research has revealed their presence in nearly all tissues in both humans and mice (Schenkel & Masopust 2014, Thome et al. 2014). Phenotypically, Trm cells are distinct from other memory T cells, lacking expression of the LN homing markers CD62L and CCR7. Instead, they express integrins CD103 and CD49a, which aid in tissue entry (Mackay et al. 2013, Ray et al. 2004), and CD69, which

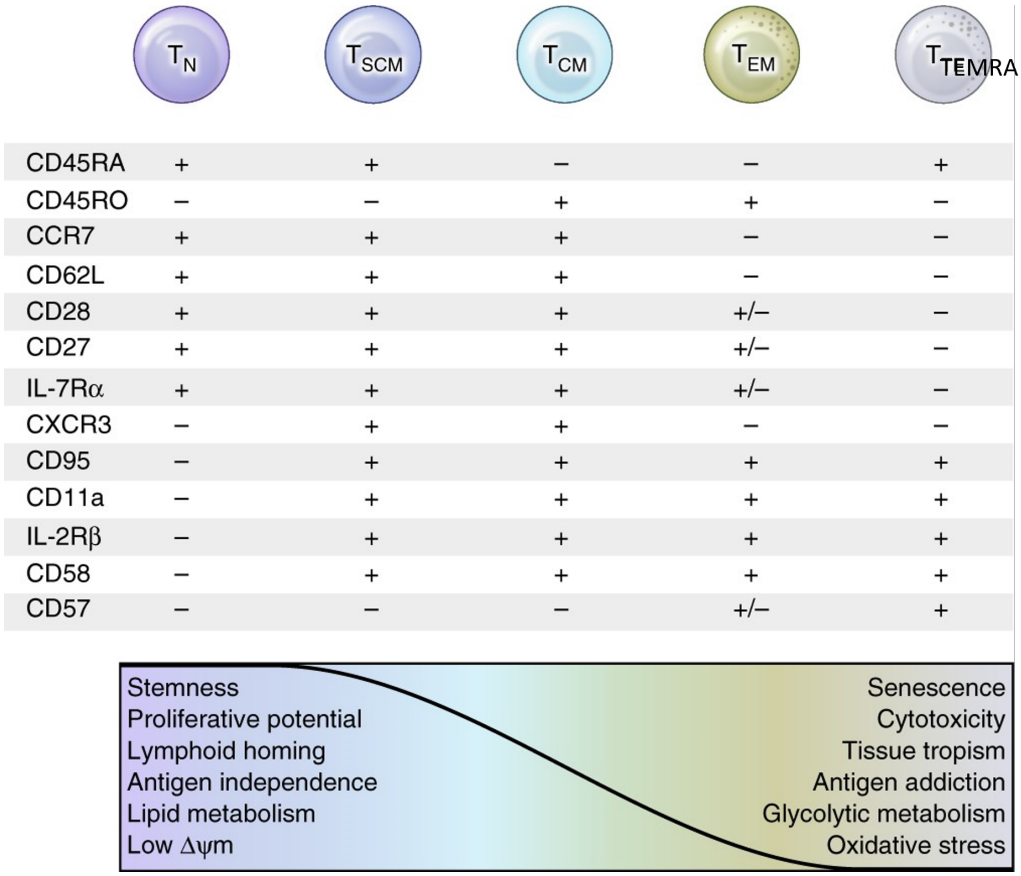



**Figure 1.3**: **Phenotypic identity of different CD8+ T memory subpopulations with functional and metabolic attributes.**. The figure is adapted from Gattinoni et al. (2017). The diagram illustrates the expression of surface markers expressed by different memory subpopulations with their functional and metabolic attributes. $\Delta\Psi$m, mitochondrial membrane potential.

promotes tissue retention (Mackay & Braun 2015). However, the expression of these proteins can vary depending on the tissue of residence. Trm cells protect the peripheral tissues through their sensing and alarm function. This involves Trm cells recognizing antigens and producing IFN-$\gamma$, leading to significant changes in gene expression of chemokine ligands, facilitating the recruitment and activation of various cells from the innate and adaptive immune systems to mount an effective immune response (Schenkel et al. 2013, Ariotti et al. 2014, Schenkel et al. 2014, Danahy et al. 2017). Trm cells exhibit distinct transcriptional profiles, which include reduced expression of KLF2 and Eomes (Mackay et al. 2015, Skon et al. 2013), low levels of T-bet and TCF1 (Mackay et al. 2015, 2016), and elevated expression of Hobit and Blimp1 (Mackay et al. 2016). Due to the unique protective properties of Trm cells in peripheral tissues, there is growing interest in developing site-directed vaccinations to induce the generation of Trm cells.

**Virtual memory T cells (Tvm)**, also known as memory phenotype (MP) cells, are a subset of antigenically naive CD8+ T cells, described in mice. In adult naive C57BL/6 mice, these cells constitute approximately 10% of total circulating CD8+ T cells (Haluszczak et al. 2009). Remarkably, despite their antigenically naive status, Tvm cells express markers typically associated with conventional memory T cells, such as high levels of CD44 and CD122 (Turner et al. 2021). Their naive state is evidenced by low-level expression of CD49d (Lee et al. 2013, Quinn et al. 2016) and their presence in germ-free mice (Haluszczak et al. 2009, La Gruta et al. 2010, Quinn et al. 2016). The differentiation of Tvm is believed to be initially influenced by high reactivity to self-peptide-MHC class I in the thymus (Miller et al. 2020), leading to elevated expression of CD5 (Quinn et al. 2016) and Eomes (Miller et al. 2020). Peripheral exposure to cytokines like IL-4 and IL-15 further maintains their differentiation (Sosinowski et al. 2013, Quinn et al. 2020). Recent evidence suggests that Tvm cells represent a distinct CD8+T cell lineage, rather than just a peripherally activated T-cell state (Miller et al. 2020). In humans, a putative Tvm population has been proposed within the Temra population (CD45RA+CD27lo) and distinguished by the expression of NKG2A and/or KIRs (Jacomet et al. 2015, Paprckova et al. 2023). Human Tvm cells, similar to their mouse counterpart, are found in cord blood and exhibit high levels of CD122, Eomes and T-bet (Jacomet et al. 2015, Paprckova et al. 2023). They are functionally equivalent to mouse Tvm cells in terms of TCR-mediated proliferation and IFN-$\gamma$ production following cytokine stimulation (Jacomet et al. 2015). Further research to identify specific markers for human Tvm cells is crucial for better understanding their role in human immunity.

**Exhausted T Cells (Tex)** are a subset of antigen-specific CD8+ T cells that were originally identified in chronic infections, and characterised by reduced effector functions (Gallimore et al. 1998, Zajac et al. 1998). These cells coexpress high levels of multiple inhibitory receptors such as PD-1 and exhibit distinct transcriptional and epigenetic profiles (Barber et al. 2006, Wherry et al. 2007, Blackburn et al. 2008, Pauken et al. 2016, Sen et al. 2016). Tex cells are commonly found in both humans and mice during chronic infections and cancer. While they might partially limit or slow disease progression, they are unable to fully control infection or tumors (McLane

et al. 2019, Wherry & Kurachi 2015). In humans, Tex cells are often classified by their elevated expression of PD-1 or other inhibitory receptors. Notably, in tissues, Tex cells may share certain features or exhibit phenotypic overlap with Trm cells. Further exploration of the Tex cell compartment reveals additional heterogeneity, which will be discussed in more detail later in section 1.5.4. The overview of CD8+ T-cell subsets and terminology is summarized in Figure 1.2

Overall, our understanding of CD8+ T cell immunity has evolved significantly, emphasizing the unique nature of the different immune cells. Advances in sampling methods and single-cell technologies offer exciting opportunities to refine our understanding of how CD8+ T cells localize to specific niches and execute pathogen-specific effector functions without causing tissue damage. Despite these significant advancements, there is still work to be done to construct a comprehensive anatomical picture.

### 1.3.3 Factors affecting the heterogeneity of memory T cell pool

**The Impact of Signal Strength on CD8+ T Cell Fate**: During infection or vaccination, naive CD8+ T cells interact with dendritic cells presenting cognate peptides in a MHC class I-restricted manner (Zinkernagel & Doherty 1974, Doherty & Zinkernagel 1975). This engagement triggers rapid proliferation and acquisition of effector functions in antigen-specific CD8+ T cells, enabling them to migrate to infection sites. T cell priming involves integrating multiple signals, including TCR signaling, co-stimulation, cytokine, chemokines, and metabolic signals (Obar & Lefrançois 2010, Kaech & Cui 2012, Chang et al. 2014). The quality and strength of these signals play roles in determining memory T cell development and differentiation (Muroyama & Wherry 2021, Martin & Badovinac 2018, Chen et al. 2017).

- **TCR signaling:** The effectiveness and nature of TCR signaling are influenced by factors such as the TCR's affinity for peptide-MHC complexes, the antigen dose presented by APCs, the duration of TCR-pMHC interactions, and the timing of TCR recognition during the infection phase (Chen & Flies 2013). Studies have shown that weaker TCR signaling during initial antigen recognition promotes a faster transition from Tem to Tcm, whereas strong

TCR signaling leads to terminal differentiation (Wherry et al. 2003, Teixeiro et al. 2009, Zehn et al. 2009, Smith-Garvin et al. 2010) (Figure 1.4).

- **Co-stimulatory signaling :** co-stimulatory molecules like CD28, 4-1BB, CD27, and OX40 promote memory formation and secondary responses, while inhibitory receptors like PD-1 and TIM-3 regulate T cell fate toward exhaustion phenotype (Figure 1.4) (Hendriks et al. 2005, Boesteanu & Katsikis 2009).

- **Inflammatory signalling:** Inflammatory signals such as IL-12, IL-27 and IFNs can impact the balance between effector and memory CD8+ T cell subsets (Figure 1.4) (Badovinac et al. 2004, Kolumam et al. 2005, Pearce & Shen 2007, Shaulov & Murali-Krishna 2008, Cui et al. 2009, Wiesel et al. 2012)(Figure 1.4). IL-15 promotes memory formation (Weninger et al. 2001, Berard et al. 2003, Richer et al. 2015), whereas IL-2 signaling influences SLECs differentiation (Kalia et al. 2010, Pipkin et al. 2010). Interestingly, the impact of IL-2 signaling on CD8+ T cell memory formation appears to be regulated temporally. Administration of recombinant IL-2 (rIL-2) during the expansion phase reduces T cell survival, whereas treatment with rIL-2 during the contraction phase enhances T cell proliferation, survival and memory formation (Blattman et al. 2003). IL-10 and IL-21 signaling, through a STAT3-SCOCS3 pathway, contribute to memory formation by regulating T cell responses to inflammation (Cui et al. 2011). Recent studies have also revealed the importance of cytokine signaling pathways in Trm development. Transforming growth factor (TGF-$\beta$) and IL-15 play crucial roles in Trm differentiation, particularly, in inducing CD103 expression on Trm precursor cells infiltrating various tissues (El-Asady et al. 2005, Zhang & Bevan 2013, Casey et al. 2012, Mackay et al. 2013, Sheridan et al. 2014).

**CD4+ T cell help**: CD4+ T cells help play a critical role in regulating the differentiation of T memory cells. Early studies demonstrated that the absence of CD4+ T cells helps compromise the development of Tcm (Janssen et al. 2003, Shedlock & Shen 2003, Sun & Bevan 2003). This effect was linked to an increase in SLECs generation, which is dependent on the transcription factor T-bet (Intlekofer et al. 2007). The exact mechanism by which CD4+ T cells influence T memory cell

differentiation is still not fully understood and may vary depending on the context. Possible mechanisms include the licensing of dendritic cells (DCs) through CD40L (Castellino et al. 2006, Bennett et al. 1998, Ridge et al. 1998), production of IL-2 (Kalia et al. 2010, Makedonas et al. 2010, Pipkin et al. 2010), production of IL-21 (Cui et al. 2011), and support for the production of effective antibodies (Bachmann et al. 2004).

**Transcription factors (TFs)**: TFs and their associated circuits play crucial roles in guiding the differentiation of T effector and memory cells. TFs involved in the formation of memory T precursors, Tcm and Tscm are Id3 (Yang et al. 2011), TCF-1 (Zhou et al. 2010, Utzschneider et al. 2016, Kratchmarov et al. 2018), Bcl6 (Ichii et al. 2002), STAT3 (Cui et al. 2011), Foxo1 (Utzschneider et al. 2016), Eomes (Banerjee et al. 2010), and Zeb1 (Guan et al. 2018, Scott & Omilusik 2019). On the other hand, the formation of Tem and SLECs is promoted by transcriptional factors such as T-bet (Intlekofer et al. 2007, Joshi et al. 2007), Id2 (Cannarile et al. 2006, Yang et al. 2011, Masson et al. 2013), Blimp-1 (Kallies et al. 2009, Rutishauser et al. 2009), STAT4 (Mollo et al. 2014) and Zed2 (Figure 1.4) (Guan et al. 2018, Scott & Omilusik 2019). Many of these TFs function in opposing pairs, where one TF drives effector-like differentiation while the other promotes memory-like differentiation. Additionally, numerous other TFs are required for the initiation stages of T cell activation, including BATF (Kurachi et al. 2014), IRF4 (Kurachi et al. 2014), c-Myb (Chen et al. 2017) and Runx3 (Wang et al. 2018), as well as signal-dependent TFs downstream of TCR signaling and/or costimulation, such as NFATs, Fos, Jun, AP-1 family members, and NF-$\kappa$B (Daniels & Teixeiro 2015, Chen et al. 2017). These TFs collectively orchestrate the diverse differentiation events leading to the formation of distinct CD8+ memory T cell subsets.

**Epigenetic regulation**: Epigenetic modifications are pivotal in controlling the fate of memory formation within CD8+ T cells, a critical characteristic that enables them to rapidly reacquire effector functions upon encountering the same pathogen. These epigenetic changes encompass DNA methylation, histone modifications, and chromatin accessibility, collectively orchestrating memory T cell behavior and function. DNA methylation primarily occurs at CpG dinucleotides in genomic regions, influencing gene expression through its repressive nature. The DNA methyltrans-

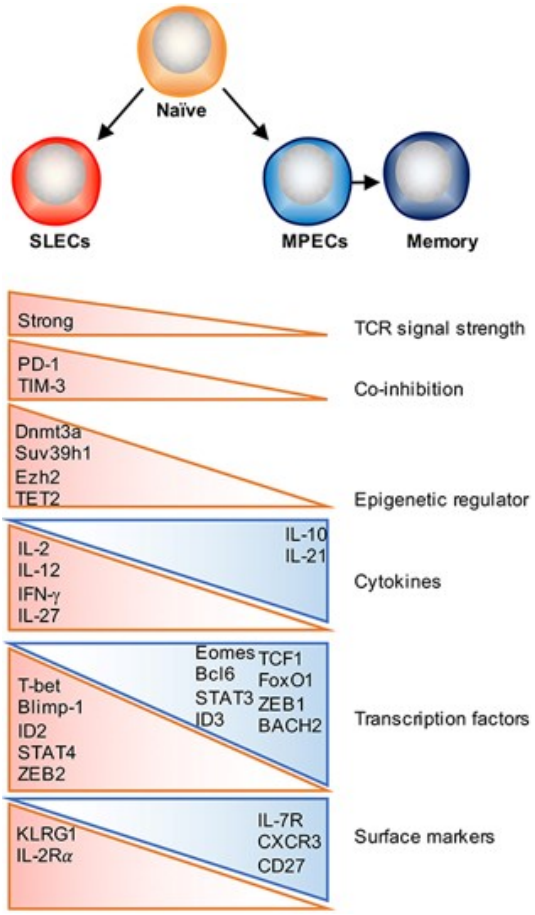



**Figure 1.4**: **Regulatory Factors Influencing Effector and Memory Cell Fate.**This figure is taken form (Chen 2018)

ferase Dnmt3a catalyzes DNA methylation at sites such as the Tcf7 promoter, thereby limiting MPEC formation (Ladle et al. 2016), while TET2, a methylcytosine dioxygenase, induces active DNA demethylation upon TCR signaling, favoring memory cell formation (Figure 1.4) (Carty et al. 2018). Further, chromatin accessibility, determined by nucleosome positioning, impacts the availability of binding sites for TFs. Studies using ATAC-seq and ChIP-seq techniques reveal insights into chromatin changes during CD8+ T cell differentiation (Buenrostro et al. 2013, He et al. 2016). Open regulatory regions in MPECs, as opposed to SLECs, govern genes associated with naïve and memory T cell properties, thereby preserving memory potential (Scott-Browne et al. 2016). In contrast, terminally differentiated SLECs exhibit increased repressive histone modification H3K27Me3 at genes related to cell survival and memory formation (Gray et al. 2017). Thus, epigenetic modifications play an essential role in memory CD8+ T cell differentiation.

## 1.4 Models of CD8+ T-Cell Memory

With the knowledge of possible factors affecting CD8+ T cell differentiation, the next question to ask is: What are the timings of fate commitment during CD8+ T memory cell differentiation? How do these subsets relate to each other, and to what extent do they share plasticity (Restifo & Gattinoni 2013)? Several models have been proposed to define the lineage of CD8+ T memory cells, with three classical models gaining popularity: a) asymmetrical division model b)progressive differentiation model, and c) transient and reversible differentiation model. Each model has experimental support but also poses contradictions when considered together.

In the asymmetrical division model, cells take divergent paths early on in the development stages, leading to the formation of both memory and effector cells. Specifically, upon the first cell division, one daughter cell becomes an effector precursor cell, while the other generates the memory T-cell pool (Chang et al. 2007, Chen et al. 2018) (Figure 1.5 A).

On the other hand, the model of progressive development and stable differentiation proposes that memory CD8+T cells directly originate from activated naive T cells and undergo gradual differentiation into Tscm to Tcm to Tem cells, orchestrated by differential gene expression (Gattinoni et al. 2011, Gray et al. 2017, Restifo & Gattinoni 2013) (Figure 1.5 B). This model is supported by the evidence that Tem CD8+ T cells are a terminally differentiated subset with limited differentiating potential (Gattinoni et al. 2011, Lugli 2013, Saeed et al. 2014) and reprogramming ability (Crompton et al. 2016). The late stage of effector fate commitment is also associated with changes in chromatin accessibility, influencing the regulation of memory and stem genes versus effector loci (Crompton et al. 2016).

In contrast, the model of transient and reversible differentiation of CD8+ T cells further contradicts the above models. It proposes that there are two gene expression programs: an "on/off/on" and on "off/on/off" for effector and memory precursor subsets, respectively (Youngblood et al. 2017, Herndler-Brandstetter et al. 2018) (Figure 1.5 C). According to this model, memory T cell clones can differentiate from certain effector subsets through gene expression reprogramming. After the resolution of an acute infection, specific transcriptional activities, such as Id2 and Foxo1, play a role in maintaining the immune phenotype and cellular plasticity of

effector-like memory population or sustaining the memory state by preventing the effector gene signatures (Omilusik et al. 2018, Delpoux et al. 2018). Deficiency in Id2 or Foxo1 leads to instability in CD8+ T cell states, causing the cells to reverse to opposite immune phenotypes. Importantly, virus-specific memory precursor effector subsets retain the plasticity to transform into long-lived memory T cells through DNA demethylation and epigenetic reprogramming (Youngblood et al. 2017).

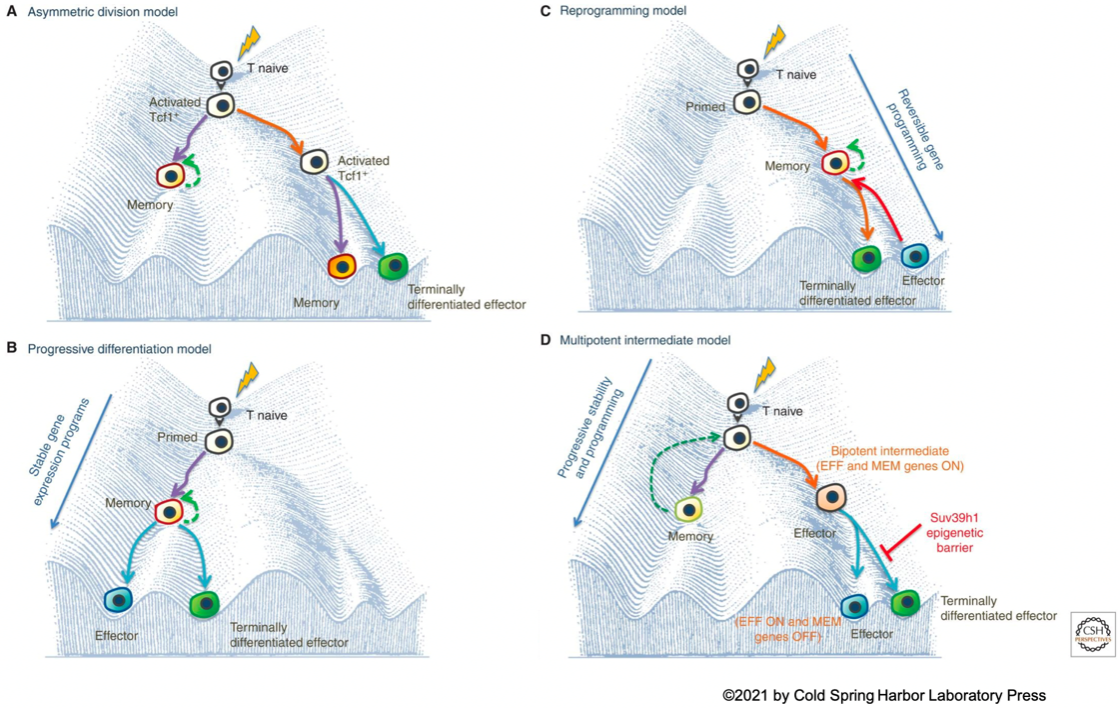



**Figure 1.5**: **Proposed models to explain CD8+ T-cell memory heterogeneity.**Figure from Pace (2021) (A) asymmetric division model, (B) progressive differentiation model, (C) reprogramming model, and (D) multipotent intermediate model.

More recent studies focusing on key epigenetic factors and utilizing quantitative multi-parametric single cell assays have provided new insights into the complex framework of CD8+T cell fate decision during lineage commitment (Henning et al. 2018). This research has led to the identification of various intermediate subsets of cycling CD8+ T cells. Among these subsets, one proliferating group exhibited characteristics of both memory and effector gene signatures, suggesting the presence of bipotent effector/memory intermediates. These bipotent intermediates may represent memory precursor/effector subsets that possess the capacity to be epigenetically reprogrammed to either become effector cells or enter into long-term memory quiescence (Pace et al. 2018) (Figure 1.5 D). Further investigations are needed to better

understand the role of chromatin-based information and dynamic changes in regulating the plasticity and fate commitment of these multipotent intermediate cells during different stages of CD8+ T cell differentiation.

So far, there is no conclusive resolution of which model reflects reality, and it is possible that in vivo elements of all models hold true. Further research is required to gain a comprehensive understanding of CD8+ T cell differentiation and fate commitment.

## 1.5 Stem-like memory T cells

Over the decade, there has been a growing interest in Tscm cells, a small subset of cells with a naive-like phenotype believed to be crucial in maintaining T cell memory. These stem like T cells are multipotent progenitors capable of self-renewal and replenishing other memory T cell subsets (as explained in section1.3.2). Labeling experiments have shown that Tscm cells exhibit greater proliferation compared to naive T cells (Ahmed et al. 2016). However, it remains unclear whether Tscm cells are less or more dynamic than the overall memory T cell population in the circulation. In this section, I will discuss the characteristics, discovery, functional properties, dynamics and maintenance of Tscm cells.

### 1.5.1 Characteristics and Discovery

The concept of memory T cells existing within naive T cell population emerged following the discovery of CD44loCD62LhiCD8+ cells in mice that displayed naive-like phenotype but possessed unique properties that distinguished them from conventional memory T cells, including high expression of stem cell antigen 1 (SCA1), IL-2R$\alpha$, CXCR3 (Zhang et al. 2005). These cells are named as Tscm cells due to their remarkable stem cell-like properties demonstrated by their ability to sustain graft-versus-host diseases (GVHD) upon serial transplantation and to reconstitute diverse memory and effector T cell subsets while exhibiting self-renewing capacities (Zhang et al. 2005). Identifying the human counterpart of Tscm cells proved challenging due to the lack of a SCA1 equivalent, but subsequent research successfully generated human Tscm cells in vitro by activating the Wnt-$\beta$-catenin signaling

pathway (Gattinoni et al. 2009).

Further insights into the functional characteristics of Tscm cells were gained through studies in nonhuman primates (NHPs). Tscm in NHP were found to be functionally distinct from conventional memory cells and serve as a precursor of Tcm cells (Lugli et al. 2013). Moreover, these cells were abundant in LN and virtually absent at mucosal surfaces in NHPs (Lugli et al. 2013).

Phenotypically, like naive T cells, Tscm cells are CD45RA+CD45RO-, and they exhibit elevated expression levels of CD27, CD28, IL-7R$\alpha$, CD62L, CD58 and CCR7 (Gattinoni et al. 2011, Lugli 2013). Functionally, unlike naive T cells, Tscm cells undergo clonal expansion and express memory markers such as CD95 and CD122 (Farber et al. 2014, Gattinoni et al. 2011). These cells exhibit superior proliferative capacity compared to Tcm cells, possess the potential to differentiate into various other classically defined T cell memory subsets (including Tcm) and retain their distinctive phenotype even after proliferation, both in vitro and in mice in vivo (Gattinoni et al. 2011, Farber et al. 2014, Zhang et al. 2005, Lugli 2013). Additionally, they rely on IL-7 and IL-15 for homeostatic maintenance, a hallmark of memory phenotype (Gattinoni et al. 2011, Lugli et al. 2013).

Transcriptionally, Tscm cells express critical TFs in the Wnt-$\beta$-catenin pathway, such as TCF7, LEF1, Eomes, FOXO1 and Id3, known to promote self-renewal (Gattinoni et al. 2011, Kratchmarov et al. 2018). Conversely, they downregulate the expression of key effector transcription factors, including TBX21, BLIMP-1, and Id2 (Gao et al. 2021). These molecular characteristics further support their identity as memory cells with stem cell-like properties.

Taken together, the accumulating evidence suggests that Tscm cells represent the primary stem cell memory population that plays a crucial role in sustaining long-term memory responses in vivo.

### 1.5.2 Longevity and persistence

Tscm cells represent a unique and long-lived subset within the memory T cell pool that lies between naive T and Tcm subsets Figure 1.3. Their ability to persist for the long term throughout an individual's life, even after antigen elimination (Lugli et al. 2013), highlights their significance in maintaining immune memory. Moreover,

vaccine-induced CD8+ Tscm cells specific to Yellow Fever (YF) antigens have been observed to sustain in a stable state for over 25 years (Fuertes Marraco et al. 2015).

Recent advances in longitudinal monitoring of engineered lymphocytes have allowed the tracking of individual T cell clonotypes over extended periods. In patients with adenosine demaminase (ADA)-deficient severe combined immunodeficiency (SCID), genetically engineered Tscm cells exhibited remarkable persistence and preserved their precursor for decades (Biasco et al. 2015). Another study followed engineered lymphocytes in leukemia patients who underwent haploidentical hematopoietic stem cell transplantation (HSCT) with retrovirally transduced donor lymphocytes expressing a suicide gene (Oliveira et al. 2015). It was found that the number of persisting gene-marked T cells was closely linked to infused Tscm cell count, indicating enhanced proliferative potential, immune-reconstitution capacity, and longevity of Tscm cells. These findings were further supported by clinical trials involving chimeric antigen receptor (CAR)–engineered autologous T cells, demonstrating the long-term presence of genetically modified T cells (Sabatino et al. 2016). Many other vaccination studies have also provided evidence of the longevity of memory (Aleksova et al. 2023) (Discuss in section 1.5.3).

Many factors contribute toward the maintenance of longevity of Tscm cells such as :

**(a) Self-renewal capacity:** As explained earlier, Tscm cells can renew themselves, allowing to maintain a stable population and persist over extended periods. The high turnover rate, supported by their high telomerase activity that preserves telomere length during cell division, plays an essential role in the self-maintenance of Tscm cells (Ahmed et al. 2016).

**(b) Reduced exposure to antigen:** During viral infection, antigen reaches the LN via two main pathways: direct drainage of virions into the subcapsular sinus through afferent lymphatics, leading to infection of the interfollicular regions (IFRs) (Groom 2015, Hickman et al. 2008, Phan et al. 2007) and local inflammation (Junt et al. 2007), or migration of antigen-presenting DCs from peripheral tissue to the lymph node (Ulvmar et al. 2014). These events concentrate viral antigens in the IFRs, influencing T cell differentiation at this site (Gerner et al. 2015).

During infection, IFR turns into an inflammatory site with high antigen load and inflammatory cytokines (Hickman et al. 2008, Galletti et al. 2020, Junt et al. 2007). IFN-$\alpha$ act as inducer of CXCR3 ligands, direct CD8+T cell differentiation away from SLEC and towards Tscm (Wu et al. 2016, Duckworth et al. 2021) (Figure 1.6). A recent study in mice by inhibiting IFN-$\alpha$ receptor (IFN-$\alpha$R) demonstrated that LCMV-induced CD8+ T cells differentiation skewed toward Tscm differentiation because of increased retention of CD8+ T cells in the central paracortex of lymph nodes (less inflammatory region)(Duckworth et al. 2021). Importantly, limiting the inflammatory environment by blocking IFN-$\alpha$ during primary viral infection promoted Tscm differentiation, resulting in enhanced stemness and robust secondary immune responses, even during subsequent challenges (Duckworth et al. 2021). Furthermore, other inflammatory cytokines such as IL-2,IL-12, IL-6 and IFN-$\gamma$ were also found to promote effector-like phenotype (Danilo et al. 2018, Sercan et al. 2010, Pipkin et al. 2010, Mitchell et al. 2010, Pham et al. 2009, Xin et al. 2016).

The presence of increased local viral load in the IFRs of inflamed LN suggests that multiple inflammatory cytokines might be produced in distinct niches. This leads to the identification of an axis between spatially separated fates, proposing an intriguing hypothesis: the default state of differentiation toward Tscm is established due to decreased inflammation through retention in the paracortex, rather than being driven by any specific memory-inducing network (Duckworth & Groom 2021). Consequently, the continuous expression of CCR7 may primarily serve to keep Tscm precursors separated from the inflammatory IFRs (Duckworth et al. 2022)

Overall, this indicates that Tscm cells preferentially reside deep in the lymphoid tissues, where exposure to continuous antigen stimulation and inflammatory environment is limited. Consequently, this helps Tscm cells to evade excessive activation and differentiation, thereby preserving their stem-like characteristics and contributing to the maintenance of Tscm longevity.

**(c) Low metabolic activity:** Numerous studies have provided valuable insights into how cellular metabolism profoundly influences the formation and longevity of memory T cells, reviewed by (Kishton et al. 2017). One key aspect is the

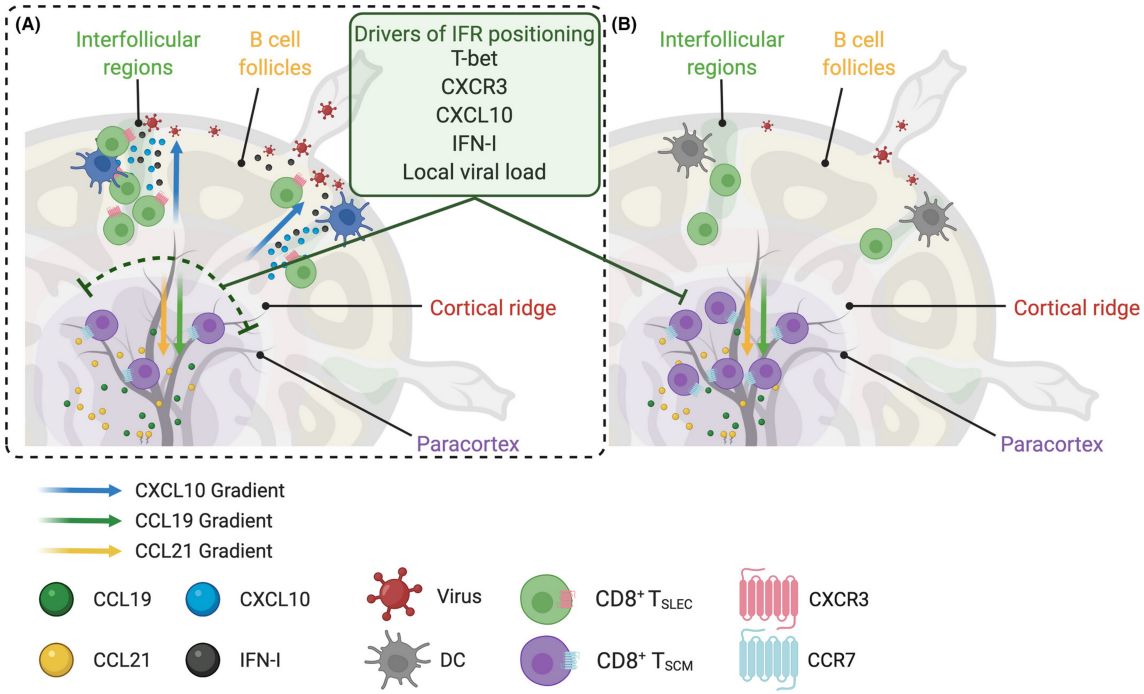



**Figure 1.6**: **Tscm generation based on spatial T cell position, taken from Duckworth et al. (2022).** A. In an infected lymph node, the Inflammatory Focal Region (IFR) experiences heightened inflammation caused by local viral infection, resulting in the upregulation of IFN-I, stromal, and DC sources of CXCL10. This environment attracts T-bet+ CXCR3+ CD8+ T cells, which become imprinted in the IFR and differentiate into SLEC. Meanwhile, in the paracortex, T cells are segregated from peripheral lymph node inflammation by the dual expression of CCR7. This reduced local inflammation in the paracortex promotes default differentiation toward Tscm.B. When there is an absence of local lymph node inflammation or reduced migration into the IFR (due to factors such as loss of CXCR3, CXCL10, or IFN-I signaling), CD8+ T cell retention in the paracortex increases due to CCR7 expression, resulting in the default formation of Tscm cells.

preference of memory T cells for oxidative phosphorylation (OxPhos) as their primary energy source. This metabolic adaption allows memory T cells to rely on mitochondrial respiration for energy production which contributes to their increased longevity and persistence as compared to effector T cells (Raynor et al. 2021). Notably, Tscm cells demonstrated a lower mitochondrial membrane potential than other T cell subsets, further emphasizing their dependence on OxPhos and fatty acid oxidation to meet their metabolic needs as observed by Sukumar et al. (2016). Additionally, the regulation of the mechanistic target of rapamycin (mTOR) signaling pathway also plays a central role in memory T cell development and metabolic control. Inhibition of mTOR during the early phase of T cell activation enhances memory T cell gener-

ation, whereas prolonged mTOR activation leads to terminal differentiation and compromises the memory pool (Scholz et al. 2016).

In conclusion, the cellular metabolism of Tscm plays a critical role in shaping its longevity and functionality.

**(d) Homeostatic maintenance:** The homeostatic maintenance of Tscm cells is crucial for their ability to provide long-lasting immunity. Homeostatic maintenance involves the continuous replenishment of Tscm cells through self-renewal and slow cell division. Further, unlike naive T cells, Tscm cells can persist independently of TCR-mediated antigen interaction (Murali-Krishna et al. 1999, Swain et al. 1999, Polic et al. 2001), as they transition to MHC independence and exhibit reduced TCR sensitivity but heightened sensitivity to cytokines. Studies have confirmed the significance of gamma chain cytokines as key players (Lodolce et al. 1998, Kennedy et al. 2000, Ku et al. 2000, Becker et al. 2002), particularly IL-15's role in promoting the survival and antigen-independent proliferation of Tscm cells (Jameson & Masopust 2018). This is evident by the high expression of IL-15 receptors on CD8+ T cells (Giri et al. 1994, Grabstein et al. 1994, Lenz et al. 2004, Zhang et al. 1998). Additionally, IL-7 plays a crucial role in the survival and homeostatic proliferation of memory cell (Kondrack et al. 2003, Lenz et al. 2004, Purton et al. 2007) by regulating Bcl-2 (an anti-apoptotic protein) (Kondrack et al. 2003, Osborne et al. 2007) and supporting cells expressing CD62L (Kawabe et al. 2021). Further, IL-7 has been demonstrated to promote the metabolic well-being of memory T cells (Cui et al. 2015). Overall, homeostatic maintenance ensures a continuous supply of functional and long-lived Tscm cells, allowing them to persist over extended periods and contribute to the long-term memory response.

### 1.5.3 Tscm cells in vaccination

The primary goal of vaccination is to establish durable protective immune memory (Castellino et al. 2009). Despite the gradual decline in vaccine-induced antibody levels over time, studies have demonstrated the persistence of memory cells in vaccinated individuals for more than 15 years (Davis 2005, Wang et al. 2004, Bauer &

Jilg 2006), underscoring their significance in evaluating vaccine effectiveness. Among memory T cell subsets, Tscm cells have garnered significant attention due to their extreme persistence as compared to other memory populations after vaccination.

In the context of YF vaccination, studies have shown that Tscm cells are the most stable and long-lasting memory T cell population, persisting for over a decade after vaccination (Akondy et al. 2017, Fuertes Marraco et al. 2015). In contrast, other memory subsets, such as Tcm and Tem cells, show limitations in long-term persistence (Akondy et al. 2017, Fuertes Marraco et al. 2015).

Similarly, in HIV infection, CD8+ Tscm cells are abundant in patients receiving anti-retroviral therapy, contributing to long-term cellular immune memory response against HIV (Vigano et al. 2015). These cells may not directly participate in the antiviral process but play a crucial role by secreting IL-2 to support their own proliferation and differentiation (Finley 2017, Fenwick et al. 2019, Sharov 2021). Recent studies have shown that vaccination with prophylactic HIV-1 vaccine candidates induces more Tscm cells and enhances antiviral responses (Munusamy Ponnan et al. 2020).

Likewise, for the hepatitis B vaccine, a recent study by Vakili et al. (2022) revealed that nonresponders to the hepatitis B vaccine exhibited lower frequencies of CD4+ Tscm cells compared to responders. Other subsets of CD4+ T cells, including naive T cells, Tcm and Tem cells, did not show significant differences between groups (Vakili et al. 2022). In the case of bacillus Calmette–Guerin (BCG) vaccination in infants, Mpande et al. (2018) found that vaccine-induced Tscm cells positively correlate with the BCG-specific Ki67+CD4+ cells. This suggests that vaccine-induced Tscm cells contribute to long-term memory and proliferative capacity of the vaccine-induced T cell response to mycobacteria (Mpande et al. 2018). Additionally, other studies developed a vaccine targeting a TF called Twist, involved in metastasis. They observed an elevated presence of CD4+ Tscm cells in vaccinated mice compared to PBS-treated mice, suggesting that the Tscm population may have the potential to generate antitumor activity (Ardiani et al. 2014, Khan et al. 2013).

Furthermore, in the context of Severe acute respiratory syndrome coronavirus 2 (SARS-CoV-2) infection, Tscm cells play a key role in maintaining memory responses following recovery from SARS-CoV-2 infection or vaccination. Tscm cells

were successfully generated in convalescent COVID-19 patients even ten months after infection (Jung et al. 2021). Similarly, the BNT162b2 vaccine induced an antigen-specific population of Tscm cells that provide a multipotent memory reservoir for at least six months after vaccination (Guerrera et al. 2021).

To further improve vaccination strategies, it is desirable to develop vaccines that can induce significant numbers of Tscm cells. However, many current vaccine formulations primarily stimulate Tem cells (Speiser et al. 2005, Melero et al. 2014), which are less efficacious compared to those inducing protective antibodies (De Gregorio & Rappuoli 2012, Sallusto et al. 2010). Current T cell vaccines might be inefficient at promoting the development of memory T cells due to suboptimal signaling via the TCR and insufficient induction of metabolic programs, transcription factors, and chromatin reorganization (Chang et al. 2014). While activating CD8+ T cells under low-level inflammation enhances memory cell formation, it is debatable whether the avoidance of effector cell differentiation is necessary for optimal memory T cell generation (Pham et al. 2009). Natural infections can lead to robust memory T cell responses, including Tscm cells, despite initially producing effector cells. Some recent vaccine studies have observed the emergence of Tscm cells along with effector cells (Ahmed & Akondy 2011). The goal of new vaccines should be to induce a broad spectrum of memory cell phenotype, incorporating Tscm cells without compromising differentiated Tem and tissue-resident memory cells, which provide immediate protection at potential sites of re-infection in peripheral tissues (Park & Kupper 2015, Zhang & Bevan 2013). Ideally, future vaccines should mimic the diversity of memory cell responses induced by human pathogens and their pathophysiological properties in vivo (Jameson & Masopust 2009, Farber et al. 2014).

In conclusion, Tscm cells hold promise in vaccination strategies for their long-lasting immunological memory. Understanding the relationship between Tscm populations and the longevity of memory responses following vaccination will be crucial in developing effective and long-lasting immune protection against various pathogens. Further research is needed to unlock the full potential of Tscm cells and to create vaccines that mimic the diversity of memory cell responses induced by natural infections.

### 1.5.4 Heterogeneity of Tscm cells in humans

Heterogeneity within Tscm population was first established by Costa Del Amo et al. (2018), where they found that Tscm cells in humans have an average half-life of less than one year and a degree of self-renewal of 430 days under physiological conditions. This observed half-life is short for a population to be considered as stem cells. Further investigation using stable isotope labeling, telomere length analysis, and cross-sectional data from vaccine recipients revealed the presence of at least two distinct Tscm subpopulations with different turnover rates. One subpopulation displayed a rapid turnover (half-life = 5 months) explaining the rapid turnover of the bulk Tscm population, while another subpopulation exhibited remarkable self-renewal capacity and serves as the basis of long-term memory (half-life = 9 years) (Costa Del Amo et al. 2018).

A recent study in humans, conducted by Galletti et al. (2020) mapped the heterogeneity of Tscm and identified two subsets of CCR7+ progenitors distinguished by PD-1 and TIGIT expression. One progenitor gives rise to a dysfunctional subset with exhausted progeny expressing these inhibitory receptors (Tpex), while the other generates a more functional progeny lacking these inhibitory receptors (Tstem). They observed that Tstem cells maintained a high degree of multipotency and proliferation potential in response to re-activation, whereas Tpex cells generated functionally impaired progeny and showed decreased proliferation potential. Interestingly, despite their dysfunctional state, Tpex cells do not lose their memory-like features (Galletti et al. 2020).

Additionally, another recent study explored Tscm heterogeneity in humans based on CD122 expression on Tscm cells. The study demonstrated that Tscm cells expressing high CD122 exhibit greater proliferation, enhanced multipotency, and increased polyfunctionality, with higher frequencies of triple positive cytokine-production cells (TNF-$\alpha$, IL-2, IFN-$\gamma$) upon exposure to recall antigen (Zhao et al. 2021). Transcriptomic analysis of the Tscm CD122hi population further supports its stem cell-like transcriptional profile with higher expression of activation and homing molecules, such as CCR6, CSCR6, IL12Rc and IL18rap, and downregulation cell proliferation inhibitors such as S100A8 and S100A9. The study also observed that the Tscm CXCR3lo population also exhibited increased proliferation and polyfunc-

tionality (Zhao et al. 2021). Several other studies have explored the CXCR3 expression in distinct T cell phenotypes (Hu et al. 2011). Recent findings by De Simone et al. (2019) demonstrated that CXCR3 expression on naive T cells identified a subset with increased effector potential. However, in a study by Zhao et al. (2021) no significant differences were observed between CXCR3hi and CXCR3int populations in terms of multipotency and self-renewal capacity. Nevertheless, CXCR3 role in Tscm differentiation was highlighted in another recent mice study, showing that CXCR3 directs the differentiation of Tscm in LNs (Duckworth et al. 2022). Loss of CXCR3 or CXCL10 resulted in the accumulation of CCR7, maintained by TCF1 transcription factor, further facilitated the retention of cells in the paracortex of LN (Duckworth et al. 2022). These findings imply that CXCR3 is involved in the differentiation pathway of Tscm cells, although it does not lead to functionally distinct subsets. This notion was further supported by a recent study by Giles et al. (2022), where the transcriptional and epigenetic profiles of CXCR3+ and CXCR3- Tscm cells in healthy humans were found to be very similar (Giles et al. 2022).

Based on the studies above, it is clear that the Tscm compartment exhibits significant heterogeneity. However, there is still a lack of understanding regarding how these various subsets are interconnected and regulate memory maintenance in humans. Further research is needed to elucidate these complexities and their implications for immune responses.

## 1.6 Study Overview and Roadmap

### 1.6.1 Aim

The primary aim of this study was to explore the heterogeneity within the Tscm population and its contribution to the long-term maintenance of memory. While the significance of the Tscm compartment in memory preservation is widely acknowledged, several questions regarding its biology remain unresolved. The theoretical existence of kinetic heterogeneity within the Tscm compartment in humans was proposed (Costa Del Amo et al. 2018); however, the precise identity, function, and phenotypic markers to identify the Tscm sub-subsets have yet to be determined. Recent research from our lab indicates that CD95 expression can be employed to

distinguish between these two distinct Tscm subsets. Notably, Tscm cells expressing high levels of CD95 exhibit a higher Ki67+ population, suggesting an enhanced self-renewal potential compared to Tscm cells expressing low or intermediate CD95 levels (Danai et al., Unpublished). Building on these findings, the goal of this study is to provide further characterization of these two Tscm subsets (identified by CD95 expression) and to investigate their roles in sustaining long-term immunity.

### 1.6.2 Hypothesis

In pursuit of the aforementioned aim, our study posits the following hypotheses:

a) Tscm population comprises two distinct subpopulations that can be distinguished based on CD95 expression.

b) Tscm plays a pivotal role in the long-term maintenance of CD8+ T cell memory due to their stem-like properties, including self-renewal and multipotency.

### 1.6.3 Research approach

**Sample selection rationale:** In this study, I have opted to employ human samples as the primary subject of investigation, and this choice is driven by several compelling reasons. While acknowledging the invaluable contributions of mouse studies to our understanding of T-cell memory, it is essential to recognize the inherent limitations when applying these findings directly to humans (Mestas & Hughes 2004, Davis 2008). Notably, the evolutionary paths of their immune systems diverge significantly. With humans enjoying substantially longer lifespans than mice, the need for specialized mechanisms to sustain immunological memory over extended periods becomes apparent. Consequently, mouse models may not comprehensively capture the complexities of human immune memory. For instance, the regulation of naïve T cell homeostasis in humans predominantly hinges on thymic output during early life, transitioning to peripheral proliferation in later stages, whereas in mice, the thymic output of naïve cells remains relatively static (Murray et al. 2003, den Braber et al. 2012). Hence, we employed samples from healthy human volunteers to profile Tscm subpopulations by assessing proliferative history and self-renewal capacity.

**Methods for quantifying memory T cell dynamics:** Researchers have used various experimental techniques to quantify the dynamics of memory T cells in humans. These techniques provide valuable insights into cell proliferation and death. Ki67, expressed in all cell cycle phases except G0 (Scholzen & Gerdes 2000), and Annexin V, an apoptosis marker, are used to measure cell proliferation and death, respectively (Koopman et al. 1994, Asquith & Borghans 2011). Additionally, markers such as telomere length (De Boer & Noest 1998)and T-cell Receptor Excision Circle (TREC) (Hazenberg et al. 2001) offer insights into a cell's replicative history (Weng et al. 1995). Telomeres shorten with each division, while TRECs dilute as cells divide. Staining with bromodeoxyuridine (BrdU) (Asquith & Borghans 2011, Dancey et al. 1976) and carboxyfluorescein succinimidyl ester (CFSE) (Quah et al. 2007) also tracks proliferation in vitro.

In our study to investigate the first hypothesis (a), we opted for the TRECs quantification method to assess the cell division history of memory CD8+ T subpopulations. The reasons for choosing it over CFSE, BrdU, and telomerase length quantification methods are: Firstly, CFSE and BrdU, while capable of tracking cell division, have severe limitations: in particular neither is currently considered ethical in humans (though limited studies have been conducted with BrdU in the past). Secondly, telomerase length analysis, although informative, comes with challenges. Telomere metabolism is highly dynamic and influenced by multiple factors, including telomerase activity, genetics, and environmental factors (Lulkiewicz et al. 2020). This variability can make it less suitable for uniform and consistent tracking of proliferative history. In contrast, TRECs offer a non-toxic, non-invasive, and in vivo marker of cell division history (Verstegen et al. 2019). Formed during V(D)J recombination in the thymus, TRECs do not replicate during mitosis and are diluted with each round of cell division. Their stability within cells provides a consistent and reliable marker for long-term tracking, making them an ideal choice for our study (Verstegen et al. 2019).

**Methods to quantify TRECs:** TRECs measurement has proven to be effective in monitoring recent thymic emigrants and T cell division history (Kwan & Puck 2015). TRECs are circular DNA byproducts formed during the rearrangement of V(D)J recombination, where excised ends are ligated to create a distinctive signal

joint (Hazenberg et al. 2001). By designing specific PCR primers and probes for the T-cell signal joint, a quantitative PCR assay can be developed. Until now, the predominant approach in most studies has involved the utilization of quantitative real-time PCR (qPCR) (Baker et al. 2009, Barbaro et al. 2017, Van Zelm et al. 2011) or digital PCR (ddPCR) (Profaizer & Slev 2020, Tessitore et al. 2017, Vidal-Folch et al. 2017) for TRECs quantification. However, due to the very low frequency of CD8+ T memory subpopulations, particularly Tscm subpopulations, we designed an in-house optimised high-throughout ddPCR protocol directly from the cell lysates of sorted memory subpopulations to measure absolute copies of TRECs per cell.

**HIV clinical trials for long-term immunity study:** In pursuit of our second hypothesis (b), I worked on multiple HIV clinical trial vaccination projects. The purpose of vaccination is to create long-lasting immunity, providing an in vivo model to study the dynamics of long-term immune protection. To explore this hypothesis, we quantified antigen-specific CD8+ T memory subpopulations from PBMCs of healthy individuals vaccinated with HIV immunogens in CUTHIVAC002 (combined skin and muscle HIV trial vaccine) and IAVI (International AIDS Vaccine Initiative)-B001 and S001 clinical trial studies, at different timepoints post-vaccination. Our objective was to study how the early immune response related to long-term protection, especially antigen-specific Tscm cells. Comprehensive information about the vaccination projects will be presented in subsequent chapters of this thesis.

## 1.7 Thesis outline

The primary aim of this study was to investigate the dynamics of Tscm subpopulations and their role in the generation and maintenance of long-term immunity. To achieve this goal, we employed an integrated approach that combined immunophenotyping, transcriptional analysis, and cell-division history tracking analysis. Additionally, we investigated the dynamics of memory T cells in HIV clinical trial vaccination samples.

**Chapter 2:** This chapter describes the material and methodology used in our study.

**Chapter 3:** This chapter focuses on the development of a high-throughput

ddPCR method directly from cell lysate (referred to as crude lysate ddPCR) for the quantification of rare targets in rare cells, in our study, TRECs.

**Chapter 4:** In this chapter, we investigate the hypothesis that CD95 expression can be used to identify Tscm subpopulations. For this, we quantified cell division history and age-related changes in the frequency of CD8+ T memory subpopulations, particularly for Tscm subpopulations. We also explored the tissue distribution of CD8+ Tscm subpopulations, within human LNs. We utilised a combination of techniques, including flow cytometry, fluorescence-activated cell sorting (FACS) and an in-house high-throughput crude lysate ddPCR protocol. We also studied differential gene expression profiles of sorted memory subpopulations by bulk RNA sequencing, our objective was to characterize Tscm subpopulations and identify potential differences in their functional and transcriptional profiles.

**Chapter 5:** The objective of this chapter is to compare various activation-induced markers (AIMs) to determine the optimal AIM marker combination for quantifying antigen-specific CD8+ T cells. Data was obtained from healthy adults vaccinated with seasonal flu vaccine.

**Chapter 6:** This chapter quantifies antigen-specific CD8+ T memory subpopulations from HIV clinical trial vaccination studies- IAVI (B001 and S001 studies) and CUTHIVAC002. Our objective was to investigate the correlation between the early Tscm pool generated post-vaccination and the rate of memory decay.

**Chapter 7:** In this chapter, we explore the tissue distribution of various immune cells within human LNs. We utilize samples from HIV-negative volunteers who were injected with HIV envelope immunogens as part of the EAVI2020_01 (European AIDS Vaccine Initiative EAVI2020 01) study.

**Chapter 8:** In the final chapter, we summarize the study's findings, contextualize them within existing research, and discuss the study's limitations. We also outline potential avenues for future research.

# Chapter 2

# Materials and Methods

## 2.1 Immunophenotyping of memory T cells

### 2.1.1 Donor information

Healthy volunteers between 18 and 65 years old with no underlying infections, allergies or autoimmune diseases were recruited to donate blood for immunophenotyping of memory T cells, TREC measurement and RNA sequencing experiments. All volunteers signed a consent form and ethical approval for the project has been obtained (EC: 20/SC/0226 and 22/WA/0214).

### 2.1.2 Peripheral Blood Mononuclear Cell (PBMC) isolation

Blood (30-100ml) from healthy donors was collected in heparin-coated BD Vacutainer® (BD Biosciences, NJ, US) 10ml tubes. PBMCs were isolated using Histopaque®Hybri-max (Sigma-Aldrich, Missouri, US). Briefly, the blood was diluted 1:1 with Phosphate-buffered saline (PBS) and 35mLs of diluted blood were carefully layered on 15mLs of Histopaque® in a 50mL tube. The samples were centrifuged (800g, 20', 20°C) with no break and at the slowest acceleration. After centrifugation, the upper layer was discarded while the mononuclear cell layer was collected in a new 50ml tube, topped up with PBS and centrifuged (300g, 10' 4°C) at maximum acceleration and break. The cells were re-suspended in FACS buffer (PBS +7% fetal calf serum (FCS) (heat-inactivated, Gibco)) and counted using acridine orange/propidium iodide stain and the Luna dual Fluorescence cell counter

| Antibody | Clone | Supplier | Dilution |
|---|---|---|---|
| V500 anti-human CD19 | HIB19 | BD Biosciences | 1:25 |
| V500 anti-human CD14 | M5E2 | BD Biosciences | 1:200 |
| Qdot605 anti-human CD27 | CLB-27/1 | ThermoFisher | 1:200 |
| BV711 anti-human CD8 | RPA-T8 | BioLegend | 1:100 |
| BV785 anti-human CD3 | SK7 | BioLegend | 1:100 |
| FITC anti-human CD95 | DX2 | BioLegend | 1:50 |
| ECD anti-human CD45RA | Ki67 | Beckman Coulter | 2:25 |
| PEcy5.5 anti-human CD4 | MHCD0418 | ThermoFisher | 1:200 |
| FITC anti-human CCR7 | 150503 | BD Biosciences | 1:25 |

**Table 2.1: Antibodies used for flow cytometry and cell sorting.**

(Logos Biosystems, South Korea). PBMCs were cryopreserved in 10% dimethyl sulfoxide (DMSO) (Merck, NJ, US) in FBS (heat-inactivated, Gibco).

### 2.1.3 Flow cytometry and cell sorting

For phenotyping different types of memory subpopulations i.e. T naive, Tem, Tcm, Temra and Tscm, a cocktail of fluorescently labeled antibodies was prepared. Details of antibodies and their dilutions are given in table 2.1. Briefly, cells were washed in FACS buffer (PBS + 3% FCS, both GibcoTM) and re-suspended in 50$\mu$l of the surface antibody cocktail. Samples were stained in the dark for 20' at room temperature and then washed twice with FACS buffer. Cells were re-suspended in the FACS buffer for acquisition. For intracellular analysis, cells were fixed/permeabilized using the FoxP3 Transcription Factor Staining Buffer Set (eBioscience, Thermo Fisher Scientific, Massachusetts, US). Cells were incubated for 20' at room temperature (RT) with the fixation buffer from the kit as per the manufacturer's instructions. Samples were washed in permeabilization buffer and stained with intracellular antibodies for 20' at RT. Cells were washed and then re-suspended in FACS buffer for acquisition.

Dead cells were excluded using Live/DeadTM Fixable Near-IR dead cell stain kit (Thermo Fisher Scientific). Samples were acquired using a BD LSRFortessa(BD Biosciences, New Jersey, US). Compensation was performed using the UltraComp eBeads(Invitrogen, Thermo Fisher Scientific) as single-stained controls. Individual cell populations were gated using fluorescence minus one (FMO) controls.

For the sorting experiment, samples were pre-enriched for CD3+T cells using EasySep Human T cell isolation kit (Stemcell Technologies, Cambridge, UK) as per

the manufacturer's instructions. T cell subsets were sorted to purity (75%) using a FACSAria III (BD Biosciences).

### 2.1.4 Data analysis

Analysis of FCS files was done using FlowJo software version 10.6.1 (FlowJo). Data were exported and visualized in R studio (1.4.1106) and graphpad (version 9.4.1).

## 2.2 Droplet Digital Polymerase Chain Reaction

Droplet Digital Polymerase Chain Reaction (ddPCR) was used to quantify TRECs from sorted memory subpopulations. This protocol was first optimised using extracted DNA (standard ddPCR) from PBMCs isolated from the blood of healthy individuals and then modified for direct cell lysate (crude lysate ddPCR). The protocol optimisation is elaborated in Chapter 3.

### 2.2.1 DNA Extraction

Genomic DNA from PBMCs and sorted memory T cell subpopulations were extracted using DNeasy Blood and Tissue Kit (Qiagen, Germany) as per manufacturer's instructions. DNA was eluted in 60$\mu$l of nuclease free water (NFW) and stored at –20°C. DNA concentration was measured fluorometrically by Qubit 3.0 (Invitrogen, Thermo Fisher Scientific, Massachusetts, US)

### 2.2.2 Cell lysate preparation

For crude lysate ddPCR, various methods were tried to make the cell lysate compatible with ddPCR as follow:

1) Thermal lysis in NFW. 1000-10,000 cells were resuspended in 10$\mu$l of NFW and boiled for 5' at 99°C on the water bath. 10$\mu$l of ProteinaseK (10mg/ml, Qiagen, Germany) was added in the tube and incubated at 57°C for 30', followed by 99°C for 30'. Next, cells were rapidly cooled on ice and centrifuged for 2' at full speed. The supernatant was used for crude lysate ddPCR.

2) Sonication. For sonication lysis protocol, 1000-10,000 cells were resuspended in 50$\mu$l of NFW and sonicated for 1 cycle of 30sec with Peak Power= 105, Duty factor= 10 and cycle/burst=200.

3) Lysis in buffer 1. Lysis reagents from the Ambion Cell to-Ct® kit (ThermoFisher, US) (henceforth Buffer 1). This kit is designed for a direct qPCR assay, we only used the lysis buffer reagents. The cell lysate was prepared according to the manufacturer's instructions, omitting the DNase DNA degradation step.

4) Lysis in buffer 2. Lysis reagents from the SuperScript™ IV CellsDirect™ cDNA Synthesis Kit (ThermoFisher, US) (henceforth Buffer 2). This kit is designed for direct cDNA preparation from cell lysate, we only used the lysis buffer reagents. The cell lysate was prepared according to the manufacturer's instructions, omitting the DNase DNA degradation step.

Cell lysate prepared using the methods above was used in the crude lysate ddPCR reaction mixture.

### 2.2.3 Cell lysate viscosity breakdown step

The cell lysate made with buffer 1 and buffer 2 then ran through the viscosity breakdown step to reduce the viscosity of lysate. Briefly, the cell lysate was heated on a thermocycler at 65°C for 1', 96°C for 2', 65°C for 4', 96°C for 1', 65°C for 1' and 96°C for 30 sec. Tubes were spun down for 1' and cooled at RT before proceeding to droplet generation.

### 2.2.4 ddPCR reaction mixture preparation

In each ddPCR reaction, two probes were used: a FAM labeled TRECs and the housekeeping gene ribonuclease P/MRP subunit p3 (RPP30) labeled with HEX. The sequences of primers and probe used for TRECs are: Forward primer 5'-CAC ATC CCT TTC AAC CAT GCT-3'; Reverse primer 5'-GCC AGC TGC AGG GTT TAG G-3', Probe Sequence: 5'-ACA CCT CTG GTT TTT GTA AAG GTG CCC ACT-3' with FAM and BQ-1 quencher (Sandgaard et al. 2014). For RPP30, we used the primer probe mix for copy number detection from BioRad.

A 22$\mu$l reaction mixture was prepared comprising 11$\mu$l 2×ddPCR Supermix for probes (no dUTP) (Bio-Rad, Pleasanton, CA, USA), 0.55$\mu$l of TRECs primers (36$\mu$M stock) and probes (10$\mu$M) each, 1.1 $\mu$l of RPP30 copy number detection (Bio-Rad), 1$\mu$l of HindIII-HF restriction enzyme (NEB, UK). The remaining 7.8$\mu$l was adjusted with NFW and extracted DNA for standard ddPCR. Or, for crude lysate ddPCR 7.8$\mu$l of cell lysate was used. For buffer 1, seven replicates were made and for buffer 2, four replicates were made to consume total cell lysate. During data analysis, these replicates were summed so that a total of 140,000 droplets/sample were screened for buffer 1 and 80,000 droplets/sample for buffer 2.

### 2.2.5 ddPCR droplet generation and thermocycler protocol

From 22$\mu$l of ddPCR reaction mixture above, 20$\mu$l was loaded into a droplet cartridge (Bio-Rad, USA) in sample loading wells. 70$\mu$l of droplet oil (Bio-Rad, USA) was loaded in the droplet oil wells. The cartridge was covered with a gasket (Bio-Rad, USA) and placed in the droplet generator (Bio-Rad #186-3002). 40$\mu$l of droplets generated in the cartridge were transferred to a 96-well plate (Bio-Rad, USA) using a multichannel pipette. The plate was sealed using foil in the plate sealer (Bio-Rad, USA). The plate was put on the thermocycler (Bio-Rad, USA) under the following conditions: 10' hold at 95°C, 45 cycles of 94°C for 30s then 59°C for 60s, next step of 98°C for 10' and final hold at 12°C. Amplified droplets were then read in the QX200 Droplet Reader (Bio-Rad, USA). The droplet reader was turned on for 30' before reading the plate.

### 2.2.6 Assay accuracy

For standard ddPCR, a standard curve of five serial dilutions (in 3 replicates) was made using CD3+ T cell DNA diluted with macrophage DNA (macrophages are negative for TRECs). The concentrations are described in table 2.2.

For crude lysate ddPCR using buffer 1 and buffer 2, 100-10,000 cells (depending upon the number of TRECs copies/cell) were used to make two-fold serial dilutions in PBS. Serially diluted cells were then lysed using either buffer 1 or buffer 2.

| Dilutions | T cell DNA (Vol in $\mu$l) | Macrophage DNA (Vol in $\mu$l) |
|---|---|---|
| Dilution 1 | 40 | 0 |
| Dilution 2 | 30 | 10 |
| Dilution 3 | 20 | 20 |
| Dilution 4 | 10 | 30 |
| Dilution 5 | 0 | 40 |

**Table 2.2: Proportion of T cell DNA and macrophage DNA used to make different dilutions.**

### 2.2.7 Limit of Blank

Limit of Blank (LOB) for crude cell lysate ddPCR was calculated using the TRECs copy number concentration that was found in a total of 22 non template controls (NTCs) and 22 monocyte cell line lysate controls (CLCs) (U-937) (gifted by a friend) reactions measured on two different days using the formula: LOB = Mean (copy number blank) + 1.645 × SD(copy number blank)).

### 2.2.8 Limit of Detection, and Limit of Quantification

A standard curve made from PBMCs diluted with U-937 monocyte cell line was used to estimate the Limit of Detection (LOD) and Limit of Quantification (LOQ) of crude lysate ddPCR, respectively. The LOD and LOQ were defined as previously described (Milosevic et al. 2018). Specifically, the LOD was defined as the lowest concentration of TRECs that could be detected with a 95% confidence calculated by the equation: LOD = LOB + 1.645 × SD(the lowest TRECs copy number dilution), While the LOQ was defined as the lowest TRECs copies that could be detected with a coefficient of variation (CV) $\leq$35% (Milosevic et al. 2018).

### 2.2.9 Repeatability of the crude lysate ddPCR assay

To assess the repeatability (intra-assay variation) of crude lysate ddPCR assay, TREC copies/cell were measured in PBMC, n=4, in triplicates. CV% was calculated to assess the repeatability.

### 2.2.10 Droplet volume size estimated by optical microscopy

The average droplet volume was compared for standard and crude lysate ddPCR. Droplet generation and acquisition of the optical microscopy images were performed on the same day. Four wells were randomly selected for both the ddPCR methods from different cartridges. 80-100 droplets/well were measured to get approximately 300 droplets in total.

The droplets were transferred to $\mu$-Slide VI flat uncoated microscopic chamber (IBIDI Germany). To obtain a uniform monolayer of droplets, the slide was held at an angle for a few seconds. An optical microscope (Leica SP8 confocal microscope) with a digital camera was used to image the droplets. Images were recorded under uniform illumination in a bright field imaging mode, with 200x magnification. The 2-D images were analyzed in ImageJ (2.9.0) following an existing procedure described by Pinheiro et al. (2012).

### 2.2.11 Data analysis

The ddPCR data were analysed in QuantaSoft analysis software version 1.7 (Bio-Rad). In each experiment, 3-8 NTCs and CLCs reactions were used to define the threshold that differentiates the positive droplets from negative droplets. The samples with more than 8000 droplets/well were used for the analysis. The copy number concentration (copies/$\mu$l) was calculated using the formula:

Concentration = -ln (N(neg)/N)/Vdroplet),

where N(neg) is number of negative droplets, N is the total droplet and Vdroplet is the volume of a droplet. We used Vdroplet as 0.70nL for our experiments as we determined it using optical microscopy as explained in section 2.2.10. This concentration was multiplied by 22 to get copies/well (as each well had 22$\mu$l reaction). Replicates were summed to calculate TRECs and RPP30 copies/sample (for Buffer 1, copies/well of seven replicates and for Buffer 2, copies/well of four replicates). Linear regression, Spearman's correlation coefficient, Bland Altman analysis and t-test were performed in GraphPad Prism version 9.4.1.

## 2.3 Antigen specific CD8+ T cell

### 2.3.1 Donor information

To optimise an experiment to quantify antigen-specific CD8+ T memory subsets, 11 healthy individuals (age 18-60 years) vaccinated with seasonal flu vaccine were recruited. Extracted DNA from the PBMCs of these samples was sent for HLA typing to Anthony Nolan organisation, UK and the remaining PBMCs were cryopreserved (as explained in section 2.1.2). Among these participants, 5 individuals possessed HLA-A2 genotype and were selected for the subsequent investigation targeting the detection of antigen-specific CD8+ T cell memory subsets. All volunteers signed a consent form and ethical approval for the project has been obtained (EC: 20/SC/0226).

### 2.3.2 Stimulation with peptide

PBMC from HLA-A2+ Flu vaccinated volunteers were thawed and rested for 3hrs at 37°C in U-bottom 96 well plates at $1 \times 10^6$ cells per well. PBMC were then stimulated with 1$\mu$g/mL Flu-M1 peptide GILGFVFTL (JPT Peptide Technologies) for 12hr, 18hr, 24hr, 36hr, 42hr and 48hr at 37°C. PBMCs were pre-labeled with an HLA-A2-Flu-M1–specific pMHC class I pentamer (ProImmune Limited). Paired unstimulated samples, incubated in RPMI1640 media supplemented with FBS and 0.01% DMSO were used as a background control.

### 2.3.3 Inhibition of TCRs and pMHC complexes

To inhibit the interactions between TCRs and pMHC complexes, PBMCs were incubated with mouse anti-human HLA-ABC antibodies (10-100 $\mu$g/mL human, DX17; BD Pharmingen) for 30' at 37°C before stimulation.

### 2.3.4 Flow cytometry

Stimulated and unstimulated cells were stained with the antibody cocktail described in table 2.3. To quantify the antigen-specific memory subpopulations from vaccination studies, a panel containing various activation-induced markers (AIMs) includ-

| Antibody | Clone | Dilution | Supplier |
|---|---|---|---|
| BV510 CD3 | UCHT1 | 1:50 | BD Biosciences |
| Alexa Fluor 647 anti-human CD95 | DX2 | 1:200 | BioLegend |
| BV421 anti-human PD-1 | EH12.2H7 | 1:100 | BioLegend |
| BV785 CD154 | 24-31 | 1:100 | BioLegend |
| PE-Cy7 anti-human CCR7 | G043H7 | 1:100 | BioLegend |
| BB515 anti-human CXCR5 | RF8B2 | 1:100 | BioLegend |
| PeCy5 HLADR | AF405 | 1:25 | BioLegend |
| BUV496 anti-human CD4 | SK3 | 1:50 | BD Biosciences |
| BUV395 anti-human CD25 | 2A3 | 1:50 | BD Biosciences |
| BV605 anti-human CD28 | CD28.2 | 1:50 | BioLegend |
| BV711 anti-human CD137 | 4B4-1 | 1:50 | BioLegend |
| APC/Cy7 anti-human CD19 | SJ25C1 | 1:50 | BioLegend |
| BV650 anti-human CD69 | FN50 | 1:25 | BioLegend |
| PerCP/Cy5.5 anti-human CD45RA | HI100 | 1:25 | BioLegend |
| APC-Cy7 anti-human CD14 | M5E2 | 2:50 | BioLegend |
| PE anti-human OX40 | Ber-ACT35 | 1:50 | BioLegend |
| PE-CF594 anti-human IRF4 | 3E4 | 1:100 | BD Biosciences |
| NovaFlour Yellow CD8 | OKT8 | 1:100 | ThermoFisher |
| Fc Block | 1 | 1:100 | BioLegend |

**Table 2.3: Antibodies used for the experiment aimed to detect antigen-specific CD8+ T cells**

ing OX40, CD154, HLA-DR, CD38, IRF4, CD69 and CD137 along with CD4 and CD8 identity markers were used to stain cells. For intracellular analysis, cells were fixed/permeabilized using a fixation/permeabilization buffer(Invitrogen). Briefly, cells were fixed by adding 200$\mu$l fixation buffer to the cell pellet and incubated for 30' at room temperature. Cells were then washed with 1X 200$\mu$l permeabilization buffer. Next, cells were stained with a titrated amount of fluorochrome attached antibody diluted in permeabilization buffer in the dark for 20' at room temperature and then washed with FACS buffer. Cells were re-suspended in FACS buffer for acquisition. Dead cells were excluded using Live/DeadTM Fixable Near-IR dead cell stain kit (Thermo Fisher Scientific). Samples were acquired using a BD LSR-Fortessa(BD Biosciences, New Jersey, US). Compensation was performed using the UltraComp eBeads(Invitrogen, Thermo Fisher Scientific) as single-stained controls. Individual cell populations were gated using fluorescence minus one (FMO) controls.

### 2.3.5 Data analysis

A comparison of different AIM markers with Flu-specific pentamer+CD8 T cells was made. Analysis of FCS files was done using FlowJo software version 10.6.1 (FlowJo). Data were exported and visualized in R studio (1.4.1106) and GraphPad (version 9.4.1) for statistical analysis.

## 2.4 Tissue distribution of memory subpopulations

### 2.4.1 Donor information and study design

This was an experimental medicine research sub-study of European AIDS Vaccination Initiative (EAVI2020_01) study. In the main study, healthy HIV-negative volunteers were enrolled and given intramuscular injections of an experimental HIV immunogen with liposomal monophosphoryl lipid A (MPLA) (a potent adjuvant) into their chosen deltoid muscle. Subsequent routine visits were conducted to collect blood samples for immunogenicity analysis.

Participants were also given the opportunity to join the lymph node study, requiring an additional visit after receiving the first or second immunogen injection. The EAVI2020_01 study (NCT04046978) received ethical approval from the London – Fulham Research Ethics Committee (18/LO/2196). All the volunteers provided written informed consent to participate in both the primary study and the lymph node study. This study was conducted in collaboration with my co-supervisor Dr. Katrina Pollock.

### 2.4.2 Blood and lymph node samples

Axillary LN samples were taken from the volunteer after vaccination following a physical examination to determine the most appropriate nodes for sampling by ultrasound-guided fine needle aspiration (US-guided FNA) technique. Paired peripheral whole blood samples (42 mL) were taken contemporaneously. PBMCs and lymph node cells (LNCs) were extracted from the blood and LN and cryopreserved at -150°C (Day et al. 2022).

| Target | Fluorochrome | Clone | Dilution | Supplier |
|---|---|---|---|---|
| Dead cells | eFluor780 | - | 1:1000 | Thermo |
| CD45RA | PE-Dazzle | HI100 | 1:25 | Biolegend |
| CD3 | AF700 | HIT3a | 1:50 | Biolegend |
| CD4 | BUV496 | SK3 | 1:33 | BD Biosciences |
| CD8 | BUV395 | RPA-T8 | 1:33 | BD Biosciences |
| CXCR5 | BB515 | RF8B2 | 1:40 | BD Biosciences |
| CCR7 | BV421 | G043H7 | 1:50 | Biolegend |
| PD-1 | BV650 | EH12.2H7 | 1:100 | Biolegend |
| CD19 | PerCPCy5.5 | HIB19 | 1:50 | Biolegend |
| CD20 | BV605 | 2H7 | 1:50 | Biolegend |
| CD27 | PE | M-T271 | 1:100 | Biolegend |
| CD21 | PE-Cy7 | Bu32 | 1:100 | Biolegend |
| IgD | BV785 | IA6-2 | 1:20 | Biolegend |
| CD14 | V500 | M5E2 | 1:100 | BD Biosciences |
| CD38 | APC | HIT2 | 1:50 | Biolegend |
| CD71 | BV711 | M-A712 | 1:50 | BD Biosciences |

**Table 2.4: Antibody cocktail 1 for phenotyping different immune cells from LNC and PBMC**

### 2.4.3 Study Immunogen

Participants were administered either one or all of three developed Mosaic HIV envelope glycoprotein immunogens named Mos3.1, Mos3.2, or Mos3.3 (Day et al. 2022). These engineered immunogens replicate the structure of natural HIV-1 viral trimers, composed of gp120 and g41, and have been adapted to create the soluble molecule gp140 (Day et al. 2022).

These model immunogens were manufactured by Polymun following current Good Manufacturing Practice (cGMP) guidelines. They were administered alongside an adjuvant - the liposomal version of the TLR-4 agonist MPLA, also manufactured by Polymun (Day et al. 2022).

### 2.4.4 Cellular subset phenotyping

For phenotyping different memory populations from PBMCs and LNCs, cells were stained in FACS buffer using a pre-optimized cocktail of fluorochrome-conjugated antibodies to identify different immune cell subtypes using flow cytometry (table 2.4). The cocktail was designed for the identification of CD14+ monocytes, CD4 and CD8+ T cell memory subsets, B cell subsets and Tfh and cTfh. Cells

| Target | Fluorochrome | Clone | Dilution | Manufacturer |
|---|---|---|---|---|
| Dead cells | eFluor506 | - | 1:500 | Thermo |
| CD45RA | PE-Dazzle | HI100 | 1:66 | Biolegend |
| CD3 | BUV395 | UCHT1 | 1:33 | BD |
| CD4 | BUV496 | SK3 | 1:33 | BD |
| CD8 | V500 | RPA-T8 | 1:100 | BD |
| CD14 | V500 | M5E2 | 1:100 | BD |
| CD19 | V500 | HIB19 | 1:100 | BD |
| CXCR5 | BB515 | RF8B2 | 1:40 | BD |
| OX40 | APC | Ber-ACT35 (ACT35) | 1:40 | Biolegend |
| PD-1 | BV421 | EH12.2H7 | 1:100 | Biolegend |
| CD25 | APC-Fire | BC96 | 1:25 | Biolegend |
| CD69 | BV650 | FN50 | 1:100 | Biolegend |
| CD154 | PE | TRAP1 | 1:25 | BD |
| PD-L1 | PE-Cy7 | 29E.2A3 | 1:40 | Biolegend |
| IRF4 | PerCP-Cy5.5 | IRF4.3E4 | 1:33 | Biolegend |

**Table 2.5: Antibody cocktail 2 for detection of activated CD8+ and CD4+ T cells following 18hr stimulation**

were resuspended in fixation buffer (eBioscience, Thermo Fisher Scientific, US) and events were acquired within 18 hours on a BD LSRFortessa (BD Biosciences, US) (Day et al. 2022).

To phenotype activated cells, PBMCs and LNCs (1 million cells/well) were stimulated for 18 hours at 37°C with various stimulation conditions - media only, EAVI Mosaic peptide pool (0.5 µg/mL) and staphylococcal enterotoxin B (SEB) (Sigma-Aldrich, St. Louis, MO; at 1µg/mL). After antigen stimulation, cells were stained with fixable viability dye eFluor506 (eBioscience, CA) and antibody cocktail 2 (table 2.5). Cells were resuspended in Fixation buffer (eBioscience, CA) and permeabilized before intracellular staining for IRF-4 PerCP Cy5.5 (IRF4.3E4; BioLegend) prior to flow cytometry analysis measured on a BD Fortessa (BD Bio- sciences, US).

### 2.4.5 Detection of antigen-specific CD8+T cells - CD137IRF4 assay

The cryopreserved PBMCs and LNCs were thawed and reconstituted in 10% human assay buffer (10% human serum (Sigma-Aldrich, St. Louis, MO) in RPMI1640 media) at a concentration of 5 million cells/mL. Cells were rested for 3 hours at 37°C, 5% CO2. After resting, 1$\mu$l of CD40 blocking antibody (0.5 $\mu$g/mL) (Miltenyi

| Surface stain | Clone | No of samples | Total volume |
|---|---|---|---|
| Alexa Fluor 647 anti-human CD95 | DX2 | 1:200 | BioLegend |
| BV785 anti-human CD3 | SK | 1:100 | BioLegend |
| BV421 anti-human PD-1 | EH12.2H7 | 1:100 | BioLegend |
| PE-Cy7 anti-human CCR7 | G043H7 | 1:100 | BioLegend |
| BB515 anti-human CXCR5 | RF8B2 | 1:100 | BioLegend |
| BUV496 anti-human CD4 | SK3 | 1:50 | BD Biosciences |
| BUV395 anti-human CD8 | RPA-T8 | 1:50 | BD Biosciences |
| BV605 anti-human CD28 | CD28.2 | 1:50 | BioLegend |
| BV711 anti-human CD137 | 4B4-1 | 1:50 | BioLegend |
| APC/Cy7 anti-human CD19 | SJ25C1 | 1:50 | BioLegend |
| BV650 anti-human CD69 | FN50 | 1:25 | BioLegend |
| PerCP/Cy5.5 anti-human CD45RA | HI100 | 1:25 | BioLegend |
| APC-Cy7 anti-human CD14 | M5E2 | 2:50 | BioLegend |
| PE anti-human CD154 | 24-31 | 1:50 | BioLegend |
| PE-CF594 anti-human IRF4 | 3E4 | 1:100 | BD Biosciences |
| Fc Block | 1 | 1:100 | BioLegend |

**Table 2.6: Antibodies used for the IRF4-CD137 experiment aimed to detect antigen-specific CD8+ T cells**

Biotech, Germany) and CXCR5-BB515 (Clone RF8B2; BD Biosciences, San Diego, CA) were added to the resting cells for a 20' incubation at 37°C. Cells were then stimulated for 18 hours at 37°C with various stimulation conditions - media only, EAVI Mosaic peptide pool (0.5 µg/mL) and SEB(Sigma-Aldrich, St. Louis, MO; at 1µg/mL). After antigen stimulation, cells were stained with NIR viability dye, and flurochrome attached antibodies listed in table 2.6. Cells were then resuspended in fixation buffer (eBioscience, CA) and permeabilized before intracellular staining for IRF-4 prior to flow cytometry analysis measured on a BD Fortessa (BD Biosciences, US).

### 2.4.6 Data analysis

Analysis was performed using FlowJo software v10.6. Unsupervised analysis was conducted using the t-SNE Plugin. Data were cleaned by gating on live singlets before concatenation of the combined files. The subsequent t-distributed Stochastic Neighbor Embedding (t-SNE) was conducted using FlowJo with 1000 iterations and a perplexity of 30. Continuous variables were summarized using the median and interquartile range (IQR) and were compared using a two-sided Mann-Whitney U test using GraphPad Prism V8/9. A p-value of $< 0.05$ was significant.

## 2.5 HIV clinical trial vaccination studies

### 2.5.1 Donor information and Study design

Samples from various HIV clinical trial vaccination studies i.e. Combined skin and muscle vaccination (CUTHIVAC) and International AIDS Vaccine Initiative (IAVI) - B001 and S001 were used to estimate the relationship between the frequency of antigen-specific Tscm cells generated following the vaccination and the longevity of memory.

CUTHIVAC002 (ClinicalTrials.gov: NCT02075983) was a randomised single-site, phase 1 clinical trial in 30 healthy HIV-negative volunteers aged 18–45 years vaccinated with GTU®MultiHIV B clade DNA vaccine(Haidari et al. 2017).

IAVI-B001 (ClinicalTrials.gov:NCT00851383) was a phase I clinical trial in healthy HIV-uninfected adults aged 18–50 years immunized with the HIV trial vaccine. This trial followed a randomized, double-blind, dose-escalation approach and included a placebo control group. The vaccine under investigation consisted of two recombinant adenovirus serotype 35 (Ad35) vectors, each carrying the essential HIV antigens gag, RT, int, nef (Ad35-GRIN), and env (Ad35-ENV) (Trial Registration: ClinicalTrials.gov NCT00851383, IAVI B001).

IAVI-S001 (Clinical Trials Registration: NCT01705990) was a multicenter, randomized, placebo-controlled, dose-escalation trial in 65 healthy adults ages 19-45 years. This trial focused on a replication-competent Sendai virus (SeV)-vectored HIV-1 vaccine administered intranasally, either alone or as part of a heterologous prime-boost regimen with a nonreplicating adenovirus vaccine (Nyombayire et al. 2017).

For CUTHIVAC: We received 18 spare samples from the main study at 22 weeks, 24 weeks and 44 weeks after vaccination (Haidari et al. 2017).

For B001: We received 20 spare samples from the main study at 2 weeks, 14 weeks and 48 wks post-boost (Keefer et al. 2012).

For S001: We received 20 spare samples from the main study at 2 wks, 16 wks and 48 wks post-boost (Nyombayire et al. 2017).

### 2.5.2 Detection of antigen-specific T cells

PBMCs were thawed and stimulated with the peptide construct similar to the vaccine (0.5 µg/mL). The protocol for this experiment is the same as described above in section 2.4.5.

### 2.5.3 Data analysis

Analysis was performed using FlowJo software v10.6. The rate of decay of antigen-specific memory was calculated from the slope of linear regression analysis between the early timepoint and the last time point following boost in R studio (1.4.1106). Correlation between the rate of decay of memory and frequency of antigen-specific Tscm cells was made in GraphPad Prism V8/9.

## 2.6 RNAseq experiment

### 2.6.1 Cell sorting

To perform the RNA sequencing experiment, memory subpopulations (Tscm subpopulations, Tnaive, Tcm, Tem and Temra) from 12 healthy individuals were sorted in FACSAria III (BD Biosciences) with high purity. Sorted T cell subsets were cultured in RPMI 1640 medium (Thermo Fisher Scientific) supplemented with 10% FBS (heat-inactivated, Gibco), 1% penicillin-streptomycin and 2mM L-glutamine (Sigma-Aldrich, Missouri, US). To evaluate the functional profile of memory subpopulations, sorted CD8+ memory T cell subsets were stimulated for 12hrs with plate-bound $\alpha$CD3 (2$\mu$g/mL) and soluble $\alpha$CD28(1$\mu$g/ml) at 37°C. The plates were pre-coated with $\alpha$-CD3 for 2h at 37°C. Stimulated cells were removed from stimulated and re-suspended in 200$\mu$L of RLT buffer (Qiagen, Germany) supplemented with 0.01% $\beta$-mercaptoethanol ($\beta$ME, Sigma-Aldrich).

### 2.6.2 RNA isolation

RNA extraction was performed utilizing the RNeasy Micro Plus Kit (Qiagen) by the manufacturer's instructions, as detailed in Appendix D of the Qiagen RNeasy handbook. The quality and quantity of the isolated RNA were assessed using the

Agilent RNA 6000 Pico Kit (Agilent Technologies) following the manufacturer's protocols. Subsequently, the RNA samples were preserved at -80 °C until they were ready for further processing.

### 2.6.3 RNAseq experiment and analysis

RNA sequencing was conducted at the Oxford Genomics Centre, where polyA-enriched, strand-specific libraries were generated using the NEBNext Ultra II Directional RNA Library Prep Kits (Illumina). We are currently analyzing this data.

# Chapter 3

# Optimizing the Crude Lysate ddPCR protocol for rare gene targets in rare cells

## 3.1 Introduction

As previously discussed in section 1.6.3, the quantification of TRECs is a highly effective approach for tracing the cellular division history of T cells. Commonly used method for TRECs quantification includes quantitative Polymerase Chain Reaction (qPCR) or ddPCR (Vidal-Folch et al. 2017, Tessitore et al. 2017, Gerstel-Thompson et al. 2010, Sottini et al. 2014). While these methods excel in measuring TRECs from blood and PBMCs, however, quantification of TRECs from low frequency memory T subpopulations e.g. Tscm (which constitute 2-4% of the total CD4+ and CD8+ T cell population in blood (Gattinoni et al. 2011, Lugli 2013)) or antigen-specific T cells (in absence of acute infection, one cell within 100 to $10^5$ T cells (Bacher & Scheffold 2013)), are problematic for two reasons: the target gene (TREC) is rare and the starting cell numbers are low. To address this challenge, we developed a highly sensitive ddPCR method called crude lysates ddPCR.

Before delving into the advancements achieved in this chapter, it's essential to establish a foundational understanding of ddPCR. As a powerful molecular biology technique, ddPCR is designed to provide absolute quantification of target genes using input nucleic acid concentration ranging from nM to pM, offering high precision

and sensitivity (Pinheiro et al. 2012). It is a form of digital PCR (dPCR), that uses water-oil emulsion droplets to partition the sample into many small partitions, each of which undergoes PCR amplification (Pinheiro et al. 2012). Poisson statistics is used to determine the absolute quantity of a target sequence in a sample based on the number of partitions in which the sequence is detected (Pinheiro et al. 2012). Unlike qPCR, ddPCR doesn't require a standard curve for absolute quantification, providing a significant advantage (Maheshwari et al. 2017, Miliaras 2014). Additionally, ddPCR lends itself not only to nucleic acid quantification but can also be utilized for analysis of gene expression (Taylor et al. 2017, Mehling et al. 2015), epigenetics (Petit et al. 2023, Manco & Dias 2022), copy number variation (Woon et al. 2022, Bao et al. 2022), rare mutations (Hashimoto et al. 2023, Ahn et al. 2022), linkage studies (Hou & Hu 2022, Holmgren et al. 2022), and quantification of next-generation sequencing libraries (Hoerres et al. 2023, Aigrain et al. 2016).

Despite these advances in ddPCR technology, it still faces challenges when dealing with limited starting material, as DNA extraction from a small number of cells (less than 1000) often results in target loss. There was a clear need for a high-throughput, sensitive, and accurate assay capable of detecting rare targets from limited clinical samples while minimizing target loss during nucleic acid extraction.

The optimisation of a high-throughput ddPCR protocol directly from cellular lysate holds immense promise across various fields of molecular biology. By eliminating the intermediate step of nucleic acid extraction, we've streamlined workflow and improved target quantification precision and efficiency. This advancement has wide-ranging implications, particularly in quantifying rare events such as circulating tumor cells, fetal DNA in maternal plasma, rare genetic mutations, and the analysis of precious clinical samples where quantity is limited but precision is crucial.

In this context, we first optimised the standard ddPCR protocol using DNA extracted from PBMCs and macrophages. In this step, we also determined the fundamental parameters such as annealing temperature and cycling protocol that would later be applied to the crude lysate ddPCR. Then, for crude lysate ddPCR, we explored various methods to make cell lysate compatible with ddPCR. We compared the results obtained from optimised crude lysate ddPCR with the standard method. We also conducted various technical assessments such as accuracy, LOD,

LOQ, repeatability, and droplet size variations. Additionally, we investigated the potential application of this method to fixed and permeabilized cells. Our approach, which eliminates the DNA extraction step and utilizes the entire cell lysate, provides accurate, sensitive, and precise measures of quantifying rare gene content in small, limited samples.

## 3.2 Results

### 3.2.1 Standardisation and validation of standard ddPCR

In this section, results for the optimisation and validation of standard ddPCR are presented, aiming at quantifying TREC copies/cell from DNA isolated from the PBMCs of healthy donors. The optimisation process focused on refining critical parameters, such as annealing temperature and cycling protocol, to enhance the precision and efficiency of standard ddPCR. Additionally, we compared the results obtained using standard ddPCR with those from the well-established qPCR method to measure the accuracy of standard ddPCR.

#### 3.2.1.1 Optimisation of annealing temperature

To optimise annealing temperature for TRECs and RPP30 primers and probes, we performed a gradient temperature experiment with temperatures ranging from 58°C to 62°C. At temperatures of 62°C, 61°C and 60°C, a clear separation was observed between TRECs-positive droplets (Figure 3.1a, top blue dots) from TRECs-negative droplets (Figure 3.1a grey dots) with minimum rain in between them (Figure 3.1a). However, the separation of RPP30-positive droplets (Figure 3.1a, green dots) from RPP30-negative (Figure 3.1a, grey dots) was less distinct at these temperatures as compared to 59°C. The best separation of both TRECs and RPP30 positives, with minimum rain in between was observed at temperature 59°C (Figure 3.1a). NTCs used in this experiment were clear, suggesting no contamination or background signal (Figure 3.1a). Consequently, 59°C was selected as the optimal annealing temperature for this ddPCR experiment. This optimisation process ensured that the standard ddPCR method was finely tuned for precise quantification of TRECs, setting the stage for further experimentation analysis.

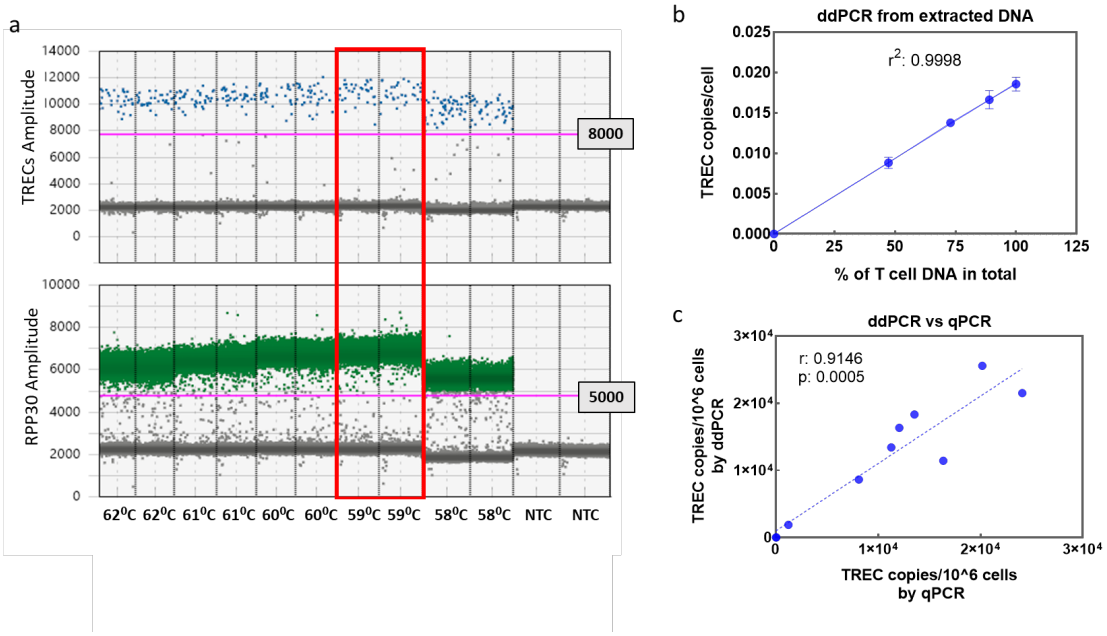



**Figure 3.1**: **Standardisation and validation of standard ddPCR**(a) Gradient temperature experiment was performed on DNA samples isolated from the blood of a healthy individual and run in duplicates. The upper part shows a 1-D dot plot displaying the results for the amplitude of TRECs-positive blue droplets, while the bottom part presents the results for RPP30, a housekeeping gene, in green droplets. The pink horizontal line represents the threshold for positive droplets, and the red squares mark the optimal temperature selected based on the best separation and minimum rain. (b) A standard curve was made by diluting T-cell DNA with macrophage DNA to assess the linearity of the assay. Samples were run in duplicates, and linear regression was performed to calculate a coefficient of determination $r^2$. (c) TREC copies/million cells were measured in n=10 DNA samples using both qPCR and ddPCR. The results were compared using Spearman coefficient analysis (rs=0.91, p=0.0005)

#### 3.2.1.2 Assessment of assay linearity using standard curve

Checking the linearity of the assay using a standard curve is a crucial step in assay validation. Linearity assessment ensures that the assay output is directly proportional to the input concentration of the target molecule and establishes the assay's quantitative reliability.

To investigate the assay linearity of the standard ddPCR experiment, we constructed a standard curve with five dilutions made by diluting CD3+ T cell DNA in macrophage DNA (as macrophages do not have TRECs). Concentrations of the dilutions are presented in table 2.2. Replicates of these dilutions were run to quantify TREC copies/cell. NTCs were also included in the experiment to check for any contamination or background signal. A linear regression curve was made by plotting

TREC copies/cell measured by ddPCR against the percentage of T cell DNA in the reaction mixture and a straight line fitted by linear regression (Figure 3.1b). The straight line fitted the data had a coefficient of determination (r2) of 0.99, indicating good agreement between the TREC copies/cell and the concentration of T cell DNA present in the sample.

#### 3.2.1.3 Accuracy evaluation: ddPCR versus qPCR

Furthermore, we assessed the accuracy of the standard ddPCR for TRECs quantification by conducting a comparative analysis with qPCR on the same samples. We did this experiment in collaboration with Dr Adam Stuart from GOS Hospital, London who routinely employs qPCR to quantify TRECs in blood for diagnosing immunodeficiency diseases, utilizing a well-established technique. In this collaborative exchange, we shared DNA samples, and independently, both parties quantified TREC copies, with Dr. Stuart's team using qPCR and we utilizing the ddPCR assay. The results revealed a strong correlation between TREC copies/million cells measured by the standard ddPCR and the qPCR assays (n=10, rs=0.91) (Figure 3.1c).

These findings confirmed that TREC copies measured by the standard ddPCR method are accurate and significantly comparable with the well-established qPCR method. Henceforth, this standard ddPCR assay had been adopted as a benchmark for our novel crude lysate ddPCR assay.

### 3.2.2 Standardisation and Validation of Crude lysate ddPCR

The optimisation of crude lysate ddPCR presented several challenges, primarily centered around the development of a cell lysate method compatible with ddPCR. Different approaches were explored to prepare cell lysate suitable for ddPCR, as discussed in the next section. Subsequently, a comprehensive technical assessment was conducted to evaluate the accuracy and reliability of crude lysate ddPCR. Notably, each experiment included at least triplicate NTCs and CLCs. The CLCs were prepared by lysing the cells of the U937 monocyte cell line, which lack TRECs but have housekeeping gene, allowing for the monitoring and quantification of any potential background signals. Accuracy was assessed by comparing the results of crude lysate ddPCR with those of the standard ddPCR.

#### 3.2.2.1 Evaluation of different methods for preparing the crude lysate

Various methods were tried to make the cell lysates compatible with ddPCR. Initially, we tried a thermal lysis method (explained in section 2.2.2), droplets were formed and TREC copies/cell were quantified. In the results, the recovery rate of cells, especially for 2000 input cells, was unsatisfactory (Figure 3.2a). Given our interest in quantifying TRECs from rare memory subpopulations, a maximum input of 2,000 cells was desired. Subsequently, we explored the sonication method (explained in section 2.2.2), which only yielded a recovery rate of 11.12% for 2000 cells (Figure 3.2b). Additionally, we experimented with the lysis buffers from DNA/RNA extraction kits (Qiagen), but these buffers, containing detergent or other harsh chemicals, hindered the droplet formation (data not presented).

Our pursuit led us to test lysis reagents from the Ambion Cell to-Ct® kit (ThermoFisher) (henceforth Buffer 1) (explained in section 2.2.2, which showed improvements but still faced recovery rate challenges and high standard deviations among replicates (data not shown). To solve this issue, we employed several strategies:

1) Addition of additional DNA polymerase and/or restriction enzyme to the reaction mixture to enhance the amplification efficiency

2) Tried different cell lysate volumes in experiments to make the cell lysates in an attempt to enhance the cell lysis

3) Increased the droplet oil volume from 70$\mu$l to 80$\mu$l to deal with viscosity

Out of these strategies, only the third was proven effective, suggesting that the viscosity of the crude lysate was impeding target gene amplification. The high viscosity of the reaction mixture caused droplets to adhere to the well's walls, reducing droplet counts to less than 10,000 (Figure 3.2c). Simply increasing the droplet oil volume was insufficient, as its mechanism for addressing viscosity was unclear. Instead, we implemented a viscosity breakdown step as discussed in section 2.2.3, and as a result, we achieved over 90% recovery for lysate prepared using buffer1 (Figure 3.2b).

We also explored other lysis reagents from the SuperScript™ IV CellsDirect™ cDNA Synthesis Kit (ThermoFisher) (henceforth Buffer 2) (explained in section 2.2.2),

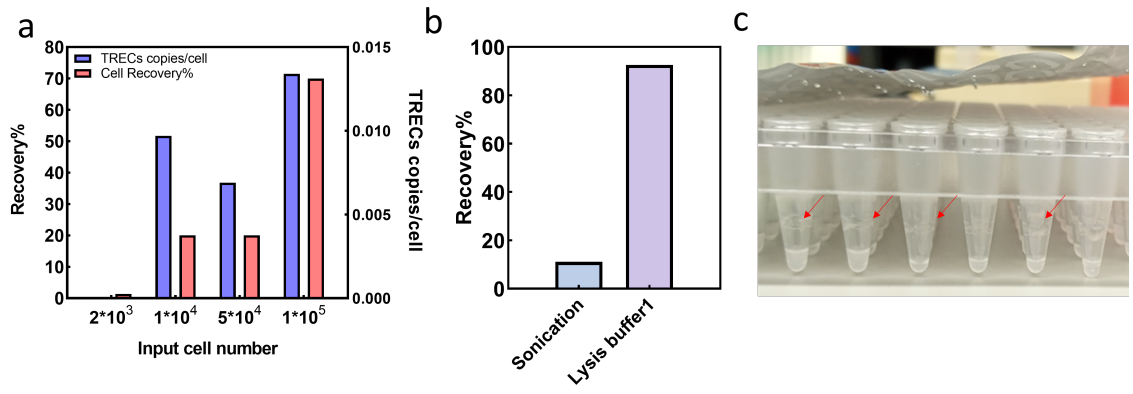



**Figure 3.2**: **Evaluation of different methods for preparing the crude lysate** (a) Graph summarizing the results obtained using thermal lysis for making cell lysates. The x-axis represents the input cell number used to make the cell lysates, while the left y-axis shows Recover% calculated as (output cell number estimated from RPP30 copies/input cell number)*100 (pink bars). The right y-axis represents TREC copies/cell (violet bars). (b) Column plot illustrating the Recovery% achieved by lysing 2000 input cells using sonication (blue column) and lysis buffer 1 (purple column) with viscosity breakdown step for preparing cell lysates. (c) Visualization of a 96-well plate after running samples in the ddPCR droplet reader, displaying droplets sticking to the walls of the wells (red arrows).

which demonstrated compatibility with ddPCR and a similar recover rate to buffer1 (data not shown here). Consequently, we proceeded with both lysis buffers - buffer 1 and buffer 2, incorporating the viscosity breakdown step in the preparation step of cell lysates for crude lysate ddPCR.

#### 3.2.2.2 Assay Linearity using Buffer 1 and Buffer2

We evaluated the linearity of the crude lysate ddPCR assay, prepared using both buffer 1 and buffer 2 and compared it with the standard ddPCR. To achieve this, we prepared standard curves by serially diluting PBMCs in PBS, subsequently lysing the diluted cells using either lysis buffer 1 or buffer 2, covering a range of 2-64 TREC copies/dilution (as determined by the standard ddPCR). These linearity assessment experiments for lysis buffer 1 or buffer2 were performed on two separate days using distinct PBMC samples, each with varying TREC copies per cell. The housekeeping gene RPP30 served as an internal control for quantifying cell numbers.

In the case of crude lysate ddPCR with Buffer 1, we established a linear relationship between the number of cells per reaction, estimated from RPP30, and the

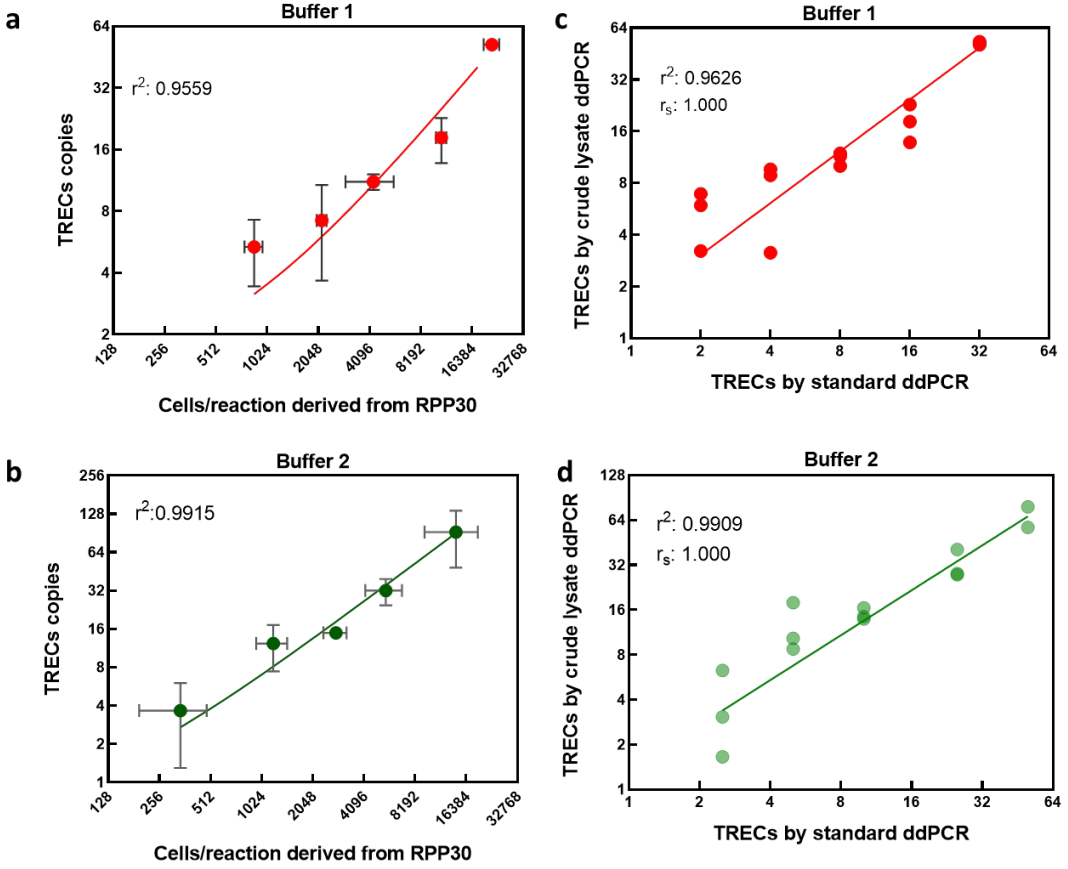



**Figure 3.3**: **Linearity and accuracy assessment of crude lysate ddPCR using lysis buffer 1 and 2.** (a-b) Linear regression analysis performed on the standard curve made by diluting PBMCs in PBS and then preparing crude lysate using lysis buffer 1 (in Red) or buffer 2 (in green). The PBMC samples used for buffer 1 and buffer 2 experiments were distinct, with varying TREC concentrations. (c-d) The accuracy of the assay was estimated by comparing the output TRECs concentration measured by crude lysate ddPCR using either lysis buffer 1 (in red) or buffer 2 (in green) with input TRECs measured using extracted DNA by standard ddPCR. Spearman coefficient analysis was performed showing rs=1 for both assays.

TREC copies. Linear regression analysis yielded an $r^2$ value of 0.95 ($p < 0.001$), indicating good linearity (Figure 3.3a). Furthermore, when we assessed accuracy by comparing it with the standard ddPCR, we observed a strong positive linear relationship and correlation ($r = 1$, $p < 0.01$) between the TREC values estimated using Buffer 1 and the standard ddPCR method (Figure 3.3c). However, the linear regression equation ($Y = 1.513X + 0.5430$) indicated that each unit increase in TREC values estimated by the standard ddPCR corresponds to a 1.513 unit increase in TREC values estimated by crude lysate ddPCR using Buffer 1. Also, it's important to note that Buffer 1 exhibited a systematic bias of overestimation. This bias, as

indicated by the positive intercept of 0.5430, suggests that Buffer 1 tends to produce TREC values higher than those measured by the standard ddPCR method.

Crude lysate ddPCR with Buffer 2 also demonstrated exceptional linearity, with an $r^2$ value >0.99 ($p < 0.001$) (Figure 3.3b). Further comparing the input TRECs estimated by standard ddPCR against the output TRECs estimated by the crude ddPCR, we observed a strong positive linear relationship and correlation ($r = 1$, $p < 0.01$) between the TREC values estimated using Buffer 2 and the standard ddPCR method (Figure 3.3d). The linear regression equation ($Y = 1.298X + 0.6991$) indicates that each unit increase in TREC values estimated by the standard ddPCR corresponds to a 1.298 unit increase in TREC values estimated by Buffer 2. Buffer 2 also exhibited a systematic bias of overestimation with a positive intercept comparable to buffer 1.

By comparing the crude lysate ddPCR assays utilizing these buffers, we found that buffer 2 exhibits a slope (1.298) that is closer to the ideal value of 1 when compared to Buffer 1 (1.513). Additionally, buffer 2 offered practical advantages as it required only 4 replicates to fully screen the total lysate volume, whereas Buffer 1 necessitated 7 replicates for this. This not only rendered buffer 2 a cost-effective choice but also reduced the susceptibility to potential sample handling errors. Consequently, buffer 2 emerges as the preferred choice for our research, and we further investigated the bias in this using actual samples in section 3.2.2.8. Consequently, we selected buffer 2 for preparing cell lysates in our subsequent experiments.

#### 3.2.2.3 Importance of viscosity breakdown protocol

To perform crude lysate ddPCR, we added an innovative step to make the cell lysates more compatible with ddPCR, called a viscosity breakdown step. The presence of intact oligonucleotides in crude cellular lysates elevates lysate viscosity, posing challenges for droplet formation and target amplification (Menacho-Melgar & Lynch 2022).

To assess the impact of a viscosity breakdown (VB) protocol performed on lysed cells before droplet formation, we conducted a comparative analysis between the crude lysate ddPCR using lysate processed with and without the VB protocol (n=5) and also compared with the standard ddPCR. The results are represented in 2-D

dot plots for all the conditions (Fig3.4a). The droplet counts in all conditions were more than 10,000. However, we found significantly higher levels of TREC copies/cell in the samples processed without the VB protocol (mean=0.046 TRECs/cell) compared to those that underwent the VB protocol (mean=0.022) and the standard ddPCR (mean=0.023) (Friedman test, p=0.008; Dunn's multiple comparisons between with VB and without VB protocol, p=0.01) (Fig3.4b). These results suggest that the viscosity of the cell lysates may interfere with the amplification and/or incomplete cell lysis may be responsible for the higher TREC levels observed in samples without the VB protocol. Consequently, we consistently utilized the VB protocol in conducting the crude lysate experiments.

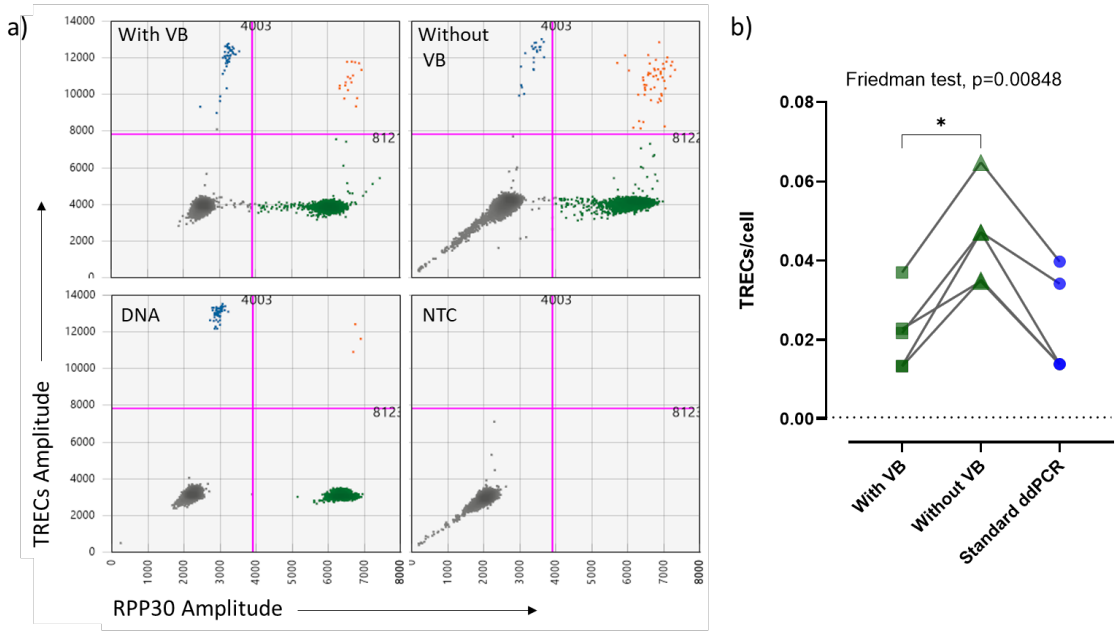



**Figure 3.4**: **Importance of viscosity breakdown step in crude lysate ddPCR.** (a) 2-D dot plot represents the results of crude lysate ddPCR performed on the PBMCs isolated from the blood of 5 healthy individuals, processed with the viscosity breakdown (VB) step (top left) and without the VB step (top right). Additionally, standard ddPCR (bottom left) and NTC (bottom right) were included as controls in this experiment. Blue dots are TRECs single positive, green dots are RPP30 single positive, Orange dots are TREC RPP30 double positive and grey dots are double negative. The pink line represents the threshold. Each dot represents a droplet in ddPCR (b) Pairwise comparisons were made between the TREC copies/cell measured by crude lysate ddPCR with VB (green squares) and without VB (green triangles) and the standard ddPCR (blue dots). Each symbol represents a donor, and pairwise comparison is shown by connecting black lines. Stats: Friedman test with Dunn's multiple comparisons, denoting significance as *<0.05

#### 3.2.2.4 Limit of Blank (LOB)

The estimation of the LOB in ddPCR is essential for establishing a reliable baseline and distinguishing true positive signals from background noise, particularly when the target concentration is low. To determine the LOB, two separate experiments were conducted on different days using NTCs and CLCs, resulting in a total of 22 samples screened.

In both sets of experiments, all NTCs neither expressed a TREC signal nor RPP30 signal (Fig3.5). Likewise, when examining the CLCs all samples were negative for TRECs (Fig3.5), except for a few very high fluorescent positive droplets that appeared along the diagonal in a 2D plot. These outliers were considered artifacts and were consequently excluded from the analysis. Hence, the LOB was determined to be zero.

Furthermore, these results not only establish the absence of nonspecific signals but also underscore the specificity of the TRECs primers and probe employed in the ddPCR assay.

#### 3.2.2.5 Limit of Detection (LOD) and Quantification (LOQ)

Estimating LOD and LOQ is vital for assessing an assay's sensitivity and ensuring reliable detection of low target concentrations, critical for data quality and regulatory compliance. To estimate the LOD and LOQ of crude lysate ddPCR assay, samples of four different TREC concentrations were made by diluting PBMCs (of known TRECs/cell content, estimated by the standard ddPCR), in the monocyte cell line (U-937) to obtain the following concentration: Dil1: 0.01 TRECs/cell (0.016±0.006 TRECs/cell), Dil2: 0.001 TRECs/cell (0.0016±0.0005 TRECs/cell), Dil3: 0.0004 TRECs/cell (0.0006±0.0002 TRECs/cell) and Dil4: 0.0002 TRECs/cell (0.0003±0.0001 TRECs/cell). Diluted cells were lysed in lysis buffer 2 and assayed by the crude lysate ddPCR. All runs were performed in triplicate. In addition, NTCs and CLCs were included as negative controls and DNA samples isolated from the same sample were used as a positive control where TRECs were quantified using the standard ddPCR.

TRECs were successfully detected in all the dilutions. Figure 3.6a displays the 2-D dot plots containing results from all the dilutions (triplicates merged) and the

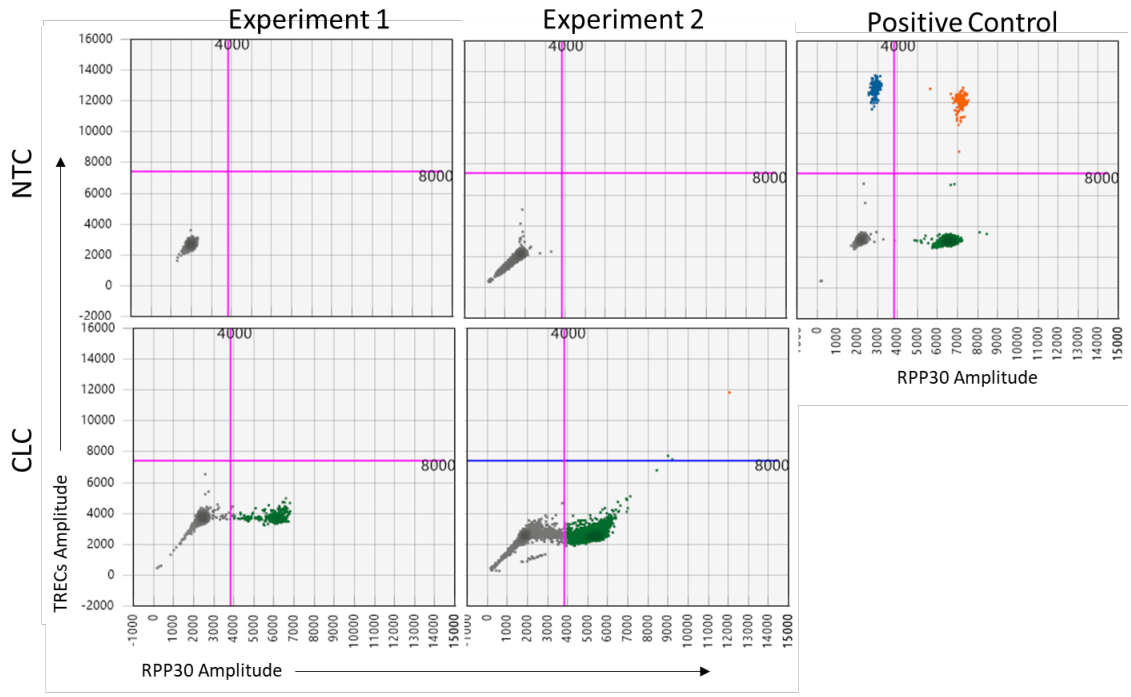



**Figure 3.5**: **Limit of Blank (LOB) of crude lysate ddPCR**. 2-D dot plots illustrate the results obtained from two separate LOB experiments performed on different days. The dot plots represent the merged droplets from all the samples in one run, in total, there were 22 samples for NTCs (top row) and CLCs (bottom row), 11 samples/run. In addition, a DNA sample isolated from PBMCs was run in triplicate by the standard ddPCR used as a positive control. In the dot plots, Blue dots are TRECs single positive, green dots are RPP30 single positive, Orange dots are TREC RPP30 double positive and grey dots are double negative. The pink line represents the threshold. Each dot represents a droplet in ddPCR.

controls (bottom three plots, red). Clearly, TRECs positive droplets (Blue and/or Orange) are present in all the dilutions. However, in Dilution 2, an unusual cluster of double-negative appeared slightly higher diagonally than the typical double-negatives, were excluded from the threshold setting manually.

Since TRECs were detected in all the samples, we selected the lowest dilution, Dil4, to estimate the LOD, calculated to be 0.0001 TRECs/cell (LOD: 0+1.645*0.00007) (Figure 3.6b). The robustness of this detection across all dilution was reaffirmed by 100% hit rate for probit analysis at all the concentration. Therefore, we considered Dil4 with average of 0.0003 TRECs/cell (95% CI 0.00015-0.0005; coefficient of variation (CV) 22%) as LOQ (Figure 3.6b).

To check the accuracy of the assay, a linear regression between input TRECs estimated by the standard ddPCR vs output TRECs estimated by the crude lysate ddPCR demonstrated excellent linearity down to 0.0003 TRECs/cell, $r^2 > 0.99$,

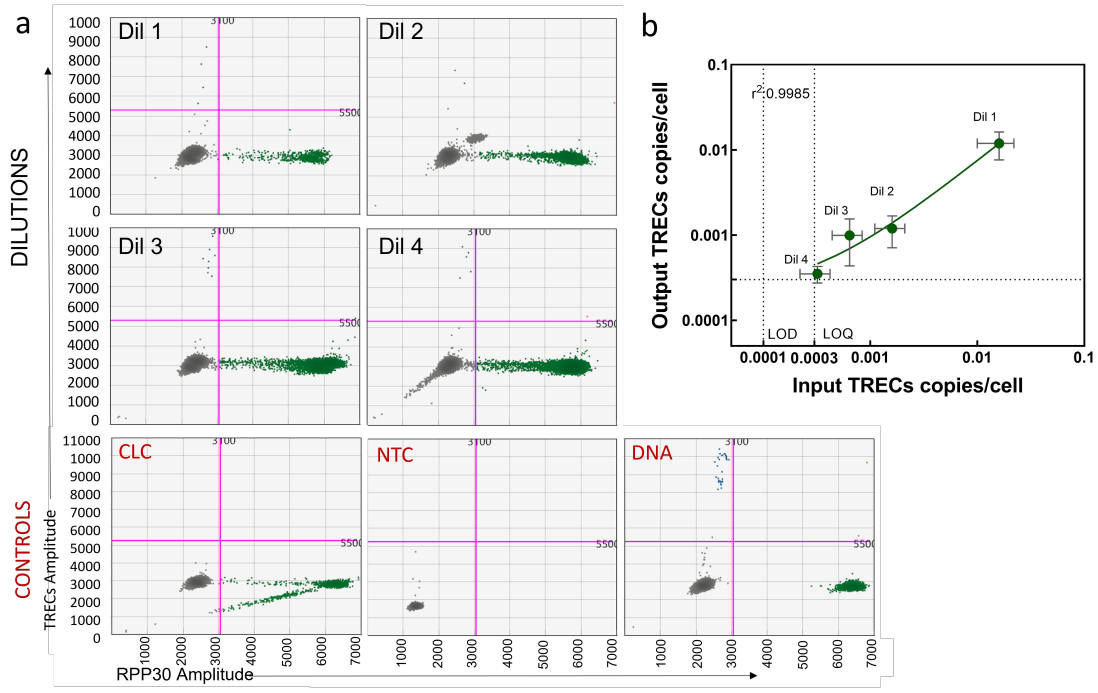



**Figure 3.6**: **Limit of Detection (LOD) and Limit of Quantification (LOQ) of crude lysate ddPCR**. (a) 2-D dot plots depict the results obtained from standard curve samples made by diluting TRECs in monocyte cell line (U937) at concentrations: Dil1: 0.01 TRECs/cell, Dil2: 0.001 TRECs/cell, Dil3: 0.0004 TRECs/cell and Dil4: 0.0002 TRECs/cell. Additional controls, including CLCs, NTCs and DNA controls, are shown in the bottom three plots (labeled in red). The dot plots represent the merged droplets from triplicate dilutions. In the dot plots, blue dots are TRECs single positive, green dots are RPP30 single positive, orange dots are TREC RPP30 double positive and grey dots are double negative. The pink line represents the threshold. Each dot represents a droplet in ddPCR. (b) Linear regression analysis was performed between the average input TREC copies/cell measured by the standard ddPCR(Dil1: 0.016±0.006 TRECs/cell, Dil2: 0.0016±0.0005 TRECs/cell, Dil3: 0.0006±0.0002 TRECs/cell and Dil4: 0.0003±0.0001 TRECs/cell) and the output TREC copies/cell measure by crude lysate ddPCR. The coefficient of determination ($r^2$) was calculated. Each dot represents the mean and the error bars indicate the standard deviation.

$p<0.001$, with good agreement between the two methods ($Y = 0.7286*X + 0.0002274$) (Figure 3.6b).

#### 3.2.2.6 Droplet volume estimation by optical microscopy

Further, our investigation focused on determining whether the cell lysis buffer had any influence on the size or volume of ddPCR droplets. To accomplish this, we conducted an optical microscopy examination to calculate the average droplet volume of ddPCR droplets generated using the crude lysate ddPCR protocol and the standard

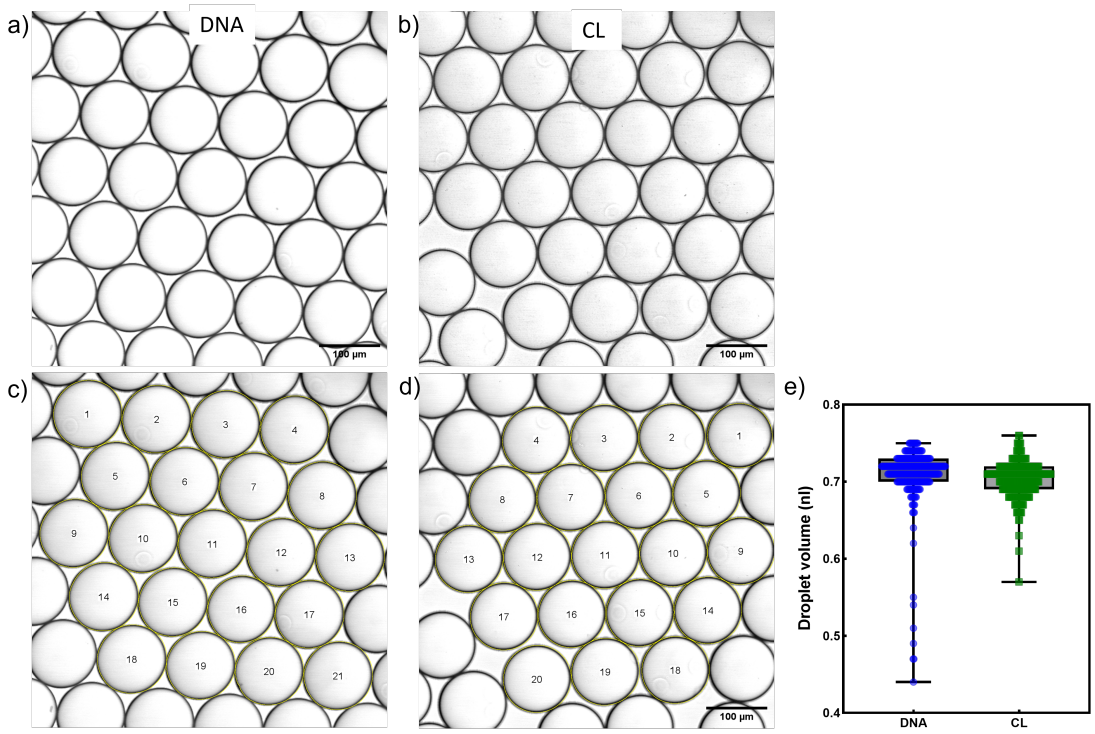



**Figure 3.7**: **Optical microscopy to measure droplet volume**. (a-b) A Monolayer of droplets was generated using extracted DNA and crude lysate (CL) observed under a Leica SP8 Confocal (Germany) optical microscope. In Figures (c) and (d), the image underwent processing using ImageJ software which involved thresholding and analyzing particle size determination. This processing adds yellow boundaries to distinguish individual droplets from one another and from the background. (e) The box-whiskers plot shows the median droplet size of droplets containing extracted DNA (in blue) and CL (in green), with each circle as one droplet.

ddPCR protocol. We screened approx. 300 droplets from 4-5 different wells for each of the protocols. We then compared the average droplet volume of ddPCR droplets generated using extracted DNA with ddPCR droplets generated using crude lysate ddPCR. To ensure the droplet size remained consistent during microscopic examination, all images were captured within a time frame of 30 minutes after droplet generation.

In the 2D image analysis step, we used area equivalent diameter measurements to calculate the diameter of the droplets and subsequently their volume. Figure 3.7 a and b represent the 2-D images captured from the droplets generated using DNA and crude lysate, respectively. Meanwhile, fig 3.7c and d represent the images obtained after conducting image analysis in the ImageJ software (version 2.9.0).

The average droplet volume for DNA droplets was 0.7096 nL (SD 0.037; 95% CI

0.7054-0.7138) and for CL droplets was 0.7034nL (SD 0.022; 95% CI 0.7010-0.7058), suggesting that lysis buffer had no discernible impact on droplet morphology. (3.7e). However, both of these volumes were much smaller than the value of 0.85nL used in QuantaSoft version 1.0.596 to calculate copy number concentrations. Hence, we used 0.70nL as droplet volume in all the analyses to quantify TREC copies/cell.

#### 3.2.2.7 Intra-assay repeatability assessment

Further, to validate the reliability and precision of crude lysate ddPCR, we examined its intra-assay repeatability. It identifies any variations or errors, crucial for quality control and trustworthy data interpretation. For this, TREC copies were quantified from the cell lysates of PBMCs (1000-8000 cells) from 4 healthy human samples. For positive control, DNA extracted from the same cells was also included in the assay. Among these four individuals, three exhibited CV% of TREC copies/reaction less than 20% (Table 3.1). However, one individual, LD8, displayed an outlier in one of the triplicate measurements, which resulted in a CV% above 35%(Table 3.1). This variation in the outlier triplicate may be attributed to the very low droplet count in this sample as compared to other triplicates, possibly due to the technical handling of the sample. On average, the CV% calculated for these four samples was 22.25% (Table 3.1).

| Sample Id | Rep1 | Rep2 | Rep3 | AVG | CV% |
|---|---|---|---|---|---|
| LD8 | 21 | 19 | 9 | 16.33 | 39.36 |
| TD1 | 15 | 12 | 14 | 1.52 | 11.17 |
| TD2 | 33 | 46 | 34 | 38 | 19.21 |
| DPG4 | 110 | 79 | 115 | 101.1457 | 19.25 |
| AVG | | | | | 22.25 |

**Table 3.1: Intra-assay variability (Crude lysate ddPCR)**. Numbers represent TREC copies/reaction

#### 3.2.2.8 Direct comparison of crude lysate ddPCR with the standard ddPCR

A direct comparison of the newly developed crude lysate ddPCR and the standard ddPCR was made by analyzing TREC copies/cells using genuine samples (rather than T cells diluted with macrophages). The samples used were sorted CD8+T

memory subpopulations for which both the ddPCRs were run simultaneously in the same plate over different days for different samples.

Average TREC copies/cell by the standard ddPCR for 17 samples was 0.0092 (range:0.00013-0.043), while for crude lysate ddPCR was 0.0108 (range: 0.00018-0.040) (Figure 3.8a). These distributions were not found to be significantly different (Wilcoxon test, p = 0.31) (Figure 3.8a).

Additionally, we performed a Bland-Altman analysis that resulted in a bias of -0.001635 between the two methods with SD of 0.008337, which indicates that, on average, standard ddPCR tends to slightly underestimate the TREC copies compared to ddPCR directly with cell lysates (Figure 3.8b). The small standard deviation suggests the differences between the methods are relatively consistent and that the level of agreement is relatively high.

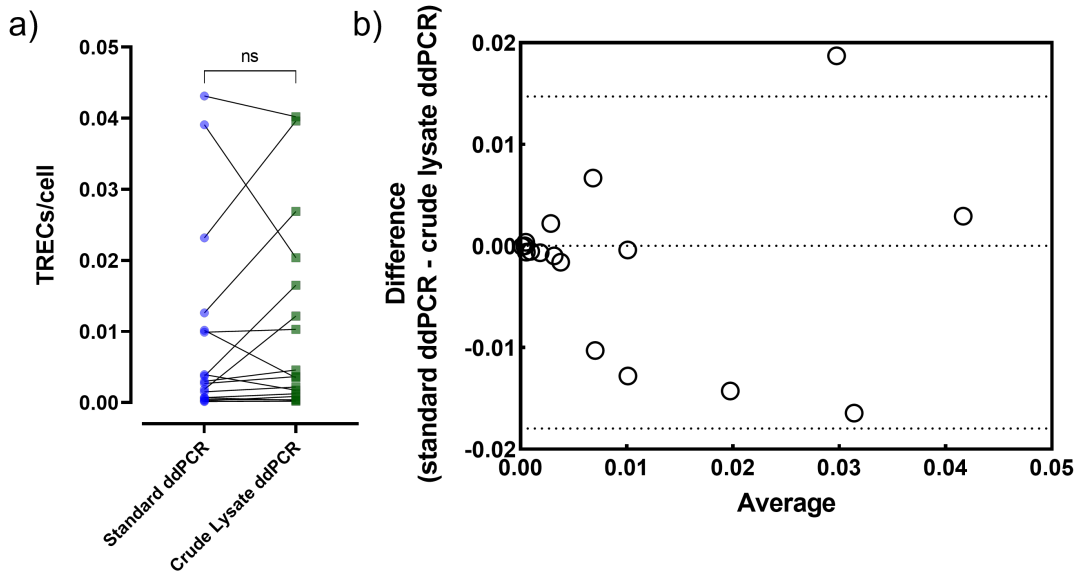



**Figure 3.8**: **Direct comparison of crude lysate ddPCR with the standard ddPCR**. (a) A pairwise comparison between TREC copies/cell detected by the standard ddPCR (in blue circles) and crude lysate ddPCR (in green squares) is plotted. Each symbol represents a donor, and pairwise comparison is shown by connecting black lines. Stats: Wilcoxon test, denoting significance as ns=non significant, *<0.05. (e) The Bland-Altman analysis is plotted as a scatter diagram with the TREC copies/cell differences between the two methods on the y-axis and the averages of these two measurements on the x-axis. Horizontal lines are drawn at the mean difference and at the limits of agreement.

#### 3.2.2.9 Impact of cell fixation and permablization

While performing the experiments on the sorted T cells, the necessity of expanding this assay for paraformaldehyde fixed and permabilised cells (fixed/permeabilized) was realised. Extracting DNA from fixed/permeabilized cells is challenging due to the cross-linking of proteins and nucleic acid caused by the fixing process. Hence, a small experiment was performed to check the reliability of the crude lysate ddPCR assay for fixed/permeabilized cells. For this, six different samples of fixed/permeabilized cells were compared with paired non-fixed/permeabilized cells and extracted DNA (standard ddPCR) samples.

Indeed, cell lysis buffer 2 demonstrated its remarkable ability to generate lysate from fixed/permeabilized cells that was fully compatible with ddPCR. More than 10,000 droplets were observed in these samples, and, most importantly, there was a clear separation between TRECs-positive and negative droplets with minimum rain in between (Figure 3.9a).

Our results revealed that the TREC count was not significantly different between the three different groups (p=0.4) with an average of 0.014 TREC copies/cell for fixed/permeabilized cells, 0.022 TREC copies/cell for non-fixed/permeabilized cells and mean=0.017 TREC copies/cell for standard ddPCR, however by eye the TRECs count was lower in fixed/permeabilized cells as compared to non-fixed/permeabilized cells for the three samples with a higher TREC concentration (Figure 3.9b). Additional research is required to increase the statistical significance of the findings, but there is potential for utilizing ddPCR directly from cell lysates in the case of fixed/permeabilized cells.

We suggest that additional optimisation is conducted before using this assay on fixed/permeabilized cells.

#### 3.2.2.10 Troubleshooting of crude lysate ddPCR

A significant portion of my Ph.D. research was dedicated to troubleshooting the crude lysate ddPCR assay, and I would like to share two key challenges I encountered to benefit future researchers using this protocol or similar ones.

First, I observed unusual droplet patterns in 2-D dot plots, as shown in Figure 3.10a. These patterns appeared suddenly in crude lysate ddPCR with lysis

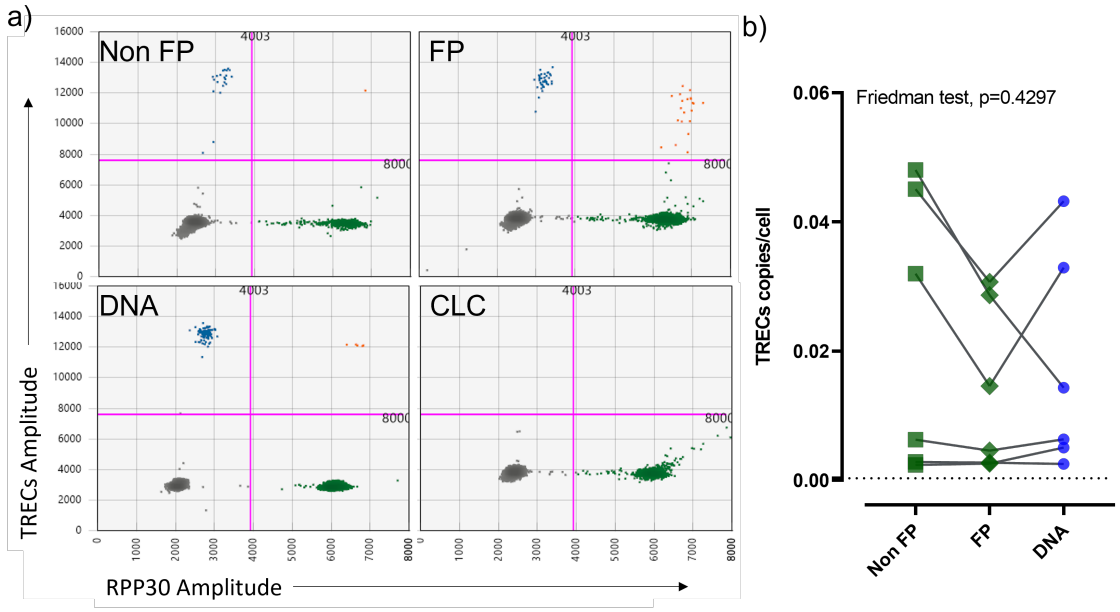



**Figure 3.9**: **Crude lysate ddPCR on fixed and permeabilized (FP) cells**. (a) The 2-D dot plots display TRECs and/or RPP30 positive droplets detected from paired FP, non FP and extracted DNA samples, representation of only one sample. Additionally, CLC, a negative control, is also shown. In the dot plots, blue dots are TRECs single positive, green dots are RPP30 single positive, orange dots are TREC RPP30 double positive and grey dots are double negative. The pink line represents the threshold. Each dot represents a droplet in ddPCR.(b) A pairwise comparison of TREC copies/cells obtained from FP (in green diamonds), non FP (in green squares) and extracted DNA (in blue circles) samples was conducted. Each symbol represents a donor, and pairwise comparison is shown by connecting black lines. Stats: Friedman test with Dunn's multiple comparisons, denoting significance as *<0.05.

buffer 1 and buffer 2 but were absent in the NTCs and positive controls. Despite not having made any changes to the protocol, I spent two weeks grappling with this issue before realizing that I had been storing the crude lysate reaction mixture on ice to prevent it from exceeding room temperature (which had occasionally risen above 25°C). This caused an increase in the viscosity of the crude lysate, disrupting droplet formation and amplification. Therefore, it is advisable to take appropriate measures to address the viscosity of the cell lysates.

Second, I encountered an unexpected challenge when my NTCs started yielding positive signals. The initial suspicion was DNA contamination in my samples. I thoroughly decontaminated the PCR workspace, replaced reagents (except for the probe, which was from a new vial), and retested, but the results remained consistent (Figure 3.10b). Upon closer examination, I noticed that the positive signal in NTCs

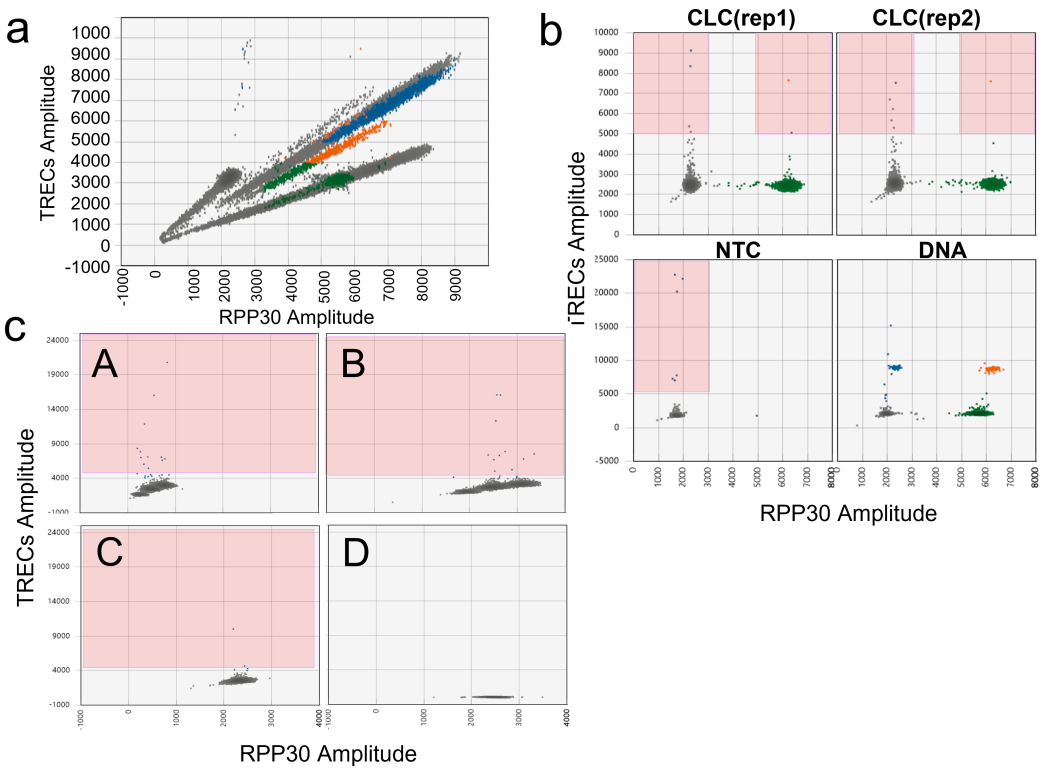



**Figure 3.10**: **Troubleshooting the crude lysate ddPCR**. (a) The 2-D dot plots display unusual droplet patterns. Data merged from 8 replicates. Different colours are automated threshold settings by QuantaSoft software. (b) 2-D dot plot represents the positive signal in replicates of CLC control and NTC. Positive control using extracted DNA was also included. (c) 2-D dot plot represents the positive signal in the different combinations of primers and probes: (A) TREC primers and probes only, (B) TREC probe without primers along with RPP30, (C) TREC primers, probes, and RPP30, and (D) RPP30 only. The pink shaded area highlights the positive signals in respective plots. Blue dots are TRECs single positive, green dots are RPP30 single positive, orange dots are TREC RPP30 double positive and grey dots are double negative. Each dot represents a droplet in ddPCR

only appeared in the TRECs region, which was unusual as TRECs are rare, and exclusively detecting TRECs in NTCs didn't make sense. This observation led me to suspect an issue with the TRECs reagents, particularly the TRECs probe. To confirm this, I experimented with various combinations of primers and probes: (A) TREC primers and probes only, (B) TREC probe without primers along with RPP30, (C) TREC primers, probes, and RPP30, and (D) RPP30 only. Surprisingly, combination (B) should not have produced any signal since it lacked TREC primers, but it did, indicating probe degradation (Figure 3.10c). Unfortunately, the probes were new, so this ruled out an issue caused by probes. By using the new TREC probe this issue was resolved completely. This experience taught me that even new

products or reagents can sometimes arrive damaged.

Both of these troubleshooting challenges consumed a significant amount of time, which is why I have included them in the results section so that any fellow researcher experiencing the same could take help from this.

### 3.2.3 Discussion

Nucleic acid target quantification is a fundamental aspect of molecular biology and diagnostics, playing a crucial role in various fields, including genomics, clinical diagnostics, and environmental monitoring. Accurate quantification of nucleic acid targets is essential for understanding biological processes, diagnosing diseases, and monitoring genetic variations. However, this task becomes particularly challenging when dealing with limited sample quantities or precious biological material. In such scenarios, the choice of quantification method becomes pivotal in achieving reliable results.

In the context of this study, we hypothesized that the development of a robust and sensitive quantification assay, specifically designed for limited-sample scenarios, could significantly advance our ability to extract valuable information from restricted biological specimens. This hypothesis was tested through the evaluation of the crude lysate ddPCR, a novel approach aimed at overcoming the challenges associated with quantifying nucleic acid targets from low-input samples.

The initial investigation aimed to explore the best method to prepare the cell lysates compatible with ddPCR, including thermal lysis, sonication, lysis buffer from DNA/RNA extraction kit as well as buffer 1 and buffer 2 (Section 3.2.2.1). Overcoming the viscosity of crude lysates emerged as a critical challenge in this process (Figure 3.2), and this challenge was successfully addressed by implementing a viscosity breakdown step (Section 2.2.3). Among the methods evaluated, the combination of buffer 1 or 2 with the viscosity breakdown step exhibited promising results (Figure 3.2), with buffer 2 emerging as the preferred choice (Section 3.2.2.2 and Figure 3.3). Consequently, we further optimised and validated this approach for direct ddPCR quantification of the rare gene target, TRECs.

Unexpectedly, we found that the droplet volume obtained using crude lysate (0.7nL) was lower than that used by QuantaSoft software v1.0.569 (0.85nL) (Sec-

tion 3.2.2.6). This decrease in volume from that expected was not attributable to the crude lysate protocol as we found an almost identical droplet volume with the standard ddPCR assay (0.7nl) (Figure 3.7e). This observation is consistent with previous studies that have also shown deviations from the default droplet volume in Biorad's system (Pinheiro et al. 2012, Dong et al. 2015, Košir et al. 2017). Notably, Košir et al. (2017) reported a droplet volume of (0.71nL, very) similar to our findings (19).

The performance of this protocol was critically assessed and compared to the standard ddPCR protocol. Overall, the novel assay demonstrated good linearity agreement in the range from 0.0003 to 0.01 TRECs/cell, where the lowest concentration corresponds to the LOQ (Figure 3.3). It's worth noting that various researchers have employed different units for reporting LOQ in TRECs quantification, such as TRECs/$\mu$g of DNA (Tessitore et al. 2017), TRECs/$\mu$l of reaction, and TRECs/$\mu$l of sample (Profaizer & Slev 2020). For instance, Profaizer & Slev (2020) optimised a ddPCR assay for TRECs quantification, Kappa-deleting recombination excision circles (KREC), and a reference gene in a single reaction, reporting results as TREC copies/$\mu$l of blood. They determined the LOQ for TRECs using standard ddPCR to be 2 copies/$\mu$l of blood. Also, their previous work using qRT-PCR only permitted the detection of 24 copies/$\mu$l of blood. To compare these reported results with our study, we transformed the units by estimating the number of T cells per $\mu$l of blood (as 45-70% of PBMCs are T cells (Lozano-Ojalvo et al. 2015), and 1 ml of blood yields $2*10^6$ PBMCs), this translates to a LOQ of 0.0014 TRECs/cell for the standard ddPCR and 0.017 TRECs/cell for qRT-PCR (Profaizer & Slev 2020), approximately 5 and 50 times higher, respectively, than our novel assay.

The quantification of TRECs as TRECs/cell in the crude lysate ddPCR provides an advantageous measure of assay recovery, making TREC copies/cell a superior unit compared to TRECs/$\mu$l. However, it's important to note that the crude lysate ddPCR using buffer 2 to prepare the cell lysates has a limitation—it has a lower upper quantification limit, and cell lysis may not work optimally when the number of cells used to prepare the lysate exceeds 10,000 cells. Therefore, for situations with ample sample quantities, utilizing the standard ddPCR or qRT-PCR remains a more suitable option.

Despite this limitation, absolute quantification of TRECs using the crude lysate ddPCR demonstrated a good agreement with standard ddPCR as analysed by Bland-Altman analysis (Figure 3.8). Additionally, the high specificity of the assay was confirmed by the absence of any signal in CLCs during the limit of blank experiment (Figure 3.5). The average coefficient of variation (CV%) for the repeatability experiment is 22.25% suggesting some source of variability (Table 3.1). The slight variability observed in these samples may arise from the viscosity of PCR mix, droplet count variations, incomplete mixing of samples or the presence of secondary DNA structures, which might disturb the random distribution of samples. Furthermore, variations in sample handling, pipetting or minor inconsistencies in assay conditions could also impact the assay's consistency. Further investigations, such as fine-tuning by PCR enhancers or cycling conditions, may offer the potential to enhance assay consistency.

Furthermore, by partitioning a single sample of cell lysates into four ddPCR reactions, we were able to comprehensively screen the entire sample to detect rare genes. Subsequently, these four samples were merged to calculate absolute quantification. This approach offered the advantage of significantly increasing the number of screened droplets per sample, from approximately 20,000 per reaction or sample to 80,000 per sample. As outlined in the dMIQE guidelines, the augmentation of droplet count per sample leads to enhanced precision and heightened analytical sensitivity (Huggett 2020, Huggett et al. 2015).

Moreover, our method stands out as a superior alternative to pre-amplification reaction. Pre-amplification involves increasing the copy number of nucleotide sequences in the reaction before polymerase chain reaction (PCR) analysis, enabling the analysis of genes with limited nucleic acid content. In pre-amplification reactions, addressing two major challenges is crucial: augmenting the reaction's capacity and ensuring target amplification specificity. This ensures efficient amplification during each PCR cycle, even for targets with significantly different initial quantities and substantial background noise (Okino et al. 2016). Failing to tackle these challenges can introduce significant bias during the pre-amplification process. By circumventing the need for pre-amplification, we eliminated related issues. Simply put, fewer steps in the process reduce the potential for introducing variability.

Our method differs from previously published studies on ddPCR directly from cell lysates for absolute quantification of genes (Ludlow et al. 2018, Zou et al. 2021, Vasudevan et al. 2021), as we utilized the whole cell lysates instead of a portion of it. Working with a larger volume of cell lysates presents challenges as it alters the viscosity of the reaction mixture, resulting in a reduction in droplet count and experiment efficiency. However, in our study, we successfully addressed these challenges by introducing a viscosity breakdown step. This approach is more robust for detecting rare events from limited clinical or biological samples.

Furthermore, we conducted experiments to evaluate the efficacy of this protocol on fixed cells. Although there were no significant differences observed between fixed/permeabilized cells and non-fixed cells, it was noted that the count of TRECs was lower in the fixed cells compared to the non-fixed cells (Figure 3.9). We suggest that further optimisation is needed before this method can be used on fixed and permeabilized samples.

It has been established that using plasmids for optimising qPCR reactions is unsuitable as it can lead to overestimation of the target (Hou et al. 2010). Therefore, for the crude lysate ddPCR optimisation, we employed regular samples (PBMCs) rather than plasmids containing TRECs DNA. In adherence to MIQE guidelines, we consistently included appropriate negative and positive controls in our experiments to assess background signals and set the threshold (Huggett 2020).

A fundamental understanding of the technique is essential for addressing challenges effectively. In our efforts to enhance the sensitivity of the crude lysate ddPCR, we explored various cycling protocol adjustments, including different ramp rates for each step, hot start protocols, and touch-down protocols (results not presented in this thesis), ultimately selecting the most effective approach. Researchers interested in adopting this protocol may also consider these variations to optimise assay sensitivity, as per their research objective.

The study's limitations include a relatively small number of replicates used for optimisation and technical assessment. Furthermore, while our LOD and LOQ assessment indicated the presence of TREC copies in all dilutions, we did not explore concentrations below 0.0003 TREC copies/cell due to the satisfactory performance within the optimised range. During experimentation, we encountered occasional ar-

tifacts, such as double negative clusters (Figure 3.6 Dil2) or isolated droplets with significantly higher TRECs and RPP30 amplitudes than the rest. These artifacts may be attributed to contamination, debris in the crude lysate, or technical variations, such as temperature fluctuations or minor inconsistencies during droplet generation.

In conclusion, the developed crude lysate ddPCR represents a significant advancement in rare gene quantification. Its efficiency, comparable performance to standard ddPCR, and potential for use with fixed cell samples make it a valuable tool for researchers in immunology and related fields. Additionally, by sidestepping the complexities of DNA extraction from limited cell numbers, this method offers several benefits, including preserving sample integrity, minimizing the risk of sample loss, and streamlining the quantification process. We used this protocol to measure TREC copies from CD8+ Tscm subpopulations explained in detail in the next chapter.

Further exploration and optimisation of this protocol will uncover its full potential and contribute to advancements in our understanding of rare gene dynamics and their implications in various biological processes.

# Chapter 4

# Characterizing the heterogeneity of the TSCM subset

## 4.1 Introduction

The human memory T-cell compartment is diverse, comprising various subpopulations that play distinct roles in maintaining memory responses during homeostasis and different types of infections. Identifying the specific subpopulation responsible for memory maintenance has been challenging due to the heterogeneity in phenotype and function among these subsets. Initially, Tcm were considered key players due to their multipotency and self-renewal capabilities (Wherry et al. 2003, Sallusto et al. 1999). However, the discovery of Tscm revealed their central role in reconstituting the memory compartment (Gattinoni et al. 2011).

Tscm cells are endowed with self-renewal and multipotent properties which are vital for maintaining immunological memory over time. These cells are also able to respond to antigen rechallenge by differentiating into effector cells thus, exhibiting all necessary traits of memory stem cells (Gattinoni et al. 2011, Fuertes Marraco et al. 2015, Oliveira et al. 2015). Due to their extreme multipotency, they are thought to be the apex of human T cell memory differentiation (Gattinoni et al. 2011, Costa Del Amo et al. 2018, Ahmed et al. 2016). Tscm cells are characterised by a set of phenotypic markers that includes naive markers (expressed by T naive cells) such as CD45RA, CD27, CD28 and CCR7 and also memory markers that separate them from naive cells such as CD95, CXCR3 and CD122 (Gattinoni et al. 2011).

Recently, Costa Del Amo et al. (2018) demonstrated heterogeneity within the human Tscm compartment. Combining deuterium labeling data, telomere length analysis and data from vaccination studies, the authors identified two kinetically heterogeneous populations with distinct proliferation rates and half-lives. As per his work, the average lifetime of a Tscm clone was relatively short, challenging the notion that Tscms function as a classical stem-cell population. However, they demonstrated that this was because the population comprises of two sub-sets; one of them is rapidly replaced (with a half-life of less than a year) whereas the other is stably maintained for over 9 years and thus suggested that the long-lived subset was the one maintaining memory over time (Costa Del Amo et al. 2018). At this stage, the phenotypic identity of the two Tscm subpopulations, their functions and their contribution to memory formation remain unsolved.

Recent research from our lab conducted by my colleague, Danai A. Koftori, found that CD95 expression could be used to distinguish the Tscm subsets and also elucidated the functional disparities between them. She revealed that Tscm cells expressing high levels of CD95 (CD95hi) displayed increased proliferation (by Ki67 staining), superior self-renewal potential, and closer transcriptional alignment with Tcm cells compared to Tscm cells expressing intermediate levels of CD95 (CD95int) (manuscript in preparation). These findings collectively demonstrated that CD95 expression levels could effectively distinguish the Tscm subpopulations.

CD95 (FAS or APO-1), a member of the tumor necrosis factor (TNF) receptor family and the FAS-FASL pathway plays a crucial role in regulating the life and death of immune cells, especially in the context of lymphocyte development and activation-induced cell death (AICD) (Zheng et al. 1995, Dhein et al. 1995). AICD is essential for maintaining immune system homeostasis. During an immune response, activated lymphocytes proliferate to generate effector cells that clear pathogens. CD95-mediated apoptosis is a significant mechanism for eliminating these activated lymphocytes, ensuring peripheral immune tolerance (Schmitz et al. 2003). Importantly, CD95 also has nonapoptotic functions in immune cells, such as promoting the activation and proliferation of T cells and the differentiation of various T cell subsets like Th2, Th9, and Th17 cells (Shen et al. 2019, Huang et al. 2021, Zu Horste et al. 2018). Paulsen et al. (2011) has shown that CD95 maintains its dual function

via the strength of the interactions with its receptor; low-strength triggers in combination with TCR co-stimulation lead to survival and activation of T cells, while high-strength interactions with CD95L result in apoptosis. CD95's role in immune cell signaling, both apoptotic and nonapoptotic, is an area of active research.

It is important to mention that Danai A. Koftori's results contradict the suggestion made by Costa Del Amo et al. (2018) that only the long-lived Tscm subset is responsible for maintaining long-term memory, as her research indicates that both Tscm subsets played crucial roles in memory maintenance. CD95hi cells actively engaged in self-renewal, contributing to the generation of other memory subsets, while CD95int cells exhibited reduced division rates but acted as a source for replenishing the CD95hi population.

With these crucial understandings as our foundation, the objective of this chapter was to further comprehensively characterized Tscm subsets and understand their dynamics through diverse approaches, including immunophenotyping, cell division history tracking, age-related variations, transcriptional analysis, and tissue distribution profiling.

## 4.2 Results

### 4.2.1 CD95 as a marker for Tscm heterogeneity

Research conducted by Danai A. Koftori (manuscript in preparation) has revealed CD95 as a potential marker for distinguishing Tscm subsets. Her findings indicate that Ki67+ Tscm cells exhibit significantly higher CD95 expression compared to Ki67- Tscm cells. To validate the observed difference in Ki67 percentage between CD95hi and CD95int subsets, we conducted a similar analysis using samples from healthy donors. Ki67, a nuclear protein commonly used to assess proliferation, is expressed during cell division and remains in the nucleus for up to three days after division (Scholzen & Gerdes 2000). Thus, Ki67 staining aids in identifying cells with varying proliferation rates.

PBMCs isolated from healthy donors aged 23-65 years were stained for Ki67, alongside other canonical CD8+ T memory cell markers. Initially, we analyzed the MFI of CD95 within Ki67+ and Ki67- subsets of different memory subpopulations

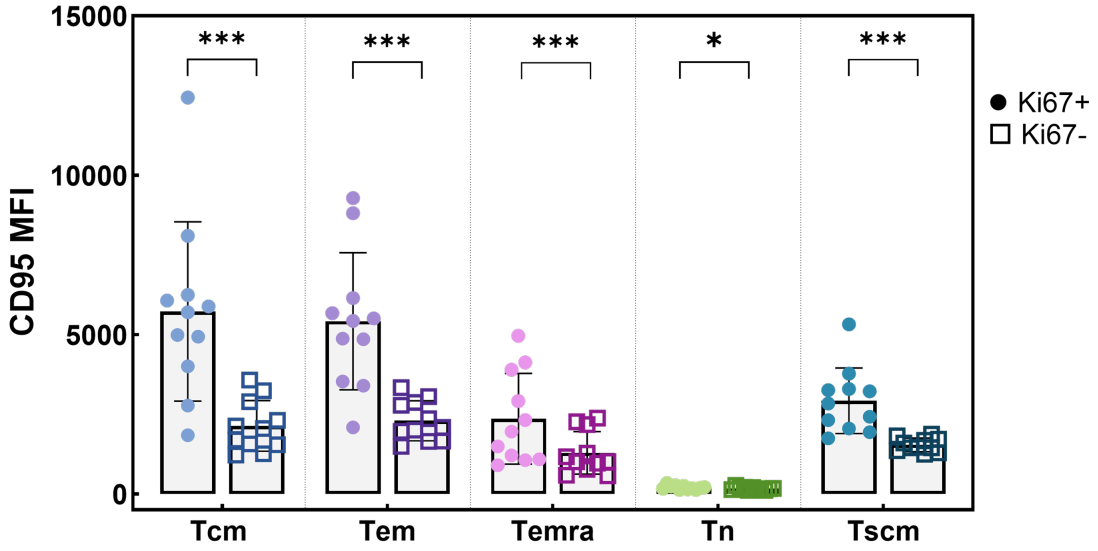



**Figure 4.1**: **Ki67+ memory CD8+ T cells exhibit increased CD95 expression.** T cells from healthy individuals were isolated and stained with Ki67 and other memory markers. Higher CD95 MFI was observed in the Ki67+ cells for all CD8+ memory subsets compared to Ki67- cells. Stats: Wilcoxon paired test. Each symbol represents one donor. Bars indicate mean ± s.e.m. *P<0.05, ***P<0.001 ****P<0.0001

and observed significantly higher CD95 MFI in Ki67+ subsets across all memory subsets compared to Ki67- cells (Figure 4.1a). Since Ki67 positivity and CD95 expression positively correlate, as observed by Danai, we used the CD95 expression level to gate the Tscm subsets. We first set the gating on the basis of the contour plot of Tscm and then further validated it using a histogram (Figure 4.2a). In the contour plot, a distinct circular cluster was observed, having denser lines toward its left, indicating a higher cell density with intermediate CD95 expression (referred as CD95int). As we move to the right of this circle, the lines become less dense, representing a population with lower density but higher CD95 expression (referred as CD95hi) (Figure 4.2a). Furthermore, in some samples (with a high frequency of CD95hi), the contour plots displayed two distinct circular clusters, each neatly bisected by the applied gates (SuppFigure 4.1). Upon comparing this observation with the histogram of CD95, a clear pattern emerged. There was a prominent peak toward the left, which corresponded to the CD95int population, while a smaller peak on the right represented the CD95hi population (Figure 4.2a). The gating strategy applied in the contour plots effectively separated these two populations,

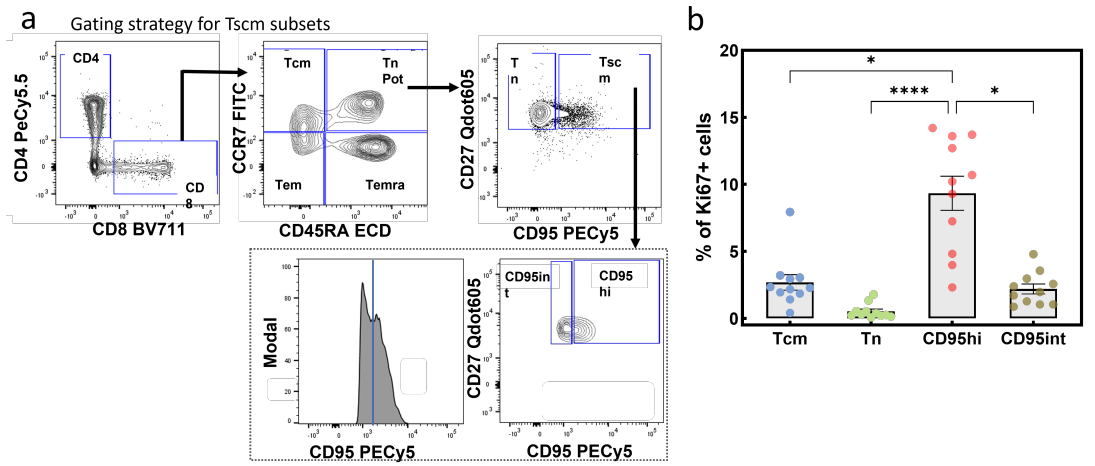



**Figure 4.2**: **CD95hi subset exhibits higher frequency of Ki67+ cells.** a) Gating strategy employed to gate CD95hi and CD95int populations. CD8+ cells were categorized into different memory subpopulations based on CD45RA and CCR7 expression, i.e., Tcm: CD45RA-CCR7+, Tem: CD45RA-CCR7-, Temra: CD45RA+CCR7-, and T naive potential (Tn Pot): CD45RA+CCR7+. Within Tn Pot cells, Tscm and naive T cells were gated based on CD95 and CD27 expressions (Tn CD27+CD95- and Tscm CD27+CD95+). All memory differentiation gates were determined using FMO controls. To delineate the Tscm subsets more precisely, contour and histogram plots are shown b) The percentage of Ki67+ cells is shown between Tcm, naive T cells (Tn), CD95hi and CD95int. Stats: Wilcoxon paired test. Each symbol represents one donor. Bars indicate mean ± s.e.m. *P<0.05, ***P<0.001 ****P<0.0001

nearly cutting through the center of the trough between these two peaks when examining concatenated samples. This gating approach remained consistent across all samples in this experiment.

In subsequent experiments with varying antibody panels or cells acquired on different machines, we repeated the same contour plot analysis to identify denser and less dense lines, followed by histogram comparison to the gate for CD95hi and CD95int populations.

In the results, CD95hi cells exhibited a high frequency of Ki67+ cells as compared to CD95int, Tcm and T naive (Figure 4.2b), indicating their high proliferation rates.

We analysed Ki67 staining in several CD8+ T cell subpopulations in addition to Tscm, including Tn, Tem, Tcm and Temra. We were particularly interested in Tcm because these cells were originally identified as the stem pool of memory cells (Fearon et al. 2001). Further studies have demonstrated the immune reconstitution and in vivo maintenance capabilities of Tcm cells compared to Tem cells (Wherry et al.

2003, Graef et al. 2014, Gattinoni 2014). Although the distinction between Tcm and Tscm cells remains unclear. Some studies suggested that Tscm possess greater stem potential than Tcm (Gattinoni et al. 2011), while others proposed that Tcm can reacquire CD45RA and hence can give rise to Tscm (Zhao et al. 2021). Given the ongoing debate surrounding the relationship between these subsets, we also aimed to compare our Tscm subsets with Tcm to explore differences and similarities. Here, through Ki67 staining, we demonstrated that CD95hi Tscm cells possessed greater proliferation potential than Tcm cells, while not any significant difference between Tcm and CD95in was observed (Gattinoni 2014), (Figure 4.2b).

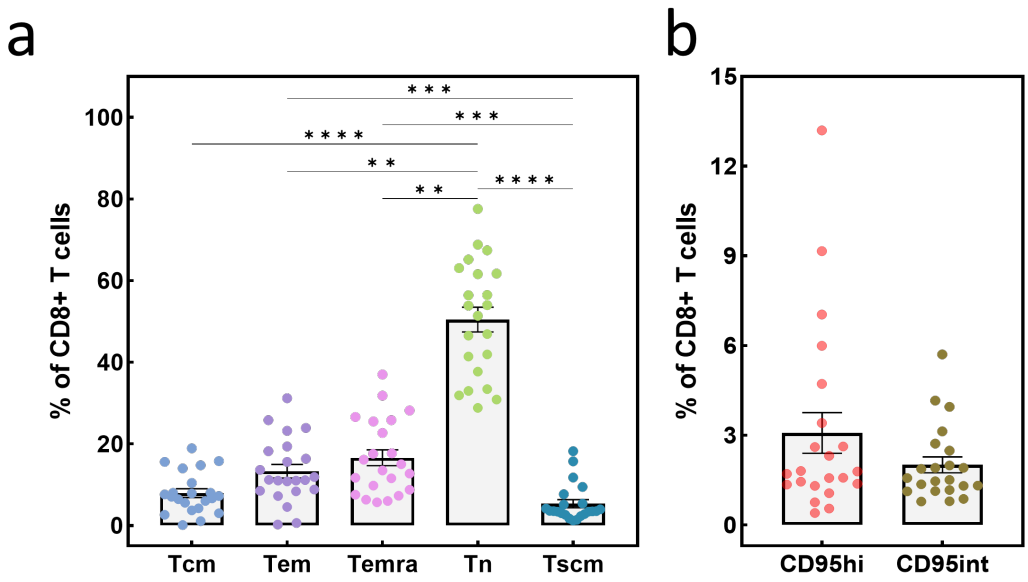



**Figure 4.3**: **Frequencies of different memory subpopulations in healthy individuals.** a) Frequencies of different memory subpopulations from CD8+ T cells, b) Frequency of Tscm subsets from CD8+ T cells (n=22, 23-65yrs with median 36yrs). Stats: One-way ANOVA with Friedman's multiple comparison test. Each symbol represents one donor. Bars indicate mean ± s.e.m. **P<0.01, ***P<0.001 ****P<0.0001

Additionally, we investigated the frequencies of different memory subpopulations in our dataset (Figure 4.3a), along with CD95hi and CD95int subsets (Figure 4.3b). In this healthy donors dataset, naive T cells constituted the highest frequency (50.45%±14.18), followed by Temra cells (16.59%±9.19), Tem (13.3 %±7.7)and Tcm (8.05%± 5.05) (Thome et al. 2016, Di Benedetto et al. 2015, Herndler-Brandstetter et al. 2012). Notably, we observed an average of 5.4%±4.5 of Tscm in CD8+ T

cells, which is slightly higher than what was defined by Gattinoni (2-3%) (Gattinoni et al. 2011). Further, the frequency of CD95hi was roughly similar to CD95int (Figure 4.3b), which contradicts Koftori's unpublished results (manuscript in preparation). Her studies indicated that CD95hi cells comprised approximately 10%-15% of the total Tscm population, while CD95int cells accounted for 80%-85% of the total Tscm population.

To better understand the reasons behind the variations in Tscm frequencies observed in our diverse dataset, which spans a wide age range (n=13 for 23-40 years; n=9 for 40-65 years; overall median=36yrs), we investigated the relationship between memory populations and age.

### 4.2.2 Age-related variations in Tscm frequencies and memory populations

Numerous studies have consistently reported that aging is associated with a shift in T cell subset distribution, transitioning from a predominance of naïve T cells toward a memory phenotype (Rodriguez et al. 2021, Li et al. 2019). However, it has remained unclear whether this age-related transformation extends to Tscm. Additionally, we aimed to investigate whether the observed increase in Tscm frequencies mentioned in the previous section is influenced by the age of the donors. To investigate this, we performed an analysis to assess age-related changes within the CD8+ T memory cell population in our dataset.

Consistent with previous studies (Rodriguez et al. 2021, Li et al. 2019), we observed a significant decrease in the frequency of CD8+ naive T cells with advancing age (Figure 4.4a). Interestingly, while all memory populations exhibited a slight age-related increase (albeit not statistically significant), the Tscm population demonstrated a notable and statistically significant increase (Figure 4.4a).

When we divided the dataset into two groups, individuals younger than 40 years and individuals older than 40 years, we observed a significant difference in the frequencies of Tscms (SuppFig 4.2a). Specifically, individuals younger than 40 years had Tscm frequencies of 3.3%±1.8%, aligning with the literature (Gattinoni et al. 2011), while those older than 40 years exhibited nearly double the Tscm frequencies averaging of 6.9%±5.3% (SuppFig 4.2a). Hence, the notable increase in Tscm

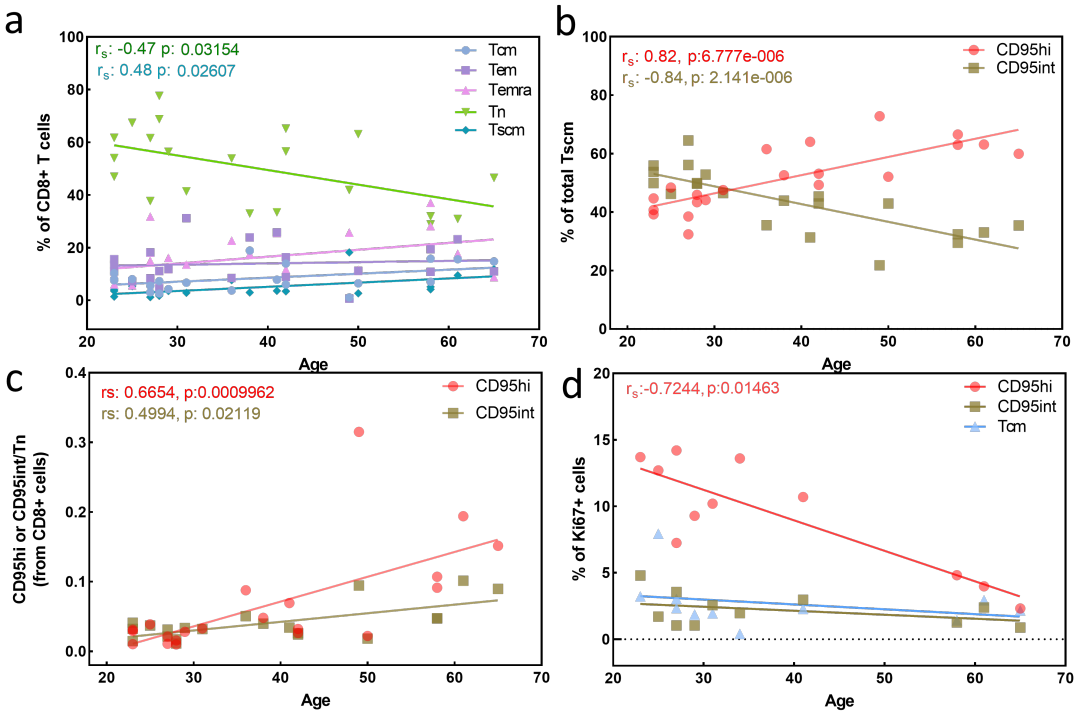



**Figure 4.4**: **Tscm accumulates with age.** The frequencies of different memory subpopulations are plotted against the age of donors (n=21). a) Frequencies of Tcm, Tem,Temra,Tn and Tscm from CD8+ T cells plotted against age. b) Frequencies of CD95hi and CD95int from total Tscm plotted against age. c) Ratio of CD95hi or CD95int/Tn plotted against age. d) % of Ki67+ cells from CD95hi, CD95int and Tcm cells plotted against age. Each symbol represents one donor. Coloured lines represent simple linear regression lines. Stats: Spearman Correlation analysis with $r_s$ is correlation cofficient

frequency with age may account for the higher Tscm frequencies observed in our dataset compared to the literature.

Our particular focus then turned to the examination of how the CD95hi and CD95int subsets within the Tscm compartment evolve over time. Remarkably, our findings show a progressive accumulation of CD95hi cells with age ($r_s$: 0.82, p: <0.0001), while CD95int cells exhibited a significant decline ($r_s$: -0.84, p 0.0001) (Figure 4.4b). Notably, we observed an interesting reversal in these two subsets' proportions at a young age (30 years), with CD95int being significantly higher than CD95hi, a relationship that inverted after this age (SuppFig 4.2b). These results indicate the complex interaction between these two subsets during the aging process.

To gain further insight into these populations, we examined the ratio of CD95hi/CD8+ Tnaive and CD95int/CD8+ Tnaive cells, calculated as frequencies from CD8+ T cells (Figure 4.4c). Surprisingly, both subsets displayed a linear increase in this ratio

with age, indicating that CD95int cells, while decreasing in their proportion from bulk Tscm cells, exhibit relative stability in their proportion compared to T naive cells.

Additionally, we explored age-related variations in Ki67+ cells within Tscm subsets and Tcm. As previously demonstrated, CD95hi cells contained the highest proportion of Ki67+ cells; however, these Ki67+ CD95hi cells exhibited a significant decline with age (Figure 4.4d). While the Ki67+ cell population within CD95hi cells decreased with age, it is important to recognize that the size of the CD95hi population itself increased. This suggests that, with advancing age, CD95hi cells lower their proliferation capacity, even though the size of this population increases over time. This phenomenon can likely be attributed to factors beyond proliferation, such as altered differentiation dynamics (Nikolich-Žugich et al. 2012, Ahmed et al. 2017), or increased survival, which could contribute to their accumulation. These factors might compensate for the reduced proliferation capacity, ultimately leading to the observed increase in the size of the CD95hi cell population.

### 4.2.3 Tscm subsets have different division histories

Cell division history analysis is a valuable tool for uncovering the origin of heterogeneity within a cell population by characterizing the diverse kinetics of cell division. Heterogeneity within a cell population can emerge from variations in cell division rates, lineage relationships, or differentiation trajectories. Understanding these distinctions in cell division kinetics is crucial for gaining insights into the complexity of cell populations and their roles in processes such as tissue development, homeostasis, disease, and other biological phenomena.

In our study, we investigated the cell division history of CD8+ T memory subpopulations by quantifying TRECs within these subpopulations. TRECs are not replicated by mitosis and instead become diluted with each cell division, meaning that subsets with an extensive division history will have a lower quantity of TREC compared to subsets that have undergone fewer divisions (Hazenberg et al. 2001, Verstegen et al. 2019). Consequently, TRECs serve as an in vivo marker of cell division history. One notable advantage of measuring TRECs in comparison to other markers like Ki67 or CFSE dilution is that TRECs provide a comprehensive view

of the proliferative history of a subset, rather than capturing only a momentary snapshot (explained in section 1.6.3).

We conducted this analysis on sorted CD8+ T memory subpopulations, which include naive T, Tem, Tcm, Temra, CD95hi and CD95int. These subpopulations were sorted at high purity from samples obtained from seven healthy individuals. We quantified TRECs using a high-throughput crude lysate ddPCR protocol that we optimized in-house (explained in Chapter 3).

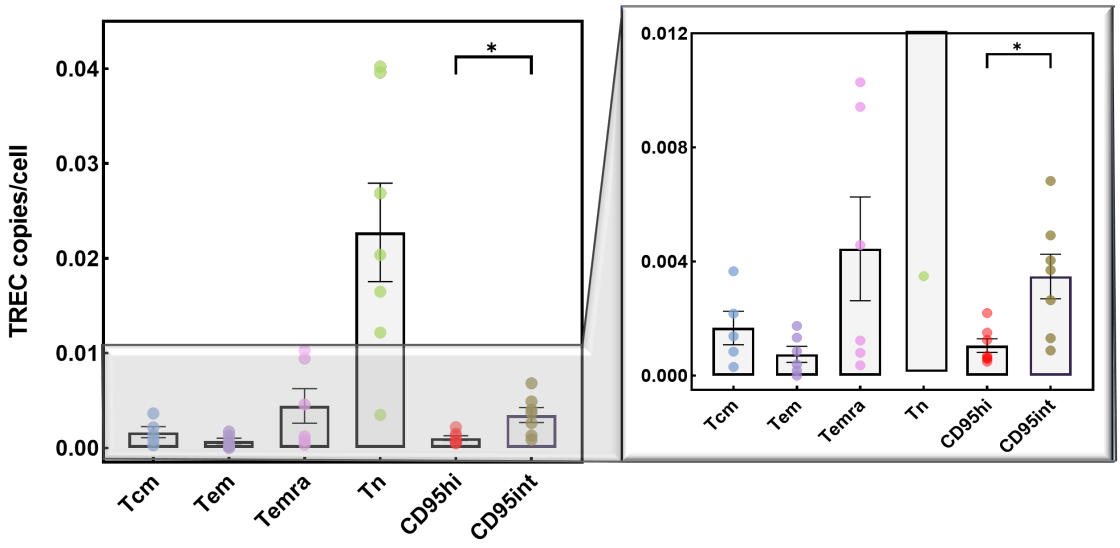



**Figure 4.5**: **CD95hi population has lower TREC count than CD95int** Number of TREC copies per cell for each memory subset isolated from n=7 healthy donors. In inset, memory subpopulations are zoomed in to view the clear difference in TREC content in them. Bars indicate mean ± s.e.m. Each dot represents a donor. Stats: Wilcoxon matched-pairs test between CD95hi and CD95int. *P<0.05

As expected, we found that T naive cells exhibited a higher TREC content compared to all memory cell subpopulations (Figure 4.5). Furthermore, we observed a significant difference in TREC content between CD95int Tscm cells and CD95hi Tscm cells (Figure 4.5). This discrepancy suggests that these two subpopulations have distinct division histories, as frequent interconversion between them would result in similar TREC contents. Additionally, it indicates that CD95hi Tscm cells have undergone more rounds of division since thymic production than CD95int Tscm cells.

### 4.2.4 Tissue specific distribution

T cells have a diverse distribution throughout the body, with only a modest fraction found in peripheral blood (Ganusov & De Boer 2007). LNs serve as central hubs for immune surveillance and responses (Pollard & Bijker 2021), making them ideal for studying Tscm cells and their role in maintaining long-term immunity and vaccine effectiveness.

To study this, we used blood and paired LN samples from European AIDS Vaccine Initiative (EAVI)2020_01 HIV trial vaccination study (section 2.4). LN samples were collected by US-guided FNA of axillary LNs from 11 healthy volunteers participating in an experimental vaccine immunogen study (Day et al. 2022). Samples were collected between 7 days and 56 days post-first immunisation but before the subsequent boost, a time point at which antigen-specific IgG was undetectable (Day et al. 2022). In this section, we are only presenting results for the distribution of Tscm along with its subsets in blood and LN. However, we also immunophenotyped other immune cells such as complete CD8+ T memory subsets, monocytes, B cells, CD4+ T memory cells, Tfh cells and compared the expression of different cells surface markers by LNCs and PBMCs, discussed in Chapter 7.

Overall, the frequencies of CD8+T cells and Tscm were significantly higher in PBMCs as compared to LNCs (Figure 4.6 a and b). Regarding Tscm subpopulations, we observed that the percentage of CD95hi was higher in PBMCs than in the LNCs (P=0.07, Mann-Whitney test), while conversely, the percentage of CD95int cells was notably elevated in LNCs (P=0.01, Mann-Whitney test) (Figure 4.6c). These results suggest that CD95int cells, characterized by a lower turnover rate, predominantly reside in LNs, while CD95hi cells, which display higher proliferation rates, circulate more prominently in the peripheral blood.

Due to the low frequency of Tscm subsets in LNCs, investigating the expression of various markers on these CD95hi and CD95int subsets was not feasible. Instead, we examined the MFI of CCR7, a homing marker, and Interferon Regulatory Factor 4 (IRF4), a transcription factor, in the bulk Tscm population. We observed a significant increase in CCR7 MFI on PBMCs, suggesting that Tscm cells in peripheral blood may have an enhanced potential for trafficking to lymphoid tissues compared to their counterparts in lymph nodes (Figure 4.6d). Conversely, the elevated ex-

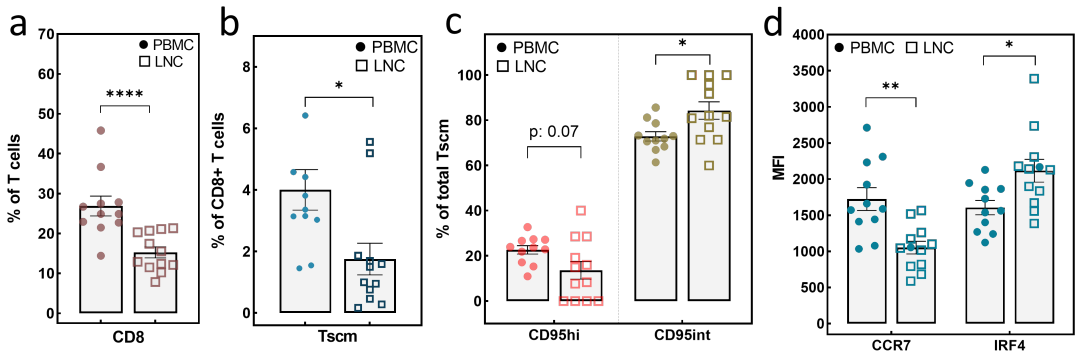



**Figure 4.6**: **Frequency of Tscm and its subsets in lymph node cells (LNC).** Comparison of different subpopulations between PBMCs and LNCs, a)CD8+ T cells, b)Tscm, c) CD95hi and CD95int. d) MFI of CCR7 and IRF4 expressed by total Tscm cells compared between PBMC and LNC. Circles represent PBMC while squares represent LNC. Bars indicate mean ± s.e.m. Each dot represents a donor. Stats: Mann-Whitney test *P<0.05, ****P<0.0001.

pression of IRF4 on LNCs indicates a distinct transcriptional profile in Tscm cells within LN, potentially reflecting different functional states or activation status of Tscm cells in these two tissues (Figure 4.6d).

To investigate the impact of external stimuli on these Tscm subsets, we stimulated both PBMCs and LNCs ex vivo with SEB, a superantigen, for 18 hours and analysed changes in their frequencies. Remarkably, we observed a significant increase in the Tscm population in response to stimulation in both PBMCs and LNCs (Figure 4.7a). This increase in Tscm frequency could be due to differentiation from naive T cells or other memory subpopulations or could result from proliferation in response to SEB. Notably, within the Tscm subsets, CD95hi Tscm cells in PBMCs exhibited a significant increase, while CD95int Tscm cells decreased significantly following stimulation (Figure 4.7b). Similar trends were observed in LNCs, although they did not reach statistical significance (Figure 4.7b). However, it's important to note that these findings should be interpreted with caution since our cells were not sorted into distinct subsets.

Additionally, we examined the expression profiles of activation and co-stimulatory molecules on CD95hi and CD95int Tscm cells in PBMC samples (Figure 4.8). Unfortunately, due to limited cell availability, we were unable to perform this analysis on LNC samples. Notably, CD95hi Tscm cells exhibited elevated levels of PD-1, CD69, IRF4, and CD137, both prior to (Figure 4.8a,b) and following SEB stimu-

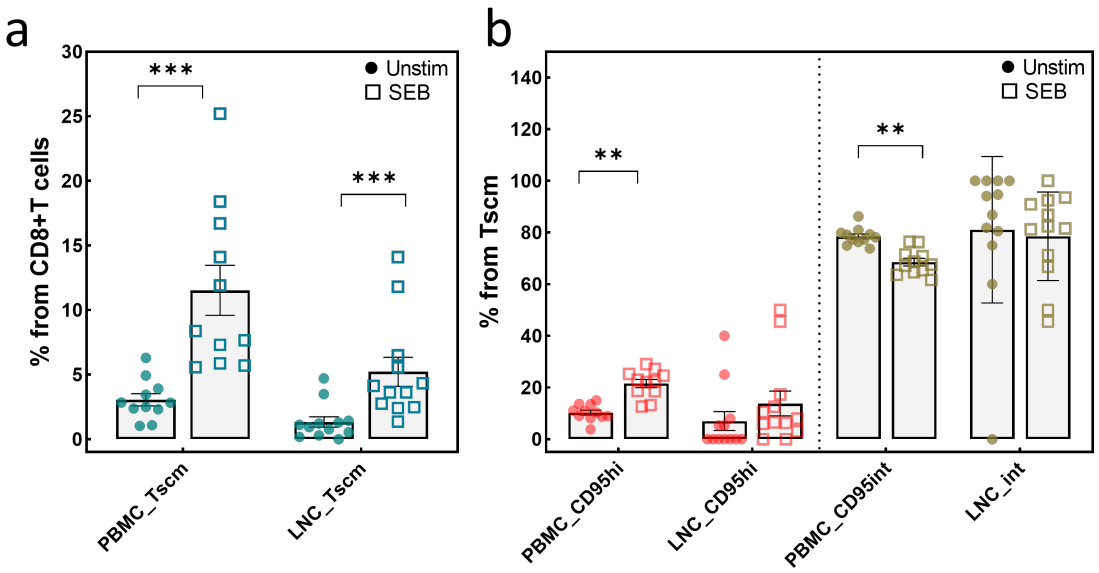



**Figure 4.7**: **Effect of SEB stimulation on Tscm subsets.** a) PBMCs and LNCs were cultured with SEB for 18 hrs and stained with different memory markers. Frequency of a)total Tscm from CD8+ Tcells and b)CD95hi and CD95int from total Tscm is compared between unstimulated and stimulated samples. Circles represent PBMC while squares represent LNC. Bars indicate mean ± s.e.m. Each dot represents a donor. Stats: Wilcoxon matched-pairs test **P<0.01, ***P<0.001.

lation (Figure 4.8a,c). This suggested that CD95hi Tscm cells are more activated and have a more pronounced co-stimulatory molecule expression profile compared to CD95int Tscm cells in PBMCs.

### 4.2.5 Transcriptional analysis of sorted memory subpopulation

The transcriptional status of immune cell subsets adds another layer of information. During T-cell differentiation, much of the fine-tuning of the activity is orchestrated by lineage-specific TFs. Cell-type specific gene expression profiles determine differential expression of phenotypic markers between subsets which confer distinct functional profiles (Montacchiesi & Pace 2022). It is therefore evident that to understand the heterogeneity of T-cell subsets and to fully characterize them, their gene expression profile has to be taken into consideration.

To investigate this, memory subpopulations, including Tn, CD95hi, CD95int, Tcm, Tem and Temra were sorted from 12 healthy individuals with high purity. Sorted cells were divided into two parts. One part was cultured with RPMI me-

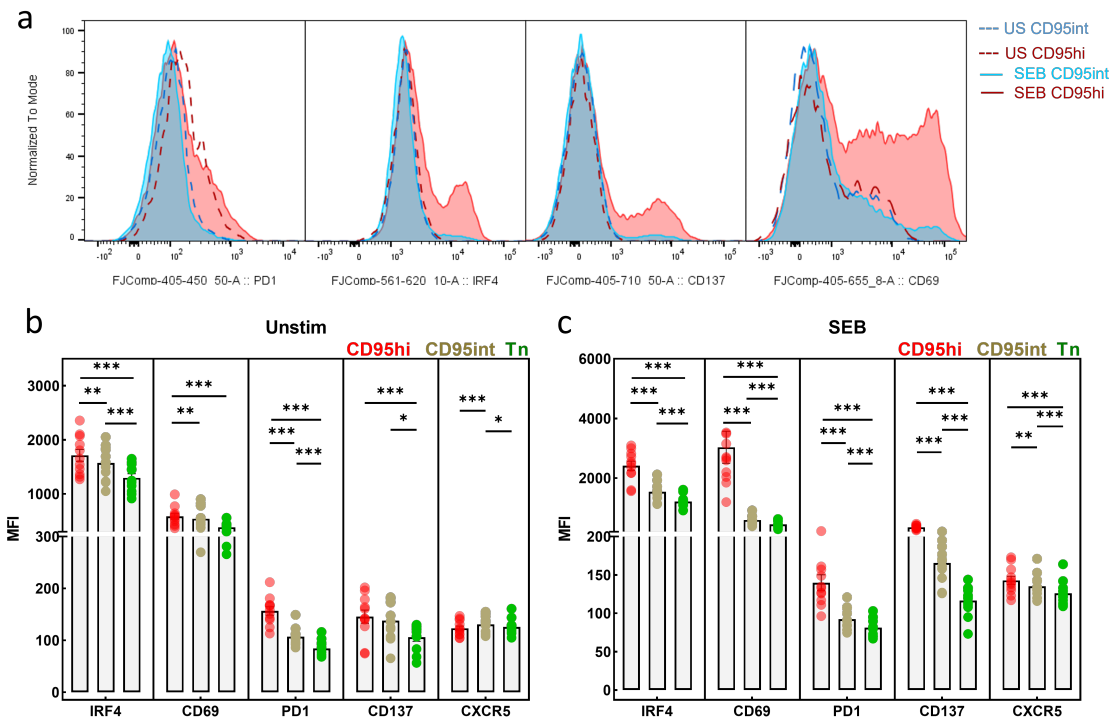



**Figure 4.8**: **Differential expression of activation and co-stimulatory markers on CD95hi and CD95int Tscm.** a) Representing histogram plots of n=11 concatenated PBMC samples, showing the expressing of PD-1, IRF4, CD137 and CD69 before (US, unstimulated, dashed line) and after SEB stimulation (solid line) on CD95hi (Red) and CD95int (blue). b-c) Column plots showing the MFI of IRF4, CD69, PD-1, CD137 and CXCR5 on CD95hi (Red), CD95int (brown) and naive T cells (green) subsets in Unstimulated (b) and SEB stimulated samples (c). Bars indicate mean ± s.e.m. Each dot represents a donor. Stats: Wilcoxon matched-pairs test *P<0.05, **P<0.01, ***P<0.001.

dia (unstimulated), while the other was stimulated by culturing with 2$\mu$g/mL $\alpha$CD3 and 1$\mu$g/mL $\alpha$CD28 antibodies. Bulk RNAseq was performed on these unstimulated and stimulated samples. The objective was to compare the transcriptional heterogeneity (a)between different memory subpopulations under unstimulated condition and (b) between unstimulated and stimulated condition. This way we are trying to understand the transcriptional dynamics and phenotypic differences between these sorted CD95hi and CD95int populations and their relationship with other memory subsets.

We are still doing the data analysis of this section.

## 4.3 Discussion

This study to understand the heterogeneity of Tscm population builds upon the previous research conducted by my labmate, Danai A. Koftori. Her earlier work revealed a correlation between Ki67 expression and CD95 within the Tscm compartment, with CD95hi cells showing a higher proportion of Ki67+ cells compared to CD95int and Tcm cells (Koftori, manuscript in preparation). She also explored the self-renewal and stemness capabilities of these subpopulations, finding that CD95hi cells displayed enhanced self-renewal and stemness potential under homeostatic conditions (IL-7/IL-15), but this ability was lost under TCR stimulation. Additionally, she examined the functional aspects of these subsets, demonstrating that CD95hi cells exhibited superior polyfunctionality in cytokine production compared to the CD95int subset (Koftori, manuscript in preparation). In continuation of this research, our study aims to delve into the cell division history, age-related changes, and tissue distribution patterns of these subsets.

To initiate our investigation, we first validated the relationship between Ki67 and CD95 expression within CD8+ T memory populations, specifically in the CD95hi and CD95int subsets. Our findings aligned with the data previously collected by Danai A. Koftori, that the frequency of Ki67+ cells is higher in CD95hi subset than CD95int and Tcm (Figure 4.1). These results were further supported by the lower TREC content in CD95hi subset suggesting that CD95hi and CD95int have different kinetics, with CD95hi exhibiting higher proliferation capacity than CD95int (Figure 4.5).

The dynamics of T cell subsets in the context of aging revealed significant alterations within Tscm populations. Notably, we observed an age-related accumulation in both total Tscm and the CD95hi subset (Figure 4.4). This increasing trend within our study can be attributed to the overall high frequencies of Tscm and CD95hi seen in our dataset as compared to D. Koftori (unpublished) and literature (Gattinoni et al. 2011, Zhao et al. 2021, Li et al. 2019, Hosokawa et al. 2016).

This age-related increasing trend of Tscm in our study contradicts with the results reported by Li et al. (2019), who observed a relatively low percentage of Tscm in CD8+ T cells ($0.98 \pm 0.53\%$) and noted stability in their frequency with age in peripheral blood across a wider age range (3-88 years, n=92). However, a

noteworthy similarity emerges when considering the ratio of Tscm to the CD8+ naïve population, which increased significantly with age in both our study and Li et al. (2019)'s findings. This suggests that while the absolute frequency of Tscm may not change substantially, their relative abundance compared to naive T cells may indeed rise over time.

Examining the ratio of Tscm to naive T cells (or CD8+ T cells) with age carries significant advantages in understanding the dynamics of the immune system during the aging process. This approach normalizes changes in the memory T cell compartment relative to the pool of naive T cells (or CD8+ T cells), providing a more precise measure of age-related alterations. It accounts for fluctuations in the total T cell population due to infections, vaccinations, or other immune challenges, allowing for a focused assessment of how memory T cells adapt over time. Importantly, it facilitates comparisons across studies and populations, enabling a standardized assessment of age-related changes in memory T cell composition.

Moreover, a study conducted by (Xia et al. 2022) supported a decreasing trend in Tscm frequency (as% of CD8+T cells) across three distinct age groups. Specifically, group 1 (18-44 years) exhibited a median Tscm frequency of 28.05% (range: 8.30-48.90%), group 2 (45-65 years) showed 11.6% (range: 2.67-31.81%), and group 3 (>65 years) displayed 6.1% (range: 1.3-21.86%). While the study by Xia et al. (2022) did not provide a direct analysis of the Tscm/Tnaive ratio with age, their provided reference ranges for Tscm and Tnaive in different age groups allowed us to calculate this ratio. Intriguingly, our calculations revealed an increasing trend in the Tscm/Tnaive ratio with age. This supports our data of significant elevation in the Tscm/Tnaive ratio, and that is primarily driven by the rising trend of CD95hi Tscm cells with increasing age. This intriguing result suggests that the frequency of CD95hi cells may play a substantial role in maintaining peripheral T cell memory homeostasis among older individuals.

While we observe an increasing trend in CD95hi cell frequency with advancing age, a noteworthy phenomenon accompanies this observation: the proportion of Ki67+ cells within the CD95hi subset decreases significantly as individuals age. This decline in Ki67 expression within CD95hi cells suggests a reduced proliferative rate among these cells with increasing age. Several plausible explanations for this

phenomenon exist. Firstly, it may stem from the complex interplay between proliferation, cellular senescence, and the maintenance of the CD95hi cell pool (Yang et al. 2021, Goronzy & Weyand 2019). It is well-established that sustained proliferation, particularly in aging cells, can activate mechanisms that lead to cellular senescence. Such mechanisms may encompass telomere shortening, DNA damage accrual, and inappropriate expression of oncogenes (Yang et al. 2021, Goronzy & Weyand 2019). In light of these considerations, CD95hi cells may transform as they age — a shift from highly proliferative cells to a state of quiescence, while remaining poised for potential immune responses. This change in proliferation dynamics may be a strategic adaptation to mitigate the risk of cellular senescence and hence lead to increased cell survival. Secondly, the age-related microenvironment could contribute to the conversion of CD95hi cells into Tpex cells, which are characterized by reduced proliferation (Zhao et al. 2021). Tpex cells are a subset of Tscm cells expressing exhaustion markers like PD-1 and TIGIT. These cells are known to exhibit diminished proliferative capacity compared to traditional Tscm cells (PD-1-TIGIT-) (Zhao et al. 2021). Furthermore, Pitsillidou et al. (2023) observed the accumulation of Tpex cells with age, reinforcing the notion that CD95hi cells may transform the Tpex subset as individuals grow older. Regrettably, our study did not directly investigate exhaustion markers on Tscm cells themselves. Therefore, further investigation is needed.

A logical question arises from this: if CD95hi cells exhibit reduced proliferation with age, what contributes to the overall increase in CD95hi cell frequency? Two potential mechanisms may be at play. Firstly, we can consider altered differentiation dynamics as a potential contributing factor (Nikolich-Žugich et al. 2012, Ahmed et al. 2017). Costa Del Amo et al. (2018) proposed that even in individuals without infections or diseases, there could be a continuous process where naïve T cells transform into Tscm cell type. Additionally, Danai's observations suggest that CD95hi can be differentiated from CD95int cells, also Tcm cells have the potential to generate CD95hi cells under cytokine stimulation, albeit in smaller proportions compared to CD95int subsets (manuscript in preparation). Furthermore, the re-acquisition of CD45RA by Tcm cells under cytokine stimulation, leading to an apparently naive phenotype (CD45RA+CCR7+), has been documented by Zhao et al. (2021), Gegi-

nat et al. (2003), suggests Tcm can give rise to Tscm. This implies that naïve T cell, CD95int or Tcm cells can differentiate to CD95hi under homeostatic conditions or cytokine stimulation, potentially contributing to the accumulation of CD95hi subpopulation. Secondly, by lowering the proliferation, these cells could counteract the cellular senescence and ultimately contribute to enhanced survival, which could also lead to its accumulation. Hence, Tscm subsets evolved in different ways with aging.

Our results indicated a significant presence of CD95int cells in LN as compared to PBMCs. Following SEB stimulation, the frequency of CD95int decreased, while the frequency of CD95hi increased in both tissues (Figure 4.7). The expansion of CD95hi could be due to their activated response to SEB stimulation or because of the differentiation of other memory subpopulations to CD95hi subsets upon stimulation. Conversely, the decrease in CD95int Tscm cells may be indicative of their transition into a more differentiated state or CD95hi upon stimulation. Since the cells were not sorted in this study, further investigation with sorted cells is needed to confirm these observations. Nevertheless, the MFI analysis of different activation and co-stimulatory molecules in PBMC samples further supported that CD95hi cells exhibit an activated phenotype, while CD95int cells maintain a more quiescent profile (Figure 4.8). Collectively, these findings strengthen our conclusion regarding the quiescent state of CD95int cells and their prevalence in LNC. Importantly, these findings align with two recent studies. In these studies, the researchers identified a subset of memory CD8+ T cells in human LN that exhibited quiescent characteristics, as evidenced by their expression of stem cell-associated TFs TCF-1 and LEF-1, and a lack of effector molecule expression (Miron et al. 2018, Reuter et al. 2017). These LN memory T cells exhibited increased proliferation to TCR-mediated stimulation and maintained higher TCR clonal diversity (Miron et al. 2018, Reuter et al. 2017). While, we did not directly investigate TCF-1 expression in our study, the negative relationship between TCF-1 and IRF4 (Man et al. 2017) suggests that CD95int cells, which expressed lower levels of IRF4 compared to CD95hi cells, may indeed express higher levels of TCF-1. Hence, we proposed that CD95int exhibits a quiescent state while maintaining the CD95hi population under homeostatic (Danai unpublished). These preliminary results prompt further exploration into the dynamics of Tscm subsets in response to immune challenges.

We were also interested in investigating any phenotypic difference between the same memory subpopulation present in different tissues. We observed that the Tscm population present in LNC and PBMCs exhibit different expressions of CCR7 and IRF4 suggesting tissue-specific variations in the phenotypes and potential functions of Tscm populations. This highlights the importance of considering the tissue microenvironment in understanding T-cell biology.

Heterogeneity within Tscm cells has also been recently observed by Zhao et al. (2021), who suggested that the Tscm compartment can be further categorized into a CD122hi subset and a CD122lo subset. The former demonstrates increased proliferation, multipotency, and polyfunctionality compared to the latter. Galletti et al. (2020) described Tscm heterogeneity based on exhaustion markers PD-1 and TIGIT, identifying Tpex (CCR7+TIGIT+PD1+) and Tstem (CCR7+TIGIT- PD1-) subsets in homeostatic conditions in humans. However, it's worth noting that we did not utilize TIGIT marker in our study directly.

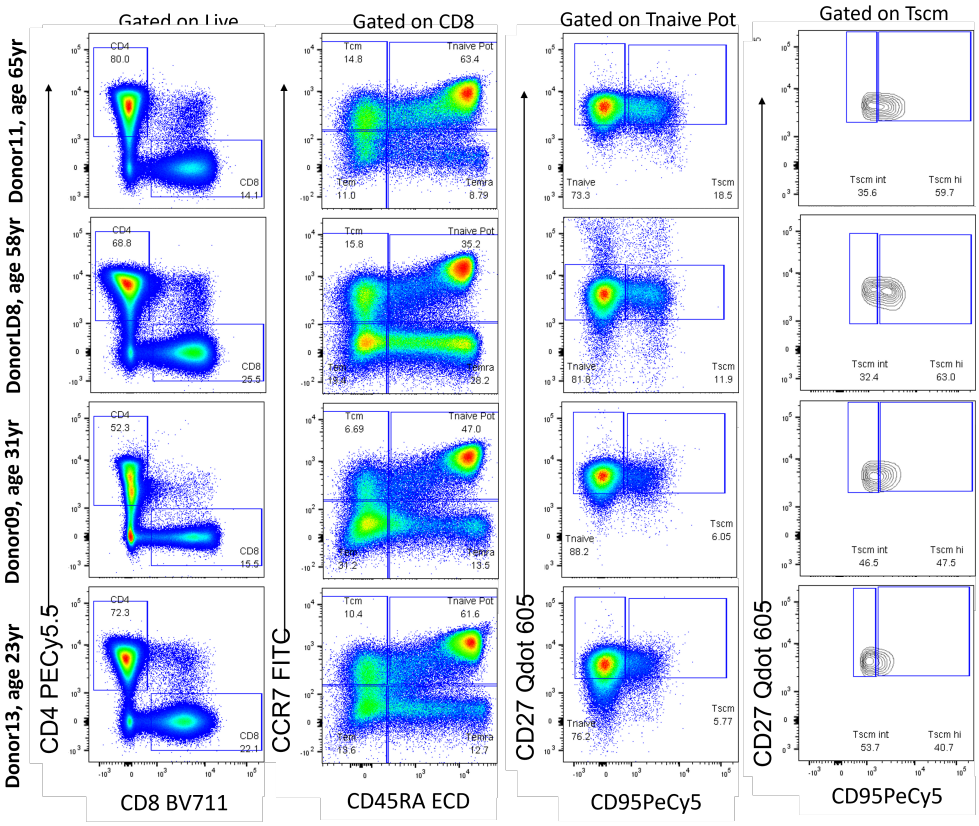
Our study has a limitation worth noting. When analyzing various memory T cell subsets, changes are often observed in the proportion or percentage of these subsets within the overall T cell population. However, such changes may not necessarily lead to significant alterations in the absolute number of cells. This discrepancy can be attributed to variations in the specific subsets being examined. For example, if there is an overall decrease in the total number of CD8 T cells, any changes in the number of specific subsets may be less pronounced due to their dilution within this smaller population. These findings suggest that both the proportion and absolute number of naïve T cells are physiologically linked to the aging process. It's important to note that this study did not involve absolute quantification of T cell subpopulations, which could provide different insights.

Previous research has highlighted potential challenges in characterizing memory T cells solely based on surface marker expression, as phenotypic markers may not consistently correlate with the cell's memory status (Jameson and Masopust, 2018; Jameson, 2021). Using Ag-specific Tscm cells for a certain pathogen such as CMV or influenza A would give us increased confidence that Tscm cells are indeed true memory cells. For this, we have investigated longitudinal HIV trial vaccination studies where we quantify HIV-specific Tscm at different time points following vaccination

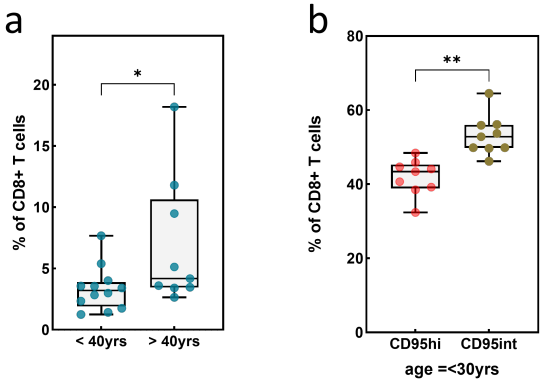
(Chapter 6). To quantify antigen-specific cells from these samples, we optimised an in-house AIM assay in the following chapter (Chapter 5).

In summary, we show that the Tscm population harbors heterogeneity with subsets defined by the expression of CD95 exhibiting reasonably distinct phenotype, age-related variability, distinct cell division history and tissue distribution. We recommend further investigations into the molecular mechanisms governing these changes and their functional implications.

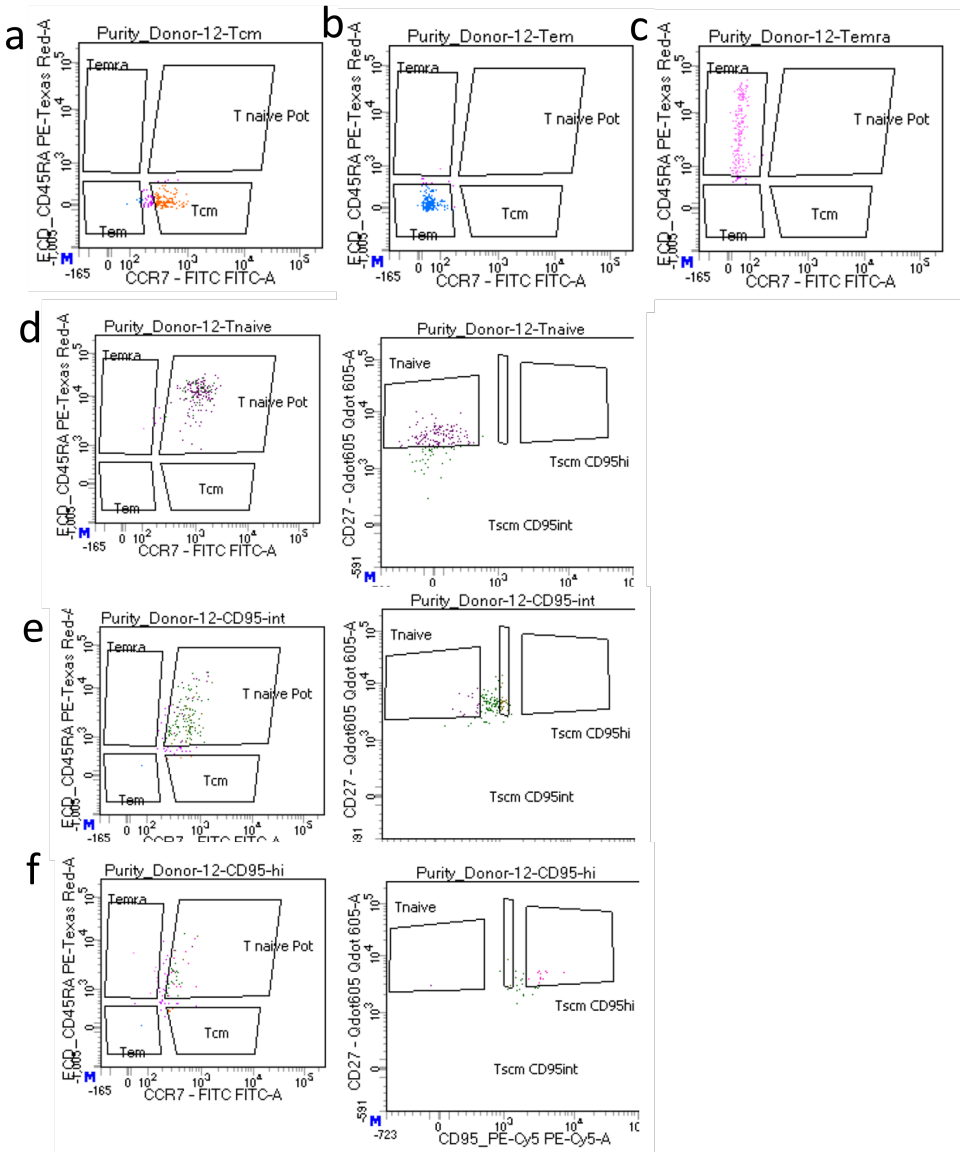
## 4.4 Supplementary Figures




**SuppFigure 4.1**: **Gating strategy for Tscm subsets in donors of different ages.**




**SuppFigure 4.2**: **a)Frequency of Tscms in individuals younger and older than 40 years. b)Frequency of Tscm subsets, CD95hi and CD95int, in individuals younger and older than 30 years**




**SuppFigure 4.3**: **Sorting purity of different memory subpopulations.** Plots representing the sorting purity of a)Tcm, b)Tem, c)Temra, d)Tn, e)CD95int, and f)CD95hi memory subpopulations. Tight gates were applied to avoid contamination with other subpopulations

# Chapter 5

# Comparison of activation-induced markers to detect antigen-specific CD8+T cells

## 5.1 Introduction

Cytotoxic T lymphocytes (CD8+ T cells) play a pivotal role in adaptive immunity, effectively controlling viruses, bacteria, and tumors. The study of CD8+ T cell responses can be categorized into two main approaches: bulk CD8+ T cell analysis, which examines these cells without considering their antigen-specificity, and the investigation of CD8+ T cells that specifically target a particular antigen of interest called antigen-specific CD8+T cell analysis.

While bulk lymphocyte analysis provides valuable insights into the overall immune system's status, it has limitations. It doesn't reveal which antigens triggered the immune response, the magnitude of these responses, or the involvement of specific immune cell subsets. Consequently, it falls short of offering a precise understanding of the intricate immune mechanisms at work during an immune response. Conversely, studying antigen-specific T cells allows researchers to focus on immune cells directly engaged in recognizing and responding to specific pathogens or antigens (Hont et al. 2022). This approach is essential for various areas of immunological research, including infectious diseases and vaccine responses.

Analyzing antigen-specific lymphocytes poses challenges due to the typically low

frequency of these cells, the vast diversity of TCRs, and the polymorphic nature of MHC (Cossarizza et al. 2021, Poloni et al. 2023). Traditional techniques for detecting antigen-specific T cells involve measuring cytokine production through methods like ELISpot (Leehan & Koelsch 2015) or intracellular cytokine secretion (ICS),(Lovelace & Maecker 2018, Rodrigues et al. 2017) tracking cellular proliferation through methods like BrdU incorporation (Kojima et al. 2021) or cytoplasmic dye dilution (Terrén et al. 2020, Stempels et al. 2022), and quantifying T cells binding to a specific MHC:peptide using multimers (Rudolph et al. 2006, Casalegno-Garduño et al. 2010, Chang 2021). While these techniques provide valuable data, they have their limitations.

Cytokine-based techniques (ICS and ELISpot) may be biased, as some subpopulations secrete more cytokines than others (Roederer et al. 2004, De Rosa et al. 2004). Additionally, they have a high limit of detection for cytokines, potentially missing cells with lower cytokine secretion and there is a need to do intracellular staining that hamper the downstream processing (Poloni et al. 2023). Proliferation-based assays can detect the presence of a response but are not suitable for quantification due to fluctuations in cell numbers during the assay, raising concerns about specificity (Duque & Rakic 2011). The use of MHC-peptide multimer complexes is a breakthrough, offering detailed information about cells with precise specificity, yet it depends on prior knowledge of individuals' MHC genotypes and the epitopes they respond to (Chang 2021).

An alternative, the activation-induced marker (AIM) T cell assay, overcomes some of these limitations. In this assay, cells are cultured with the antigen of interest, and activation is detected through flow cytometry, based on the upregulation of TCR-stimulated markers such as CD69, CD137, CD154, and OX40 (Reiss et al. 2017, Betts et al. 2003, Frentsch et al. 2005). The AIM assay is accurate and straightforward, enabling comprehensive characterization of the total pool of antigen-specific cells without prior knowledge of specific epitopes or individual MHC genotypes.

Different markers are used by different researchers to define antigen-specific CD8+T cells as follows:

### 5.1.1 OX40-CD25 combination

OX40 is a membrane-bound costimulatory molecule found on both CD4+ and CD8+ T cells, and its expression is transiently induced by TCR-specific activation (Lee et al. 2006, Mallett et al. 1990, Paterson et al. 1987). OX40 expression shows delayed kinetics, with optimal expression occurring approximately 24-48 hours after stimulation for both CD4+ and CD8+ T cells (Walker et al. 1999, Rogers et al. 2001, Bansal-Pakala et al. 2004). However, it's worth noting that CD8+ T cells tend to exhibit lower levels of OX40 expression compared to CD4 T cells (Croft 2009).

Initially, researchers used OX40 in combination with CD25 to detect CD4+ T cells responsive to antigens or peptides derived from various infections or vaccinations, including influenza, mycobacteria, CMV, tetanus toxoid, and HIV-1 (Zaunders et al. 2009, Keoshkerian et al. 2012). This marker combination was particularly useful for estimating antigen-specific CD4+ T cells, including rare germinal center Tfh (GC Tfh) cells that are challenging to detect using ICS due to their minimal cytokine secretion (Dan et al. 2016).

However, the use of OX40 as a biomarker for CD8+ T cell antigen specificity has been limited, with relatively fewer studies compared to CD4+ T cells. A recent study by Bowyer et al. (2018) applied OX40 in combination with both CD25 and CD107 in the AIM assay, with 20 hours of peptide stimulation, to detect vaccine-specific CD8+ T cells from the PBMCs of individuals vaccinated with an Ebola vaccine candidate. The results indicated that the AIM assay detected antigen-specific CD8+ T cells at 1.2-1.8 times higher levels than ICS, with comparable lower limits of detection (Bowyer et al. 2018). However, this study lacked an in-depth investigation of key parameters such as the optimal stimulation time for OX40 expression on CD8+ T cells, a comparison with established methods like tetramer staining, and an assessment of potential bystander activation in CD8+ T cells. Additionally, most of the references used in this study pertained to CD4+ T cells, emphasizing the need for further research to validate and optimize the OX40-CD25 combination specifically for CD8+ T cells.

In conclusion, while OX40 in combination with CD25 has shown promising results as an AIM assay for CD4 T cells, further research is needed to assess its sensitivity and specificity for CD8+ T cells.

### 5.1.2 HLADR-CD38 combination

HLA-DR and CD38 are widely recognized as markers of immune activation, particularly on CD8+ T cells, during various viral infections such as EBV, YFV, Influenza, Dengue, Ebola, and HIV-1 (Callan et al. 1998, Chandele et al. 2016, Fox et al. 2012, Hua et al. 2014, Miller et al. 2008). HLA-DR is a MHC class II surface receptor that is constitutively expressed by professional APCs and plays a crucial role in processing and presenting exogenous antigens to CD4-restricted T cells. Interestingly, in the late 1970s and 1980s, researchers reported the expression of MHC class II surface receptors, including HLA-DR, on activated T cells, leading to the classification of T cells as non-professional APCs (Lanzavecchia et al. 1988, Ko et al. 1979).

The expression of HLA-DR on T cells follows a delayed kinetic pattern, with surface expression occurring approximately 3 to 5 days after T-cell activation (Holling et al. 2004, Caruso et al. 1997). CD38, on the other hand, is a transmembrane molecule present on the surface of various immune cells, including T cells, B cells, Natural Killer cells, neutrophils, and myeloid cells (Choe et al. 2011, Bolzoni et al. 2019, García-Rodríguez et al. 2018). CD38 is involved in crucial cellular processes such as cell adhesion, activation, migration, apoptosis, and differentiation (Choe et al. 2011, Bolzoni et al. 2019, García-Rodríguez et al. 2018). In T cells, CD38 is constitutively expressed by naive T cells and shows minimal expression in resting memory cells. However, its expression is elevated upon T-cell activation (Dianzani et al. 1994).

The combination of HLADR+CD38+ markers is widely employed for ex-vivo detection of antigen-specific CD8+ T cells in various vaccination studies including, EBV (Callan et al. 1998), YF (Miller et al. 2008)and Malaria (Schwenk et al. 2013) vaccinations. These studies have noted that early after vaccination, antigen-specific tetramer+ CD8+ T cells exhibited a significant portion of the HLA-DR+ CD38+ phenotype, resembling an effector phenotype. However, at later timepoints, particularly beyond three months, these antigen-specific tetramer+ cells gradually reduced their HLADR and CD38 expression (Miller et al. 2008, Schwenk et al. 2013, Callan et al. 1998). This gradual reduction can present challenges when using this marker combination to study antigen-specific long-term memory responses that naturally develop after a disease or immunization. Nevertheless, the use of this

marker combination for ex-vivo detection of antigen-specific CD8+ T cells offers distinct advantages in studying immune responses without the need to restimulate the cells. However, it's worth noting that this approach may lead to the omission of antigen-specific cells at later timepoints, primarily because most of these cells have transitioned into a quiescent memory state by that time and have downregulated HLA-DR and CD38 markers of activation. Hence, HLADR+CD38+ phenotype on CD8+ T cells represents an activated effector phenotype and serves as a valuable marker for assessing early immune responses following infection or immunization.

It is important to note that this phenotype may also constitute a discrete subset of hyper-activated pathogenic cells, as observed in diseases like HIV (Ndhlovu et al. 2015, Sachdeva et al. 2010, Hua et al. 2014) and COVID-19 (Song et al. 2020, Du et al. 2021). In these studies, the frequency of HLADR+CD38+ CD8+ T cells population positively correlates with the severity of the disease and is heterogeneous. HLA-DR+CD38hi subpopulations exhibited exhaustion and inhibitory markers, stimulatory checkpoints, impaired cytotoxicity, highly apoptotic and more exhausted transcriptional regulation as compared to HLA-DR+CD38dim, Indicating that HLA-DR and CD38 co-expression on CD8+ T cells could be a result of immune exhaustion or hyperactivation in HIV and COVID (Sachdeva et al. 2010, Song et al. 2020).

To conclude, the HLA-DR+ CD38+ CD8+ T cell phenotype is an activated effector phenotype that could potentially be used to determine early immune responses after infection or immunization, while considering that it also could constitute a discrete subset of hyper-activated pathogenic phenotype as in HIV and COVID. It is clear that the expression of HLA-DR and CD38 become greatly reduced at the later timepoints both during infection/immunization, which challenges the use of this combination to study the antigen-specific long-term memory responses generated naturally after a disease or immunization. However, further studies could investigate if restimulation would help to detect antigen-specific populations at later timepoints.

### 5.1.3 CD137 and its combinations

CD137, also known as 4-1BB, ILA, and TNFSFR9, is a co-stimulatory receptor belonging to the tumor necrosis factor receptor (TNFR) superfamily. It is preferentially expressed by antigen-activated CD8+T cells, as well as by $\gamma\delta$+ T cells and CD4+ Treg cells. CD137 binds to its ligand, 4-1BB-L, present on APCs, and plays a role in promoting T cell activation, proliferation, and survival (Wolfl et al. 2007). Its expression is induced early, typically within 16-24 hours of T-cell stimulation, making it useful for identifying and selecting antigen-specific CD8+ T cells (Maino et al. 1995). CD137 is particularly valuable as a marker for several reasons:

- **Direct Staining and Viability:** CD137's early activation kinetics allow for direct staining, and the cells remain viable, enabling the sorting of antigen-specific cells or other downstream applications (Wolfl et al. 2007, Wölfl et al. 2008, Wehler et al. 2008).
- **Broad Expression:** CD137 upregulates on all subpopulations of CD8+ T cells, including T naïve, T memory, and T effector phenotypes(Wolfl et al. 2007, Wölfl et al. 2008, Wehler et al. 2008).
- **Low Background:** In healthy individuals, the background level of CD137 in unstimulated samples is low compared to other early activation markers such as CD69 and CD25 (Wolfl et al. 2007, Wölfl et al. 2008, Wehler et al. 2008).
- **Limited Bystander Activation:** CD137 is directly activated through TCR signaling, reducing the likelihood of bystander activation (Wolfl et al. 2007, Wölfl et al. 2008, Wehler et al. 2008).

Furthermore, studies have demonstrated that the frequency of CD137+ CD8 T cells correlates well with pMHC multimer+ cells, indicating a low frequency of false-positive antigen-specific cells detected by CD137

Recent studies, particularly in the context of COVID infection and vaccination, have combined CD137 with a second activation marker, CD69, and defined the 'CD8+CD69+CD137+' phenotype as AIM+ cells (Dan et al. 2021, Jung et al. 2021, Grifoni et al. 2020, Tarke et al. 2021). Other markers like OX40, TNF, CD107, and CD154 have also been used in combination with CD137 to boost the detection of

antigen-specific CD8+ T cells. Takahama et al. (2021) suggested combining CD137 with CD107, TNF, and OX40 as AIM+ CD8 T cells, but this approach requires further validation and comparison with a validated method like multimers. Similarly, Van de Sandt et al. (2016) and Klinger et al. (2013)have used CD137 in combination with CD69 and CD107 or alone to study CD8+ T cell activation in response to specific pathogens. Additionally, recent studies have explored novel combinations, such as CD137 with IRF4, to measure antigen-specific CD8+ T cell responses and observed high specificity and sensitivity (Wu et al. 2019). This study has shown promising results, suggesting that CD137-IRF4 may be a superior AIM assay marker combination for antigen-specific cell identification. CD137 alone seems a robust marker for identifying antigen-specific CD8+ T cells, but the choice of whether to use a second activation marker alongside CD137 in AIM assays depends on the specific research objectives and the need for additional sensitivity and specificity in the assay. Further validation and comparative studies are essential to determine the most effective marker combinations for specific research applications.

Reviewing this literature search, it appears that while there has been extensive research on various AIM markers for identifying antigen-specific CD8+ T cells, there is still a lack of comprehensive comparative studies that directly evaluate the performance of different AIM marker combinations. Additionally, there is limited research that specifically investigates the reliability and universality of these markers across different contexts and diseases. Therefore, there is a study gap in understanding which AIM marker combinations are the most effective and whether a universal marker or marker combination can be identified for accurately quantifying antigen-specific CD8+ T cells.

We hypothesize that the choice of AIM marker combinations significantly impacts the accuracy and specificity of quantifying antigen-specific CD8+ T cells. To test this hypothesis, we conducted a comparative study that assessed the performance of various AIM marker combinations in the context of flu vaccination and compared the results with pentamer+ true antigen-specific CD8+ T cells.

## 5.2 Results

### 5.2.1 Dynamic of AIM marker combinations on Flu-specific CD8+T cells over time

The objective of this study was to identify the most effective combination of AIM markers, ensuring a reliable quantification of cells specific to the Flu antigen. To accomplish this goal, we isolated the PBMCs from the blood of HLA-A2+ individuals who had received influenza vaccination (15-40 days post-vaccination). These PBMCs were subsequently subjected to stimulation with the HLA-A2–restricted influenza M1 (Flu-M1) peptide, GILGFVFTL, for various time intervals, including 12, 18, 24, 36, 42, and 48 hours stimulation, at a temperature of 37°C. Following stimulation, cells were stained with various AIM markers, including HLA-DR, CD38, OX40, CD25, IRF4, CD137 and CD69. In addition, CD8+ T cells were prelabeled using a HLA-A2-Flu-M1–specific MHC class I pentamer. Subsequently, we compared the frequencies of distinct AIM marker combinations expressed by Flu-specific CD8+ T cells, characterised as CD8+Pentamer+ T cell population across these diverse time points. The Gating Strategy is shown in Figure 5.1.

We observed that the majority of pentamer+ cells upregulated expression of CD69, IRF4, and CD137, while the levels of co-expressed HLA-DR and CD38 remained negligible even up to 24 hours post-stimulation (Figure 5.2). Notably, after 12hr of peptide stimulation, nearly 80% (median) of pentamer+ cells displayed co-expression for CD69 and CD137 and CD137 alone, surpassing the levels of IRF4CD137, IRF4CD25 and OX40CD25 co-expressions (median:65%) albeit non-significantly (Figure 5.2). In contrast, after 24hr of stimulation, no difference was observed between the expression of CD137 alone, CD69CD137, and IRF4CD137 combinations (Figure 5.2). It is important to note that the frequency of different AIM markers within Pentamer+CD8+ T cells in unstimulated samples remained consistently below 5% (Figure not shown here).

The Results for the 36-hour, 42-hour, and 48-hour timepoints have not presented as the peak expression of CD137, CD69, and IRF4 was consistently observed between the 12-hour and 24-hour marks. The inclusion of these later time points was aimed at investigating the kinetics of markers upregulated at later stages post-activation,

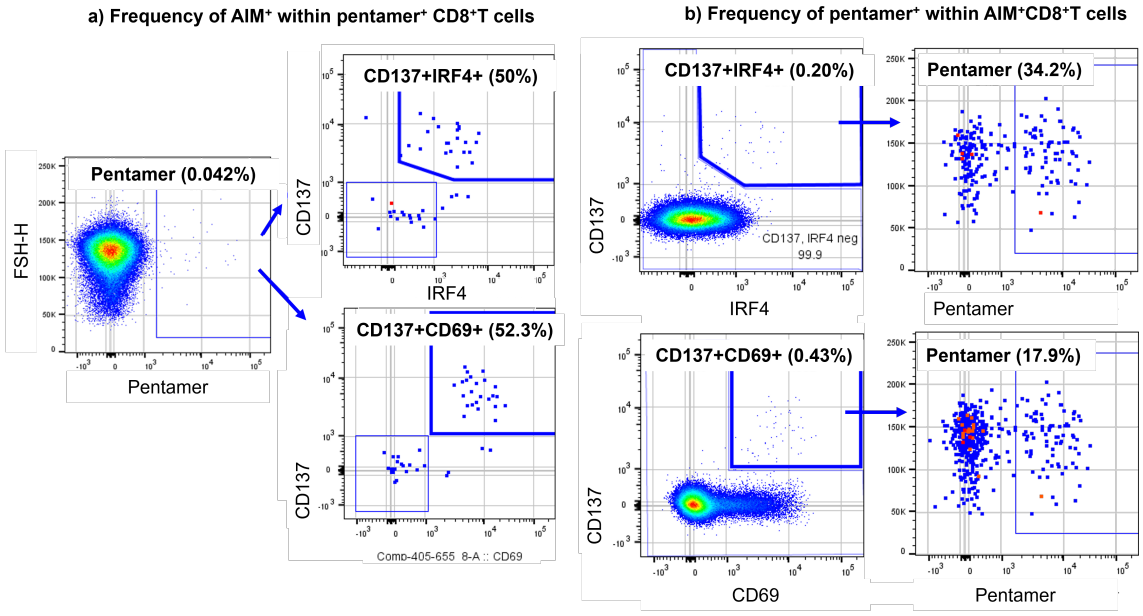



**Figure 5.1**: **Gating strategy used to gating Flu-specific CD8+ T cells and its comparison with AIM combinations** The Left figures illustrates the gating strategy employed to quantify the frequency of different AIM+ cells expressed by pentamer+CD8+ T cells. Firstly, pentamer cells were gated on live CD8+ T cells, and various combinations were explored within this population. The left panel (a) represents the frequency of CD137+IRF4+ cells (top plot) and CD137+CD69+ cells (bottom plot) expressed by Pentamer+CD8+ T cells. The Right figure (b) illustrates the gating strategy employed to quantify the frequency of pentamer+CD8+ T cells expressed by different AIM+ marker combinations. The frequency of Pentamer+ cells expressed by CD8+AIM+ cells, using CD137IRF4+ (top panel) and CD69CD137 (bottom panel) AIM combinations.

such as OX40. As illustrated in Figure 5.2, our data indicates a rising trend in the expression of OX40CD25 and also IRF4CD25 double-positive pentamer+ CD8 T cells over time, suggesting their delayed upregulation.

### 5.2.2 Performance assessment of AIM markers: Sensitivity Specificity

Evaluating the sensitivity and specificity of various AIM marker combinations represent a pivotal aspect of our study, particularly concerning the detection of antigen-specific T cells. Sensitivity, calculated by the ratio of number of True Positives to the sum of number of True Positives and False Negatives, indicates how effectively markers can correctly identify true positive cells. Specificity, calculated by the ratio of number of True negatives to the sum of number of True negatives and False

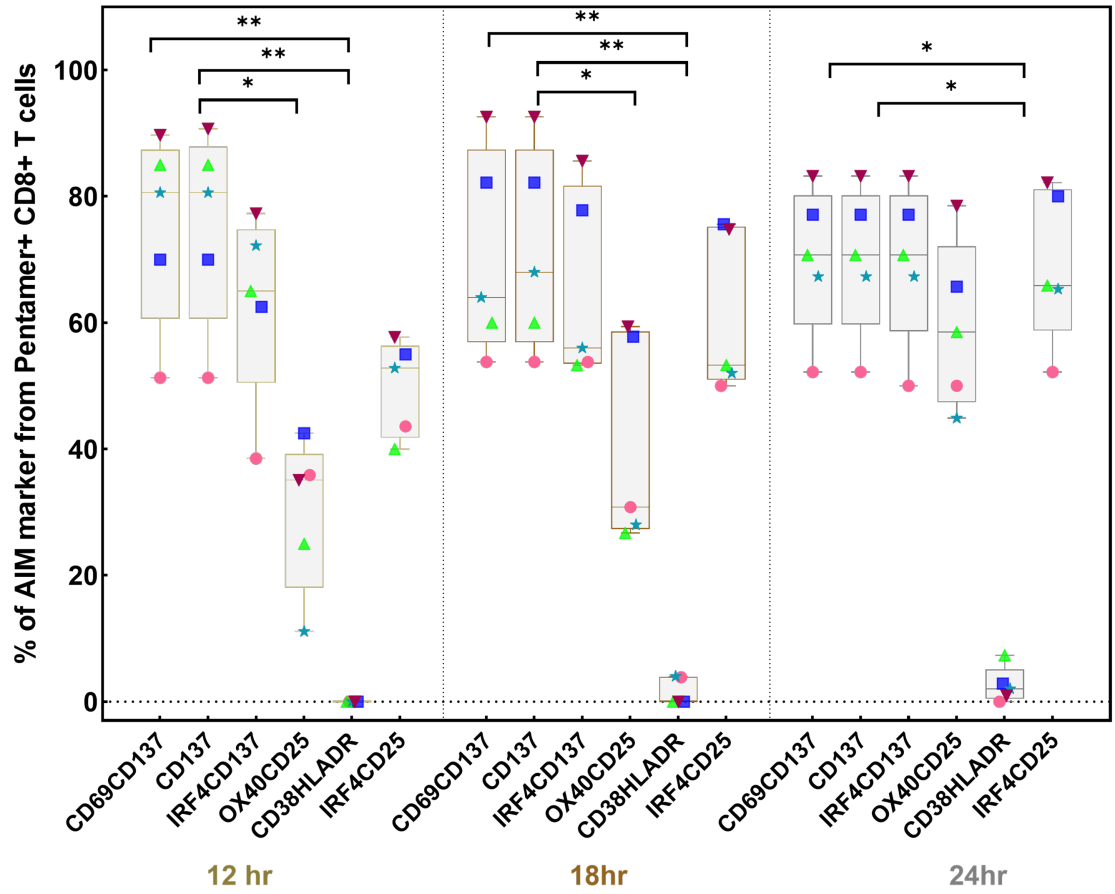



**Figure 5.2**: **Frequencies of various AIM Marker Combinations from CD8+ Pentamer+ T Cells at 12hr, 18hr, and 24hr Timepoints.** PBMCs were stimulated with the flu-M1 peptide for 12 hours, 18 hours, and 24 hours, followed by staining with various AIM markers. The figure displays a box and whisker plot showing all data points, including lower quartile, median, and upper quartile values for the frequencies of AIM marker combinations expressed by CD8+ Pentamer+ T cells. Different colored symbols represent different donors. Statistical analysis: Friedman test with Dunn's multiple comparisons, results displayed: *p<0.05, **p<0.01, ***p<0.001.

positives, illustrates the ability to minimize false positive results. These are crucial parameters for assessing markers' performance. Therefore, to determine the AIM marker combination that provides the most accurate identification of antigen-specific CD8+ T cells, we calculated the specificity and sensitivity in our data.

Sensitivity analysis revealed that after 12hr, 18hr and 24hr of stimulation, no significant differences were observed between CD69CD137, CD137 alone and IRF4CD137 combinations, significantly surpassing the other two combinations of OX40CD25 and HLADRCD38 (Figure 5.3).(Figure 5.3). Furthermore, we observed an increasing

sensitivity for OX40CD25 with time while HLDR-CD38 did not exhibit a comparable trend, Consequently, we chose to focus our further analysis on comparing the CD69CD137, CD137 alone, and IRF4CD137 combinations.

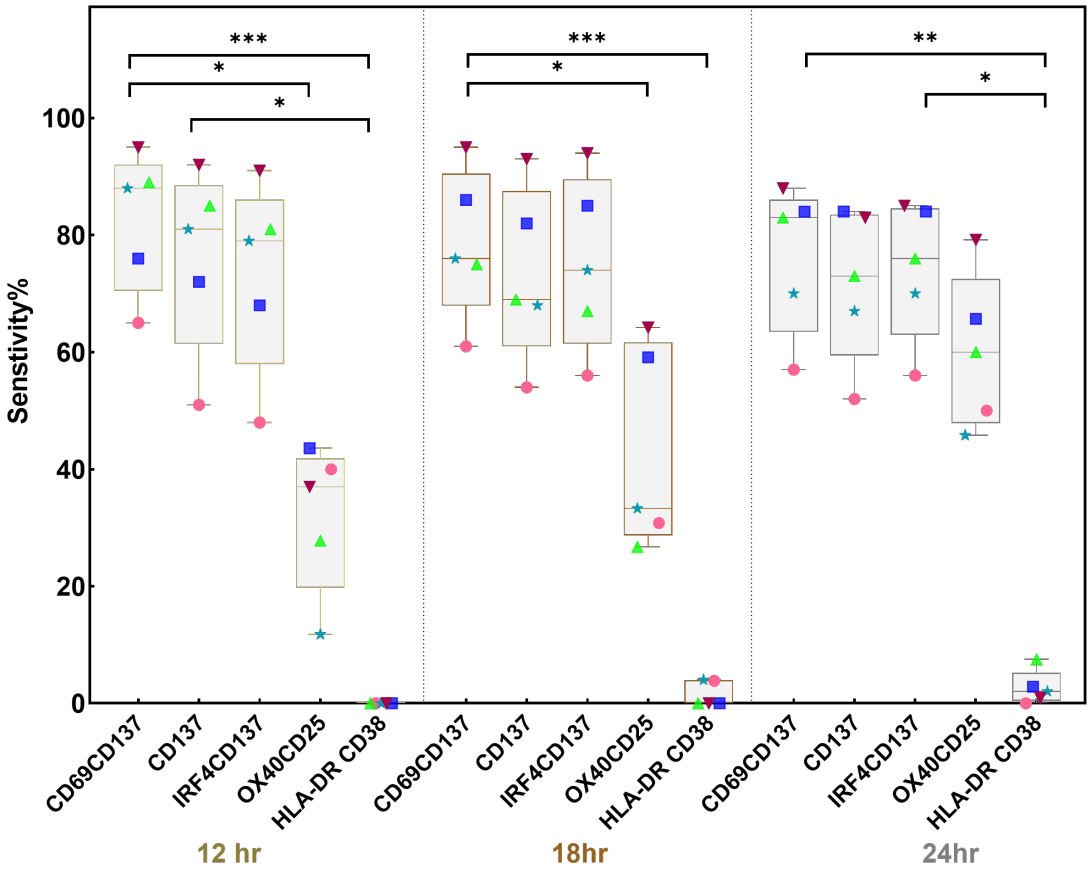



**Figure 5.3**: **Sensitivity of different AIM marker combinations to detect antigen-specific CD8+ T cells**. Sensitivity% was calculated as (Freq of Pentamer+AIM+ cells/(Freq of Pentamer+AIM+cells + Freq of Pentamer+AIM- cells)*100. The figure displays a box and whisker plot showing all data points, including lower quartile, median, and upper quartile values for the sensitivity of AIM marker combinations. Different colored symbols represent different donors. Statistical analysis: Friedman test with Dunn's multiple comparisons, results displayed: *p<0.05, **p<0.01, ***p<0.001.

Our study had a limitation in determining specificity due to the experimental design. The standard method for calculating specificity, which relies on the calculation of true negatives and true positives, was not possible in our data. The reason is that we used only one specific pentamer designed for a particular HLA allele in our study. It's possible that some cells might be antigen-specific but not detected by the chosen pentamer because the Flu peptide can be presented by different HLA alleles (Choo et al. 2014). Hence, pentamer- cells do not represent True negatives. There-

fore, the traditional specificity formula was not applicable. Instead, we assessed specificity by looking at the frequency of pentamer+ cells within the AIM+CD8+ T cell population. This approach considers our use of AIM marker combinations as a broad indicator of antigen specificity and then pinpoints the proportion of these AIM+CD8+ T cells that are also pentamer+. This method provides a more reliable measure of specificity in the context of our study's goals and potential limitations.

With this, the IRF4CD137 combination emerged as the most specific marker combination for detecting antigen-specific CD8+ T cells at all the timepoints Figure 5.4. The frequency of Pentamer+ cells within AIM+CD8+ T cells was not 100% or near because of the same reason stated above that we only used one pentamer specific for one HLA allele. Nonetheless, given that our study is a comparative analysis, this limitation does not significantly impact our overall analysis. Notably, the lower specificity observed with the CD69CD137 combination, despite its excellent sensitivity, was unexpected.

Overall, CD69CD137 and CD137 were highly sensitive, but their low specificity indicated that they might yield a high number of false positives, making them less specific. To investigate this, we measured the background levels in these markers.

### 5.2.3 Background levels for AIM marker combinations

Based on our earlier findings, the decreased specificity of the CD69CD137 and CD137 marker combination may be attributed to its tendency to detect not only true positives but also false positives. To gain a deeper understanding of this phenomenon, we analyzed background levels by assessing both the fold change (expressed as the ratio of positive cells in stimulated samples to unstimulated samples) and false positives (expressed as frequency of AIM+ in unstimulated samples). Intriguingly, our results revealed the highest background levels in the CD69CD137 and CD137 alone marker combination, which exhibited an upward trend over time (Figure 5.5). In contrast, the IRF4CD137 combination displayed lower and consistent background levels throughout the study (Figure 5.5).

These findings suggest that CD69CD137 and CD137 alone may suffer from reduced specificity due to their increasing background levels, which could contribute to the detection of false positives over time. In contrast, the IRF4CD137 combina-

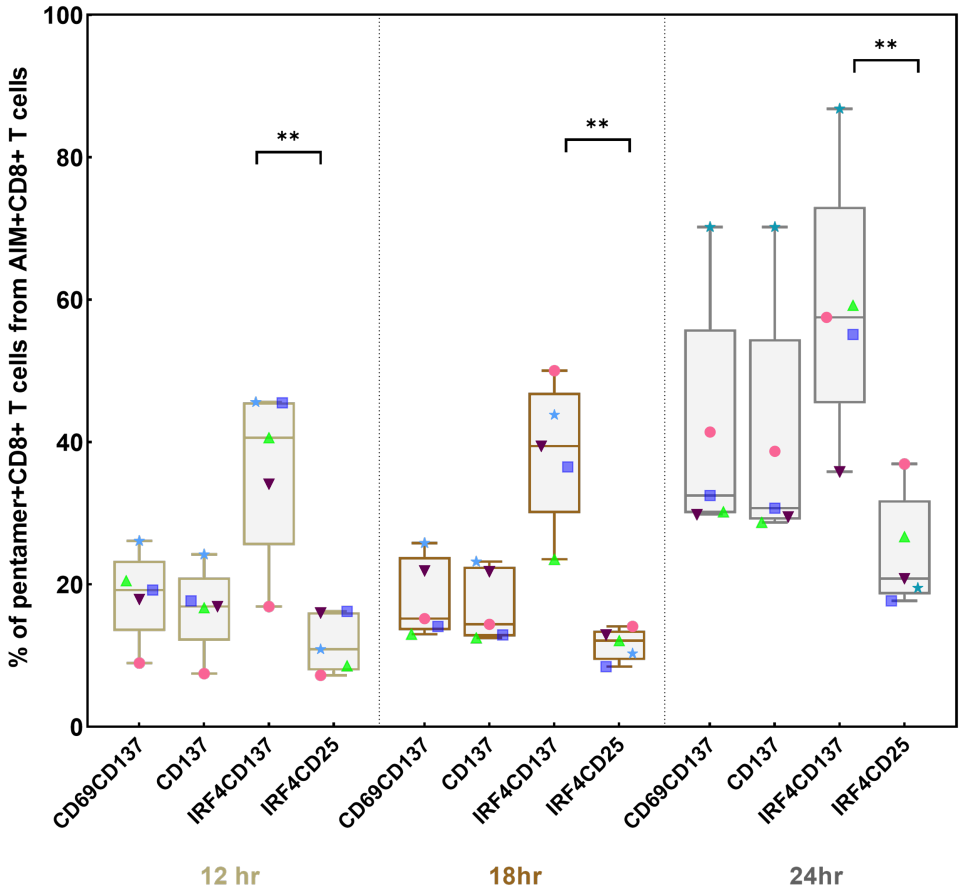



**Figure 5.4**: **Specificity of different AIM marker combinations to detect antigen-specific CD8+ T cells**. Specificity was calculated by assessing the frequency of pentamer+cells within AIM+CD8+ T cells. The figure displays a box and whisker plot showing all data points, including lower quartile, median, and upper quartile values for the specificity of AIM marker combinations. Different colored symbols represent different donors. Statistical analysis: Friedman test with Dunn's multiple comparisons, results : *p<0.05, **p<0.01, ***p<0.001.

tion maintains better specificity by maintaining lower and stable background levels throughout the experimental period.

### 5.2.4 Bystander responses to different AIM marker combinations

One potential reason for the detection of false positives using these markers could be bystander activation of the cells. Bystander activation, characterized by the non-TCR-mediated upregulation of surface markers, may arise due to cell culture contaminants or factors secreted by neighboring cells, potentially leading to false-

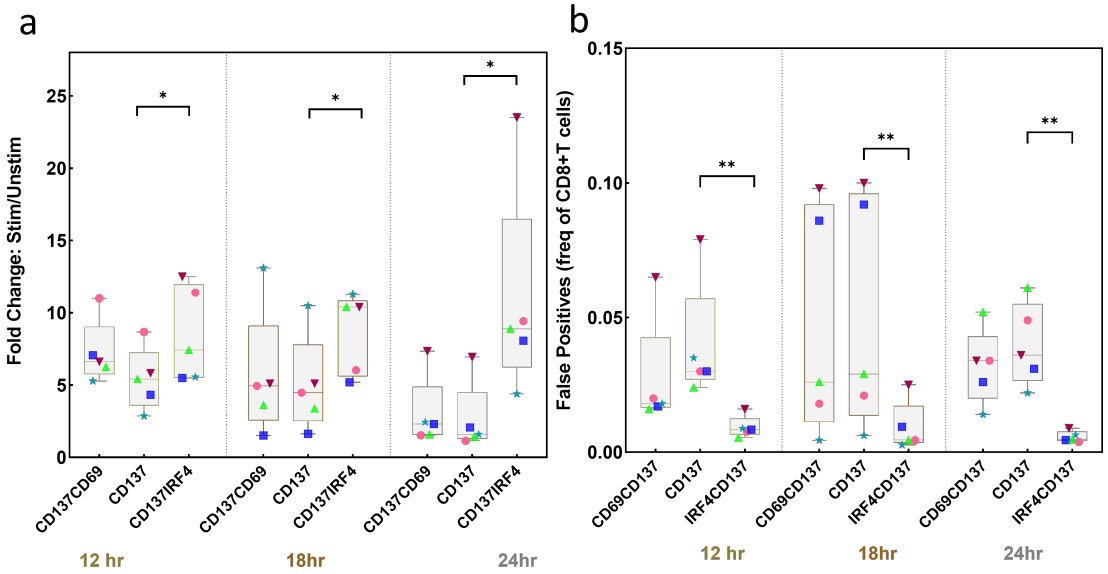



**Figure 5.5**: **Comparison of background levels in different AIM marker combinations** a) A box and whisker plot showing all data points, including lower quartile, median, and upper quartile values for the fold change of AIM marker combinations b) Frequency of false positive from CD8+ T cells observed in various AIM marker combination. Different colored symbols represent different donors. Statistical analysis: Friedman test with Dunn's multiple comparisons, results, results displayed: *p<0.05, **p<0.01, ***p<0.001.

positive results. Therefore, evaluating bystander activation within the context of this study is essential for identifying the optimal AIM combination. We aimed to minimize bystander activation in our assay to enhance its specificity.

To investigate this phenomenon, we inhibited the interactions between TCRs and pMHC complexes in PBMCs isolated from the blood of healthy individuals. This inhibition was achieved by adding varying concentrations of pan-MHC class I monoclonal antibodies (mAbs) ranging from 10 to 100 $\mu$g/mL into the cell cultures. To induce robust yet antigen-specific CD8+ T-cell responses in PBMC cultures, we utilized a CEFX peptide pool, a common positive control containing MHC class I peptides derived from antigens expressed by CMV, EBV, and influenza virus. Our results revealed that the frequency of IRF4CD137+CD8+ T cells decreased proportionately with increasing concentrations of pan-MHC class I mAb (Figure 5.6b). In contrast, increase trend in CD69CD137+ CD8+ T cell was observed with the increasing concentration of blocking antibody, with highest frequency seen at the highest concentration (Figure 5.6a). We also validate this finding on PBMCs isolated from HIV trial vaccinated individuals, stimulated with the HIV peptide pool

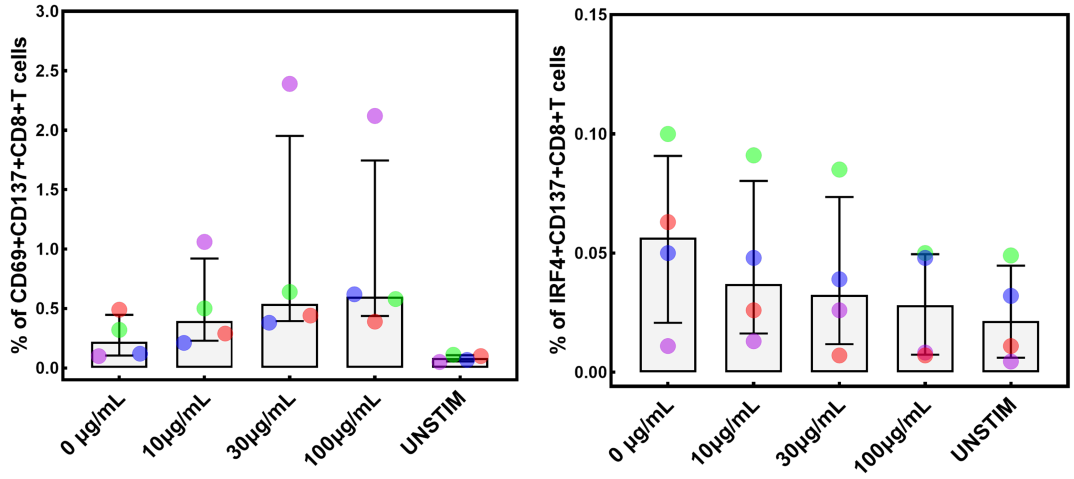



**Figure 5.6**: **IRF4CD137 expression is MHC-TCR dependent** PBMCs were treated for 30 minutes with increasing concentrations of pMHC class I mAb (0-100 g/mL) and then cultured with CEFX peptides for 18 hours. Frequency of a) CD69CD137 b)IRF4CD137 from CD8+T cells were analysed. Columns represent the Median and bars represent IQR range. Different colored symbols represent different donors.

and observed the similar trend. Further confirmed the findings (Figure 5.9).

These results suggest that IRF4 expression is more sensitive to TCR signaling, while CD137CD69 expression remains largely unaffected by TCR-MHC stimulation.

### 5.2.5 Evaluation of marker expression consistency across memory subtypes

In our pursuit of identifying the most suitable AIMs for accurate detection of antigen-specific CD8+ T cells, we conducted an in-depth examination of marker expression patterns within various memory subtypes. While previous analyses have primarily focused on bulk CD8+ T cells, it is equally vital to evaluate the uniformity of marker expression across distinct memory subpopulations. If a marker's effectiveness is limited to specific memory subsets, its applicability for antigen-specific T-cell detection becomes constrained, potentially resulting in a skewed representation of certain memory populations while overlooking others. Therefore, comprehending which marker combinations exhibit consistent expression across all memory subtypes offers valuable insights into the reliability and versatility of AIMs.

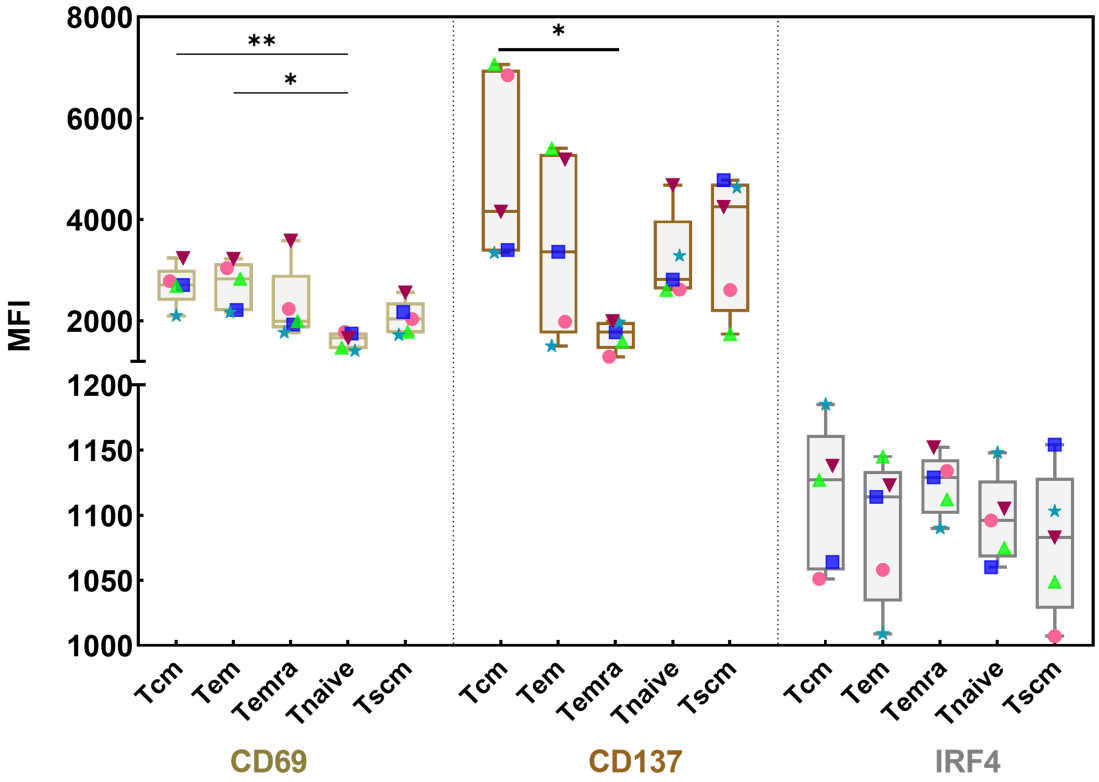



**Figure 5.7**: **IRF4 is uniformly expressed by all CD8+ T memory subpopulations** Median fluorescence intensity (MFI) of CD69, CD137 and IRF4 expressed by CD8+ Tcm, Tem, naive T, Temra and Tscm cells after 18 hours of Flu-M1 peptide stimulation in healthy donor PBMCs. Box and whisker showing all data points, including lower quartile, median, and upper quartile values. Different colored symbols represent different donors. Statistical analysis: Kruskalis-Wallis test, results displayed: *p<0.05, **p<0.01, ***p<0.001.

To gain valuable insights into marker expression patterns across various CD8+ T memory cell populations, we conducted an in-depth analysis using the Flu-pentamer dataset. Our focus was on assessing the MFI of CD69, CD137, and IRF4 across different CD8+ T memory cell subsets. Interestingly, our examination revealed diverse expression levels of CD69 and CD137 among these memory subpopulations, indicating variability in its expression (Figure 5.7). In contrast, both IRF4 consistently demonstrated expression across all the memory subtypes we studied (Figure 5.7). These findings shed light on the dynamic nature of CD69 and CD137 expression while highlighting the robust and consistent expression of IRF4 within various memory subpopulations. This information has significant implications for the selection of optimal AIM combination in our study.

### 5.2.6 Co-expression of different AIM markers

Through rigorous analysis, we identified three predominant AIM combinations: IRF4CD137, CD137 alone, and CD69CD137, each demonstrating unique sensitivity and specificity profiles. Building on this foundation, we then investigated the co-expression of these marker on CD8+ T cells.

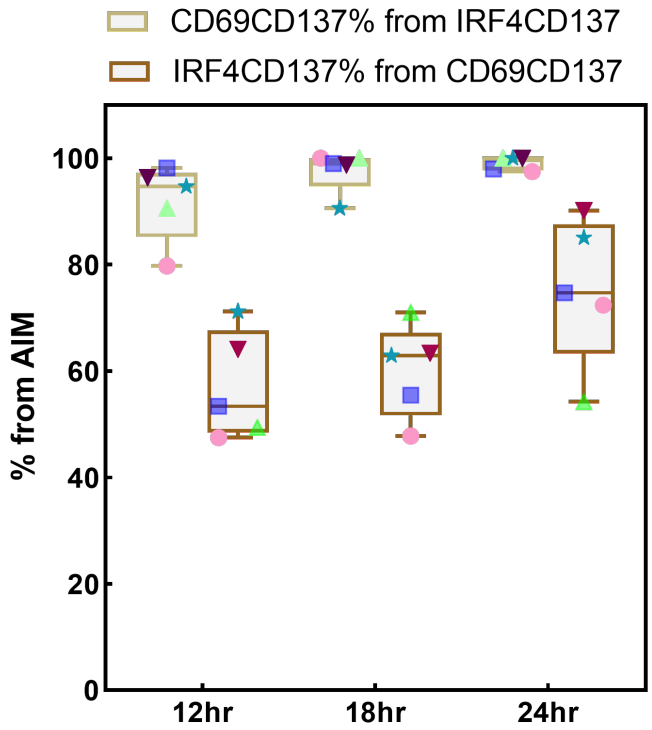



**Figure 5.8**: **IRF4CD137+ CD8+ T cells co-express CD69CD137 markers** A Box and whisker showing all data points, including lower quartile, median, and upper quartile values of frequency of cells expressing CD69CD137 from IRF4CD137+ cells and frequency of cells expressing IRF4CD137 from CD69CD137+ cells at 12hr, 18hr and 24hr after stimulation. Different colored symbols represent different donors.

Notably, a significant proportion of IRF4CD137+ CD8+ T cells (median: 90% and above at all time points) co-expressed CD69CD137. The highest frequency of IRF4CD137 combination within CD69CD137 (median: 72%) was observed after 24 hr of stimulation.

## 5.3 Discussion

This study conducted a systematic comparison of various AIM markers commonly used to quantify antigen-specific CD8+ T cells from human PBMCs. The results suggest that the choice of the best AIM combination depends on the trade-off between sensitivity and specificity that aligns with your research objective. The CD69CD137 combination offers high sensitivity but lower specificity, while the IRF4CD137 combination provides high specificity but slightly lower sensitivity.

Importantly, we observed that IRF4CD137's specificity is TCR-MHC dependent (Wu et al. 2019), which is a desirable feature. This means it accurately identifies antigen-specific cells rather than bystander-activated ones. On the other hand, CD69CD137 is not dependent on TCR-MHC interactions, which allows it to capture a wider range of cells.

These findings underscore the importance of selecting AIM marker combinations that align with specific research objectives. If the primary goal is to maximize sensitivity and capture as many antigen-specific T cells as possible, CD69CD137 may be preferred. However, for studies where minimizing false positives and ensuring the accurate identification of antigen-specific T cells are important, the IRF4CD137 combination stands out as the superior choice. Researchers are encouraged to carefully weigh the trade-off between sensitivity and specificity when selecting AIM marker combinations tailored to their study requirements.

As this comparative analysis was conducted to apply the findings to HIV trial vaccination study cohorts, where the accurate quantification of HIV-specific CD8+ Tscm cells is crucial to study Tscm dynamics, the choice of the most appropriate AIM marker combination becomes paramount. The extensive evaluation of various AIMs, considering their sensitivity, specificity, and consistency across memory subpopulations, indicates that the CD137IRF4 combination is the optimal choice for this purpose. This combination offers several advantages, including high specificity, reduced background noise, consistency in expression across diverse memory cell types, and its relevance to the study, given its TCR-MHC-dependent stimulation.

Furthermore, this analysis highlights the importance of conducting essential pilot experiments to confirm the specificity and sensitivity of selected AIM markers,

as the immune responses to different pathogens or antigens may exhibit variations in activation marker patterns, as observed in the comparison of our findings with the EBV study. Callan et al. (1998) investigated immune responses to primary and three-year post-EBV infection using tetramer technology in combination with various activation markers, including HLADR, CD38, CD45RA, CD45RO, and CD62L. Their observations revealed that during the primary response, a high percentage of tetramer-positive cells were CD38 and HLA-DR positive, suggesting a strong association between these activation markers and antigen-specific T cell populations (Callan et al. 1998). However, our investigation did not reveal a similar relationship between HLADRCD38+ cells and pentamer-positive flu-specific CD8+ T cells. This discrepancy suggests that the immune responses to different pathogens or antigens may exhibit variations in terms of the activation markers expressed by specific CD8+ T cell populations. In other words, the activation marker patterns observed in response to one infection (EBV in the Callan study) may not necessarily apply to the response to another antigen (flu in our study), highlighting the complexity and specificity of immune responses. This highlights the importance of conducting a pilot run to confirm the specificity and sensitivity of the chosen AIM marker.

Further, the importance of conducting a pilot experiment run to validate the AIM markers can be learned from another EBV study conducted by Bowyer et al. (2018). In this EBV study, Bowyer et al. (2018) applied OX40 in combination with both CD25 and CD107 in the AIM assay, with 20 hours of stimulation, to detect vaccine-specific CD8+ T cells following vaccination with an EBV vaccine candidate. However, as shown in our study and by others, OX40 and CD25 are late upregulation markers. Hence, selecting 20 hours of stimulation may lead to the loss of a significant proportion of antigen-specific CD8+ T cells. Additionally, a recent study assessed cytokine analysis with AIM assays to evaluate the functional capabilities of AIM+ antigen-specific cells in individuals vaccinated against COVID-19 (Altosole et al., 2022). They also did not observe any correlation between OX40 expression and cytokine secretion nor with other AIM markers. As a result, OX40 was excluded from their assay due to its limited informativeness in this context (Altosole et al., 2022). Hence, this highlights the significance of evaluating the timings of marker upregulation to ensure that AIM assays capture the full spectrum of antigen-specific

T cells, especially when considering late upregulation markers like OX40.

Recently, in the context of COVID infection and vaccination studies, many researchers have adopted a combination of CD137 with a second activation marker, specifically CD69, defining the 'CD8+CD69+CD137+' phenotype as AIM+ cells to assess viral-specific CD8+ T cell immune responses (Dan et al. 2016, Grifoni et al. 2020, Jung et al. 2021, Tarke et al. 2021). Based on the outcomes of our study, we propose that, instead of CD69, other activation-induced markers whose upregulation depends on TCR-MHC interactions should be considered in combination with CD137 for AIM assays. Several alternative markers have been explored alongside CD137, including OX40, TNF, CD107, and CD154. For instance, Takahama et al. (2021) recommended using CD137 in conjunction with CD107, TNF, and OX40 to enhance the detection of antigen-specific CD8 T cells (Takahama et al. 2021). However, it's important to note that this study has certain limitations. It optimized the experimental conditions using SEB stimulation, and these conditions might not be replicable with peptide stimulation. Furthermore, the study employed only a 3-hour stimulation for OX40, which might not be sufficient to capture the late upregulation of this marker. These considerations underscore the need for comprehensive assessments of AIM markers in the context of specific experimental conditions and research objectives. Hence further research is needed. Recently Wu et al. (2019) investigated the performance of CD137 in combination with IRF4 and revealed that IRF4CD137 marker combination is sensitive and robust to determine Ag-specific CD8+ T cells in human blood samples. These findings are aligned with the findings of our results.

The limitation of using IRF4 in combination with CD137 is that IRF4 is an intracellular marker, so its detection requires cell permeabilization, which makes it less suitable for studying live cells or downstream applications. However, its advantages may outweigh this limitation in certain experimental contexts.

To conclude, this analysis provides insights into the robustness and reliability of AIMs and highlights the trade-off between sensitivity and specificity, offering a comprehensive understanding of their utility in antigen-specific T cell detection. It is essential to consider these factors when selecting AIMs for future studies or clinical applications.

### 5.3.1 Supplementary

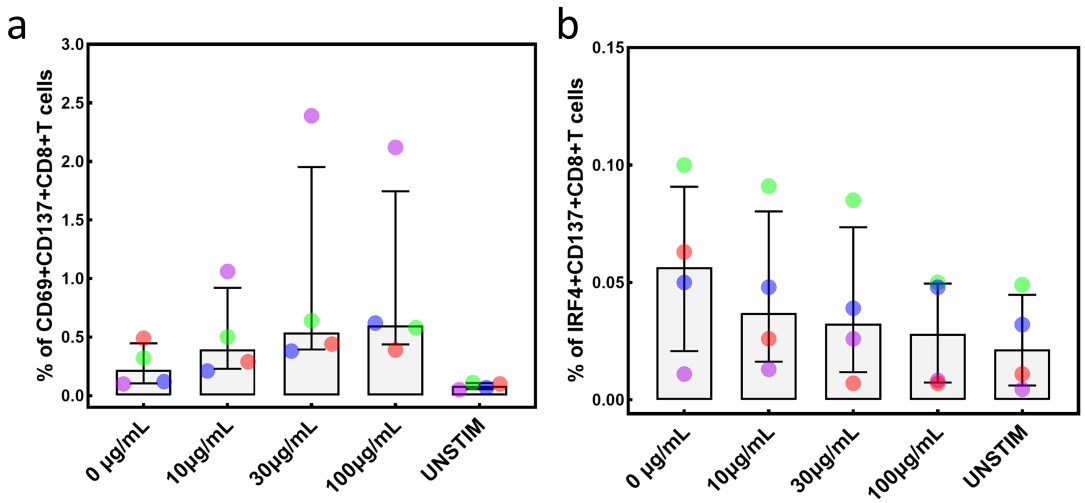



**Figure 5.9**: **IRF4CD137 expression is MHC-TCR dependent in HIV vaccinated individuals** PBMCs, isolated from the blood of HIV negative donors vaccinated with HIV candidate vaccine in study B001 (n=4), treated for 30 minutes with increasing concentrations of pMHC class I mAb (0-100 $\mu$g/mL) and then cultured with HIV peptide pool similar to vaccine construct for 18 hours. Frequency of a) CD69CD137 and b)IRF4CD137 from CD8+T cells were analysed. Columns represent the Median and bars represent the IQR range. Different colored symbols represent different donors.

# Chapter 6

# Antigen-specific CD8+Tscm and their role in sustaining memory post-vaccination

## 6.1 Introduction

The development of an effective vaccine is a remarkable achievement in modern medicine, as it serves as a crucial tool in preventing and controlling infectious diseases. However, one of the key challenges in vaccine design is ensuring that the induced immune responses are long-lasting, especially in resource-poor or logistically challenging settings where repeated vaccinations may be impractical. Understanding the mechanisms behind the persistence of T cell-mediated immunity over extended periods remains a critical aspect of vaccine research.

While the maintenance of T-cell memory is essential for long-term protection, the specific factors governing the longevity of these responses have not been fully understood. Emerging evidence highlights the vital role of Tscm in maintaining immune memory due to their stem-like properties, including self-renewal and multipotency (Fuertes Marraco et al. 2015, Biasco et al. 2015, Aleksova et al. 2023, Gattinoni et al. 2017). This notion gains support from studies involving simian immunodeficiency virus (SIV) infection in non-human primates (NHPs) (Lugli et al. 2013) and YF-vaccination study (Fuertes Marraco et al. 2015). In these studies, researchers observed the presence of antigen-specific Tscm cells during the early

stages of vaccination, a period dominated by effector T cells. Remarkably, in the YF vaccination study, these Tscm cells exhibited remarkable stability and eventually became the predominant YF-specific memory T cell population circulating in the body, even decades after the initial immunization (Fuertes Marraco et al. 2015). Given the well-established life-long protection provided by YF vaccination, this may suggest that Tscm cells play a central role in the maintenance of long-term T-cell memory. These findings underscore the potential significance of Tscm cells in the preservation of immune memory and suggest their importance as a focus of further research.

Moreover, a recent investigation involving individuals vaccinated with BNT162b2 against COVID-19 revealed compelling insights into the role of vaccine-induced Tscm generated early after vaccination in predicting future immunological responses (Guerrera et al. 2021). This study observed that the number of Tscm cells generated after the initial vaccine dose emerged as a robust predictor of both CD4+ and CD8+ T cell activation at later timepoints (Guerrera et al. 2021). By using the raw data for antigen-specific Tscm and other memory subpopulations from this published study, we correlated the rate of decay of memory with the frequency of CD4+ Tscm and CD8+ Tscm cells generated at early timepoint after vaccination and observed a significant negative correlation for CD8+ Tscm cells. That means individuals with a large vaccine-induced CD8+Tscm maintain T-cell memory to the antigen better than others. These findings provide a strong rationale for extending this research to other vaccinations.

To investigate the above-mentioned rationale, we used HIV trial vaccination studies involving healthy HIV-uninfected adults who were vaccinated with HIV trial vaccines. We selected HIV trial vaccination studies mainly for two reasons: 1) These samples provide an opportunity to investigate primary immune responses in individuals who have not previously been exposed to HIV. This "naive" response allows us to observe the early dynamics of HIV-specific Tscm and its potential role in long-term immunity development 2) These samples were readily available to us.

Samples from three HIV vaccine trials: CUTHIVAC002 and IAVI - B001 and S001 HIV trial vaccinations were utilized. CUTHIVAC002 was a randomised single-site, phase 1 clinical trial in 30 healthy HIV-negative males and females (aged 18–45)

vaccinated with HIV DNA-C CN54ENV immunizations. These immunizations were administered via both intramuscular and intradermal methods, with and without electroporation, followed by a boost with recombinant HIV CN54gp140 (Haidari et al. 2017).

IAVI-B001 was a phase I clinical trial in healthy HIV-uninfected males and females (aged 18–50 years) immunized with HIV trial vaccine. This trial followed a randomized, double-blind, dose-escalation approach and included a placebo control group. The vaccine under investigation consisted of two recombinant adenovirus serotype 35 (Ad35) vectors, each carrying the essential HIV antigens gag, RT, int, nef (Ad35-GRIN), and env (Ad35-ENV) (Keefer et al. 2012).

IAVI-S001 was a multicenter, randomized, placebo-controlled, dose-escalation trial in 65 healthy HIV-uninfected males and females (aged 19-45 years). This trial focused on a replication-competent Sendai virus (SeV) -vectored HIV-1 vaccine administered intranasally, either alone or as part of a heterologous prime-boost regimen with a nonreplicating adenovirus vaccine. This trial assessed the vaccine's safety and immunogenicity. The study's findings indicated that SeV-Gag effectively primed T-cell responses and boosted antibody responses. However, it was noted that SeV-Gag alone, in this specific configuration, did not exhibit sufficient immunogenicity for further development as a standalone vaccine candidate (Nyombayire et al. 2017).

Notably, the Tscm subset had not been previously explored in these trials. Therefore, using samples from these studies, we aimed to investigate whether the observed negative correlation between the rate of memory decay and early-generated antigen-specific Tscm cells, as seen in the COVID-BNT162b2 study, holds true in the context of HIV-1 vaccination. This research could offer valuable insights into the significant role of Tscm cells and their subsets in sustaining long-term immunity following HIV-1 vaccination, thereby offering valuable information for the design of vaccines and the maintenance of immune memory.

## 6.2 Results

PBMC samples from the the HIV trial vaccination studies were stimulated with the peptide pool similar to the respective vaccine construct for 18hr and antigen-specific cells were detected using IRF4CD137 staining and referred as AIM+ cells. The samples were taken at 3 timepoints post-boost as shown in Figure 6.1.

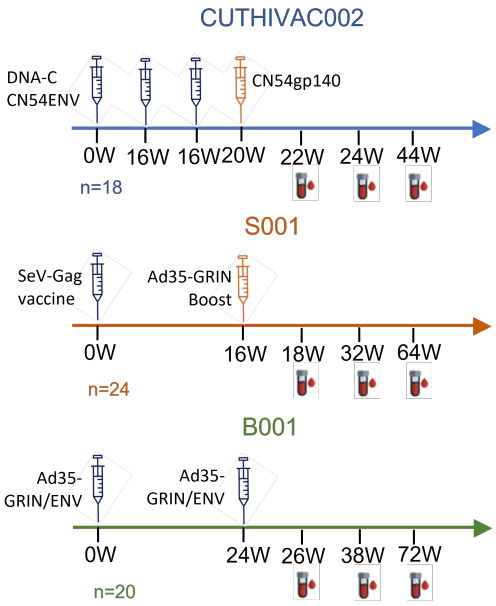



**Figure 6.1**: **Timepoints for sample collection and analysis post vaccination.** For each of the 3 studies blood was collected at 3 timepoints indicated above by the red vial symbols.

### 6.2.1 Assessment of HIV-specific CD8+T cell responses

We examined the CD8+T cell immune response following vaccination. The gating strategy for identifying different memory subpopulations is provided in SuppFigure 6.1. In the CUTHIVAC study, following background subtraction from parallel unstimulated samples, it was determined that 60% of donors exhibited detectable levels of AIM+CD8+ cells at 2 weeks post-boost (22W) (Figure 6.2a, blue). Notably, there was a slight non-significant increase in the average frequency of AIM+CD8+ T cells from 0.4%±0.48% at 22W to 0.84%±0.87% at 44W (calculated after exclusion of negative values) (Figure 6.2b, blue).

In the case of the S001 trials, at 2 weeks post-boost, all donors exhibited detectable AIM+CD8+ T cells, with an average frequency of 0.11%±0.10% (Fig-

ure 6.2a and b, orange). However, a marked decline in AIM+CD8+ cells was observed at 32W, and this decrease persisted at 64W, with only one individual out of 24 demonstrating a positive response (Figure 6.2a, orange).

For the B001 trials, approximately 60% of individuals displayed a positive response to peptide stimulation at two weeks post-boost (26W) (Figure 6.2a, green), with a frequency of 0.051%± 0.07% AIM+CD8+ T cells (Figure 6.2b, green). The frequency of AIM+CD8+ T cells remained consistent at 32W (i.e., 14 weeks post-boost). However, a significant decline in frequency, with the frequency halving of 26W, was observed at the latest timepoint (72W) (Figure 6.2b, green).

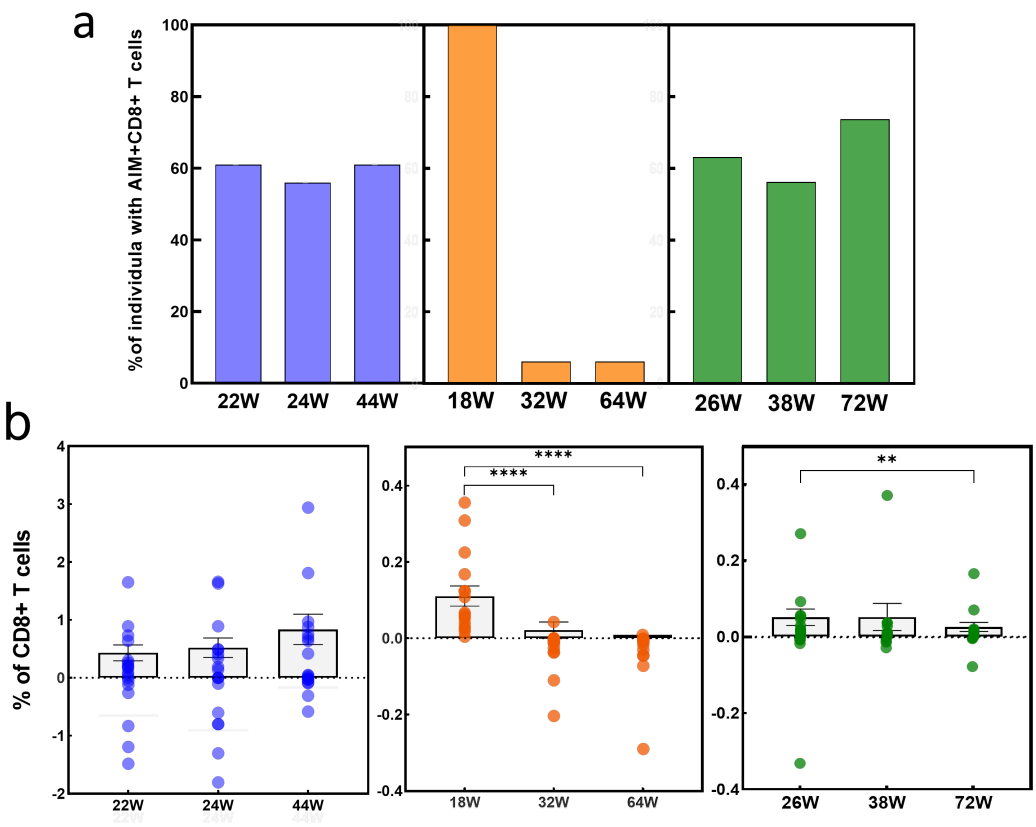



**Figure 6.2**: **Frequency of HIV-specific CD8+ T cell post-boost across HIV trial vaccination studies.** a) Percentage of individuals having AIM+CD8+ T cells at different timepoints post-boost. b)Frequency of AIM+CD8+ T cells observed at three timpoints post-boost in CUTHIVAC (blue, n=18), S001 (orange, n=24) and B001 (green, n=20). The background was subtracted. Each dot represents one donor. Some donors had negative values because of the high background signal. These donors were excluded from doing statistical analysis. Bars indicate mean ± s.e.m. Stat: Kruskal-Wallis test, **<0.01,****<0.0001.

In the context of the CUTHIVAC study, it's important to note that no significant

differences were observed in AIM+CD8+ T cell frequencies between the 2-week and 22-week post-boost timepoints suggesting a stable immune response. It raised intriguing questions about the factors contributing to this sustained response.

In the S001 study, since everyone had a negative AIM+CD8+T cell by the second timepoint, it was impossible to calculate the rate of decay. Finally, in the B001 study, a significant gradual decline in HIV-specific CD8+ T cells from 2 to 48 weeks post 2nd vaccination was observed.

Consequently, B001 and CUTHIVAC studies aligned perfectly with our objective, which aimed to correlate the rate of change in HIV-specific memory following vaccination with the early memory cells generated and assess whether the magnitude of early memory generation could predict the future immune response.

In addition, we investigated various HIV-specific memory subpopulations across all the studies, and the comparative analysis of these subpopulations is presented in the following subsections.

### 6.2.2 HIV-specific memory CD8+ T subpopulations across trial studies

To investigate the dynamics of HIV-specific memory T cell subpopulations following vaccination, we conducted a comprehensive analysis across these studies. This investigation aimed to elucidate the changes in memory T cell subpopulations over time and their distinct patterns of evolution. Intriguingly, the CUTHIVAC study revealed that a majority of the AIM+CD8+ T cell fraction predominantly consisted of Temra cells, constituting more than 70% across all the timepoints studied (Figure 6.3a). Conversely, HIV-specific Tscm cells exhibited a significant decline over time following boost (Figure 6.3a).

In contrast, the S001 trial exhibited a distinct pattern, with approximately 40% of HIV-specific Tem and 30% of Tcm cells generated at the 2-week post-boost timepoint (Figure 6.3a). This high frequency of Tem cells early after vaccination was anticipated. However, the fraction of Tcm cells was notably higher compared to the same timepoint in the other two studies. Over time, the HIV-specific Tem and Tcm populations decreased, while Tscm and Temra subpopulations increased. Notably, due to the limited availability of individuals for memory subpopulation assessment

at the 32-week and 64-week timepoints after primary vaccination in the S001 study, statistical testing was not feasible.

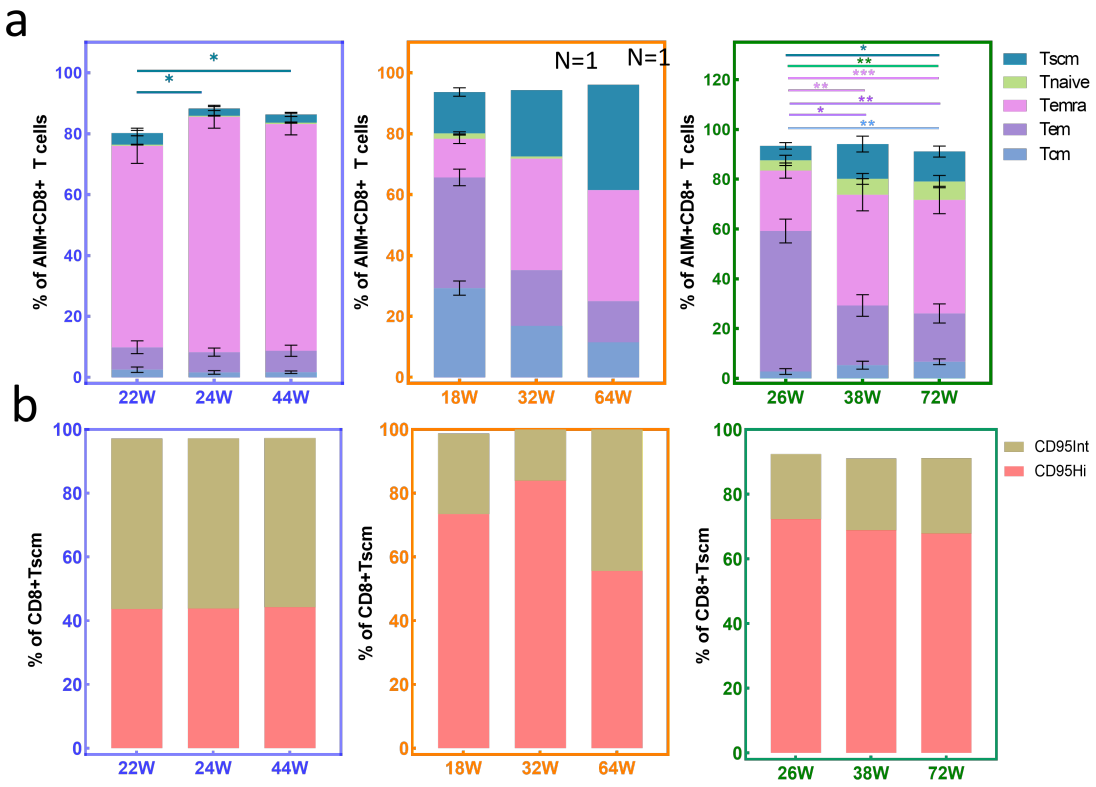



**Figure 6.3**: **Dynamics of HIV-specific CD8+T memory subpopulation post-boost.** a) Frequency of different HIV-specific CD8+ T memory subpopulations from AIM+CD8+ T cells measured across different timepoints. b) Frequency of HIV-specific CD8+ Tscm subpopulations from AIM+CD8+Tscm cells measured across different timepoints. CUTHIVAC study is represented by a blue graph border (n=9), S001 by an orange graph border (n=16, except at 32W and 64W), and B001 by a green graph border (n=12). Different colors within bars represent different subpopulations and Bars indicate mean ± s.e.m. Stat: Kruskal-Wallis test, *<0.05, **<0.01,***<0.001.

The B001 vaccine construct elicited a memory response with around 60% Tem cells two weeks after the boost, which subsequently declined significantly over time. In contrast, other subsets, including Tcm, Tscm, Tnaive, and Temra, exhibited a significant increase over time (see figure Figure 6.3a).

Furthermore, a closer examination of Tscm subpopulations revealed that in both B001 and S001 studies, the CD95hi subset consistently exhibited a higher frequency at all timepoints compared to the CD95int subset, with no significant variation over time (Figure 6.3b). In contrast, the CUTHIVAC study displayed a predominance of the CD95int subset over the CD95hi subset (Figure 6.3b).

These observations suggest that the composition and dynamics of HIV-specific memory T cell populations differ among the vaccination studies under investigation.

### 6.2.3 Comparative analysis of early immune responses generated by the vaccinations

In the previous section, we conducted a comparative analysis of the immune dynamics of HIV-specific memory cells induced following vaccination over time. In this section, our focus shifts to a specific timepoint i.e. 2 weeks post-boost, across three HIV vaccine trials. Given the predictive nature of early immune phenotypes on long-term immunity, our objective was to assess the initial response profiles in these vaccination studies and subsequently evaluate their longevity.

Our findings revealed a noteworthy disparity in the immune responses among the three cohorts. Specifically, the CUTHIVAC study exhibited a significantly higher frequency of HIV-specific Temra cells compared to both the B001 and S001 studies at two weeks post-boost(Figure 6.4a). On the other hand, HIV-specific Tcm and Tscm cells were the most abundant in the S001 study (Figure 6.4a). Interestingly, the B001 study displayed the highest frequency of Tem cells (Figure 6.4a). These observations suggest that the CUTHIVAC study, which maintained a stable immune response for up to 22 weeks post-boost, leaned towards an effector phenotype characterized by a predominance of AIM+CD8+ Temra cells. In contrast, the early response in the B001 study exhibited an effector-like bias with a high proportion of Tem cells and a smaller proportion of Temra cells, which had detectable HIV-specific cells even at 48 weeks post-boost. Conversely, the S001 study displayed a robust memory-phase response marked by the prevalence of Tcm and Tscm cells shortly after the boost and evidence of a sudden drop in memory by 16 weeks post-boost.

Finally, the CUTHIVAC cohort exhibited a significantly higher frequency of CD95int cells as compared to both the S001 and B001 studies, while CD95hi was more prevalent in the B001 and S001 studies compared to CUTHIVAC (Figure 6.4b).

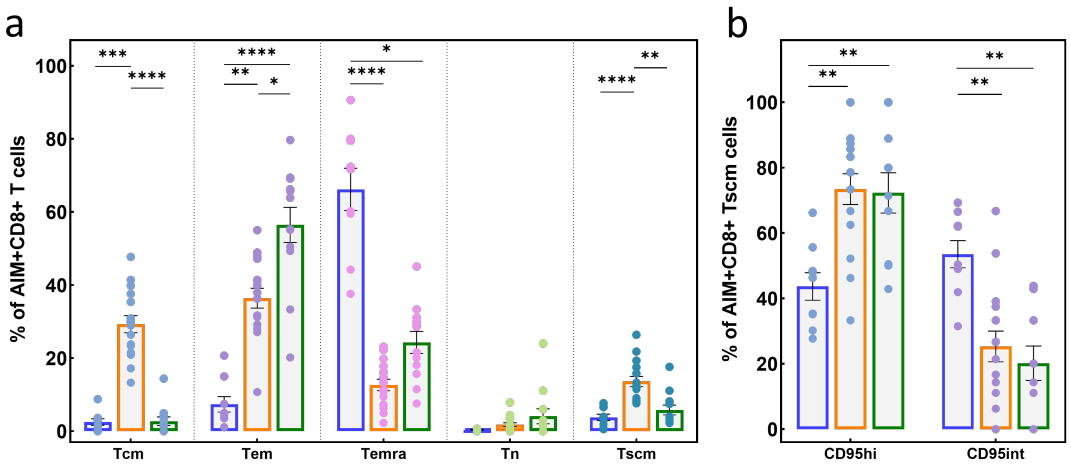



**Figure 6.4**: **Comparison of memory profile two weeks post-boost among HIV trial vaccine studies.** a Frequency of different memory subpopulations from CD8+ T cells two weeks post-boost. b) Frequency of Tscm subpopulations from CD8+Tscm cells two weeks post-boost. CUTHIVAC study is represented by a Blue bar border, S001 by the orange bar, and S001 by the green bar. Each dot represents one donor. Bars indicate mean ± s.e.m. Stat: One-way ANOVA with Friedman multiple comnparison, *<0.05, **<0.01,***<0.001, ****<0.0001.

### 6.2.4 Understanding the interplay between Tscm and long-term memory maintenance

We aimed to investigate the relationship between early T-cell responses induced by the CUTHIVAC and B001 vaccines and the durability of these responses over time.

For this, we conducted an in-depth analysis to determine whether the differentiation status of T cells, particularly the frequency of HIV-specific Tscm and its subsets at 2 weeks post-boost, plays a role in influencing the persistence of vaccine-induced CD8+ T cell responses. We first calculated the rate of memory decay, measured from 2 weeks post-boost to 22 weeks or 48 weeks post-boost in CUTHIVAC and B001, respectively. Subsequently, we performed correlation analyses to investigate the relationship between the size of different T cell memory subpopulations at the 2-week post-boost and the rate of decay of AIM+CD8+ T cells, considering both the total memory population and its individual memory subpopulations.

In the CUTHIVAC study, we did not observe any significant correlation between the size of early immune subsets with the rate of decay or persistence of memory (data not shown). This lack of correlation may be attributed to the relatively short duration of the vaccination study that we examined. Additionally, the sample size of

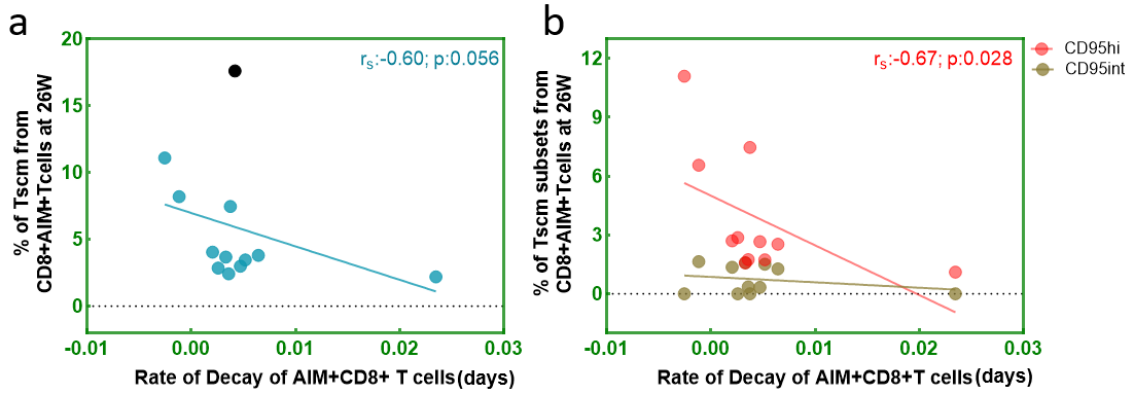



**Figure 6.5**: **Relation between frequency of HIV-specific CD8+ Tscm at 2 weeks post-boost with the rate of decay of memory.** a) for Tscm and b) for Tscm subpopulations. Each dot represents one donor. A black dot is an outlier calculated by Grubb's test and excluded from statistical analysis. Coloured lines represent simple linear regression lines. Stats: Spearman Correlation analysis with $r_s$ as correlation cofficient

individuals who showed a positive response to the vaccine was relatively small (n=9). Consequently, this study did not provide insights into the long-term implications of early immune subset sizes in the context of CUTHIVAC vaccination.

However, in the B001 study, among all the subpopulations examined, only the frequency of HIV-specific Tscm exhibited a significant negative correlation with the rate of decay of total HIV-specific CD8+ T memory cells (Figure 6.5a). Moreover, upon closer look at the memory subpopulations, it was revealed that the CD95hi subset significantly contributed to this relationship (r: -0.67, p = 0.028), whereas CD95int did not exhibit statistical significance (Figure 6.5b). These findings suggest that individuals with a high frequency of HIV-specific CD8+Tscm cells, particularly CD95hi, early after vaccination tend to experience a slower rate of memory decay compared to their counterparts.

Building upon this insight, we extended our analysis to explore the correlation between HIV-specific Tscm pool and the rate of decay of Tcm, Tem, and Temra subpopulations independently. Notably, we observed a significant negative relationship between the rate of decay of vaccine-induced Tem cells and the frequency of Tscm at 2 weeks post-boost (Figure 6.6a). In Figure 6.6 an inset, we displayed the response after excluding extreme data points to ensure that the relationship persisted without being driven by outliers. Furthermore, when we delved into Tscm subsets, we found that CD95hi exhibited a significant negative relationship with the decay of

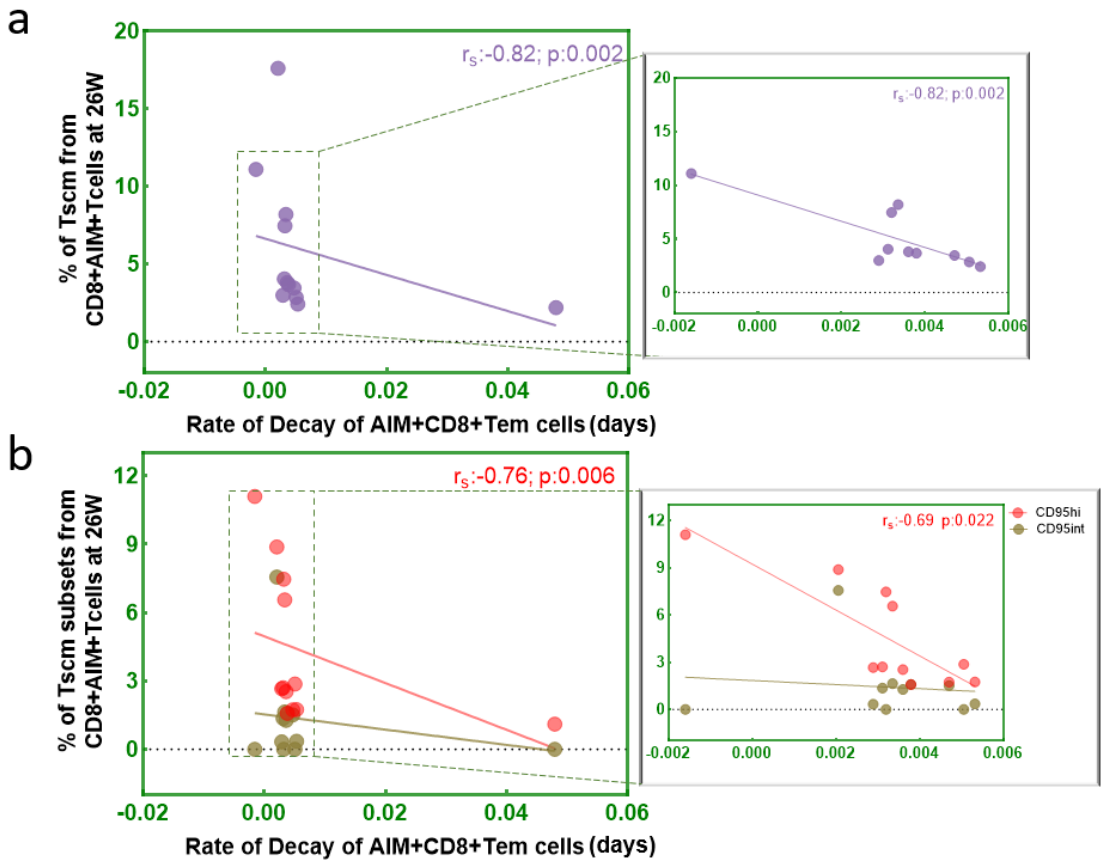



**Figure 6.6**: **Relation between frequency of HIV-specific CD8+ Tscm at 2-week post-boost with the rate of decay of Tem in B001 study.** a) for Tscm b) for Tscm subpopulations. In inset, we excluded the extreme points to notice the trend carefully. Each dot represents one donor. A black dot is an outlier calculated by Grubb's test and excluded from statistical analysis. Coloured lines represent simple linear regression lines. Stats: Spearman Correlation analysis with $r_s$ as correlation coefficient

vaccine-induced Tem cells, whereas CD95int did not share this pattern(Figure 6.6b).

Additionally, we identified a similar negative relationship between the rate of decay of vaccine-induced Tcm cells and the frequency of early Tscm, although it did not reach statistical significance for the bulk Tscm (r: -0.54, p: 0.09) and its subsets (CD95hi, r: -0.47, p: 0.15) (Figure 6.7a,b). Intriguingly, this relationship exhibited a reversal when examining Temra cells (Figure 6.7c). Individuals with higher levels of Tscm displayed a higher rate of decay of vaccine-induced Temra (r: 0.34, p: 0.29), while CD95int exhibited a negative relationship with them (r: -0.57, p: 0.07), as opposed to CD95hi (r: 0.26, p: 0.43), which was opposite to what was observed for other memory subpopulations (Figure 6.7c,d).

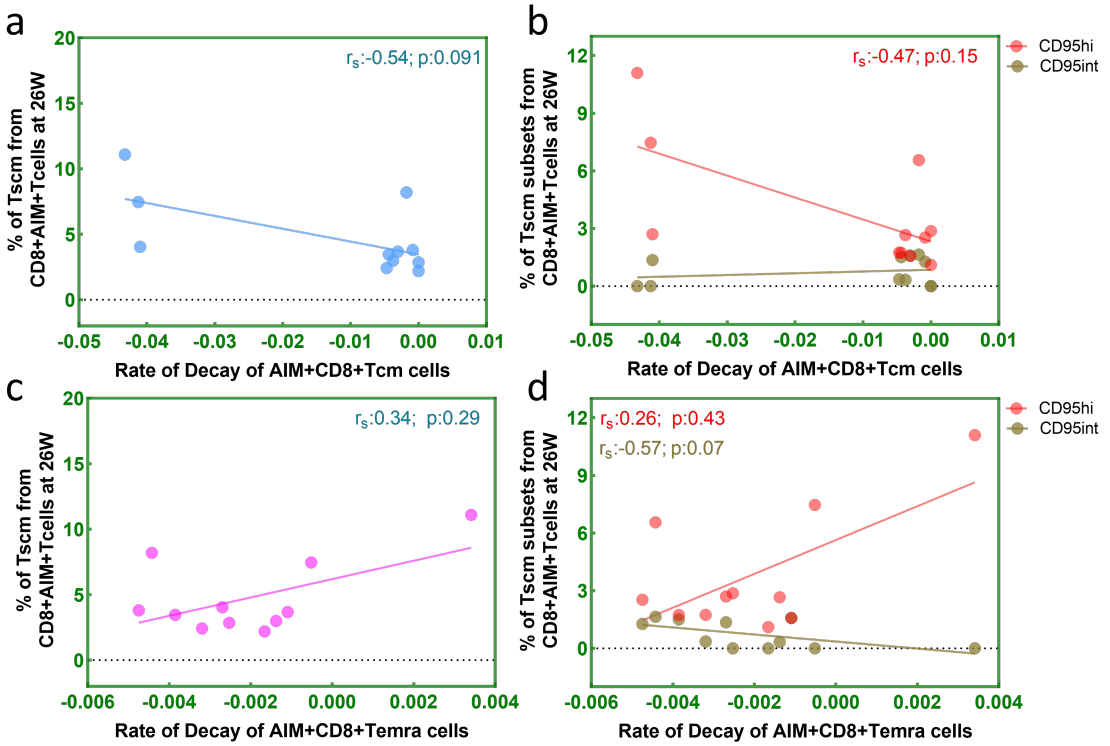



**Figure 6.7**: **Relation between frequency of HIV-specific CD8+ Tscm at 2 week post-boost with the rate of decay of Tcm and Temra in B001 study.** a) for Tscm vs rate of decay of Tcm b) for Tscm subpopulations vs rate of decay of Tcm. c) for Tscm vs rate of decay of Temra d) for Tscm subpopulations vs rate of decay of Temra. Each dot represents one donor. Coloured lines represent simple linear regression lines. Stats: Spearman Correlation analysis with $r_s$ as correlation coefficient

### 6.2.5 Discussion

In our pursuit to characterise the Tscm subsets and investigate their heterogeneity, in this chapter, we presented the results that showcased different dynamics of HIV-specific Tscm subsets in healthy volunteer vaccinated with HIV trial vaccine. We investigated three distinct vaccination studies - CUTHIVAC, B001 and S001, focused on the post-boost timepoints to ensure a detectable number of CD8+ AIM+ T cells. Our primary objective was to explore whether the early emergence and characteristics of these memory subpopulations could serve as a predictor of vaccine responsiveness.

In the CUTHIVAC study, where memory responses were monitored for 22 weeks post-boost, we observed relative stability in the frequency of AIM+CD8+ T cells during this timeframe. Notably, a significant proportion of the HIV-specific CD8+ T

cell response in this study was attributed to Temra cells. Similar Temra response has also been noted in recent studies after vaccination against COVID-19 and COVID-19 infection. A study by Li et al. (2022) observed a positive association between the emergence of SARS-CoV-2–specific CD8+ T cells and the size of the Temra pool. However, our study did not reveal any significant correlation between the emergence of Temra (or Tscm) subsets at early timepoints and the durability of memory generated. Further, another study by Adamo et al. (2022) has shown that SARS-CoV-2-specific CD8+ Temra cells express TCF1, a TF which is associated with a less-differentiated, more "stem cell-like" state in T cells, despite Temra cells typically being considered terminally differentiated. Hence, this raises an important question about the role of Temra cells in sustaining long-term immunity. This finding prompts further investigation into the functional and molecular characteristics of antigen-specific CD8+ Temra cells.

The observed stability in the AIM+CD8+ T cell response in the CUTHIVAC vaccination study raises questions about the durability of vaccine-induced CD8+ T cell immunity and the role of specific memory subpopulations in maintaining it. However, the short follow-up period following vaccination (22 weeks) leaves questions unanswered regarding the long-term durability of memory responses post-vaccination.

S001 study exhibited a distinctive pattern of immune responses following vaccination, characterized by a substantial early surge in memory responses, particularly Tscm and Tcm cells (Figure 6.4), with very few Temra cells. However, this heightened memory response in S001 did not translate into long-term immunity, as evidenced by the marked decline in AIM+CD8+ cells by 16 weeks post-boost. While, the B001 study, characterized by an initial effector immune response, exhibited a peak at 2 weeks post-boost with a high HIV-specific CD8+ Tem phenotype that gradually transitioned into the memory phase over time.

By comparing the dynamics and durability of AIM+CD8+ T cells in these studies we conclude that going through an effector phase early after the vaccination could be associated with the stable immune response seen in CUTHIVAC and B001 studies that endured for up to 22 weeks and >48 weeks after the boost, respectively. In contrast, an early surge in memory responses without going through an

effector phase following the S001 boost did not translate into long-term immunity. This comparative analysis underscores the importance of a well-regulated and robust effector phase following vaccination, mirroring the two-phase pattern observed in natural infections, in establishing long-term immunity (Adamo et al. 2023).

Further, in the B001 study, the only study for which we could calculate the rate of decay of memory, we identified a significant negative correlation between the frequency of HIV-specific Tscm cells, specifically CD95hi Tscm, at 2 weeks post-boost and the rate of decay of HIV-specific total CD8+ memory and HIV-specific CD8+ Tem. This implies that individuals with a higher abundance of CD95hi Tscm cells early after vaccination tend to experience a slower decline in memory responses. The early expansion of Tscm CD95hi appears to play a pivotal role in maintaining the Tem cell pool for an extended duration, potentially contributing to the longevity and effectiveness of the vaccine-induced immune response. These results are supported by Danai's unpublished results, where she investigated the impact of TCR stimulation on the phenotype of Tscm subsets and observed that 7 days after TCR stimulation, both CD95hi and CD95int cells gave rise to predominately Tem followed by Temra and Tcm cells. Tcm cells however, mostly retained their identity or differentiated into Tem cells. The early generation (within 1 week) of Tscm cells, albeit in low frequency, after YF vaccination (Fuertes Marraco et al. 2019) and BNT162b2 vaccination had been noted earlier (Jung et al. 2022). In addition, Tscm's positive relationship with the durability of vaccine-induced memory CD8+ T cell after BNT162b2 vaccination is beautifully shown by Jung et al. (2022). Hence, it could be postulated that even present at relatively low initial frequencies, Tscm subsets generation early after the vaccination determines the durability of vaccine-induced CD8+T cell responses, by maintaining an early effector phase to combat the infection and then gradually transits to the memory phase.

Furthermore, delving into the role of Tscm subpopulations, the predominance of HIV-specific CD95hi Tscm cells in the B001 and S001 studies, and their significant relationship with the rate of decay of HIV-specific CD8+ T cells suggests a potentially more active and less quiescent subset. In contrast, CD95int Tscm cells represent a less differentiated and more quiescent memory cell population in these studies.

However, intriguingly, in the B001 study, CD95int Tscm cells displayed a negative relationship with the rate of decay of Temra cells. This unexpected relationship could explain the higher frequencies of Temra cells in CUTHIVAC, where CD95int frequencies were higher than CD95hi. This underscores that the frequencies of HIV-specific CD95int/CD95hi at peak response could influence the nature of the memory response. Our observation indicated that in CUTHIVAC, a high frequency of CD95int may lead to more Temra cells, whereas in B001 and S001, a high frequency of CD95hi might regulate the Tem phenotype. Importantly, the frequencies of CD95hi and CD95int remained relatively stable over time after the boost in all vaccination cohorts, suggesting that the initial balance of CD95int and CD95hi Tscm subsets established early after vaccination may have a lasting impact on the nature of memory responses.

Recent work by Scudier (2022) also attempted to characterize Tscm heterogeneity based on CD29 and Plexin B2 markers, that subset with CD29lo Plexin B2hi named as LT-Tscm while CD29hi Plexin B2lo termed as ST-Tscm. ST-Tscm were found to be more proliferative and more differentiated than LT-Tscm. Further, they examined the dynamics of Ag-specific LT-Tscm and ST-Tscm in 3 donors vaccinated with YF-17D vaccine, and noted that LT-Tscm were less abundant than ST-Tscm at any timepoint. As we know, peak response in YF-specific peak response is exhibited by a higher proportion of Tem cells than Temra (Akondy et al. 2009). Hence, this also supports that a higher frequency of ST-Tscm (analogous to CD95hi in our case) than LT-Tscm (analogous to CD95int in our case) maintains the Tem pool while the other way around could lead to an effector response by Temra cells. Further, it would be intriguing to enumerate the CD95hi and CD95int frequencies in the case of COVID vaccination, as its effector phase is characterised by a higher frequency of Temra cells.

However, it's important to recognize that these interpretations are primarily based on subset frequencies. To gain a more comprehensive understanding, functional and transcriptional studies are essential. Factors such as the presence of specific transcriptional factors and differential functionalities in response to particular antigens may further determine the balance of immune responses.

Overall, this suggests that early Tscm responses may serve as a foundation for

sustaining long-term immune memory, by balancing the effector and memory phenotypes. The requirement of this balance response is supported by the statement given by Adamo et al. (2022) that "Understanding how the immune system maintains the balance between effector response and memory formation could provide insights on why some infections result in robust and long-lasting T cell memory, whereas others fail to do so". In our study, we potentially unravel that Tscm plays a pivotal role in achieving this balance, influencing the quality and durability of vaccine-induced immunity. It is important to acknowledge that other factors may also influence the quality and durability of vaccine-induced immunity.

The heterogeneity in immune responses among these vaccination studies can be partly attributed to the differences in the vaccine types and their modes of administration. CUTHIVAC employed a DNA-based vaccine, which typically involves the administration of DNA containing specific antigens to stimulate an immune response. This method may have influenced the immune response dynamics in unique ways, potentially contributing to the observed stability in immunity. DNA vaccines have the advantage of providing a broader range of antigens for the immune system to target (Khan et al. 2013), which can lead to a balanced development of memory and effector cells. Similar response has been observed in mRNA-based COVID-19 vaccines (Mayer-Blackwell et al. 2023, Jung et al. 2021, Dan et al. 2021).

In contrast, S001 utilized a SeV -vectored HIV-1 vaccine, administered intranasally either alone or as part of a heterologous prime-boost regimen with a nonreplicating adenovirus vaccine. This mode of delivery, coupled with the use of a viral vector, can elicit distinct immune responses. The intranasal route may have influenced mucosal immunity, while the viral vector can trigger robust cellular and humoral responses. The unique combination of these factors could have contributed to the early memory response observed in the S001 study.

B001, on the other hand, employed two recombinant Ad35 vectors, each carrying essential HIV antigens. Ad35 are known for their capacity to induce strong cellular immune responses. The use of two Ad35 vectors targeting various HIV antigens may have led to a predominantly effector response, followed by memory development.

Overall, the heterogeneity in vaccine types, delivery methods, and antigen compositions among these studies likely underlies the variations in immune response

profiles. Each approach has its advantages and may trigger distinct pathways in the immune system, leading to different patterns of immune cell development and persistence.

From the number of factors shaping the immune response, however, in this study, our analysis primarily centered on understanding the CD8+ T cell immune responses, which represent a crucial arm of the adaptive immune system. However, an exhaustive understanding of vaccine-induced immunity requires the consideration of other immune components, including CD4+ T cells, B cells, and the humoral immune response.

This study presents several limitations that should be considered when interpreting the findings. First and foremost, the sample size in this investigation was relatively small, with a maximum of 24 participants in the S001 study. With an overall positive response rate of approximately 60% across all vaccination studies, the effective sample size varied between 10 to 16 individuals, which may limit the generalizability of the results. A larger and more diverse cohort would enhance the robustness and comprehensiveness of the conclusions drawn from this study.

Additionally, the reliance on specific timepoints for data collection post-boost is a notable limitation. The dynamics of memory cell populations can be influenced by a multitude of factors, and the selected timepoints may not capture all potential changes that could occur following primary vaccinations. A more continuous or frequent data collection approach could provide a more nuanced understanding of the evolving immune response.

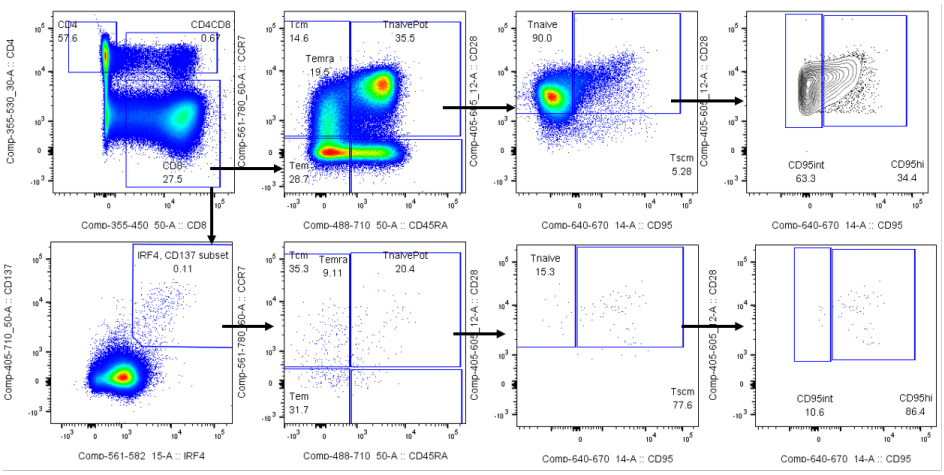
Furthermore, while correlations were used as the primary analytical tool in this study to explore relationships between Tscm subsets and memory cell decay, it is crucial to acknowledge that establishing causation based solely on correlations is challenging. To confirm the causal links between Tscm subsets and memory cell longevity, future mechanistic studies involving experimental interventions and functional assessments will be essential.

We only investigated the phenotype of different HIV-specific CD8+ memory cells, however, further investigations into the functional properties and maintenance mechanisms of these memory subsets are essential to gain a comprehensive understanding of vaccine-induced immunity.

Finally, there is the possibility of unmeasured variables or confounding factors that were not accounted for in the analysis. Immune responses are complex and multifaceted, influenced by genetic variations, prior exposure histories, and individual variability. While this study aimed to uncover specific relationships, the existence of additional factors that could impact the outcomes cannot be ruled out. The gender-based bias in this study was not analysed because we didn't have the demographic data to analyse this. In light of these limitations, it is imperative to approach the study's findings with caution and recognize the potential avenues for further research in this field.

In summary, these findings underscore the intricate nature of vaccine-induced immune responses. Notably, early Tscm responses emerge as pivotal factors in shaping the delicate equilibrium among diverse memory phenotypes, ultimately influencing the quality and durability of vaccine-triggered immunity. This study emphasizes the paramount importance of achieving a balanced immune response after vaccination, where the emphasis shifts from quantity to the diversity and quality of the response. By strategically orchestrating the timing and characteristics of immune reactions, we may enhance the durability and efficacy of vaccine-induced immunity. Further research is needed to fully understand the mechanisms and their implications for vaccine design and effectiveness.

### 6.2.6 Supplementary Figures




**SuppFigure 6.1**: **Gating strategy for bulk CD8+ memory T subpopulations and antigen-specific CD8+ memory T subpopulations in HIV immunized donors in CUTHIVAC, B001 and S001 study.**

# Chapter 7

# Immune cell profiles in blood and lymph nodes post intramuscular HIV envelope immunization

## 7.1 Introduction

The human immune system is an intricate network of cells and molecules, working together to protect the body from invading pathogens and maintain its overall health. Understanding the dynamics of immune responses is essential for the development of effective vaccines, particularly for infectious diseases such as HIV. While peripheral blood serves as a readily accessible source for monitoring immune responses, it provides only a partial view of the complex interplay occurring within the entire immune system. To gain a comprehensive understanding of vaccine-induced immune responses, it is crucial to investigate immune cell dynamics at the site of primary immune activation— the Lymph Nodes (LNs) (Pollard & Bijker 2021).

LNs are anatomical structures strategically distributed throughout the body, serving as critical hubs for immune surveillance and coordination. Within these nodes, a multitude of immune cell populations, including T cells, B cells, and antigen-presenting cells, converge and interact to mount immune responses against pathogens or antigens following infection or vaccination (Moysi et al. 2022). Investigating immune responses in LNs offers a unique opportunity to decipher the intricacies of antigen recognition, immune cell priming, and the subsequent expan-

sion of antigen-specific immune cells.

In the context of HIV vaccine research, it's critical to study immune responses within LNs after immunization. Vaccine strategies for HIV often involve repeated exposure to specific epitopes to mimic the natural infection process, aiming to elicit broadly neutralizing antibodies (Cirelli et al. 2019). This strategy has shown promising results in increasing the frequency of T follicular helper cell (Tfh) and in generating broadly neutralizing antibodies in LNs in animal studies (Havenar-Daughton et al. 2016, Crotty 2019, Sok & Burton 2018).

However, most clinical vaccine research relies on blood samples, offering only a limited perspective of LN responses. Understanding how CD4+ T cells assist B cells within germinal centers of LNs is crucial for generating broadly neutralizing antibodies. Unfortunately, there's a lack of data on lymphatic responses in humans following vaccination (Moysi et al. 2022).

Recent findings have shed light on the significance of lymphoid tissues in vaccine responses. Studies have revealed that LNs can exhibit immune responses as early as two days following intradermal injection of certain antigens, such as tuberculin (Tatovic et al. 2015). Additionally, research in children immunized with influenza vaccines has shown that lymphoid tissues like tonsils can play a pivotal role in the generation of antibody responses against specific vaccine strains (Amodio et al. 2018). Notably, in individuals living with HIV who are on antiretroviral therapy, LNs have been found to exhibit distinct responses, which change after influenza vaccination, a pattern not observed in HIV-negative volunteers (Moysi et al. 2018). Hence, studying LNs directly could enhance our understanding of vaccine-induced immune responses and expedite HIV vaccine development (Hagan et al. 2015).

To investigate this, we used the samples from the EAVI2020_01 HIV immunogen study, also known as the European AIDS Vaccine Initiative EAVI2020_01 study (NCT04046978). This study used repeated intramuscular injections of rationally designed HIV Env Mosaic immunogens, specifically engineered to stabilize the native conformation of the Env glycoprotein. Env glycoprotein is known to stimulate the production of broadly neutralizing antibodies against HIV (Lyumkis et al. 2013, Julien et al. 2013, Do Kwon et al. 2015). Remarkably, in this study, we incorporated an innovative diagnostic technique i.e. US-guided FNA to extract the LN sample in

addition to blood (Havenar-Daughton et al. 2020). While this technique is not yet widely integrated into clinical vaccine research, it has demonstrated its feasibility within research contexts. We tested this technique in a clinical setting as a part of the EAVI2020_01 study(Day et al. 2022).

This LN study encompassed a multifaceted approach, beginning with an assessment of the feasibility of employing US-guided FNA to obtain LN samples in a clinical setting. Subsequently, it delved into the comparison of HIV-specific responses generated by HIV Mosaic immunogens. The primary objective was then centered on contrasting the cellular landscape between blood and LNCs.

Crucially, this study unlocked the potential for studying critical T cell types residing in secondary lymphoid tissues, both contralateral and ipsilateral to the injection site. By enabling the direct investigation of immune responses within LNs following intramuscular injection of HIV Mosaic immunogens, this study yielded valuable insights into vaccine-induced immunity against HIV — a significant step forward in the pursuit of an effective HIV vaccine.

## 7.2 Results

### 7.2.1 Tolerability and yield of US-guided FNA procedure

To assess the feasibility, safety, and tolerability of US-guided FNA of axillary LNs following intramuscular injection of HIV Mosaic immunogens into the deltoid muscle, participants enrolled in the EAVI2020_01 study were given the option to contribute LNC along with paired phlebotomy. Out of the participants, 11 individuals willingly joined the LN study and subsequently underwent sampling procedures. The LN FNA was conducted within 0-56 days after the initial injection of the study immunogen. To identify the most suitable nodes for sampling, a physical examination was done on the participants.

The FNA procedure was well-tolerated and did not result in any serious or high-grade adverse events. Safety assessments were performed 15-30 minutes post-FNA and at the follow-up visit. Importantly, no severe complications or safety concerns arose, demonstrating the overall safety of the procedure. Of the participants, 10 out of 11 (91%) reported immediate adverse events, with 7 out of 11 (64%) continuing to

report adverse events post-procedure. These events were all classified as mild, with no instances of moderate or severe adverse events. Notably, none of the reported adverse events were deemed related to the procedure itself. The most common immediate adverse event was mild tenderness or pain at the FNA site, experienced by 6 out of 11 participants (55%), followed by minor bruising at the FNA site, reported by 2 out of 11 participants (18%). One participant briefly experienced mild superficial swelling at the FNA site, which resolved by the following day. Another participant reported slight paraesthesia at the FNA site, which also resolved. An isolated case of post-FNA nausea occurred in one participant, with no additional associated symptoms or clinical issues. This resolved, allowing the participant to undergo FNA of the contralateral axilla without further complications. Finally, one participant reported bruising the day after the procedure. Fortunately, the majority of adverse events reported at the follow-up visit (6 out of 10, 60%) were resolved within 48 hours, and all adverse events were ultimately resolved within five days. This concludes that the FNA procedure is tolerable and can be well included in clinical settings.

It is important to note that Dr. Katrina Pollock conducted this procedure along with the safety assessments.

### 7.2.2 Cellular landscape of blood and LN is divergent

To investigate the cellular composition of both human tissues, including blood and LNs, we conducted immunophenotyping using paired LNC and PBMC obtained from six participants. This analysis was done by Suzanne Day. A specialized cocktail of 15 fluorochrome-conjugated antibodies was employed to define major lymphocyte and monocyte lineages as well as specific cell subsets. The subsequent unsupervised clustering analysis of the concatenated and down-sampled immunophenotyping data revealed seventeen distinct cell clusters, representing monocytes, T cells, and B cell memory subsets (Figure 7.1a).

One important observation in t-SNE plots was the substantial disparity in the breadth and frequency of cell types between blood and LNs. CD14+ monocytes, which were notably enriched in PBMC, were nearly absent in LNC (Figure 7.1a). In LNC, B cells and CD4+ T cells predominated, with CD8+ T cells forming a

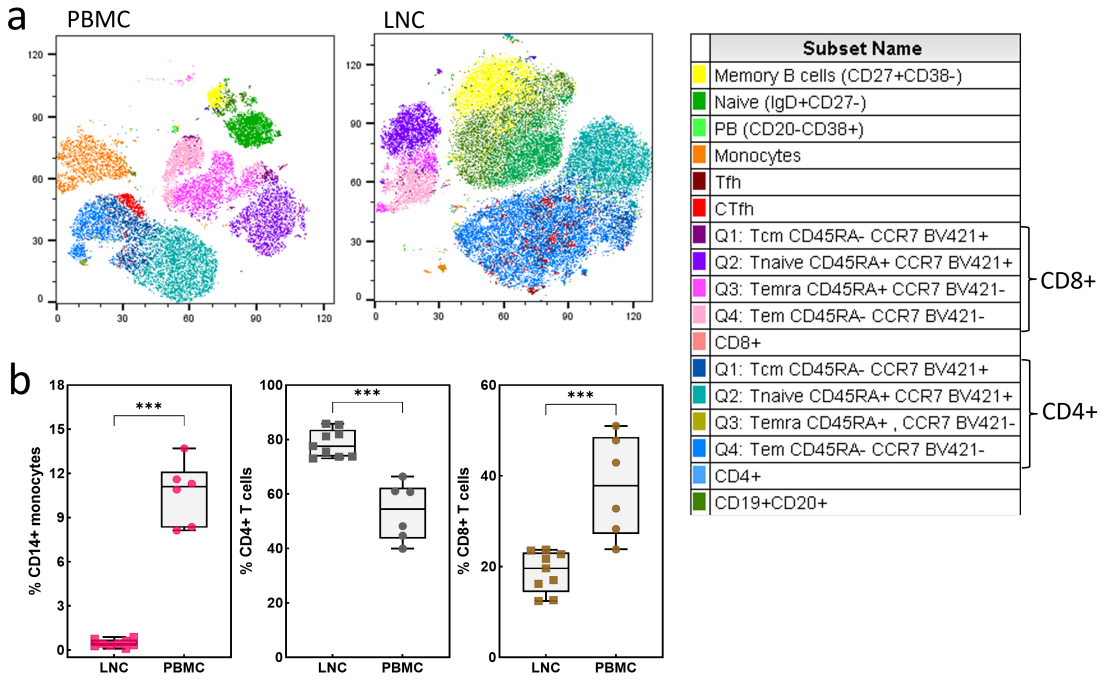



**Figure 7.1**: **Cellular diversity in PBMCs and LNCs.** a) t-distributed Stochastic Neighbor Embedding (t-SNE) representation of PBMCs (left panel) and LNCs (middle panel). The data were manually cleaned (gated on FlowJo based on time> Lymphocytes> FCS singlets> SSC> Singlets> Viability) and concatenated, down-sampling each participant's live population to 10,000 events. Seventeen cell subsets were defined by manual cell gating and are displayed on the plots by color distribution as shown in the legend (right panel) (b) Frequency of CD14+ monocytes (pink) from lymphocytes, CD4+ T cells (grey) and CD8+ T (Brown) from live CD3+ T cells. Each panel shows individual data points for LNC (squares), PBMC (circles), and the median and interquartile range as a box and whisker plot. The results of Mann-Whitney U tests are shown with ***p<0.001. (Day et al. 2022)

smaller cluster (Figure 7.1a). Both tissues contained naive and memory CD4+ and CD8+ T cells, along with memory and naive B cells being abundant in LNC. In PBMC, circulatory Tfh (cTfh) formed a distinct cluster, while in LNC, cTfh and germinal center Tfh (labeled as Tfh) cells were integrated into the CD4+ T cell cluster (Figure 7.1a).

To validate our findings from unsupervised analyses, we conducted sequential two-dimensional analyses. It was confirmed that LNC had a scarcity of CD14+ monocytes compared to PBMC, with median (IQR) frequencies of 0.42% (0.28-0.7%) and 11.1% (8.3%-12.1%), respectively (p<0.001) (Figure 7.1b). Additionally, we observed a significant enrichment of CD4+ T cells in LNC compared to PBMC, with median frequencies of 77.6% (73.8-83.7%) and 54.5% (43.5-62.35%), respectively

(p<0.001) (Figure 7.1b). Conversely, the frequencies of CD8+ T cells were higher in PBMC than in LNC, with median frequencies of 37.9% (27.2-48.6%) and 19.6% (14.4-23.1%), respectively (p<0.001) (Figure 7.1a). Consequently, the CD4:CD8 ratio of T cell subset frequency was significantly higher for LNC compared to PBMC, with median (IQR) values of 4.0 (3.2-5.9) and 1.5 (0.9-2.3), respectively (p<0.001) (figure not shown).

This differential distribution of immune cell subsets between these two tissues underscores the specialized roles they play in immune responses.

### 7.2.3 Memory T subset distribution is tissue specific

Given the potential impact of immune challenge with HIV Mosaic immunogen on T cell memory within reacting LNs, we examined the composition of memory T cell subsets in LNC. Here, we are presenting the data for naive T cells, Tcm, Temra, and Tem. Data for Tscm has already been presented in Chapter 4 (section 4.2.4).

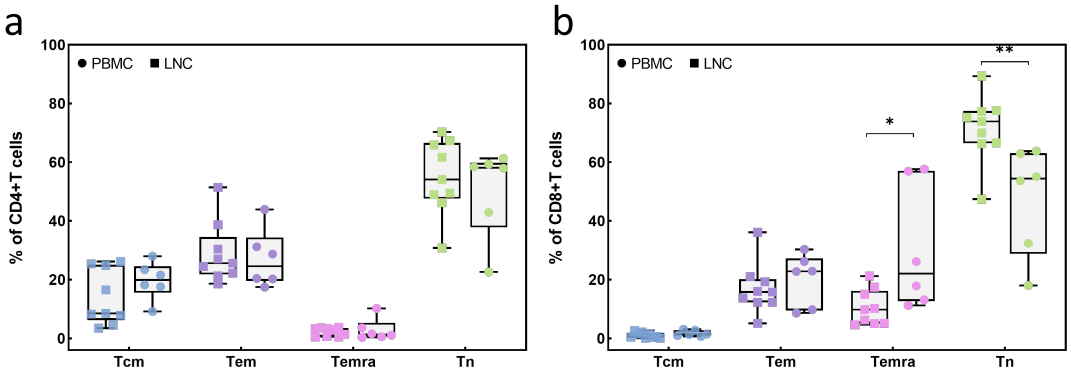



**Figure 7.2**: **Comparative analysis of frequencies of different memory population in PBMCs and LNCs.** a) Frequencies of CD4+ memory T cells in PBMC (circle) and LNC (square). b) Frequencies of CD8+ memory T cells in PBMC (circle) and LNC (square). Each panel shows individual data points for LNC, PBMC, and the median and interquartile range as a box and whisker plot. The results of Mann-Whitney U tests are shown with ***p < 0.001. (Day et al. 2022)

In CD4+ T cells, the frequency of memory subsets in blood and LN exhibited similar patterns (Figure 7.2a). However, naive CD8+ T cells were more abundant in LNC compared to peripheral blood, with median percentages of 73.9% (IQR 66.5-77.5%) and 54.4% (IQR 28.8-63.1%), respectively (p<0.01). Conversely, CCR7-CD45RA+ (Temra) CD8+ T cells were more prevalent in peripheral blood than in LNC (p<0.05) (Figure 7.2b). These differences in memory T cell subsets between

LNs and blood may have implications for immune responses following HIV Mosaic immunogen exposure.

### 7.2.4 Naive CD8+ T cells in the LN are heterogenous

Building upon our earlier observation that CD8+ T memory cells exhibit differential distribution between LNC and PBMCs, we proceeded to delve deeper into the distinctions within CD8+ T cell populations between these two anatomical compartments. To achieve this, we performed an unsupervised pairwise analysis, focusing on two participants for whom adequate CD8+ T cell data from both left and right LNs and PBMC were available (n=2). Equal numbers of CD8+ T cell events (1531) were downsampled from the data, and t-SNE analysis was applied to the concatenated downsampled CD8+ T cells, with samples distinguished by their SampleID (Figure 7.3a-c).

This analysis revealed that several CD8+ T cell subtypes were abundant in LNC but virtually absent in PBMC (Figure 7.3c). FlowSOM analysis of the concatenated CD8+ T cell data generated 25 distinct populations (Figure 7.4a). A unique cluster of CD8+ T cells displaying a naive phenotype was exclusive to PBMC (population 0), while six clusters were found exclusively in LNC (Pop 2, 3, 4, 7, 8, 13). Additionally, there were three rare subsets of CXCR5+CD8+ T cells specific to LNC (Figure 7.4b,c). To validate the observed differences among CD8+ naive T cells in all samples, we conducted conventional pairwise 2-dimensional analysis in CD8+ T cells from PBMC (n=9) and left and right LNC (n=12). In CD8+ naive T cells, markers such as CCR7, CD45RA, CD95, and CD28 were significantly more highly expressed in PBMC compared to LNC ($p<0.0001$ and $p<0.001$). Conversely, CXCR5 and IRF4 showed higher expression levels in LNC compared to PBMC ($p<0.01$ and $p<0.0001$). Notably, markers such as PD-1, CD69, and CD137 exhibited similar expression levels in these CD8+ T cells between blood and LNs (Figure 7.5).

These findings highlight the heterogeneity of CD8+ T cell populations between these two anatomical sites and suggest that the LNs play a distinct role in shaping and housing certain CD8+ T cell subtypes.

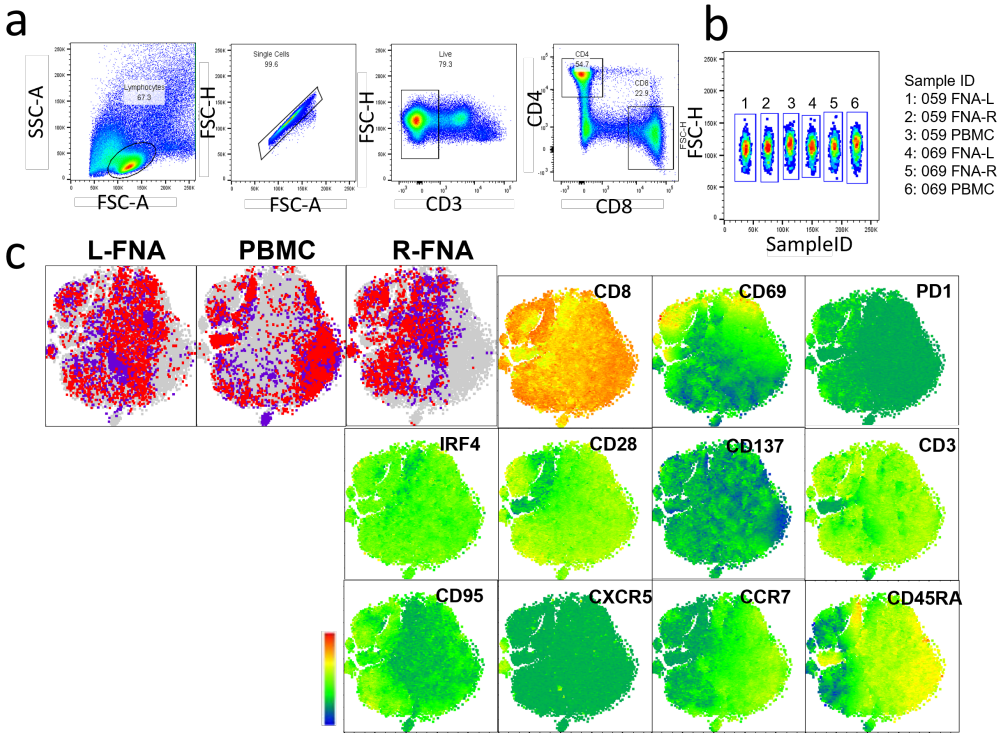



**Figure 7.3**: **Comparison of phenotypic features in CD8+ T Cells between LN and Blood.** a) We conducted pairwise analysis of CD8+ T cells using down-sampled data from LNC and PBMC (1531 events from each participant, n=2). b) Samples were distinguished by their respective sample IDs. c) Subsequently, we applied t-SNE analysis to these samples with a perplexity of 30, gating the data to identify L-FNA, PBMC, and R-FNA using Sample IDs. Dots in the plots represent individual cells, with purple and red colors denoting different participants, while grey dots represent ungated cells. Heatmap statistics plots show the expression of different markers expressed in the cells. (Day et al. 2022)

### 7.2.5 Tfh with a germinal center (GC)-like phenotype are exclusive to the LN

CD4+ Tfh plays a crucial role in supporting B cell's immune responses by orchestrating the formation of germinal center (GC) and facilitating the production of high-affinity antibodies. In previous studies, cTfh cells have been extensively examined as proxies for conventional Germinal central-Tfh (GC-Tfh) cells, primarily due to the challenges involved in directly studying the latter. However, the relationship between these two cell types and their relative significance in shaping immune response remains unclear. To address this question, we aimed to characterize the phenotypic traits of cTfh and LN-resident Tfh in samples obtained simultaneously after HIV Envelope immunogen injection.

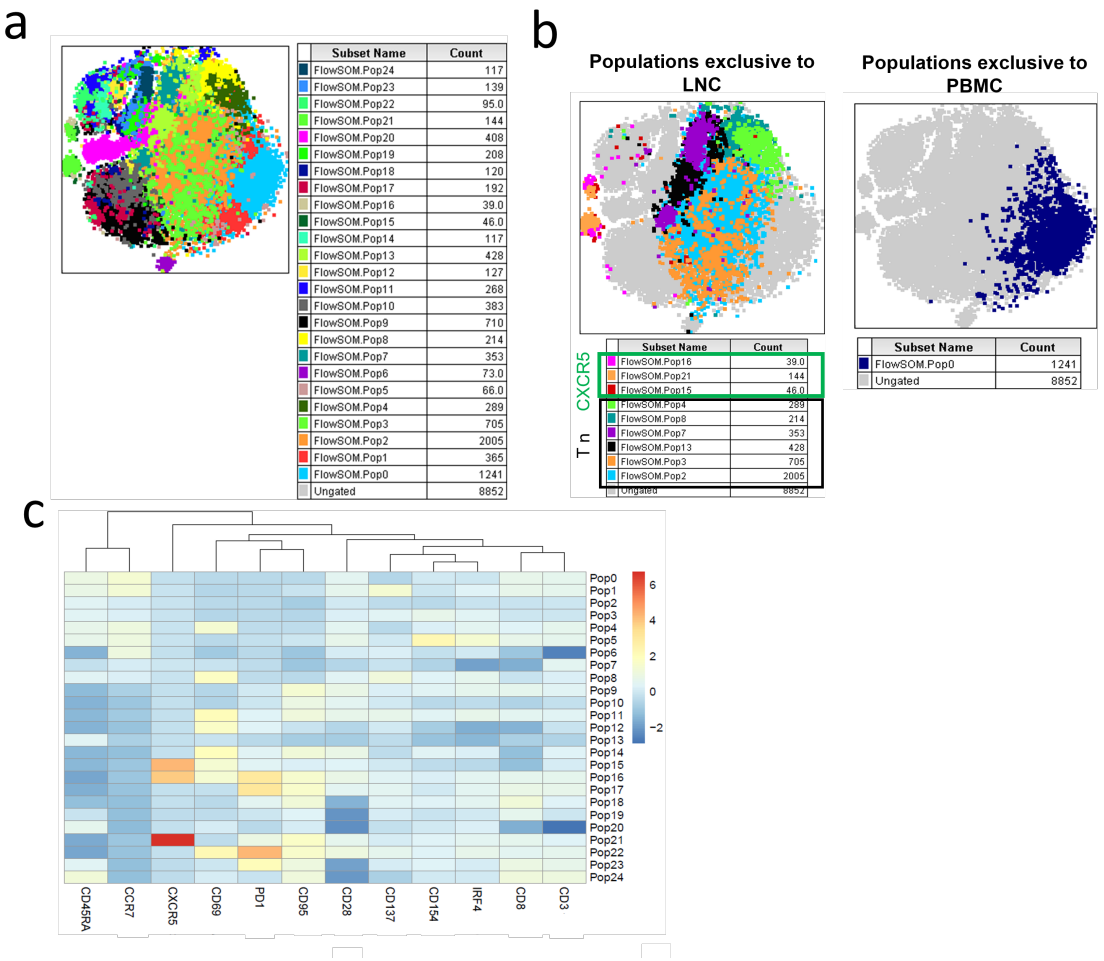



**Figure 7.4**: **Different CD8+ T subsets between LN and Blood.** a) FlowSOM analysis on Figure 7.3 revealed 25 metaclusters. b) We identified distinct cell subpopulations using FlowSOM and visualized them as subpopulations exclusive to either LNC or PBMC through the manual overlay. c) A population heatmap illustrates the relative expression of markers on the 25 metaclusters for FlowSOM populations.(Day et al. 2022)

LN-resident Tfh cells were delineated using sequential gating, defining Tfh as live CD3+CD4+CD19-CD45RA- CXCR5+PD-1+ cells, while cTfh were identified as CD3+CD4+CD19-CD45RA-CXCR5+ cells (Figure 7.6a). Notably, Tfh cells were notably more frequent in LNCs but rare or nearly absent in PBMC, with median (IQR) frequencies of 1.0% (0.7-1.3%) versus 0.14% (0.09-0.17%), respectively ($p<0.001$) (Figure 7.6b). In contrast, the frequency of cTfh exhibited no significant difference between LNC and PBMC, with median (IQR) values of 4.9% (3.4-6.6%) and 7.8% (5.1-9.4%), respectively (Figure 7.6b).

Since CD69 serves as an activation marker for T cells in peripheral blood and is constitutively expressed on GC-Tfh cells, we conducted additional immunophe-

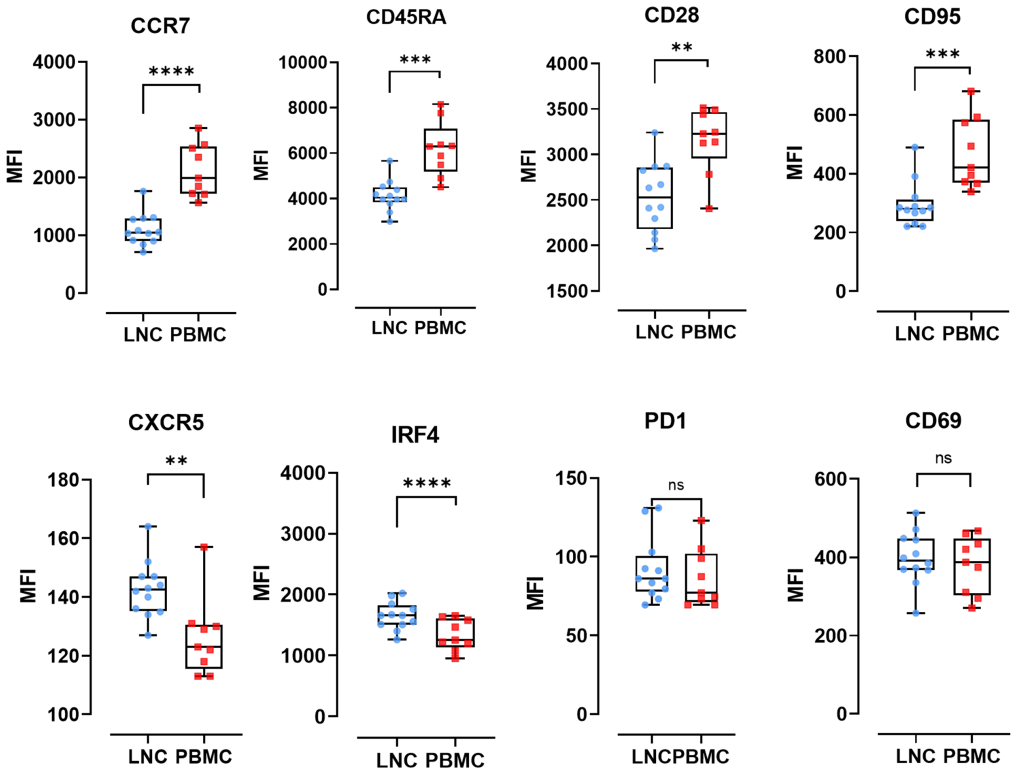



**Figure 7.5**: **Different CD8+ T naïve phenotype in LNC and PBMC.** Two-dimensional analysis compared the median fluorescence intensity of various markers expressed on CD8+ T naïve cells (n=12 for LNC, left and right, and n=9 for PBMC). Significance levels are indicated as follows: *p<0.05, **p<0.01, ***p<0.001, ****p<0.0001. (Day et al. 2022)

notyping experiments involving four participants, accounting for cell number availability. This experiment included CD69 as a marker and utilized paired LNC and PBMC samples that had undergone overnight resting in cell culture medium. Unsupervised clustering analysis was performed on the concatenated data of CD4+ T cells obtained from the paired left and right fine needle aspiration (FNA) and PBMC samples (Figure 7.7a). The expression profiles of immunophenotyping markers were subsequently compared (Figure 7.7b). To gain a deeper understanding of the immunophenotype exclusive to either LNC or PBMC, we employed FlowSOM analysis, revealing the existence of twenty distinct cell populations (Figure 7.7c). Of these, five populations were exclusive to LNC, while one population was unique to PBMC (Figure 7.8a). Remarkably, CD4+ T cell populations 3, 4, 5, and 6 exhibited high CXCR5 expression and were exclusively present in LNC, except for population 4,

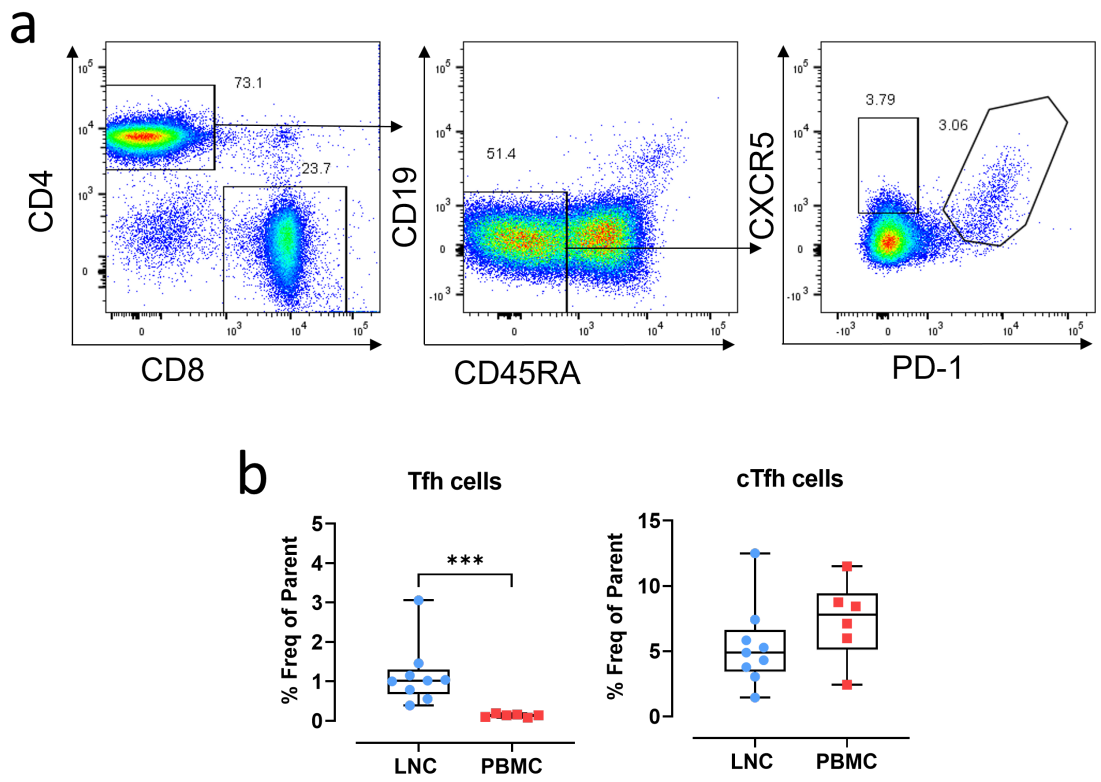



**Figure 7.6**: **LN-resident Tfh (Tfh) and Circulating Tfh (cTfh) in Blood and LN.** a) Presented is a representative gating strategy used to identify Tfh and cTfh. Tfh were gated among live CD4+ T cells that were CD45RA-CD19- and expressed both CXCR5 and PD-1. Meanwhile, cTfh were gated among live CD4+ T cells expressing CXCR5 alone. (B) The frequencies of Tfh (left panel) and cTfh (right panel) within CD4+ T cells in LNC and PBMC were compared. Data are from n=6 participants. Significance levels are indicated as follows: *p<0.05, **p<0.01, ***p<0.001 (Day et al. 2022).

which was distributed between blood and LN. Notably, population 10, found exclusively in PBMC, displayed high levels of PD-1 and CD95 expression (Figure 7.8a).

Further examination of the four CD4+ T cell populations exhibiting high CXCR5 expression (populations 3, 4, 5, and 6) confirmed that population 4 was distributed between both blood and LNs, while populations 3, 5, and 6 were exclusive to LNs, concomitantly expressing CD69 (Figure 7.8b). The MFI of CD69 expression on CD4+CD45RA-CXCR5+ Tfh cells was significantly higher among these cells in LNC compared to PBMC ($p<0.0001$) (Figure 7.8c). Moreover, PD-1 expression reached its highest levels on Tfh cells in LNC, was lower on cTfh in PBMC ($p<0.01$), and significantly lower on CD4+ naive T cells in PBMC ($p<0.001$) (Figure 7.8c). Collectively, these experiments conclusively established that CD69 is highly expressed

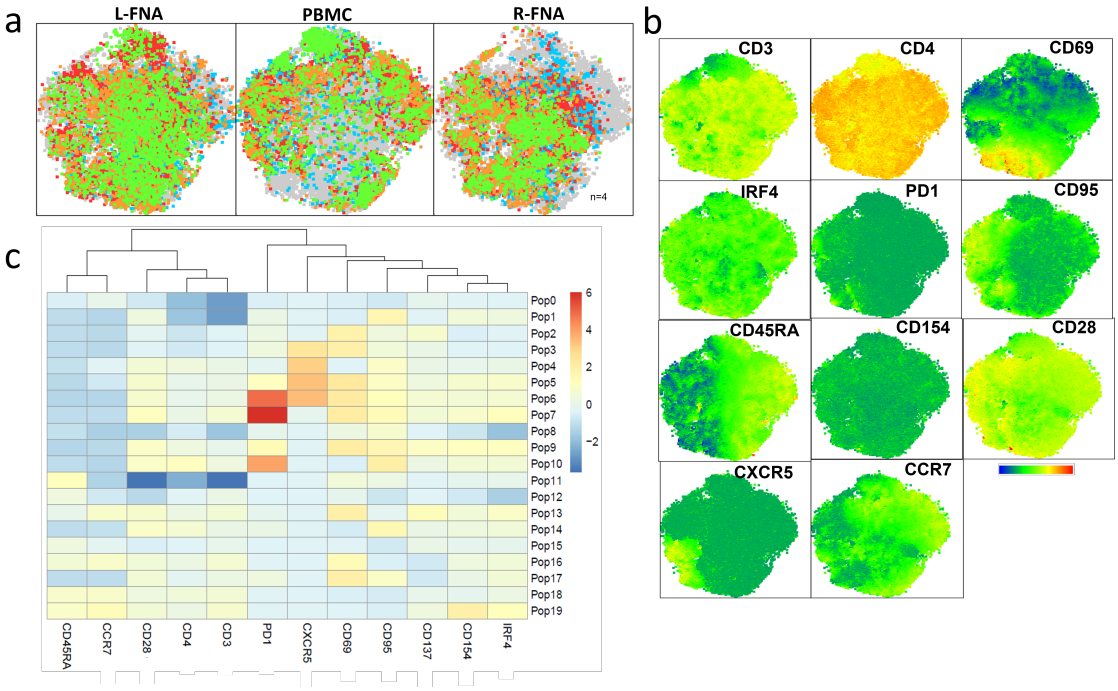



**Figure 7.7**: **t-SNE and FlowSOM analysis of paired LN and blood samples on Live CD4+ T Cells.** a) t-SNE analysis was performed on paired LNC and PBMC samples, with each dataset downsampled to include 2063 events representing CD4+ T cells from each of the four participants (n=4). A perplexity value of 30 was used for t-SNE analysis. SampleID was utilized to distinguish between L-FNA, PBMC, and R-FNA samples. The color coding (green, red, orange, and blue) indicates different participants, while grey dots represent ungated cells not present in the subset. (b) Expression levels of immunophenotyping markers are represented in heatmap statistical plots on the tSNE plots generated by concatenating paired LNC and PBMC samples on live CD4+ T cells. The legend on the right indicates the scale of expression, ranging from low (in blue) to high (in red). c) Population heatmap analysis of the twenty FlowSOM-defined cell populations on tSNE plots, which resulted from concatenating paired LNC and PBMC on live CD4+ T cells. This downsampled dataset included 2063 events representing CD4+ T cells from each of the four participants (n=4). The heatmap illustrates the expression patterns of various immunophenotyping and activation markers (Day et al. 2022).

on Tfh cells in LN but not on cTfh cells in peripheral blood. Additionally, a specific subset of CD4+ T cells in LNC, corresponding to FlowSOM population 6, displayed a phenotype consistent with activated GC-Tfh cells, characterized by CD45RA-CCR7-CD28+PD- 1hiCXCR5hiCD69hiCD95+CD137+CD154+IRF4+ expression.

### 7.2.6 Induction of HIV-specific T cell response in LN

To assess whether the injection of HIV Mosaic induced CD4+ HIV-specific T cells in the LNs, we conducted ex vivo stimulation experiments. PBMC samples were ob-

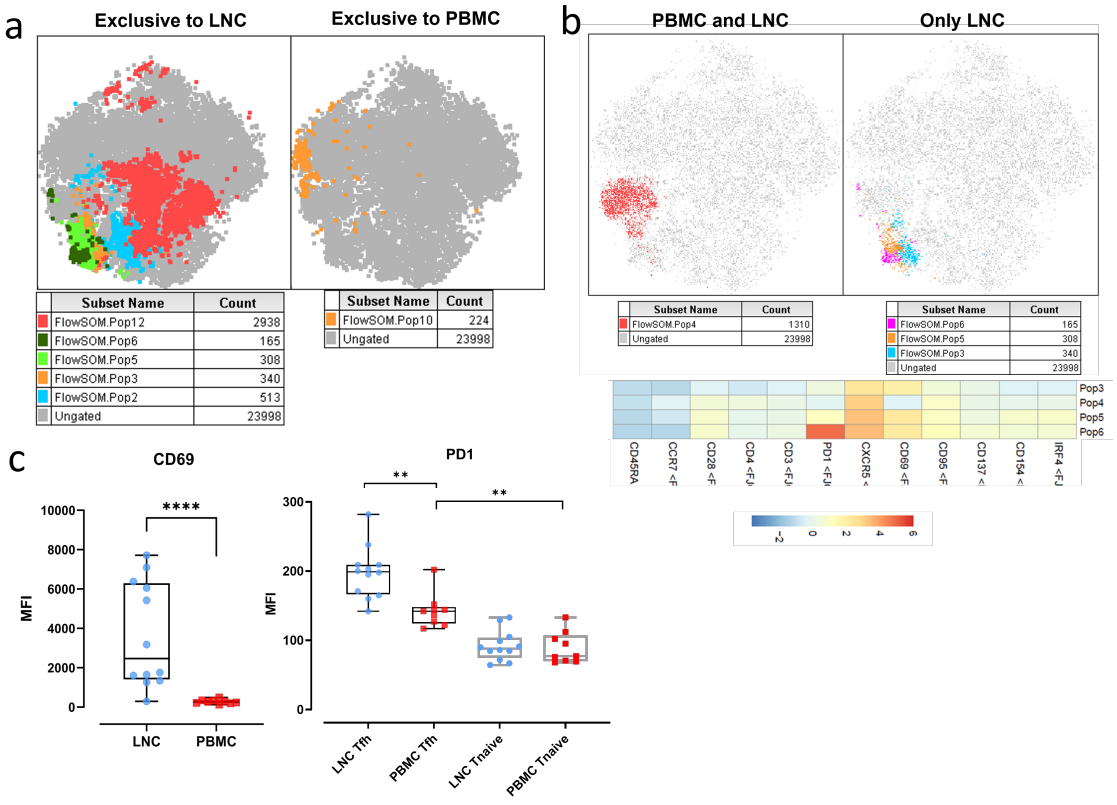



**Figure 7.8**: **Phenotypic differences in Tfh and ctfh cells.** a)FlowSOM Population exclusive to LNC (left panel) and to PBMC (right panel). b)Overlay on t-SNE Analysis of CXCR5+ CD4+ FlowSOM populations present in PBMC and LNC (left panel) and exclusively in LNC (right panel). Subpopulations identified manually are presented in the legend below each tSNE plot. Heatmap represents the expression level of different markers on these populations. c) Comparison of MFI of CD69 and PD1 expression on CD4+ CXCR5+ CD45RA- Tfh Cells and CD45RA+CCR7+ naïve T Cells expressing PD-1 in LNC and PBMC. Statistical Analysis by Mann-Whitney U Tests: **p<0.01, ***p<0.001, ****p<0.0001. (Day et al. 2022)

tained from n=5 participants, and corresponding LNC samples were collected from the same n=5 participants. These samples were subjected to an AIM assay using SEB and the HIV Mosaic peptide pool spanning the full length of the Env proteins utilized in the injection. Activation of CD4+ T cells was identified by the concurrent expression of CD25 and OX40, a well-established marker combination for antigen-specific CD4+ T cells(Figure 7.9a) (19–21). Responding cells were defined as those exhibiting a frequency of CD25+OX40+ cells equal to or greater than 0.01%after background response subtraction. Using this criterion, 6 out of 8 LNC samples and all 5 PBMC samples exhibited responses to the HIV immunogens, while 7 out of 8 LNC samples and all 5 PBMC samples responded to the superantigen SEB. Notably,

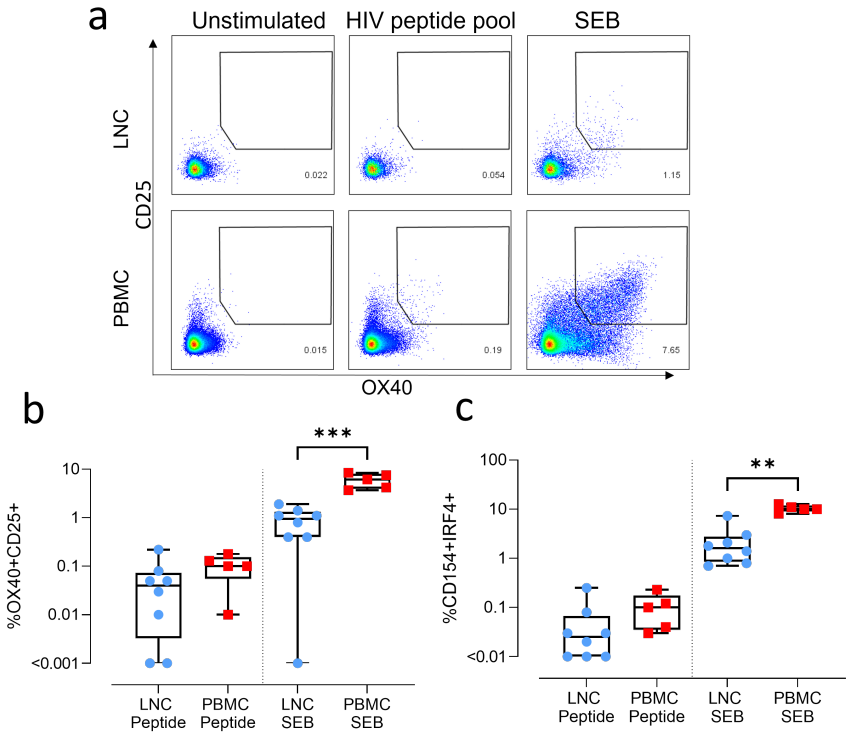



**Figure 7.9**: **Induction of HIV-Specific CD4+ T Cells in LN and suppression of superantigen response compared to blood.** a) Representative gating strategy for AIM assay, unstimulated cells (left panel) or cells stimulated for 18 hours with a peptide pool covering the full length of HIV mosaic envelope trimers used in the immunogen injection (middle panel) or with SEB (Right Panel). CD25 and OX40 Expression in CD4 T Cells in LNC (Top Row) and PBMC (Bottom Row) is Shown. b) Box and whisker plot showing all data points: lower quartile, median, and upper quartile values for LNC and PBMC stimulated with HIV MOSAIC peptide pool (Left) or SEB (Right) in the AIM Assay. b)Frequency of OX40+CD25+ Cells in CD4+ T Cells is shown. c) Frequency of CD154+IRF4+ Cells in CD4+ T Cells is Shown (Day et al. 2022).

the frequency of responsive cells to the EAVI Mosaic peptide pool was comparable between PBMC and LNC. Interestingly, the frequency of responses to SEB was significantly higher in PBMC compared to LNC ($p<0.001$) (Figure 7.9b). The assay also included the measurement of CD154/CD40L-expressing cells, revealing that 5 out of 8 LNC samples and all 5 PBMC samples responded to the HIV immunogens, while 8 out of 8 LNC samples and all 5 PBMC samples responded to the superantigen SEB. Similarly, the frequency of responding CD4+ T cells to SEB was higher in PBMC ($p<0.01$) (Figure 7.9c).

Further, to investigate the frequencies of activation level of different memory subpopulations, both PBMC and LNC were cultured with SEB for 18 hours, and

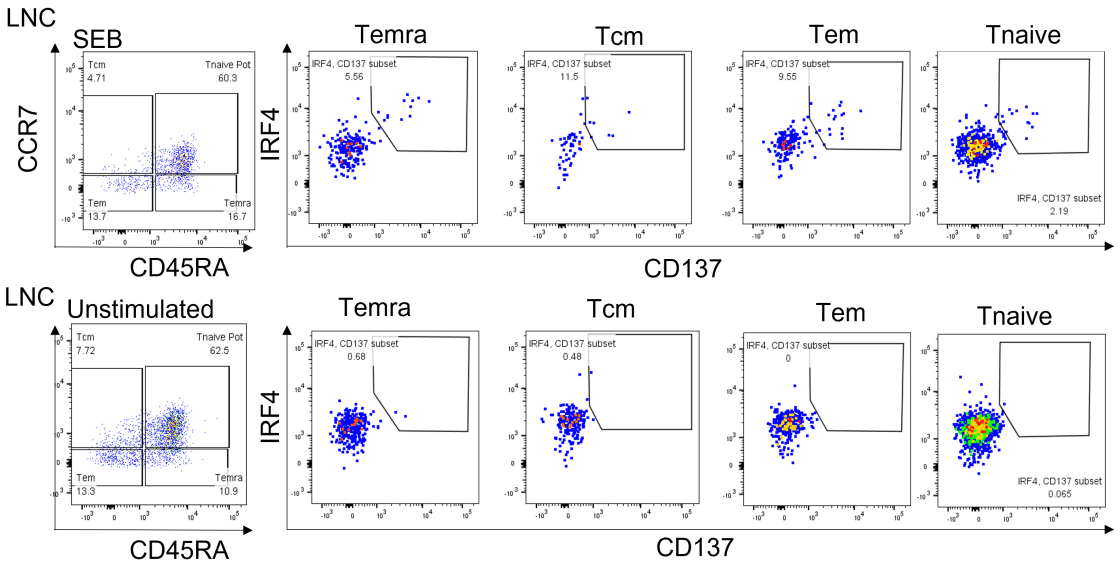



**Figure 7.10**: **Representative gating strategy for SEB stimulated LNC CD8+T memory subpopulation for IRF4CD137 assay.** CD8+ T Cells with Panels from Left to Right Showing Temra, Tcm, Tem, and Tnaive Subsets (Day et al. 2022).

the expression of IRF4 was assessed alongside concurrent expression of CD154 in CD4+ cells and CD137 in CD8+ T cells (n=6 for right FNA, n=6 for left FNA, and n=11 for PBMC) (Figure 7.10).

In CD4+ T cells, the co-expression of CD154 and IRF4 was more prevalent in naïve (CD45RA+CCR7+) and Tem (CD45RA-CCR7-) subpopulations in PBMC than in LNC ($p<0.05$ for both), with a particularly significant difference observed in Tcm (CD45RA-CCR7+) ($p<0.001$) (Figure 7.11a). This indicates that the expression of IRF4 and CD154 in CD4+ T cells was more responsive to SEB stimulation in PBMC compared to LNC. A similar trend was observed in CD8+ T cells expressing CD137 and IRF4, with significantly higher expression in CD8+ Tcm in PBMC compared to LNC ($p<0.001$) (Figure 7.11b). Pairwise comparisons of the activation status of different memory subpopulations after 18 hours of SEB stimulation between left and right FNA samples showed no significant differences for the IRF4+CD154+CD4+ T cell memory subpopulation and the IRF4+CD137+CD8+ T cell memory subpopulation (data not shown). This showed that the memory populations in PBMCs are more responsive to SEB stimulation as compared to LNCs.

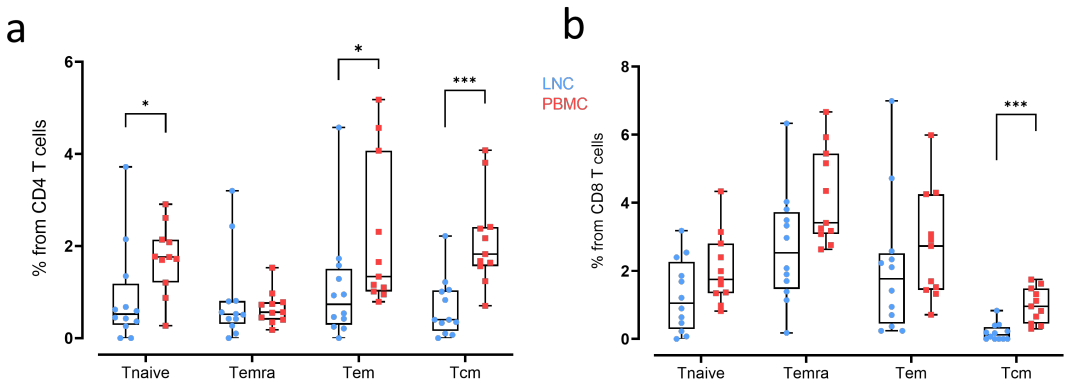



**Figure 7.11**: **Comparison of activation status of T memory subpopulations in PBMC and LNC after stimulation with SEB.** a)PBMC and LNC cultured with SEB for 18 hrs in the IRF4 assay; n=6 for right FNA, n=6 for left FNA, and n=11 for PBMC. Background signals were subtracted. Frequencies shown are the percentage from the parent (CD4 or CD8) population. Frequencies of CD154+IRF4+ among CD4+T Cells that are Naïve (CD45RA+CCR7+), Temra (CD45RA+CCR7-), Tem (CD45RA-CCR7-), and Tcm (CD45RA-CCR7+) in LNC (Blue Circles) and from PBMC (Red Squares). b) Frequency of CD137+IRF4+ memory subpopulation in CD8+ T Cells: LNC (Blue Circles) and PBMC (Red Squares). Statistical Results Displayed: *p<0.05, **p<0.01, ***p<0.001. (Day et al. 2022)

## 7.3 Discussion

The results of this comprehensive analysis of axillary LNC and PBMC following HIV Env antigen injection shed light on the complex interplay between these two compartments in the immune response to vaccination. Notably, LNC demonstrated a remarkable enrichment of immune cell populations, including CD4+ T cells, CD8+ T cells, and B cells, immediately after intramuscular vaccination. This enrichment was particularly significant, as it included the presence of HIV Mosaic-specific CD4+ T cells in individuals who had tested negative for HIV prior to vaccination. Further, these responses in LNs appeared to mirror the timing observed in non-human primates responding to a similar vaccine design (Havenar-Daughton et al. 2016). These findings highlight the pivotal role of LNs in initiating immune responses to HIV antigens, often preceding the detection of antibodies in the bloodstream.

One of the most striking observations was the stark contrast in the composition of immune cells between LNC and PBMC. LNC exhibited a substantially higher CD4:CD8 T cell ratio, a noteworthy feature that is distinct from the blood (Francis-

Morris et al. 2020). Additionally, LNC harbored predominantly naive CD8+ T cells, characterized by unique phenotypic markers such as increased expression of IRF4 and CXCR5, coupled with decreased expression of CD28, CD95, CCR7, and CD45RA. These distinctive features underscore the existence of a specialized immune microenvironment within LNs, further emphasizing their role as immune orchestrators. Further, the population exclusive to PBMC included CD4+ T cells expressing CD95 and PD-1, markers associated with apoptosis and exhaustion. This population is also observed in the peripheral blood of COVID-19 patients (Bellesi et al. 2020).

Within LNC, the presence of GC-like Tfh expressing PD-1 and CD69 hints at their potential involvement in supporting GC reactions. Conversely, CXCR5+PD-1-CD69- cTfh were found to be abundant in both compartments, possibly representing a resting memory T cell population as previously described (Locci et al. 2013, Bentebibel et al. 2013). These findings suggest that CD69+PD-1+ Tfh cells may reside within human LNs, while memory CD4+CXCR5+ T cells appear to move between the blood and LNs. Analysing LN-residing Tfh cells revealed that they highly expressed CXCR5 and CD69 and displayed varying levels of PD-1, CD154, and IRF4. LN-residing Tfh with high PD-1 expression also expressed activation markers consistent with Tfh gaining GC function, in line with the notion that Tfh cells are transitioning in and out of GC function during their memory development (Crotty 2014). Further research involving the simultaneous analysis of blood and LN-residing Tfh cells following vaccination will help clarify whether CD69+PD-1+ Tfh cells possess additional features of GC-Tfh cells and how they relate to cTfh cells.

Another interesting observation was the differential response of LNC and PBMC to the superantigen SEB. These differences may be attributed to variations in antigen presentation, particularly the relative absence of CD14+ monocytes in LNC. This raises questions regarding the identity of antigen-presenting cells in LNs and their role in antigen-specific responses, which warrant further investigation.

The study did have a limitation that is being executed during the COVID-19 pandemic, we adopted a pragmatic approach. This practical strategy involved adjusting the timing of study visits and data collection to accommodate real-world

constraints. Since the study did not specifically assess the HIV-specific response for all the assays, the difficulty in managing potential lymphatic stimulation from other immunogens, including those related to COVID-19 vaccination, adds complexity to interpreting the observed responses to HIV vaccination.

Overall, these findings carry significant implications for vaccine research, particularly in the quest for an effective HIV vaccine. Understanding the dynamics and distinct immune cell compositions within LNs, and their role in shaping immune responses, provides a valuable roadmap for vaccine design and optimization. The direct investigation of adaptive cellular responses within LNs during vaccination offers a potent avenue for expanding our understanding of vaccine development and effectiveness, with the ultimate aim of advancing our efforts to combat HIV infection.

## 7.4 Publication

The results of this chapter have been published in *Frontiers in Immunology* under the title "**Comparison of blood and lymph node cells after intramuscular injection with HIV envelope immunogens**" with me listed as the first co-author (Day et al. 2022).

# Chapter 8

# Discussion

## 8.1 Summary and Outlook

In my doctoral research, we investigated Tscm subpopulations and their roles in shaping immune responses in healthy individuals. Our work built upon the foundational research by Costa Del Amo et al. (2018) and Danai A. Koftori (manuscript in preparation), that the human Tscm compartment exhibits kinetic heterogeneity and contains at least two subsets. We tested the hypothesis that CD95 expression can be used to identify these kinetically distinct Tscm subset and these subsets play a role in maintaining long-term immunity. Indeed, our results show clear differences between CD95int and CD95hi subpopulations, with the CD95int subset exhibiting a quiescent profile, while the CD95hi subset displays an activated phenotype. Importantly, we suggest that both populations play an important role in the maintenance of immune responses. In addition to accomplish the primary objectives, I have made two technical advancements that includes crude lysate ddPCR assay for quantifying rare gene targets from rare cells and optimised AIM assay to quantify antigen-specific CD8+ T cells.

In the paragraphs below, I have provided the highlights of each chapter:

To investigate the dynamics of Tscm subsets, we intended to assess their cell division history by quantifing TRECs content. Given that Tscm cells are present at very low frequency in blood and TRECs are rare in memory subpopulations, we developed a high-throughput crude lysate ddPCR protocol (Chapter 3). This protocol represents a significant advancement in quantifying rare genes from rare

cells, showing excellent linearity within the range of 0.0003 to 0.01 TRECs per cell. The method not only matches the efficiency of standard ddPCR but also offers compatibility with fixed and permeabilized cell samples. By eliminating the need for DNA extraction, it enables the analysis of limited clinical samples, preserves sample integrity, reduces the risk of sample loss, and streamlines the quantification process.

In Chapter 4, we set out to test the hypothesis that CD95 expression can be used to identify different Tscm subsets and that these subsets exhibit distinct dynamics. Indeed, our observations revealed clear differences between CD95int and CD95hi subpopulations. CD95int cells displayed a quiescent profile characterized by low proliferation rates, low expression of activation and co-stimulatory molecules even after SEB stimulation, and relative stability in its frequency with aging. These cells were notably abundant in human LNs. In contrast, the CD95hi subset exhibited an activated phenotype with high proliferation rates, extensive cell division history, increased expression of activation molecules, and an accumulation with age.

In chapters 5 and 6, our attention shifted to the exploration of the dynamics of antigen-specific CD8+ Tscm subsets following vaccination. We aimed to understand their contribution to maintaining long-term memory responses following vaccination. To achieve this, we optimized an AIM assay to detect antigen-specific CD8+ T cells (Chapter 5). In this study, we compared different AIM marker combinations and suggested that the choice of the most suitable AIM combination depends on the desired balance between sensitivity and specificity, aligned with specific research objectives. We selected the IRF4CD137 AIM combination for our HIV trial vaccination studies as it offered several advantages, including high specificity, reduced background noise, consistency in expression across different memory subpopulations, and relevance to the study due to its TCR-MHC-dependent stimulation.

In Chapter 6, we investigated the dynamics of HIV-specific Tscm cells following HIV vaccination in healthy individuals. Notably, in vaccination studies such as B001 and S001, HIV-specific CD95int cells were less prominent, while CD95hi cells started expanding soon after vaccination and exhibited a negative correlation with the rate of decay of CD8+ T cell memory. These findings further reinforce the conclusions outlined in Chapter 4, highlighting the quiescent nature of CD95int and the active

profile of CD95hi. Further, HIV-specific Tscm cells and their subsets generated early after vaccination determine the longevity of vaccine-induced memory CD8+ T cell responses. They provide a foundation for sustaining long-term immune memory by maintaining a balance between effector and memory phenotypes. These findings are supported by: firstly, the early emergence (within 1 week) of antigen-specific Tscm after YF vaccination (Fuertes Marraco et al. 2019) and COVID-BNT162b2 vaccination (Jung et al. 2022). Secondly, their role in sustaining immunity is shown in recent COVID vaccination studies (Jung et al. 2021), where they observed a positive correlation between the frequency of Tscm cell generated early after the vaccination with the durability of T cell response (Jung et al. 2022, Guerrera et al. 2021) and antibody responses (Agallou et al. 2023).

In addition to our primary investigations discussed above, in Chapter 7, we recognize the critical significance of exploring immune dynamics within LNs. Our finding sheds light on the unique immune landscape within LNs as compared to PBMCs and highlights the critical importance of considering the tissue microenvironment in understanding T-cell biology.

The results have been extensively discussed in their respective chapters. Here, I am presenting an overview of the way I accomplished the objectives:

1) In Chapter 3, crude lysate ddPCR assay was established and its technical assessment was done to quantify TRECs from sorted memory cell populations:

   **a)** Firstly, the standard ddPCR assay protocol was optimised and validated by comparing it with a well-established qPCR technique to quantify TRECs from PBMCs.

   **b)** Different methods, including thermal lysis, sonication, lysis buffers from DNA/RNA extraction kits, lysis Buffer 1, and lysis buffer 2, were explored to make the cell lysate compatible with ddPCR. Lysis buffer 1 and buffer 2 offered the best results with the highest reproducibility.

   **c)** Linearity of the crude lysate ddPCR using buffer 1 was compared with that of using buffer 2. For this, standard curves using PBMCs from healthy individuals were made. We observed that Buffer 2 exhibited a slope (1.298) that is closer to the ideal value of 1 when compared to Buffer 1 (1.513). Therefore, buffer 2 was taken forward.

**d)** We added an innovative step to deal with the problem caused by the high viscosity of crude lysate i.e. viscosity breakdown step, that enhanced the accuracy of our results.

**e)** The LOD of crude lysate ddPCR using buffer2 was determined to be 0.0001 TRECs/cell (or 1 TREC/10,000 cells) and LOQ 0.0003 TRECs/cell (or 3 TRECs/10,000 cells). This protocol demonstrated good repeatability with average CV% below 25%, ensuring precise quantification of low target concentrations with confidence.

**f)** A direct comparison of the newly developed crude lysate ddPCR and the standard ddPCR was made by analyzing TRECs copies/cells from sorted memory subpopulations and observed a high level of agreement (assessed using Bland-Altman analysis).

**g)** Additionally, this method also offered compatibility with fixed and permeabilised cell samples.

2) In Chapter 4, we comprehensively characterized Tscm subsets through various approaches, including immunophenotyping, cell division history tracking, age-related variations, transcriptional analysis, and tissue distribution profiling.

**a)** Initially, we investigated the association between CD95 expression and Ki67 positivity. We observed that CD95hi cells had higher frequency of Ki67+ cells as compared to CD95int and Tcm.

**b)** We defined our gating strategy to identify Tscm subsets using contour and histogram plots.

**c)** We observed accumulation of CD95hi subset in healthy donors with age, while CD95int were relatively stable. However, the proliferation capacity of CD95hi cells was reduced significantly with age, indicated by the reduced frequency of Ki67+ cells within this subset in older individuals.

**d)** Significantly higher TRECs were observed in CD95hi subset as compared to CD95int, indicating higher division history of CD95hi than CD95int.

**e)** We further investigated the tissue distribution patterns of Tscm subsets in PBMCs and LNCs and observed higher percentage of CD95int cells in LNCs

as compared to PBMCs. Differential expression of different markers on PBMC Tscm and LNC Tscm suggested different functional states or activation status of Tscm cells in these two tissues.

**f)** Additionally, we investigated the expression of different activation markers such as CD137, IRF4, PD-1 and CD69 on Tscm subsets, and observed CD95hi Tscm cells have a more pronounced activation molecule expression profile compared to CD95int.

3) In Chapter 5, we compared different AIM markers to identify the best AIM marker combinations to detect antigen-specific CD8+ T cells. For this, we utilised samples from healthy donors vaccinated with the flu vaccine. We stimulated the PBMCs with Flu-M1 peptide and detected true Flu-specific CD8+ T cells by Pentamer staining and compared it with AIM marker combinations to assess their accuracy:

**a)** CD69CD137, CD137 and IRF4CD137 had nearly similar sensitivity for detecting antigen-specific CD8+ T, which means these markers are effective at correctly identifying true positive cells. However, when considering specificity, which measures the ability to minimize false positive results, the IRF4CD137 combination was found to be the best at all timepoints. In other words, while CD69CD137 and CD137 were highly sensitive, they may also yield a higher number of false positives, making them less specific

**b)** We assessed the bystander activation in these markers combination by blocking the MHC-TCR interactions and found that IRF4 expression is more sensitive to MHC-TCR signaling, while CD137CD69 expression remains largely unaffected by TCR-MHC stimulation.

**c)** Additionally, CD69 and CD137 expression on different memory subpopulations was variable while IRF4 exhibits consistent expression within various memory subpopulations.

**d)** A significant proportion of IRF4CD137combination co-expressed CD69.

4) In Chapter 6, we studied the dynamics of different HIV- specific CD8+ T memory subpopulations following HIV vaccination in healthy donors. We

used samples from three HIV trial vaccination studies: CUTHIVAC, S001 and B001.

**a)** Firstly, we investigated the HIV-specific CD8+ T cell response and observed that CUTHIVAC has a relatively stable response within the timeframe studies, while in S001, CD8+ T cell response dropped drastically by 32 weeks post-boost, and for B001 a gradual decline was observed till last time point assessed (72 W).

**b)** Comparing initial responses in different vaccines, we observed that the CUTHIVAC study has an initial effector response characterised by the high frequency of Temra cells. S001 dominated the initial memory response indicated by a higher frequency of Tcm and Tscm cells. While B001 had an effector response characterised by a high frequency of Tem cells.

**c)** Two weeks post-boost, CUTHIVAC had a higher frequency of CD95int as compared to CD95hi. While the reversed trend is observed for B001 and S001.

**d)** We observed a negative correlation between the frequency of HIV-specific Tscm generated early after vaccination with the rate of decay of HIV-specific CD8+ T cell memory.

**e)** The frequency of HIV-specific CD95hi early after vaccination exhibited a negative correlation with the rate of decay of HIV-specific Tem and Tcm, while HIV-specific CD95int cells exhibited a negative correlation with the rate of decay of Temra.

5) In Chapter 7, we compared the immune profile of different immune cells present in human LN and blood following HIV envelope immunogen challenge in healthy donors (EAVI study): **a)** Notably, LNC exhibited a significantly higher CD4:CD8 T cell ratio and negligible frequency of monocytes, distinguishing features compared to peripheral blood.

**b)** LNC pre-dominantly housed naive CD8+ T cells, characterized by unique phenotypic markers such as increased expression of IRF4 and CXCR5, alongside decreased expression of CD28, CD95, CCR7, and CD45RA.

**c)** The phenotype of LNC-resident Tfh cells is different from cTfh present in blood. LNC-resident Tfh cells exhibited higher expression of PD-1 and CD69.

**d)** Another interesting observation was the differential response of LNC and PBMC to the superantigen SEB

In summary, my doctoral research in addition to investigating Tscm subpopulations and their roles in shaping immune responses in healthy individuals, I also optimised innovative methodologies to quantify cellular division history. This journey was marked by the validation of our hypotheses, a thorough understanding of Tscm subset dynamics, and the illumination of their crucial contributions to long-term memory and immunity. Our findings, supported by a growing body of research, underscore the significance of early-emerging Tscm cells in sustaining long-term immune responses and emphasize the importance of understanding tissue-specific immune landscapes.

## 8.2 Limitations

Our study, while valuable in elucidating the dynamics of memory T cell subsets and their relationship to immune responses, has several notable limitations. These limitations are essential to consider when interpreting the findings.

**Limited Insight into Absolute Quantification:** The primary focus of our analysis was on changes in the frequencies of various memory T cell subsets. While we extensively examined the relative frequencies of Tscm subsets and how they change with vaccination or aging, we did not assess the actual numeric changes in these populations. This limitation becomes evident when we consider the relative frequencies alone. For instance, our research observed shifts in the relative frequencies of Tscm subsets following vaccination and with advancing age, suggesting changes in the immune response. However, without absolute quantification, we are unable to definitively conclude whether these shifts represent genuine numerical changes in the Tscm populations or if they are a result of broader fluctuations in the overall T cell composition unrelated to the vaccine's effectiveness or aging process. Absolute quantification would have provided a more precise understanding of the actual alterations in Tscm populations, shedding light on the efficacy of the vaccines and the dynamics of these crucial memory T cell subsets both in response to vaccinations and with age. To provide a more comprehensive understanding of

changes in memory T cell subsets, future studies could incorporate methods for the absolute quantification of these subpopulations.

**Challenges in Lymph Node Sampling:** Our study faced challenges with limited Tscm cell numbers in LN samples, affecting statistical reliability and may have introduced potential sampling bias and data variability. It's important to note that this is not due to the inadequacy of the FNA technique to extract LN cells. Rather, our study was designed as a preliminary investigation to assess the feasibility of using FNA in a clinical setting for longitudinal studies of LNCs following vaccination. Therefore, we divided our LNC samples into separate parts to conduct different analyses. Despite this limitation, we successfully achieved our main objective in this study.

**Small Sample Size:** A notable limitation of the vaccination studies in this investigation is the relatively small sample size. With a maximum of 24 participants in the S001 study and an effective sample size ranging from 10 to 16 individuals, the generalizability of the results may be constrained. A larger and more diverse cohort would enhance the robustness and comprehensiveness of the conclusions drawn from this study.

**Specific Timepoint Data Collection:** The reliance on specific timepoints for data collection post-booster vaccinations is a limitation. Memory cell populations are dynamic and can be influenced by multiple factors. The selected timepoints may not capture all potential changes that could occur following primary vaccinations. More continuous or frequent data collection would provide a better understanding of the evolving immune response.

**Causation and Correlation:** While correlations were used as the primary analytical tool to explore relationships between Tscm subsets and memory cell decay, it is important to recognize the difficulty in establishing causation based solely on correlations. Future mechanistic studies involving experimental interventions and functional assessments will be essential to confirm causal links.

**Unmeasured Variables and Confounding Factors:** The possibility of unmeasured variables or confounding factors that were not accounted for in the analysis is acknowledged. Immune responses are complex and multifaceted, influenced by genetic variations, prior exposure histories, and individual variability. This study

aimed to uncover specific relationships, but it cannot rule out the existence of additional factors that could impact the outcomes.

**Gender-Based Bias:** We did not perform a gender-based analysis in the vaccination studies due to the lack of demographic data for analysis. This limitation should be noted when considering the study's findings.

**ddPCR Limitations:** The study had a limited number of replicates for optimization and technical assessment. While LOD and LOQ analysis showed satisfactory results, concentrations below 0.0003 TRECs copies/cell were not explored. Occasional artifacts, such as double negative clusters and isolated droplets with abnormal amplitudes, may be attributed to contamination, debris, or technical variations.

**Use of IRF4 and CD137:** Using IRF4 as an intracellular marker in combination with CD137 required cell permeabilization, limiting its suitability for live cell studies or downstream applications. Despite this limitation, the high specificity of these markers in filtering out background noise can be advantageous for certain experimental contexts.

In light of these limitations, it is imperative to approach the study's findings with caution and recognize the potential avenues for further research in this field.

## 8.3 Future work

The future work of this research branches into more immediate questions and further exploratory work. **Immediate questions include further phenotyping for characterizing Tscm subsets**, connecting their functionality, exhaustion patterns, and quiescent gene markers. It could include assessing cytokines/cytotoxic secretion and activation markers for functionality; CD39, CXCR5, PD-1, TIGIT for exhaustion markers and FOXP1 as a quiescent gene marker. We are currently analyzing bulk RNAseq data from sorted memory CD95hi and CD95int subpopulations to further characterise these subpopulations. However, this technique or scRNAseq could be used to further understand the dynamics of these subsets longitudinally following vaccination.

Another **immediate question that needs clarification in future work in-**

**cludes if CD95hi and CD95int cells are indeed two subsets as we propose or if they transiently upregulate CD95 under certain conditions**. Notably, earlier sections of this thesis have underscored the pivotal role of epigenetics in governing the differentiation pathways and functionality of immune subsets (Pace, 2021). It would be particularly insightful to delve into the chromatin landscape of CD95hi and CD95int subsets, comparing their similarities and differences with other memory subsets and naive T cells. An intriguing study by Gilles et al., involving healthy humans, has revealed epigenetic similarities among Tcm, CXCR3+ TSCM, and CXCR3- Tscm cells while shedding light on significant inflection points in the differentiation process (Giles et al., 2022).

Furthermore, the issue of whether CD95int and CD95hi cells share TCR sequences or possess distinct clonal identities remains unresolved. Our research and findings, alongside Danai's work, have led to the proposition that CD95int cells maintain the CD95hi subset and serve as a source for its replenishment. This logic implies that both subsets might have originated during the primary response, potentially resulting in a substantial overlap in their repertoire. Galletti et al. conducted valuable research on Tstem and Tpex subsets in humans, revealing distinct spectra of recognized antigens and hinting at parallel differentiation pathways (Galletti et al., 2020). Leveraging TCR sequencing (TCR-seq) for the examination of CD95hi and CD95int subsets could provide analogous insights into their differentiation and functional characteristics. Next, reassessing tissue distribution patterns, especially considering the limited Tscm cell data from LNC in our initial study, offers a more comprehensive understanding of the distribution of these subsets and whether they genuinely constitute two distinct entities.

To further **explore the dynamics of these subsets**, one could take a lead from our Ki67 and CD95hi data. We observed that CD95hi subsets exhibited a decline in their proliferation capacity indicated by a reduction in Ki67+ cells, despite their accumulation with age. Researchers can further explore whether our hypothesis of converting CD95hi to Tpex with age is true. Alternatively, an investigation of the half-life of these cells to understand their enhanced survival could be done. This research is particularly significant for comprehending the role of these subsets in regulating immune responses, especially in older individuals.

Additionally, this study has focused on characterizing the subsets under homeostatic conditions or after HIV vaccination, but it has been shown that infections by different pathogens can lead to the generation of phenotypically and functionally distinct memory subsets (Aalderen et al., 2021). The ontogeny of the 2 subsets is a critical feature of their identity and it would be worth exploring more. For example, an interesting question to address would be if one subset is more likely to arise under chronic infection settings compared to the other. Isolating naive cells from healthy individuals and exposing them to different stimuli of chronic or acute infection could be a way to answer this question.

**Next aspect is to understand the mechanism of regulation governed by Tscm cells**. In our study, we proposed that Tscm and its subsets regulate the maintenance of memory by establishing a balance between the effector and memory phase. Exploring the mechanisms governing this regulation would be interesting. Particularly, if this is true then how do Tscm cells actively control their population size through self-renewal and differentiation into effector phase cells?

Likewise, it would also be interesting to investigate the metabolomics of these subsets, as studies have shown that memory cells exhibit different metabolomes than naive T cells. Expanding this research on Tscm subsets would be further interesting.

Finally, **understanding how environmental contexts shape the maintenance of these subsets** underlines their functional significance in diverse environments and provides insights into their therapeutic targeting. A study by Fuertes et al. has shown that CCR7hi Tscm cells (which are similar to CD95int as mentioned in Chapter 4) have the highest% of YF-specific cells 25 years after vaccination and are more stable over time compared to CCR7lo suggesting something similar could be the case for CD95hi and CD95int subsets as previously mentioned.

By addressing these areas and questions, future research can provide a more comprehensive understanding of memory T cell dynamics, immune responses, and long-term immunity. These insights are crucial for the development of more effective vaccines and vaccination strategies.

## 8.4 Final words

In conclusion, we observed two kinetically distinct subsets in the human Tscm compartment - CD95hi and CD95int. Both Tscm subsets are important in the maintenance of memory. We believe that throughout this thesis we have managed to capture and describe the heterogeneity of the Tscm compartment using both healthy human samples and HIV trial vaccination samples. Our efforts have substantiated the notion that these proposed subsets are genuinely discrete entities, each possessing distinct and defining attributes. How the dynamics of Tscm and its subsets are maintained and what regulatory mechanisms are exerted by them to maintain long-term immunity - is the next step of this work but beyond the scope of this thesis.

# Thesis-Related Publications: Current and Upcoming

## Published as First co-author

- Day, S., Kaur, C.*, Cheeseman, H.M., de Groot, E., McFarlane, L.R., Tanaka, M., Coelho, S., Cole, T., Lemm, N.M., Lim, A. and Sanders, R.W., 2022. Comparison of blood and lymph node cells after intramuscular injection with HIV envelope immunogens. Frontiers in Immunology, 13, p.991509.

## Upcoming

- Kaur, C.*, Stuart, A., Kibirige, C. and Asquith, B., **In Prep.** Absolute Quantification of rare gene targets in limited samples using crude lysate and ddPCR
- Koftori, D., Kaur, C.*, Zhang, Y., Hadcocks, L., Yan, A., Ladell, K., Pollock, K., Macallan, D. and Asquith, B., **Submitted.** Two distinct subpopulations of human stem-like memory T cells with different dynamics, function and homing properties
- Kaur, C.*, Cheeseman, H., Pollock, K., and Asquith, B., **In prep.** Comparison of activation-induced markers to detect antigen-specific CD8+T cells
- Kaur, C.*, Hayes, P., Makinde, J., Cheeseman, H., Pollock, K., and Asquith, B., Evaluation of antiviral T cell responses and Tscm cells in volunteers enrolled in CUTHIVAC002 and IAVI HIV trial vaccination studies.

# Acronyms

**PBMC** Peripheral Blood Mononuclear Cells

**LN** Lymph node

**Tfh** T follicular helper cell

**GC** germinal center

**US-guided FNA** ultrasound-guided fine needle aspiration

**FNA** fine needle aspiration

**LNC** lymph node cell

**t-SNE** t-distributed Stochastic Neighbor Embedding

**cTfh** circulatory Tfh

**GC-Tfh** Germinal central-Tfh

**TREC** T-cell Receptor Excision Circle

**PBS** Phosphate-buffered saline

**FCS** fetal calf serum

**DMSO** dimethyl sulfoxide

**FMO** fluorescence minus one

**ddPCR** Droplet Digital Polymerase Chain Reaction

**NFW** nuclease free water

**RPP30** ribonuclease P/MRP subunit p3

**LOB** Limit of Blank

**NTC** non template control

**CLC** cell line lysate control

**LOD** Limit of Detection

**LOQ** Limit of Quantification

**SEB** staphylococcal enterotoxin B

**CUTHIVAC** Combined skin and muscle vaccination

**IAVI** International AIDS Vaccine Initiative

**EAVI** European AIDS Vaccine Initiative

**SIV** simian immunodeficiency virus

**NHPs** non-human primates

**YF** Yellow Fever

**SLECs** short-lived effector cells

**MPECs** memory precursor effector cells

**Tcm** Central memory T cell

**Tem** Effector memory T cells

**Temra** Effector memory RA+ T cells

**CMV** cytomegalovirus

**Tscm** Memory stem T cells

**HIV** Human immunodeficiency viruses

**Trm** Tissue-resident memory cells

**Tvm** Virtual memory T cells

**Tex** Exhausted T Cells

**TF** Transcription factor

**GVHD** graft-versus-host diseases

**NHP** nonhuman primate

**IFR** interfollicular region

**SARS-CoV-2** Severe acute respiratory syndrome coronavirus 2

**qPCR** quantitative Polymerase Chain Reaction

**CV** coefficient of variation

**TNF** tumor necrosis factor

**IRF4** Interferon Regulatory Factor 4

**TCR** T cell receptor

**MHC** major histocompatibility complex

**ICS** intracellular cytokine secretion

**AIM** activation-induced marker

**APC** antigen presenting cell

**SeV** Sendai virus

**Ad35** adenovirus serotype 35

# Bibliography


Adamo, S., Gao, Y., Sekine, T., Mily, A., Wu, J., Storgärd, E., Westergren, V., Filén, F., Treutiger, C.-J., Sandberg, J. K. et al. (2023), 'Memory profiles distinguish cross-reactive and virus-specific t cell immunity to mpox', *Cell Host & Microbe* **31**(6), 928–936.

Adamo, S., Michler, J., Zurbuchen, Y., Cervia, C., Taeschler, P., Raeber, M. E., Baghai Sain, S., Nilsson, J., Moor, A. E. & Boyman, O. (2022), 'Signature of long-lived memory cd8+ t cells in acute sars-cov-2 infection', *Nature* **602**(7895), 148–155.

Agallou, M., Koutsoni, O. S., Michail, M., Zisimopoulou, P., Tsitsilonis, O. E. & Karagouni, E. (2023), 'Antibody and t-cell subsets analysis unveils an immune profile heterogeneity mediating long-term responses in individuals vaccinated against sars-cov-2', *The Journal of Infectious Diseases* **227**(3), 353–363.

Ahmed, A. S. I., Sheng, M. H., Wasnik, S., Baylink, D. J. & Lau, K.-H. W. (2017), 'Effect of aging on stem cells', *World journal of experimental medicine* **7**(1), 1.

Ahmed, R. & Akondy, R. S. (2011), 'Insights into human cd8+ t-cell memory using the yellow fever and smallpox vaccines', *Immunology and cell biology* **89**(3), 340–345.

Ahmed, R. & Gray, D. (1996), 'Immunological memory and protective immunity: understanding their relation', *Science* **272**(5258), 54–60.

Ahmed, R., Miners, K. L., Lahoz-Beneytez, J., Jones, R. E., Roger, L., Baboonian, C., Zhang, Y., Wang, E. C., Hellerstein, M. K., McCune, J. M. et al. (2020), 'Cd57+ memory t cells proliferate in vivo', *Cell reports* **33**(11).

Ahmed, R., Roger, L., Del Amo, P. C., Miners, K. L., Jones, R. E., Boelen, L., Fali, T., Elemans, M., Zhang, Y., Appay, V. et al. (2016), 'Human stem cell-like memory t cells are maintained in a state of dynamic flux', *Cell reports* **17**(11), 2811–2818.

Ahn, S. G., Bae, S. J., Kim, Y., Ji, J. H., Chu, C., Kim, D., Lee, J., Cha, Y. J., Lee, K.-A. & Jeong, J. (2022), 'Primary endocrine resistance of er+ breast cancer with esr1 mutations interrogated by droplet digital pcr', *npj Breast Cancer* **8**(1), 58.

Aigrain, L., Gu, Y. & Quail, M. A. (2016), 'Quantitation of next generation sequencing library preparation protocol efficiencies using droplet digital pcr assays-a systematic comparison of dna library preparation kits for illumina sequencing', *BMC genomics* **17**, 1–11.

Akondy, R. S., Fitch, M., Edupuganti, S., Yang, S., Kissick, H. T., Li, K. W., Youngblood, B. A., Abdelsamed, H. A., McGuire, D. J., Cohen, K. W. et al. (2017), 'Origin and differentiation of human memory cd8 t cells after vaccination', *Nature* **552**(7685), 362–367.

Akondy, R. S., Monson, N. D., Miller, J. D., Edupuganti, S., Teuwen, D., Wu, H., Quyyumi, F., Garg, S., Altman, J. D., Del Rio, C. et al. (2009), 'The yellow fever virus vaccine induces a broad and polyfunctional human memory cd8+ t cell response', *The Journal of Immunology* **183**(12), 7919–7930.

Alberts, B., Johnson, A., Lewis, J., Raff, M., Roberts, K. & Walter, P. (2002), B cells and antibodies, *in* 'Molecular Biology of the Cell. 4th edition', Garland Science.

Aleksova, M., Todorova, Y., Emilova, R., Baymakova, M., Yancheva, N., Andonova, R., Zasheva, A., Grifoni, A., Weiskopf, D., Sette, A. et al. (2023), 'Virus-specific stem cell memory cd8+ t cells may indicate a long-term protection against evolving sars-cov-2', *Diagnostics* **13**(7), 1280.

Amodio, D., Cotugno, N., Macchiarulo, G., Rocca, S., Dimopoulos, Y., Castrucci, M. R., De Vito, R., Tucci, F. M., McDermott, A. B., Narpala, S. et al. (2018), 'Quantitative multiplexed imaging analysis reveals a strong association between immunogen-specific b cell responses and tonsillar germinal center immune

dynamics in children after influenza vaccination', *The Journal of Immunology* **200**(2), 538–550.

Ardiani, A., Gameiro, S. R., Palena, C., Hamilton, D. H., Kwilas, A., King, T. H., Schlom, J. & Hodge, J. W. (2014), 'Vaccine-mediated immunotherapy directed against a transcription factor driving the metastatic process', *Cancer research* **74**(7), 1945–1957.

Ariotti, S., Hogenbirk, M. A., Dijkgraaf, F. E., Visser, L. L., Hoekstra, M. E., Song, J.-Y., Jacobs, H., Haanen, J. B. & Schumacher, T. N. (2014), 'Skin-resident memory cd8+ t cells trigger a state of tissue-wide pathogen alert', *Science* **346**(6205), 101–105.

Arstila, T. P., Casrouge, A., Baron, V., Even, J., Kanellopoulos, J. & Kourilsky, P. (1999), 'A direct estimate of the human $\alpha\beta$ t cell receptor diversity', *Science* **286**(5441), 958–961.

Asquith, B. & Borghans, J. A. (2011), Modelling lymphocyte dynamics in vivo, *in* 'Mathematical Models and Immune Cell Biology', Springer, pp. 141–169.

Bacher, P. & Scheffold, A. (2013), 'Flow-cytometric analysis of rare antigen-specific t cells', *Cytometry Part A* **83**(8), 692–701.

Bachmann, M. F., Hunziker, L., Zinkernagel, R. M., Storni, T. & Kopf, M. (2004), 'Maintenance of memory ctl responses by t helper cells and cd40-cd40 ligand: antibodies provide the key', *European journal of immunology* **34**(2), 317–326.

Bachmann, M. F., Wolint, P., Schwarz, K., Jager, P. & Oxenius, A. (2005), 'Functional properties and lineage relationship of cd8+ t cell subsets identified by expression of il-7 receptor $\alpha$ and cd62l', *The Journal of Immunology* **175**(7), 4686–4696.

Badovinac, V. P., Porter, B. B. & Harty, J. T. (2004), 'Cd8+ t cell contraction is controlled by early inflammation', *Nature immunology* **5**(8), 809–817.

Baker, M. W., Grossman, W. J., Laessig, R. H., Hoffman, G. L., Brokopp, C. D., Kurtycz, D. F., Cogley, M. F., Litsheim, T. J., Katcher, M. L. & Routes, J. M.

(2009), 'Development of a routine newborn screening protocol for severe combined immunodeficiency', *Journal of Allergy and Clinical Immunology* **124**(3), 522–527.

Banerjee, A., Gordon, S. M., Intlekofer, A. M., Paley, M. A., Mooney, E. C., Lindsten, T., Wherry, E. J. & Reiner, S. L. (2010), 'Cutting edge: The transcription factor eomesodermin enables cd8+ t cells to compete for the memory cell niche', *The Journal of Immunology* **185**(9), 4988–4992.

Bansal-Pakala, P., Halteman, B. S., Cheng, M. H.-Y. & Croft, M. (2004), 'Costimulation of cd8 t cell responses by ox40', *The Journal of Immunology* **172**(8), 4821–4825.

Bao, X., Qin, D., Ma, J., Zhou, X., Wang, J., Yao, C., Zhang, L. & Du, L. (2022), 'Accurate detection of $\alpha$-globin gene copy number variants with two reactions using droplet digital pcr', *Hematology* **27**(1), 198–203.

Barbaro, M., Ohlsson, A., Borte, S., Jonsson, S., Zetterström, R. H., King, J., Winiarski, J., von Döbeln, U. & Hammarström, L. (2017), 'Newborn screening for severe primary immunodeficiency diseases in sweden—a 2-year pilot trec and krec screening study', *Journal of clinical immunology* **37**, 51–60.

Barber, D. L., Wherry, E. J., Masopust, D., Zhu, B., Allison, J. P., Sharpe, A. H., Freeman, G. J. & Ahmed, R. (2006), 'Restoring function in exhausted cd8 t cells during chronic viral infection', *Nature* **439**(7077), 682–687.

Bauer, T. & Jilg, W. (2006), 'Hepatitis b surface antigen-specific t and b cell memory in individuals who had lost protective antibodies after hepatitis b vaccination', *Vaccine* **24**(5), 572–577.

Becker, T. C., Wherry, E. J., Boone, D., Murali-Krishna, K., Antia, R., Ma, A. & Ahmed, R. (2002), 'Interleukin 15 is required for proliferative renewal of virus-specific memory cd8 t cells', *The Journal of experimental medicine* **195**(12), 1541–1548.

Bellesi, S., Metafuni, E., Hohaus, S., Maiolo, E., Marchionni, F., D'Innocenzo, S., La Sorda, M., Ferraironi, M., Ramundo, F., Fantoni, M. et al. (2020), 'Increased

cd95 (fas) and pd-1 expression in peripheral blood t lymphocytes in covid-19 patients', *British journal of haematology* **191**(2), 207–211.

Bennett, S. R., Carbone, F. R., Karamalis, F., Flavell, R. A., Miller, J. F. & Heath, W. R. (1998), 'Help for cytotoxic-t-cell responses is mediated by cd40 signalling', *Nature* **393**(6684), 478–480.

Bentebibel, S.-E., Lopez, S., Obermoser, G., Schmitt, N., Mueller, C., Harrod, C., Flano, E., Mejias, A., Albrecht, R. A., Blankenship, D. et al. (2013), 'Induction of icos+ cxcr3+ cxcr5+ th cells correlates with antibody responses to influenza vaccination', *Science translational medicine* **5**(176), 176ra32–176ra32.

Berard, M., Brandt, K., Paus, S. B. & Tough, D. F. (2003), 'Il-15 promotes the survival of naive and memory phenotype cd8+ t cells', *The Journal of Immunology* **170**(10), 5018–5026.

Betts, M. R., Brenchley, J. M., Price, D. A., De Rosa, S. C., Douek, D. C., Roederer, M. & Koup, R. A. (2003), 'Sensitive and viable identification of antigen-specific cd8+ t cells by a flow cytometric assay for degranulation', *Journal of immunological methods* **281**(1-2), 65–78.

Biasco, L., Scala, S., Basso Ricci, L., Dionisio, F., Baricordi, C., Calabria, A., Giannelli, S., Cieri, N., Barzaghi, F., Pajno, R. et al. (2015), 'In vivo tracking of t cells in humans unveils decade-long survival and activity of genetically modified t memory stem cells', *Science translational medicine* **7**(273), 273ra13–273ra13.

Blackburn, S. D., Shin, H., Freeman, G. J. & Wherry, E. J. (2008), 'Selective expansion of a subset of exhausted cd8 t cells by $\alpha$pd-l1 blockade', *Proceedings of the National Academy of Sciences* **105**(39), 15016–15021.

Blattman, J. N., Antia, R., Sourdive, D. J., Wang, X., Kaech, S. M., Murali-Krishna, K., Altman, J. D. & Ahmed, R. (2002), 'Estimating the precursor frequency of naive antigen-specific cd8 t cells', *The Journal of experimental medicine* **195**(5), 657–664.

Blattman, J. N., Grayson, J. M., Wherry, E. J., Kaech, S. M., Smith, K. A. &

Ahmed, R. (2003), 'Therapeutic use of il-2 to enhance antiviral t-cell responses in vivo', *Nature medicine* **9**(5), 540–547.

Boesteanu, A. C. & Katsikis, P. D. (2009), Memory t cells need cd28 costimulation to remember, *in* 'Seminars in immunology', Vol. 21, Elsevier, pp. 69–77.

Bolzoni, M., Toscani, D., Costa, F., Vicario, E., Aversa, F. & Giuliani, N. (2019), 'The link between bone microenvironment and immune cells in multiple myeloma: Emerging role of cd38', *Immunology Letters* **205**, 65–70.

Bowyer, G., Rampling, T., Powlson, J., Morter, R., Wright, D., Hill, A. V. & Ewer, K. J. (2018), 'Activation-induced markers detect vaccine-specific cd4+ t cell responses not measured by assays conventionally used in clinical trials', *Vaccines* **6**(3), 50.

Brenchley, J. M., Karandikar, N. J., Betts, M. R., Ambrozak, D. R., Hill, B. J., Crotty, L. E., Casazza, J. P., Kuruppu, J., Migueles, S. A., Connors, M. et al. (2003), 'Expression of cd57 defines replicative senescence and antigen-induced apoptotic death of cd8+ t cells', *Blood, The Journal of the American Society of Hematology* **101**(7), 2711–2720.

Buenrostro, J. D., Giresi, P. G., Zaba, L. C., Chang, H. Y. & Greenleaf, W. J. (2013), 'Transposition of native chromatin for fast and sensitive epigenomic profiling of open chromatin, dna-binding proteins and nucleosome position', *Nature methods* **10**(12), 1213–1218.

Butcher, E. C. & Picker, L. J. (1996), 'Lymphocyte homing and homeostasis', *Science* **272**(5258), 60–67.

Callan, M., Tan, L., Annels, N., Ogg, G., Wilson, J., O'callaghan, C., Steven, N., McMichael, A. & Rickinson, A. (1998), 'Direct visualization of antigen-specific cd8+ t cells during the primary immune response to epstein-barr virus in vivo', *The Journal of experimental medicine* **187**(9), 1395–1402.

Cannarile, M. A., Lind, N. A., Rivera, R., Sheridan, A. D., Camfield, K. A., Wu, B. B., Cheung, K. P., Ding, Z. & Goldrath, A. W. (2006), 'Transcriptional regulator id2 mediates cd8+ t cell immunity', *Nature immunology* **7**(12), 1317–1325.

Carty, S. A., Gohil, M., Banks, L. B., Cotton, R. M., Johnson, M. E., Stelekati, E., Wells, A. D., Wherry, E. J., Koretzky, G. A. & Jordan, M. S. (2018), 'The loss of tet2 promotes cd8+ t cell memory differentiation', *The Journal of Immunology* **200**(1), 82–91.

Caruso, A., Licenziati, S., Corulli, M., Canaris, A. D., De Francesco, M. A., Fiorentini, S., Peroni, L., Fallacara, F., Dima, F., Balsari, A. et al. (1997), 'Flow cytometric analysis of activation markers on stimulated t cells and their correlation with cell proliferation', *Cytometry: The Journal of the International Society for Analytical Cytology* **27**(1), 71–76.

Casalegno-Garduño, R., Schmitt, A., Yao, J., Wang, X., Xu, X., Freund, M. & Schmitt, M. (2010), 'Multimer technologies for detection and adoptive transfer of antigen-specific t cells', *Cancer immunology, immunotherapy* **59**(2), 195–202.

Casey, K. A., Fraser, K. A., Schenkel, J. M., Moran, A., Abt, M. C., Beura, L. K., Lucas, P. J., Artis, D., Wherry, E. J., Hogquist, K. et al. (2012), 'Antigen-independent differentiation and maintenance of effector-like resident memory t cells in tissues', *The Journal of Immunology* **188**(10), 4866–4875.

Castellino, F., Galli, G., Del Giudice, G. & Rappuoli, R. (2009), 'Generating memory with vaccination', *European journal of immunology* **39**(8), 2100–2105.

Castellino, F., Huang, A. Y., Altan-Bonnet, G., Stoll, S., Scheinecker, C. & Germain, R. N. (2006), 'Chemokines enhance immunity by guiding naive cd8+ t cells to sites of cd4+ t cell–dendritic cell interaction', *Nature* **440**(7086), 890–895.

Chandele, A., Sewatanon, J., Gunisetty, S., Singla, M., Onlamoon, N., Akondy, R. S., Kissick, H. T., Nayak, K., Reddy, E. S., Kalam, H. et al. (2016), 'Characterization of human cd8 t cell responses in dengue virus-infected patients from india', *Journal of virology* **90**(24), 11259–11278.

Chang, J. (2021), 'Mhc multimer: a molecular toolbox for immunologists', *Molecules and Cells* **44**(5), 328.

Chang, J. T., Palanivel, V. R., Kinjyo, I., Schambach, F., Intlekofer, A. M., Banerjee, A., Longworth, S. A., Vinup, K. E., Mrass, P., Oliaro, J. et al. (2007), 'Asymmetric

t lymphocyte division in the initiation of adaptive immune responses', *science* **315**(5819), 1687–1691.

Chang, J. T., Wherry, E. J. & Goldrath, A. W. (2014), 'Molecular regulation of effector and memory t cell differentiation', *Nature immunology* **15**(12), 1104–1115.

Chen, e. a. (2018), 'Transcriptional and epigenetic regulation of effector and memory cd8 t cell differentiation', *Frontiers in immunology* **9**, 2826.

Chen, L. & Flies, D. B. (2013), 'Molecular mechanisms of t cell co-stimulation and co-inhibition', *Nature reviews immunology* **13**(4), 227–242.

Chen, Y.-H., Kratchmarov, R., Lin, W.-H. W., Rothman, N. J., Yen, B., Adams, W. C., Nish, S. A., Rathmell, J. C. & Reiner, S. L. (2018), 'Asymmetric pi3k activity in lymphocytes organized by a pi3k-mediated polarity pathway', *Cell reports* **22**(4), 860–868.

Chen, Z., Stelekati, E., Kurachi, M., Yu, S., Cai, Z., Manne, S., Khan, O., Yang, X. & Wherry, E. J. (2017), 'mir-150 regulates memory cd8 t cell differentiation via c-myb', *Cell reports* **20**(11), 2584–2597.

Chicz, R. M., Urban, R. G., Lane, W. S., Gorga, J. C., Stern, L. J., Vignali, D. A. & Strominger, J. L. (1992), 'Predominant naturally processed peptides bound to hla-dr1 are derived from mhc-related molecules and are heterogeneous in size', *Nature* **358**(6389), 764–768.

Choe, C.-u., Lardong, K., Gelderblom, M., Ludewig, P., Leypoldt, F., Koch-Nolte, F., Gerloff, C. & Magnus, T. (2011), 'Cd38 exacerbates focal cytokine production, postischemic inflammation and brain injury after focal cerebral ischemia', *PLoS One* **6**(5), e19046.

Chong, L. K., Aicheler, R. J., Llewellyn-Lacey, S., Tomasec, P., Brennan, P. & Wang, E. C. (2008), 'Proliferation and interleukin 5 production by cd8hicd57+ t cells', *European journal of immunology* **38**(4), 995–1000.

Choo, J. A., Liu, J., Toh, X., Grotenbreg, G. M. & Ren, E. C. (2014), 'The immunodominant influenza a virus m158–66 cytotoxic t lymphocyte epitope exhibits

degenerate class i major histocompatibility complex restriction in humans', *Journal of virology* **88**(18), 10613–10623.

Cirelli, K. M., Carnathan, D. G., Nogal, B., Martin, J. T., Rodriguez, O. L., Upadhyay, A. A., Enemuo, C. A., Gebru, E. H., Choe, Y., Viviano, F. et al. (2019), 'Slow delivery immunization enhances hiv neutralizing antibody and germinal center responses via modulation of immunodominance', *Cell* **177**(5), 1153–1171.

Cossarizza, A., Chang, H.-D., Radbruch, A., Abrignani, S., Addo, R., Akdis, M., Andrä, I., Andreata, F., Annunziato, F., Arranz, E. et al. (2021), 'Guidelines for the use of flow cytometry and cell sorting in immunological studies', *European journal of immunology* **51**(12), 2708–3145.

Costa Del Amo, P., Lahoz-Beneytez, J., Boelen, L., Ahmed, R., Miners, K. L., Zhang, Y., Roger, L., Jones, R. E., Marraco, S. A. F., Speiser, D. E. et al. (2018), 'Human tscm cell dynamics in vivo are compatible with long-lived immunological memory and stemness', *PLoS biology* **16**(6), e2005523.

Croft, M. (2009), 'Control of immunity by the tnfr-related molecule ox40 (cd134)', *Annual review of immunology* **28**, 57–78.

Crompton, J. G., Narayanan, M., Cuddapah, S., Roychoudhuri, R., Ji, Y., Yang, W., Patel, S. J., Sukumar, M., Palmer, D. C., Peng, W. et al. (2016), 'Lineage relationship of cd8+ t cell subsets is revealed by progressive changes in the epigenetic landscape', *Cellular & molecular immunology* **13**(4), 502–513.

Crotty, S. (2014), 'T follicular helper cell differentiation, function, and roles in disease', *Immunity* **41**(4), 529–542.

Crotty, S. (2019), 'T follicular helper cell biology: a decade of discovery and diseases', *Immunity* **50**(5), 1132–1148.

Cui, G., Staron, M. M., Gray, S. M., Ho, P.-C., Amezquita, R. A., Wu, J. & Kaech, S. M. (2015), 'Il-7-induced glycerol transport and tag synthesis promotes memory cd8+ t cell longevity', *Cell* **161**(4), 750–761.

Cui, W., Joshi, N. S., Jiang, A. & Kaech, S. M. (2009), 'Effects of signal 3 during cd8 t cell priming: Bystander production of il-12 enhances effector t cell expansion but promotes terminal differentiation', *Vaccine* **27**(15), 2177–2187.

Cui, W. & Kaech, S. M. (2010), 'Generation of effector cd8+ t cells and their conversion to memory t cells', *Immunological reviews* **236**(1), 151–166.

Cui, W., Liu, Y., Weinstein, J. S., Craft, J. & Kaech, S. M. (2011), 'An interleukin-21-interleukin-10-stat3 pathway is critical for functional maturation of memory cd8+ t cells', *Immunity* **35**(5), 792–805.

Dan, J. M., Lindestam Arlehamn, C. S., Weiskopf, D., da Silva Antunes, R., Havenar-Daughton, C., Reiss, S. M., Brigger, M., Bothwell, M., Sette, A. & Crotty, S. (2016), 'A cytokine-independent approach to identify antigen-specific human germinal center t follicular helper cells and rare antigen-specific cd4+ t cells in blood', *The Journal of Immunology* **197**(3), 983–993.

Dan, J. M., Mateus, J., Kato, Y., Hastie, K. M., Yu, E. D., Faliti, C. E., Grifoni, A., Ramirez, S. I., Haupt, S., Frazier, A. et al. (2021), 'Immunological memory to sars-cov-2 assessed for up to 8 months after infection', *Science* **371**(6529), eabf4063.

Danahy, D. B., Anthony, S. M., Jensen, I. J., Hartwig, S. M., Shan, Q., Xue, H.-H., Harty, J. T., Griffith, T. S. & Badovinac, V. P. (2017), 'Polymicrobial sepsis impairs bystander recruitment of effector cells to infected skin despite optimal sensing and alarming function of skin resident memory cd8 t cells', *PLoS pathogens* **13**(9), e1006569.

Dancey, J., Deubelbeiss, K. A., Harker, L. A., Finch, C. A. et al. (1976), 'Neutrophil kinetics in man.', *The Journal of clinical investigation* **58**(3), 705–715.

Daniels, M. A. & Teixeiro, E. (2015), 'Tcr signaling in t cell memory', *Frontiers in immunology* **6**, 617.

Danilo, M., Chennupati, V., Silva, J. G., Siegert, S. & Held, W. (2018), 'Suppression of tcf1 by inflammatory cytokines facilitates effector cd8 t cell differentiation', *Cell reports* **22**(8), 2107–2117.

Davis, J. P. (2005), 'Experience with hepatitis a and b vaccines', *The American journal of medicine* **118**(10), 7–15.

Davis, M. M. (2008), 'A prescription for human immunology', *Immunity* **29**(6), 835–838.

Day, S., Kaur, C., Cheeseman, H. M., de Groot, E., McFarlane, L. R., Tanaka, M., Coelho, S., Cole, T., Lemm, N.-M., Lim, A. et al. (2022), 'Comparison of blood and lymph node cells after intramuscular injection with hiv envelope immunogens', *Frontiers in Immunology* **13**, 991509.

De Boer, R. J. & Noest, A. J. (1998), 'T cell renewal rates, telomerase, and telomere length shortening', *The Journal of Immunology* **160**(12), 5832–5837.

De Gregorio, E. & Rappuoli, R. (2012), 'Vaccines for the future: learning from human immunology', *Microbial biotechnology* **5**(2), 149–155.

De Rosa, S. C., Lu, F. X., Yu, J., Perfetto, S. P., Falloon, J., Moser, S., Evans, T. G., Koup, R., Miller, C. J. & Roederer, M. (2004), 'Vaccination in humans generates broad t cell cytokine responses', *The Journal of Immunology* **173**(9), 5372–5380.

De Simone, G., Mazza, E., Cassotta, A., Davydov, A. N., Kuka, M., Zanon, V., De Paoli, F., Scamardella, E., Metsger, M., Roberto, A. et al. (2019), 'Cxcr3 identifies human naive cd8+ t cells with enhanced effector differentiation potential', *The Journal of Immunology* **203**(12), 3179–3189.

Delpoux, A., Michelini, R. H., Verma, S., Lai, C.-Y., Omilusik, K. D., Utzschneider, D. T., Redwood, A. J., Goldrath, A. W., Benedict, C. A. & Hedrick, S. M. (2018), 'Continuous activity of foxo1 is required to prevent anergy and maintain the memory state of cd8+ t cells', *Journal of Experimental Medicine* **215**(2), 575–594.

den Braber, I., Mugwagwa, T., Vrisekoop, N., Westera, L., Mögling, R., de Boer, A. B., Willems, N., Schrijver, E. H., Spierenburg, G., Gaiser, K. et al. (2012), 'Maintenance of peripheral naive t cells is sustained by thymus output in mice but not humans', *Immunity* **36**(2), 288–297.

Dhein, J., Walczak, H., Bäumler, C., Debatin, K.-M. & Krammer, P. H. (1995), 'Autocrine t-cell suicide mediated by apo-1/(fas/cd95)', *Nature* **373**(6513), 438–441.

Di Benedetto, S., Derhovanessian, E., Steinhagen-Thiessen, E., Goldeck, D., Müller, L. & Pawelec, G. (2015), 'Impact of age, sex and cmv-infection on peripheral t cell phenotypes: results from the berlin base-ii study', *Biogerontology* **16**, 631–643.

Dianzani, U., Funaro, A., DiFranco, D., Garbarino, G., Bragardo, M., Redoglia, V., Buonfiglio, D., De Monte, L. B., Pileri, A. & Malavasi, F. (1994), 'Interaction between endothelium and cd4+ cd45ra+ lymphocytes. role of the human cd38 molecule.', *Journal of immunology (Baltimore, Md.: 1950)* **153**(3), 952–959.

Do Kwon, Y., Pancera, M., Acharya, P., Georgiev, I. S., Crooks, E. T., Gorman, J., Joyce, M. G., Guttman, M., Ma, X., Narpala, S. et al. (2015), 'Crystal structure, conformational fixation and entry-related interactions of mature ligand-free hiv-1 env', *Nature structural & molecular biology* **22**(7), 522–531.

Doherty, P. C. & Zinkernagel, R. M. (1975), 'H-2 compatibility is required for t-cell-mediated lysis of target cells infected with lymphocytic choriomeningitis virus.', *The Journal of experimental medicine* **141**(2), 502–507.

Dong, L., Meng, Y., Sui, Z., Wang, J., Wu, L. & Fu, B. (2015), 'Comparison of four digital pcr platforms for accurate quantification of dna copy number of a certified plasmid dna reference material', *Scientific reports* **5**(1), 13174.

Du, J., Wei, L., Li, G., Hua, M., Sun, Y., Wang, D., Han, K., Yan, Y., Song, C., Song, R. et al. (2021), 'Persistent high percentage of hla-dr+ cd38high cd8+ t cells associated with immune disorder and disease severity of covid-19', *Frontiers in Immunology* **12**, 735125.

Duckworth, B. C. & Groom, J. R. (2021), 'Conversations that count: cellular interactions that drive t cell fate', *Immunological Reviews* **300**(1), 203–219.

Duckworth, B. C., Lafouresse, F., Wimmer, V. C., Broomfield, B. J., Dalit, L., Alexandre, Y. O., Sheikh, A. A., Qin, R. Z., Alvarado, C., Mielke, L. A. et al.

(2021), 'Effector and stem-like memory cell fates are imprinted in distinct lymph node niches directed by cxcr3 ligands', *Nature immunology* **22**(4), 434–448.

Duckworth, B. C., Qin, R. Z. & Groom, J. R. (2022), 'Spatial determinates of effector and memory cd8+ t cell fates', *Immunological Reviews* **306**(1), 76–92.

Duque, A. & Rakic, P. (2011), 'Different effects of bromodeoxyuridine and [3h] thymidine incorporation into dna on cell proliferation, position, and fate', *Journal of Neuroscience* **31**(42), 15205–15217.

El-Asady, R., Yuan, R., Liu, K., Wang, D., Gress, R. E., Lucas, P. J., Drachenberg, C. B. & Hadley, G. A. (2005), 'Tgf-$\beta$–dependent cd103 expression by cd8+ t cells promotes selective destruction of the host intestinal epithelium during graft-versus-host disease', *The Journal of experimental medicine* **201**(10), 1647–1657.

Farber, D. L., Yudanin, N. A. & Restifo, N. P. (2014), 'Human memory t cells: generation, compartmentalization and homeostasis', *Nature Reviews Immunology* **14**(1), 24–35.

Fearon, D. T., Manders, P. & Wagner, S. D. (2001), 'Arrested differentiation, the self-renewing memory lymphocyte, and vaccination', *Science* **293**(5528), 248–250.

Fenwick, C., Joo, V., Jacquier, P., Noto, A., Banga, R., Perreau, M. & Pantaleo, G. (2019), 'T-cell exhaustion in hiv infection', *Immunological reviews* **292**(1), 149–163.

Finley, J. (2017), 'Elimination of cancer stem cells and reactivation of latent hiv-1 via ampk activation: Common mechanism of action linking inhibition of tumorigenesis and the potential eradication of hiv-1', *Medical Hypotheses* **104**, 133–146.

Fox, A., Hoa, L. N. M., Horby, P., van Doorn, H. R., Trung, N. V., Ha, N. H., Cap, N. T., Phu, V. D., Ha, N. M., Ngoc, D. N. T. et al. (2012), 'Severe pandemic h1n1 2009 infection is associated with transient nk and t deficiency and aberrant cd8 responses', *PloS one* **7**(2), e31535.

Francis-Morris, A., Mackie, N., Eliahoo, J., Ramzan, F., Fidler, S. & Pollock, K. (2020), 'Compromised cd 4: Cd 8 ratio recovery in people living with hiv aged over 50 years: an observational study', *HIV medicine* **21**(2), 109–118.

Frentsch, M., Arbach, O., Kirchhoff, D., Moewes, B., Worm, M., Rothe, M., Scheffold, A. & Thiel, A. (2005), 'Direct access to cd4+ t cells specific for defined antigens according to cd154 expression', *Nature medicine* **11**(10), 1118–1124.

Fuertes Marraco, S. A., Bovay, A., Nassiri, S., Maby-El Hajjami, H., Ouertatani-Sakouhi, H., Held, W. & Speiser, D. E. (2019), 'The human cd8 t stem cell-like memory phenotype appears in the acute phase in yellow fever virus vaccination', *Biorxiv* p. 808774.

Fuertes Marraco, S. A., Soneson, C., Cagnon, L., Gannon, P. O., Allard, M., Maillard, S. A., Montandon, N., Rufer, N., Waldvogel, S., Delorenzi, M. et al. (2015), 'Long-lasting stem cell–like memory cd8+ t cells with a naïve-like profile upon yellow fever vaccination', *Science translational medicine* **7**(282), 282ra48–282ra48.

Galletti, G., De Simone, G., Mazza, E. M., Puccio, S., Mezzanotte, C., Bi, T. M., Davydov, A. N., Metsger, M., Scamardella, E., Alvisi, G. et al. (2020), 'Two subsets of stem-like cd8+ memory t cell progenitors with distinct fate commitments in humans', *Nature immunology* **21**(12), 1552–1562.

Gallimore, A., Glithero, A., Godkin, A., Tissot, A. C., Plückthun, A., Elliott, T., Hengartner, H. & Zinkernagel, R. (1998), 'Induction and exhaustion of lymphocytic choriomeningitis virus–specific cytotoxic t lymphocytes visualized using soluble tetrameric major histocompatibility complex class i–peptide complexes', *The Journal of experimental medicine* **187**(9), 1383–1393.

Ganusov, V. V. & De Boer, R. J. (2007), 'Do most lymphocytes in humans really reside in the gut?', *Trends in immunology* **28**(12), 514–518.

Gao, S., Liang, X., Wang, H., Bao, B., Zhang, K., Zhu, Y. & Shao, Q. (2021), 'Stem cell-like memory t cells: a perspective from the dark side', *Cellular Immunology* **361**, 104273.

García-Rodríguez, S., Rosal-Vela, A., Botta, D., Cumba Garcia, L. M., Zumaquero, E., Prados-Maniviesa, V., Cerezo-Wallis, D., Lo Buono, N., Robles-Guirado, J.-Á., Guerrero, S. et al. (2018), 'Cd38 promotes pristane-induced chronic inflammation and increases susceptibility to experimental lupus by an apoptosis-driven and trpm2-dependent mechanism', *Scientific reports* **8**(1), 3357.

Gattinoni, L. (2014), 'Memory t cells officially join the stem cell club', *Immunity* **41**(1), 7–9.

Gattinoni, L., Lugli, E., Ji, Y., Pos, Z., Paulos, C. M., Quigley, M. F., Almeida, J. R., Gostick, E., Yu, Z., Carpenito, C. et al. (2011), 'A human memory t cell subset with stem cell–like properties', *Nature medicine* **17**(10), 1290–1297.

Gattinoni, L., Speiser, D. E., Lichterfeld, M. & Bonini, C. (2017), 'T memory stem cells in health and disease', *Nature medicine* **23**(1), 18–27.

Gattinoni, L., Zhong, X.-S., Palmer, D. C., Ji, Y., Hinrichs, C. S., Yu, Z., Wrzesinski, C., Boni, A., Cassard, L., Garvin, L. M. et al. (2009), 'Wnt signaling arrests effector t cell differentiation and generates cd8+ memory stem cells', *Nature medicine* **15**(7), 808–813.

Geginat, J., Lanzavecchia, A. & Sallusto, F. (2003), 'Proliferation and differentiation potential of human cd8+ memory t-cell subsets in response to antigen or homeostatic cytokines', *Blood* **101**(11), 4260–4266.

Gerner, M. Y., Torabi-Parizi, P. & Germain, R. N. (2015), 'Strategically localized dendritic cells promote rapid t cell responses to lymph-borne particulate antigens', *Immunity* **42**(1), 172–185.

Gerstel-Thompson, J. L., Wilkey, J. F., Baptiste, J. C., Navas, J. S., Pai, S.-Y., Pass, K. A., Eaton, R. B. & Comeau, A. M. (2010), 'High-throughput multiplexed t-cell–receptor excision circle quantitative pcr assay with internal controls for detection of severe combined immunodeficiency in population-based newborn screening', *Clinical chemistry* **56**(9), 1466–1474.

Giles, J. R., Manne, S., Freilich, E., Oldridge, D. A., Baxter, A. E., George, S., Chen, Z., Huang, H., Chilukuri, L., Carberry, M. et al. (2022), 'Human epigenetic and transcriptional t cell differentiation atlas for identifying functional t cell-specific enhancers', *Immunity* **55**(3), 557–574.

Giri, J. G., Ahdieh, M., Eisenman, J., Shanebeck, K., Grabstein, K., Kumaki, S., Namen, A., Park, L. S., Cosman, D. & Anderson, D. (1994), 'Utilization of the

beta and gamma chains of the il-2 receptor by the novel cytokine il-15.', *The EMBO journal* **13**(12), 2822–2830.

Golstein, P., Wigzell, H., Blomgren, H. & Svedmyr, E. A. (1972), 'Cells mediating specific in vitro cytotoxicity: ii. probable autonomy of thymus-processed lymphocytes (t cells) for the killing of allogeneic target cells', *The Journal of experimental medicine* **135**(4), 890–906.

Goronzy, J. J. & Weyand, C. M. (2019), 'Mechanisms underlying t cell ageing', *Nature Reviews Immunology* **19**(9), 573–583.

Grabstein, K. H., Eisenman, J., Shanebeck, K., Rauch, C., Srinivasan, S., Fung, V., Beers, C., Richardson, J., Schoenborn, M. A., Ahdieh, M. et al. (1994), 'Cloning of a t cell growth factor that interacts with the $\beta$ chain of the interleukin-2 receptor', *Science* **264**(5161), 965–968.

Graef, P., Buchholz, V. R., Stemberger, C., Flossdorf, M., Henkel, L., Schiemann, M., Drexler, I., Höfer, T., Riddell, S. R. & Busch, D. H. (2014), 'Serial transfer of single-cell-derived immunocompetence reveals stemness of cd8+ central memory t cells', *Immunity* **41**(1), 116–126.

Gray, S. M., Amezquita, R. A., Guan, T., Kleinstein, S. H. & Kaech, S. M. (2017), 'Polycomb repressive complex 2-mediated chromatin repression guides effector cd8+ t cell terminal differentiation and loss of multipotency', *Immunity* **46**(4), 596–608.

Grifoni, A., Weiskopf, D., Ramirez, S. I., Mateus, J., Dan, J. M., Moderbacher, C. R., Rawlings, S. A., Sutherland, A., Premkumar, L., Jadi, R. S. et al. (2020), 'Targets of t cell responses to sars-cov-2 coronavirus in humans with covid-19 disease and unexposed individuals', *Cell* **181**(7), 1489–1501.

Groom, J. R. (2015), 'Moving to the suburbs: T-cell positioning within lymph nodes during activation and memory', *Immunology and cell biology* **93**(4), 330–336.

Guan, T., Dominguez, C. X., Amezquita, R. A., Laidlaw, B. J., Cheng, J., Henao-Mejia, J., Williams, A., Flavell, R. A., Lu, J. & Kaech, S. M. (2018), 'Zeb1, zeb2,

and the mir-200 family form a counterregulatory network to regulate cd8+ t cell fates', *Journal of Experimental Medicine* **215**(4), 1153–1168.

Guerrera, G., Picozza, M., D'Orso, S., Placido, R., Pirronello, M., Verdiani, A., Termine, A., Fabrizio, C., Giannessi, F., Sambucci, M. et al. (2021), 'Bnt162b2 vaccination induces durable sars-cov-2–specific t cells with a stem cell memory phenotype', *Science immunology* **6**(66), eabl5344.

Hagan, T., Nakaya, H. I., Subramaniam, S. & Pulendran, B. (2015), 'Systems vaccinology: enabling rational vaccine design with systems biological approaches', *Vaccine* **33**(40), 5294–5301.

Haidari, G., Cope, A., Miller, A., Venables, S., Yan, C., Ridgers, H., Reijonen, K., Hannaman, D., Spentzou, A., Hayes, P. et al. (2017), 'Combined skin and muscle vaccination differentially impact the quality of effector t cell functions: the cuthivac-001 randomized trial', *Scientific reports* **7**(1), 13011.

Haluszczak, C., Akue, A. D., Hamilton, S. E., Johnson, L. D., Pujanauski, L., Teodorovic, L., Jameson, S. C. & Kedl, R. M. (2009), 'The antigen-specific cd8+ t cell repertoire in unimmunized mice includes memory phenotype cells bearing markers of homeostatic expansion', *Journal of Experimental Medicine* **206**(2), 435–448.

Hamann, D., Baars, P. A., Rep, M. H., Hooibrink, B., Kerkhof-Garde, S. R., Klein, M. R. & Lier, R. A. v. (1997), 'Phenotypic and functional separation of memory and effector human cd8+ t cells', *The Journal of experimental medicine* **186**(9), 1407–1418.

Hashimoto, Y., Masunaga, N., Kagara, N., Abe, K., Yoshinami, T., Tsukabe, M., Sota, Y., Miyake, T., Tanei, T., Shimoda, M. et al. (2023), 'Detection of ultra-rare esr1 mutations in primary breast cancer using lna-clamp ddpcr', *Cancers* **15**(9), 2632.

Havenar-Daughton, C., Carnathan, D. G., de la Peña, A. T., Pauthner, M., Briney, B., Reiss, S. M., Wood, J. S., Kaushik, K., van Gils, M. J., Rosales, S. L. et al.

(2016), 'Direct probing of germinal center responses reveals immunological features and bottlenecks for neutralizing antibody responses to hiv env trimer', *Cell reports* **17**(9), 2195–2209.

Havenar-Daughton, C., Newton, I. G., Zare, S. Y., Reiss, S. M., Schwan, B., Suh, M. J., Hasteh, F., Levi, G. & Crotty, S. (2020), 'Normal human lymph node t follicular helper cells and germinal center b cells accessed via fine needle aspirations', *Journal of immunological methods* **479**, 112746.

Hazenberg, M. D., Verschuren, M. C., Hamann, D., Miedema, F. & Dongen, J. J. (2001), 'T cell receptor excision circles as markers for recent thymic emigrants: basic aspects, technical approach, and guidelines for interpretation', *Journal of molecular medicine* **79**(11), 631–640.

He, B., Xing, S., Chen, C., Gao, P., Teng, L., Shan, Q., Gullicksrud, J. A., Martin, M. D., Yu, S., Harty, J. T. et al. (2016), 'Cd8+ t cells utilize highly dynamic enhancer repertoires and regulatory circuitry in response to infections', *Immunity* **45**(6), 1341–1354.

Hendriks, J., Xiao, Y., Rossen, J. W., Van Der Sluijs, K. F., Sugamura, K., Ishii, N. & Borst, J. (2005), 'During viral infection of the respiratory tract, cd27, 4-1bb, and ox40 collectively determine formation of cd8+ memory t cells and their capacity for secondary expansion', *The Journal of Immunology* **175**(3), 1665–1676.

Henning, A. N., Roychoudhuri, R. & Restifo, N. P. (2018), 'Epigenetic control of cd8+ t cell differentiation', *Nature Reviews Immunology* **18**(5), 340–356.

Henson, S. & Akbar, A. (n.d.), 'Klrg1—more than a marker for t cell senescence. age (dordr). 2009; 31: 285–91'.

Herndler-Brandstetter, D., Ishigame, H., Shinnakasu, R., Plajer, V., Stecher, C., Zhao, J., Lietzenmayer, M., Kroehling, L., Takumi, A., Kometani, K. et al. (2018), 'Klrg1+ effector cd8+ t cells lose klrg1, differentiate into all memory t cell lineages, and convey enhanced protective immunity', *Immunity* **48**(4), 716–729.

Herndler-Brandstetter, D., Landgraf, K., Tzankov, A., Jenewein, B., Brunauer, R., Laschober, G. T., Parson, W., Kloss, F., Gassner, R., Lepperdinger, G. et al.

(2012), 'The impact of aging on memory t cell phenotype and function in the human bone marrow', *Journal of leukocyte biology* **91**(2), 197–205.

Hickman, H. D., Takeda, K., Skon, C. N., Murray, F. R., Hensley, S. E., Loomis, J., Barber, G. N., Bennink, J. R. & Yewdell, J. W. (2008), 'Direct priming of antiviral cd8+ t cells in the peripheral interfollicular region of lymph nodes', *Nature immunology* **9**(2), 155–165.

Hoerres, D., Dai, Q., Elmore, S., Sheth, S., Gupta, G. P., Kumar, S. & Gulley, M. L. (2023), 'Calibration of cell-free dna measurements by next-generation sequencing', *American Journal of Clinical Pathology* p. aqad055.

Hoffman, W., Lakkis, F. G. & Chalasani, G. (2016), 'B cells, antibodies, and more', *Clinical journal of the American Society of Nephrology: CJASN* **11**(1), 137.

Holling, T. M., Schooten, E. & van Den Elsen, P. J. (2004), 'Function and regulation of mhc class ii molecules in t-lymphocytes: of mice and men', *Human immunology* **65**(4), 282–290.

Holmgren, A., Hansson, L., Bjerkaas-Kjeldal, K., Impellizzeri, A. A. R., Gilfillan, G. D., Djurovic, S. & Hughes, T. (2022), 'Mapping the expression of an ank3 isoform associated with bipolar disorder in the human brain', *Translational Psychiatry* **12**(1), 45.

Hont, A. B., Powell, A. B., Sohai, D. K., Valdez, I. K., Stanojevic, M., Geiger, A. E., Chaudhary, K., Dowlati, E., Bollard, C. M. & Cruz, C. R. Y. (2022), 'The generation and application of antigen-specific t cell therapies for cancer and viral-associated disease', *Molecular Therapy* **30**(6), 2130–2152.

Hosokawa, K., Muranski, P., Feng, X., Townsley, D. M., Liu, B., Knickelbein, J., Keyvanfar, K., Dumitriu, B., Ito, S., Kajigaya, S. et al. (2016), 'Memory stem t cells in autoimmune disease: high frequency of circulating cd8+ memory stem cells in acquired aplastic anemia', *The Journal of Immunology* **196**(4), 1568–1578.

Hou, L. & Hu, Z. (2022), 'Performance of anmbrs treating low strength wastewater with different carbon sources at decreasing hrts and its linkage to methanosaeta

with high specific affinity', *Environmental Science: Water Research & Technology* **8**(4), 849–861.

Hou, S., Hyland, L., Ryan, K. W., Portner, A. & Doherty, P. C. (1994), 'Virus-specific cd8+ t-cell memory determined by clonal burst size', *Nature* **369**(6482), 652–654.

Hou, Y., Zhang, H., Miranda, L. & Lin, S. (2010), 'Serious overestimation in quantitative pcr by circular (supercoiled) plasmid standard: microalgal pcna as the model gene', *PloS one* **5**(3), e9545.

Hu, J. K., Kagari, T., Clingan, J. M. & Matloubian, M. (2011), 'Expression of chemokine receptor cxcr3 on t cells affects the balance between effector and memory cd8 t-cell generation', *Proceedings of the National Academy of Sciences* **108**(21), E118–E127.

Hua, S., Lecuroux, C., Saez-Cirion, A., Pancino, G., Girault, I., Versmisse, P., Boufassa, F., Taulera, O., Sinet, M., Lambotte, O. et al. (2014), 'Potential role for hiv-specific cd38-/hla-dr+ cd8+ t cells in viral suppression and cytotoxicity in hiv controllers', *PloS one* **9**(7), e101920.

Huang, X., Zhu, J., Liu, T., Li, F., Yang, T., Li, H., Chen, F., Zhang, Y., Wang, Y., Fu, L. et al. (2021), 'Increased expression of cd95 in cd4+ effector memory t cells promotes th17 response in patients with myasthenia gravis', *Journal of Neuroimmune Pharmacology* pp. 1–16.

Huggett, J. F. (2020), 'The digital miqe guidelines update: minimum information for publication of quantitative digital pcr experiments for 2020', *Clinical chemistry* **66**(8), 1012–1029.

Huggett, J. F., Cowen, S. & Foy, C. A. (2015), 'Considerations for digital pcr as an accurate molecular diagnostic tool', *Clinical chemistry* **61**(1), 79–88.

Ichii, H., Sakamoto, A., Hatano, M., Okada, S., Toyama, H., Taki, S., Arima, M., Kuroda, Y. & Tokuhisa, T. (2002), 'Role for bcl-6 in the generation and maintenance of memory cd8+ t cells', *Nature immunology* **3**(6), 558–563.

Intlekofer, A. M., Takemoto, N., Kao, C., Banerjee, A., Schambach, F., Northrop, J. K., Shen, H., Wherry, E. J. & Reiner, S. L. (2007), 'Requirement for t-bet in the aberrant differentiation of unhelped memory cd8+ t cells', *The Journal of experimental medicine* **204**(9), 2015–2021.

Intlekofer, A. M., Takemoto, N., Wherry, E. J., Longworth, S. A., Northrup, J. T., Palanivel, V. R., Mullen, A. C., Gasink, C. R., Kaech, S. M., Miller, J. D. et al. (2005), 'Effector and memory cd8+ t cell fate coupled by t-bet and eomesodermin', *Nature immunology* **6**(12), 1236–1244.

Jacomet, F., Cayssials, E., Basbous, S., Levescot, A., Piccirilli, N., Desmier, D., Robin, A., Barra, A., Giraud, C., Guilhot, F. et al. (2015), 'Evidence for eomesodermin-expressing innate-like cd8+ kir/nkg2a+ t cells in human adults and cord blood samples', *European journal of immunology* **45**(7), 1926–1933.

Jacquemont, L., Tilly, G., Yap, M., Doan-Ngoc, T.-M., Danger, R., Guérif, P., Delbos, F., Martinet, B., Giral, M., Foucher, Y. et al. (2020), 'Terminally differentiated effector memory cd8+ t cells identify kidney transplant recipients at high risk of graft failure', *Journal of the American Society of Nephrology: JASN* **31**(4), 876.

Jameson, S. C. & Masopust, D. (2009), 'Diversity in t cell memory: an embarrassment of riches', *Immunity* **31**(6), 859–871.

Jameson, S. C. & Masopust, D. (2018), 'Understanding subset diversity in t cell memory', *Immunity* **48**(2), 214–226.

Janeway Jr, C. A., Carding, S., Jones, B., Murray, J., Portoles, P., Rasmussen, R., Rojo, J., Saizawa, K., West, J. & Bottomly, K. (1988), 'Cd4+ t cells: specificity and function', *Immunological reviews* **101**(1), 39–80.

Janssen, E. M., Lemmens, E. E., Wolfe, T., Christen, U., von Herrath, M. G. & Schoenberger, S. P. (2003), 'Cd4+ t cells are required for secondary expansion and memory in cd8+ t lymphocytes', *Nature* **421**(6925), 852–856.

Jiang, X., Clark, R. A., Liu, L., Wagers, A. J., Fuhlbrigge, R. C. & Kupper, T. S.

(2012), 'Skin infection generates non-migratory memory cd8+ trm cells providing global skin immunity', *Nature* **483**(7388), 227–231.

Joshi, N. S., Cui, W., Chandele, A., Lee, H. K., Urso, D. R., Hagman, J., Gapin, L. & Kaech, S. M. (2007), 'Inflammation directs memory precursor and short-lived effector cd8+ t cell fates via the graded expression of t-bet transcription factor', *Immunity* **27**(2), 281–295.

Julien, J.-P., Cupo, A., Sok, D., Stanfield, R. L., Lyumkis, D., Deller, M. C., Klasse, P.-J., Burton, D. R., Sanders, R. W., Moore, J. P. et al. (2013), 'Crystal structure of a soluble cleaved hiv-1 envelope trimer', *Science* **342**(6165), 1477–1483.

Jung, J. H., Rha, M.-S., Sa, M., Choi, H. K., Jeon, J. H., Seok, H., Park, D. W., Park, S.-H., Jeong, H. W., Choi, W. S. et al. (2021), 'Sars-cov-2-specific t cell memory is sustained in covid-19 convalescent patients for 10 months with successful development of stem cell-like memory t cells', *Nature communications* **12**(1), 4043.

Jung, S., Jung, J. H., Noh, J. Y., Kim, W.-J., Yoon, S.-Y., Jung, J., Kim, E. S., Kim, H. B., Cheong, H. J., Kim, W. J. et al. (2022), 'The generation of stem cell-like memory cells early after bnt162b2 vaccination is associated with durability of memory cd8+ t cell responses', *Cell Reports* **40**(4).

Junt, T., Moseman, E. A., Iannacone, M., Massberg, S., Lang, P. A., Boes, M., Fink, K., Henrickson, S. E., Shayakhmetov, D. M., Di Paolo, N. C. et al. (2007), 'Subcapsular sinus macrophages in lymph nodes clear lymph-borne viruses and present them to antiviral b cells', *Nature* **450**(7166), 110–114.

Kaech, S. M. & Cui, W. (2012), 'Transcriptional control of effector and memory cd8+ t cell differentiation', *Nature Reviews Immunology* **12**(11), 749–761.

Kaech, S. M. & Wherry, E. J. (2007), 'Heterogeneity and cell-fate decisions in effector and memory cd8+ t cell differentiation during viral infection', *Immunity* **27**(3), 393–405.

Kaech, S. M., Wherry, E. J. & Ahmed, R. (2002), 'Effector and memory t-cell dif-

ferentiation: implications for vaccine development', *Nature Reviews Immunology* **2**(4), 251–262.

Kalia, V., Sarkar, S., Subramaniam, S., Haining, W. N., Smith, K. A. & Ahmed, R. (2010), 'Prolonged interleukin-2r$\alpha$ expression on virus-specific cd8+ t cells favors terminal-effector differentiation in vivo', *Immunity* **32**(1), 91–103.

Kallies, A., Xin, A., Belz, G. T. & Nutt, S. L. (2009), 'Blimp-1 transcription factor is required for the differentiation of effector cd8+ t cells and memory responses', *Immunity* **31**(2), 283–295.

Kawabe, T., Yi, J. & Sprent, J. (2021), 'Homeostasis of naive and memory t lymphocytes', *Cold Spring Harbor Perspectives in Biology* **13**(9), a037879.

Keefer, M. C., Gilmour, J., Hayes, P., Gill, D., Kopycinski, J., Cheeseman, H., Cashin-Cox, M., Naarding, M., Clark, L., Fernandez, N. et al. (2012), 'A phase i double blind, placebo-controlled, randomized study of a multigenic hiv-1 adenovirus subtype 35 vector vaccine in healthy uninfected adults'.

Kennedy, M. K., Glaccum, M., Brown, S. N., Butz, E. A., Viney, J. L., Embers, M., Matsuki, N., Charrier, K., Sedger, L., Willis, C. R. et al. (2000), 'Reversible defects in natural killer and memory cd8 t cell lineages in interleukin 15–deficient mice', *The Journal of experimental medicine* **191**(5), 771–780.

Keoshkerian, E., Helbig, K., Beard, M., Zaunders, J., Seddiki, N., Kelleher, A., Hampartzoumian, T., Zekry, A. & Lloyd, A. R. (2012), 'A novel assay for detection of hepatitis c virus-specific effector cd4+ t cells via co-expression of cd25 and cd134', *Journal of immunological methods* **375**(1-2), 148–158.

Khan, M. A., Chen, H.-c., Zhang, D. & Fu, J. (2013), 'Twist: a molecular target in cancer therapeutics', *Tumor Biology* **34**, 2497–2506.

Kishton, R. J., Sukumar, M. & Restifo, N. P. (2017), 'Metabolic regulation of t cell longevity and function in tumor immunotherapy', *Cell metabolism* **26**(1), 94–109.

Klinger, M., Kong, K., Moorhead, M., Weng, L., Zheng, J. & Faham, M. (2013), 'Combining next-generation sequencing and immune assays: a novel method for identification of antigen-specific t cells', *PLoS One* **8**(9), e74231.

Klonowski, K. D., Williams, K. J., Marzo, A. L., Blair, D. A., Lingenheld, E. G. & Lefrançois, L. (2004), 'Dynamics of blood-borne cd8 memory t cell migration in vivo', *Immunity* **20**(5), 551–562.

Ko, H., Fu, S. M., Winchester, R. J., Yu, D. & Kunkel, H. (1979), 'Ia determinants on stimulated human t lymphocytes. occurrence on mitogen-and antigen-activated t cells.', *The Journal of experimental medicine* **150**(2), 246–255.

Kojima, H., Kashiwakura, Y., Kanno, Y., Hashiguchi, M. & Kobata, T. (2021), 'Fine-tuning of antigen-specific immune responses by regulatory t cells activated via antigen recognition–independent and humoral factor–dependent mechanisms', *Scandinavian Journal of Immunology* **93**(6), e13020.

Kolumam, G. A., Thomas, S., Thompson, L. J., Sprent, J. & Murali-Krishna, K. (2005), 'Type i interferons act directly on cd8 t cells to allow clonal expansion and memory formation in response to viral infection', *The Journal of experimental medicine* **202**(5), 637–650.

Kondrack, R. M., Harbertson, J., Tan, J. T., McBreen, M. E., Surh, C. D. & Bradley, L. M. (2003), 'Interleukin 7 regulates the survival and generation of memory cd4 cells', *The Journal of experimental medicine* **198**(12), 1797–1806.

Koopman, G., Reutelingsperger, C., Kuijten, G., Keehnen, R., Pals, S. & Van Oers, M. (1994), 'Annexin v for flow cytometric detection of phosphatidylserine expression on b cells undergoing apoptosis'.

Košir, A. B., Divieto, C., Pavšič, J., Pavarelli, S., Dobnik, D., Dreo, T., Bellotti, R., Sassi, M. P. & Žel, J. (2017), 'Droplet volume variability as a critical factor for accuracy of absolute quantification using droplet digital pcr', *Analytical and bioanalytical chemistry* **409**, 6689–6697.

Kratchmarov, R., Magun, A. M. & Reiner, S. L. (2018), 'Tcf1 expression marks self-renewing human cd8+ t cells', *Blood advances* **2**(14), 1685–1690.

Ku, C. C., Murakami, M., Sakamoto, A., Kappler, J. & Marrack, P. (2000), 'Control of homeostasis of cd8+ memory t cells by opposing cytokines', *Science* **288**(5466), 675–678.

Kurachi, M., Barnitz, R. A., Yosef, N., Odorizzi, P. M., DiIorio, M. A., Lemieux, M. E., Yates, K., Godec, J., Klatt, M. G., Regev, A. et al. (2014), 'The transcription factor batf operates as an essential differentiation checkpoint in early effector cd8+ t cells', *Nature immunology* **15**(4), 373–383.

Kwan, A. & Puck, J. M. (2015), History and current status of newborn screening for severe combined immunodeficiency, *in* 'Seminars in perinatology', Vol. 39, Elsevier, pp. 194–205.

La Gruta, N. L., Rothwell, W. T., Cukalac, T., Swan, N. G., Valkenburg, S. A., Kedzierska, K., Thomas, P. G., Doherty, P. C., Turner, S. J. et al. (2010), 'Primary ctl response magnitude in mice is determined by the extent of naive t cell recruitment and subsequent clonal expansion', *The Journal of clinical investigation* **120**(6), 1885–1894.

Ladle, B. H., Li, K.-P., Phillips, M. J., Pucsek, A. B., Haile, A., Powell, J. D., Jaffee, E. M., Hildeman, D. A. & Gamper, C. J. (2016), 'De novo dna methylation by dna methyltransferase 3a controls early effector cd8+ t-cell fate decisions following activation', *Proceedings of the National Academy of Sciences* **113**(38), 10631–10636.

Lanzavecchia, A., Roosnek, E., Gregory, T., Berman, P. & Abrignani, S. (1988), 'T cells can present antigens such as hiv gp120 targeted to their own surface molecules', *Nature* **334**(6182), 530–532.

Lee, J.-Y., Hamilton, S. E., Akue, A. D., Hogquist, K. A. & Jameson, S. C. (2013), 'Virtual memory cd8 t cells display unique functional properties', *Proceedings of the National Academy of Sciences* **110**(33), 13498–13503.

Lee, S.-W., Park, Y., Song, A., Cheroutre, H., Kwon, B. S. & Croft, M. (2006), 'Functional dichotomy between ox40 and 4-1bb in modulating effector cd8 t cell responses', *The Journal of Immunology* **177**(7), 4464–4472.

Leehan, K. M. & Koelsch, K. A. (2015), 'T cell elispot: for the identification of specific cytokine-secreting t cells', *Western Blotting: Methods and Protocols* pp. 427–434.

Lenz, D. C., Kurz, S. K., Lemmens, E., Schoenberger, S. P., Sprent, J., Oldstone, M. B. & Homann, D. (2004), 'Il-7 regulates basal homeostatic proliferation of antiviral cd4+ t cell memory', *Proceedings of the National Academy of Sciences* **101**(25), 9357–9362.

Li, L., Muftuoglu, M., Liang, S., Basyal, M., Jiangxing, L., Akdogan, M. E., Chen, K., Andreeff, M., Flowers, C. R. & Parmar, S. (2022), 'In-depth analysis of sars-cov-2–specific t cells reveals diverse differentiation hierarchies in vaccinated individuals', *JCI insight* **7**(7).

Li, M., Yao, D., Zeng, X., Kasakovski, D., Zhang, Y., Chen, S., Zha, X., Li, Y. & Xu, L. (2019), 'Age related human t cell subset evolution and senescence', *Immunity & Ageing* **16**, 1–7.

Ligotti, M. E., Accardi, G., Aiello, A., Aprile, S., Calabrò, A., Caldarella, R., Caruso, C., Ciaccio, M., Corsale, A. M., Dieli, F. et al. (2023), 'Sicilian semi-and supercentenarians: identification of age-related t cell immunophenotype to define longevity trait', *Clinical and Experimental Immunology* p. uxad074.

Locci, M., Havenar-Daughton, C., Landais, E., Wu, J., Kroenke, M. A., Arlehamn, C. L., Su, L. F., Cubas, R., Davis, M. M., Sette, A. et al. (2013), 'Human circulating pd-1+ cxcr3- cxcr5+ memory tfh cells are highly functional and correlate with broadly neutralizing hiv antibody responses', *Immunity* **39**(4), 758–769.

Lodolce, J. P., Boone, D. L., Chai, S., Swain, R. E., Dassopoulos, T., Trettin, S. & Ma, A. (1998), 'Il-15 receptor maintains lymphoid homeostasis by supporting lymphocyte homing and proliferation', *Immunity* **9**(5), 669–676.

Lovelace, P. & Maecker, H. T. (2018), 'Multiparameter intracellular cytokine staining', *Flow cytometry protocols* pp. 151–166.

Lozano-Ojalvo, D., López-Fandiño, R. & López-Expósito, I. (2015), 'Pbmc-derived t cells', *The Impact of Food Bioactives on Health: in vitro and ex vivo models* pp. 169–180.

Ludlow, A. T., Shelton, D., Wright, W. E. & Shay, J. W. (2018), 'ddtrap: a method

for sensitive and precise quantification of telomerase activity', *Digital PCR: Methods and Protocols* pp. 513–529.

Lugli, e. a. (2013), 'Identification, isolation and in vitro expansion of human and nonhuman primate t stem cell memory cells', *Nature protocols* **8**(1), 33–42.

Lugli, E., Dominguez, M. H., Gattinoni, L., Chattopadhyay, P. K., Bolton, D. L., Song, K., Klatt, N. R., Brenchley, J. M., Vaccari, M., Gostick, E. et al. (2013), 'Superior t memory stem cell persistence supports long-lived t cell memory', *The Journal of clinical investigation* **123**(2).

Lugli, E., Goldman, C. K., Perera, L. P., Smedley, J., Pung, R., Yovandich, J. L., Creekmore, S. P., Waldmann, T. A. & Roederer, M. (2010), 'Transient and persistent effects of il-15 on lymphocyte homeostasis in nonhuman primates', *Blood, The Journal of the American Society of Hematology* **116**(17), 3238–3248.

Lulkiewicz, M., Bajsert, J., Kopczynski, P., Barczak, W. & Rubis, B. (2020), 'Telomere length: how the length makes a difference', *Molecular Biology Reports* **47**, 7181–7188.

Lyumkis, D., Julien, J.-P., De Val, N., Cupo, A., Potter, C. S., Klasse, P.-J., Burton, D. R., Sanders, R. W., Moore, J. P., Carragher, B. et al. (2013), 'Cryo-em structure of a fully glycosylated soluble cleaved hiv-1 envelope trimer', *Science* **342**(6165), 1484–1490.

Mackay, L. K. & Braun, e. a. (2015), 'Cutting edge: Cd69 interference with sphingosine-1-phosphate receptor function regulates peripheral t cell retention', *The Journal of Immunology* **194**(5), 2059–2063.

Mackay, L. K., Minnich, M., Kragten, N. A., Liao, Y., Nota, B., Seillet, C., Zaid, A., Man, K., Preston, S., Freestone, D. et al. (2016), 'Hobit and blimp1 instruct a universal transcriptional program of tissue residency in lymphocytes', *Science* **352**(6284), 459–463.

Mackay, L. K., Rahimpour, A., Ma, J. Z., Collins, N., Stock, A. T., Hafon, M.-L., Vega-Ramos, J., Lauzurica, P., Mueller, S. N., Stefanovic, T. et al. (2013), 'The

developmental pathway for cd103+ cd8+ tissue-resident memory t cells of skin', *Nature immunology* **14**(12), 1294–1301.

Mackay, L. K., Wynne-Jones, E., Freestone, D., Pellicci, D. G., Mielke, L. A., Newman, D. M., Braun, A., Masson, F., Kallies, A., Belz, G. T. et al. (2015), 'T-box transcription factors combine with the cytokines tgf-$\beta$ and il-15 to control tissue-resident memory t cell fate', *Immunity* **43**(6), 1101–1111.

Maheshwari, Y., Selvaraj, V., Hajeri, S. & Yokomi, R. (2017), 'Application of droplet digital pcr for quantitative detection of spiroplasma citri in comparison with real time pcr', *PLoS One* **12**(9), e0184751.

Mahnke, Y. D., Brodie, T. M., Sallusto, F., Roederer, M. & Lugli, E. (2013), 'The who's who of t-cell differentiation: human memory t-cell subsets', *European journal of immunology* **43**(11), 2797–2809.

Maino, V. C., Suni, M. A. & Ruitenberg, J. J. (1995), 'Rapid flow cytometric method for measuring lymphocyte subset activation', *Cytometry: The Journal of the International Society for Analytical Cytology* **20**(2), 127–133.

Makedonas, G., Hutnick, N., Haney, D., Amick, A. C., Gardner, J., Cosma, G., Hersperger, A. R., Dolfi, D., Wherry, E. J., Ferrari, G. et al. (2010), 'Perforin and il-2 upregulation define qualitative differences among highly functional virus-specific human cd8+ t cells', *PLoS pathogens* **6**(3), e1000798.

Mallett, S., Fossum, S. & Barclay, A. N. (1990), 'Characterization of the mrc ox40 antigen of activated cd4 positive t lymphocytes–a molecule related to nerve growth factor receptor.', *The EMBO journal* **9**(4), 1063–1068.

Man, K., Gabriel, S. S., Liao, Y., Gloury, R., Preston, S., Henstridge, D. C., Pellegrini, M., Zehn, D., Berberich-Siebelt, F., Febbraio, M. A. et al. (2017), 'Transcription factor irf4 promotes cd8+ t cell exhaustion and limits the development of memory-like t cells during chronic infection', *Immunity* **47**(6), 1129–1141.

Manco, L. & Dias, H. C. (2022), 'Dna methylation analysis of elovl2 gene using droplet digital pcr for age estimation purposes', *Forensic Science International* **333**, 111206.

Martin, M. D. & Badovinac, V. P. (2018), 'Defining memory cd8 t cell', *Frontiers in immunology* **9**, 2692.

Masopust, D., Vezys, V., Marzo, A. L. & Lefrançois, L. (2001), 'Preferential localization of effector memory cells in nonlymphoid tissue', *Science* **291**(5512), 2413–2417.

Masopust, D., Vezys, V., Wherry, E. J., Barber, D. L. & Ahmed, R. (2006), 'Cutting edge: gut microenvironment promotes differentiation of a unique memory cd8 t cell population', *The Journal of Immunology* **176**(4), 2079–2083.

Masson, F., Minnich, M., Olshansky, M., Bilic, I., Mount, A. M., Kallies, A., Speed, T. P., Busslinger, M., Nutt, S. L. & Belz, G. T. (2013), 'Id2-mediated inhibition of e2a represses memory cd8+ t cell differentiation', *The Journal of Immunology* **190**(9), 4585–4594.

Mayer-Blackwell, K., Ryu, H., Codd, A. S., Parks, K. R., MacMillan, H. R., Cohen, K. W., Stewart, T. L., Seese, A., Lemos, M. P., De Rosa, S. C. et al. (2023), 'mrna vaccination boosts s-specific t cell memory and promotes expansion of cd45raint temra-like cd8+ t cells in covid-19 recovered individuals', *Cell Reports Medicine* **4**(8).

McLane, L. M., Abdel-Hakeem, M. S. & Wherry, E. J. (2019), 'Cd8 t cell exhaustion during chronic viral infection and cancer', *Annual review of immunology* **37**, 457–495.

Mehling, M., Frank, T., Albayrak, C. & Tay, S. (2015), 'Real-time tracking, retrieval and gene expression analysis of migrating human t cells', *Lab on a Chip* **15**(5), 1276–1283.

Melero, I., Gaudernack, G., Gerritsen, W., Huber, C., Parmiani, G., Scholl, S., Thatcher, N., Wagstaff, J., Zielinski, C., Faulkner, I. et al. (2014), 'Therapeutic vaccines for cancer: an overview of clinical trials', *Nature reviews Clinical oncology* **11**(9), 509–524.

Menacho-Melgar, R. & Lynch, M. D. (2022), 'Measuring oligonucleotide hydrolysis in cellular lysates via viscosity measurements', *Bio-protocol* **12**(2), e4304–e4304.

Meraviglia, S., Di Carlo, P., Pampinella, D., Guadagnino, G., Presti, E. L., Orlando, V., Marchetti, G., Dieli, F. & Sergi, C. (2019), 'T-cell subsets (tcm, tem, temra) and poly-functional immune response in patients with human immunodeficiency virus (hiv) infection and different t-cd4 cell response', *Annals of Clinical & Laboratory Science* **49**(4), 519–528.

Mestas, J. & Hughes, C. C. (2004), 'Of mice and not men: differences between mouse and human immunology', *The Journal of Immunology* **172**(5), 2731–2738.

Miliaras, N. (2014), 'Digital pcr comes of age', *Genetic Engineering & Biotechnology News* **34**(4), 14–16.

Miller, C. H., Klawon, D. E., Zeng, S., Lee, V., Socci, N. D. & Savage, P. A. (2020), 'Eomes identifies thymic precursors of self-specific memory-phenotype cd8+ t cells', *Nature immunology* **21**(5), 567–577.

Miller, J. D., van der Most, R. G., Akondy, R. S., Glidewell, J. T., Albott, S., Masopust, D., Murali-Krishna, K., Mahar, P. L., Edupuganti, S., Lalor, S. et al. (2008), 'Human effector and memory cd8+ t cell responses to smallpox and yellow fever vaccines', *Immunity* **28**(5), 710–722.

Milosevic, D., Mills, J. R., Campion, M. B., Vidal-Folch, N., Voss, J. S., Halling, K. C., Highsmith, W. E., Liu, M. C., Kipp, B. R. & Grebe, S. K. (2018), 'Applying standard clinical chemistry assay validation to droplet digital pcr quantitative liquid biopsy testing', *Clinical chemistry* **64**(12), 1732–1742.

Miron, M., Kumar, B. V., Meng, W., Granot, T., Carpenter, D. J., Senda, T., Chen, D., Rosenfeld, A. M., Zhang, B., Lerner, H. et al. (2018), 'Human lymph nodes maintain tcf-1hi memory t cells with high functional potential and clonal diversity throughout life', *The Journal of Immunology* **201**(7), 2132–2140.

Mitchell, D. M., Ravkov, E. V. & Williams, M. A. (2010), 'Distinct roles for il-2 and il-15 in the differentiation and survival of cd8+ effector and memory t cells', *The Journal of Immunology* **184**(12), 6719–6730.

Mollo, S. B., Ingram, J. T., Kress, R. L., Zajac, A. J. & Harrington, L. E. (2014),

'Virus-specific cd4 and cd8 t cell responses in the absence of th1-associated transcription factors', *Journal of leukocyte biology* **95**(5), 705–713.

Montacchiesi, G. & Pace, L. (2022), 'Epigenetics and cd8+ t cell memory', *Immunological reviews* **305**(1), 77–89.

Moon, J. J., Chu, H. H., Pepper, M., McSorley, S. J., Jameson, S. C., Kedl, R. M. & Jenkins, M. K. (2007), 'Naive cd4+ t cell frequency varies for different epitopes and predicts repertoire diversity and response magnitude', *Immunity* **27**(2), 203–213.

Moysi, E., Pallikkuth, S., De Armas, L. R., Gonzalez, L. E., Ambrozak, D., George, V., Huddleston, D., Pahwa, R., Koup, R. A., Petrovas, C. et al. (2018), 'Altered immune cell follicular dynamics in hiv infection following influenza vaccination', *The Journal of clinical investigation* **128**(7), 3171–3185.

Moysi, E., Paris, R. M., Le Grand, R., Koup, R. A. & Petrovas, C. (2022), 'Human lymph node immune dynamics as driver of vaccine efficacy: an understudied aspect of immune responses', *Expert Review of Vaccines* **21**(5), 633–644.

Mpande, C. A., Dintwe, O. B., Musvosvi, M., Mabwe, S., Bilek, N., Hatherill, M., Nemes, E., Scriba, T. J. & Team, S. C. I. (2018), 'Functional, antigen-specific stem cell memory (tscm) cd4+ t cells are induced by human mycobacterium tuberculosis infection', *Frontiers in immunology* **9**, 324.

Munusamy Ponnan, S., Hayes, P., Fernandez, N., Thiruvengadam, K., Pattabiram, S., Nesakumar, M., Srinivasan, A., Kathirvel, S., Shankar, J., Goyal, R. et al. (2020), 'Evaluation of antiviral t cell responses and tscm cells in volunteers enrolled in a phase i hiv-1 subtype c prophylactic vaccine trial in india', *PloS one* **15**(2), e0229461.

Murali-Krishna, K., Altman, J. D., Suresh, M., Sourdive, D. J., Zajac, A. J., Miller, J. D., Slansky, J. & Ahmed, R. (1998), 'Counting antigen-specific cd8 t cells: a reevaluation of bystander activation during viral infection', *Immunity* **8**(2), 177–187.

Murali-Krishna, K., Lau, L. L., Sambhara, S., Lemonnier, F., Altman, J. & Ahmed, R. (1999), 'Persistence of memory cd8 t cells in mhc class i-deficient mice', *Science* **286**(5443), 1377–1381.

Muroyama, Y. & Wherry, E. J. (2021), 'Memory t-cell heterogeneity and terminology', *Cold Spring Harbor Perspectives in Biology* **13**(10), a037929.

Murray, J. M., Kaufmann, G. R., Hodgkin, P. D., Lewin, S. R., Kelleher, A. D., Davenport, M. P. & Zaunders, J. J. (2003), 'Naive t cells are maintained by thymic output in early ages but by proliferation without phenotypic change after age twenty', *Immunology and Cell Biology* **81**(6), 487–495.

Ndhlovu, Z. M., Kamya, P., Mewalal, N., Kløverpris, H. N., Nkosi, T., Pretorius, K., Laher, F., Ogunshola, F., Chopera, D., Shekhar, K. et al. (2015), 'Magnitude and kinetics of cd8+ t cell activation during hyperacute hiv infection impact viral set point', *Immunity* **43**(3), 591–604.

Newell, E. W., Sigal, N., Bendall, S. C., Nolan, G. P. & Davis, M. M. (2012), 'Cytometry by time-of-flight shows combinatorial cytokine expression and virus-specific cell niches within a continuum of cd8+ t cell phenotypes', *Immunity* **36**(1), 142–152.

Nikolich-Žugich, J., Li, G., Uhrlaub, J. L., Renkema, K. R. & Smithey, M. J. (2012), Age-related changes in cd8 t cell homeostasis and immunity to infection, *in* 'Seminars in immunology', Vol. 24, Elsevier, pp. 356–364.

Nyombayire, J., Anzala, O., Gazzard, B., Karita, E., Bergin, P., Hayes, P., Kopycinski, J., Omosa-Manyonyi, G., Jackson, A., Bizimana, J. et al. (2017), 'First-in-human evaluation of the safety and immunogenicity of an intranasally administered replication-competent sendai virus–vectored hiv type 1 gag vaccine: Induction of potent t-cell or antibody responses in prime-boost regimens', *The Journal of Infectious Diseases* **215**(1), 95.

Obar, J. J. & Lefrançois, L. (2010), 'Memory cd8+ t cell differentiation', *Annals of the New York Academy of Sciences* **1183**(1), 251–266.

Okino, S. T., Kong, M., Sarras, H. & Wang, Y. (2016), 'Evaluation of bias associated with high-multiplex, target-specific pre-amplification', *Biomolecular detection and quantification* **6**, 13–21.

Oliveira, G., Ruggiero, E., Stanghellini, M. T. L., Cieri, N., D'Agostino, M., Fronza, R., Lulay, C., Dionisio, F., Mastaglio, S., Greco, R. et al. (2015), 'Tracking genetically engineered lymphocytes long-term reveals the dynamics of t cell immunological memory', *Science translational medicine* **7**(317), 317ra198–317ra198.

Omilusik, K. D., Nadjsombati, M. S., Shaw, L. A., Yu, B., Milner, J. J. & Goldrath, A. W. (2018), 'Sustained id2 regulation of e proteins is required for terminal differentiation of effector cd8+ t cells', *Journal of Experimental Medicine* **215**(3), 773–783.

Osborne, L. C., Dhanji, S., Snow, J. W., Priatel, J. J., Ma, M. C., Miners, M. J., Teh, H.-S., Goldsmith, M. A. & Abraham, N. (2007), 'Impaired cd8 t cell memory and cd4 t cell primary responses in il-7r$\alpha$ mutant mice', *The Journal of experimental medicine* **204**(3), 619–631.

Pace, L. (2021), 'Temporal and epigenetic control of plasticity and fate decision during cd8+ t-cell memory differentiation', *Cold Spring Harbor Perspectives in Biology* **13**(12), a037754.

Pace, L., Goudot, C., Zueva, E., Gueguen, P., Burgdorf, N., Waterfall, J. J., Quivy, J.-P., Almouzni, G. & Amigorena, S. (2018), 'The epigenetic control of stemness in cd8+ t cell fate commitment', *Science* **359**(6372), 177–186.

Paprckova, D., Salyova, E., Michalik, J. & Stepanek, O. (2023), 'Bystander activation in memory and antigen-inexperienced memory-like cd8 t cells', *Current Opinion in Immunology* **82**, 102299.

Park, C. O. & Kupper, T. S. (2015), 'The emerging role of resident memory t cells in protective immunity and inflammatory disease', *Nature medicine* **21**(7), 688–697.

Paterson, D., Jefferies, W., Green, J., Brandon, M., Corthesy, P., Puklavec, M. & Williams, A. (1987), 'Antigens of activated rat t lymphocytes including a

molecule of 50,000 mr detected only on cd4 positive t blasts', *Molecular immunology* **24**(12), 1281–1290.

Patin, E., Hasan, M., Bergstedt, J., Rouilly, V., Libri, V., Urrutia, A., Alanio, C., Scepanovic, P., Hammer, C., Jönsson, F. et al. (2018), 'Natural variation in the parameters of innate immune cells is preferentially driven by genetic factors', *Nature immunology* **19**(3), 302–314.

Pauken, K. E., Sammons, M. A., Odorizzi, P. M., Manne, S., Godec, J., Khan, O., Drake, A. M., Chen, Z., Sen, D. R., Kurachi, M. et al. (2016), 'Epigenetic stability of exhausted t cells limits durability of reinvigoration by pd-1 blockade', *Science* **354**(6316), 1160–1165.

Paulsen, M., Valentin, S., Mathew, B., Adam-Klages, S., Bertsch, U., Lavrik, I., Krammer, P. H., Kabelitz, D. & Janssen, O. (2011), 'Modulation of cd4+ t-cell activation by cd95 co-stimulation', *Cell Death & Differentiation* **18**(4), 619–631.

Pearce, E. L. & Shen, H. (2007), 'Generation of cd8 t cell memory is regulated by il-12', *The Journal of Immunology* **179**(4), 2074–2081.

Perl, A. & Morel, L. (2023), 'Expanding scope of temra in autoimmunity', *Ebiomedicine* **90**.

Petit, J., Carroll, G., Zhao, J., Roper, E., Pockney, P. & Scott, R. (2023), 'Evaluation of epigenetic methylation biomarkers for the detection of colorectal cancer using droplet digital pcr', *Scientific Reports* **13**(1), 8883.

Pham, N.-L. L., Badovinac, V. P. & Harty, J. T. (2009), 'A default pathway of memory cd8 t cell differentiation after dendritic cell immunization is deflected by encounter with inflammatory cytokines during antigen-driven proliferation', *The Journal of Immunology* **183**(4), 2337–2348.

Phan, T. G., Grigorova, I., Okada, T. & Cyster, J. G. (2007), 'Subcapsular encounter and complement-dependent transport of immune complexes by lymph node b cells', *Nature immunology* **8**(9), 992–1000.

Pinheiro, L. B., Coleman, V. A., Hindson, C. M., Herrmann, J., Hindson, B. J., Bhat, S. & Emslie, K. R. (2012), 'Evaluation of a droplet digital polymerase

chain reaction format for dna copy number quantification', *Analytical chemistry* **84**(2), 1003–1011.

Pipkin, M. E., Sacks, J. A., Cruz-Guilloty, F., Lichtenheld, M. G., Bevan, M. J. & Rao, A. (2010), 'Interleukin-2 and inflammation induce distinct transcriptional programs that promote the differentiation of effector cytolytic t cells', *Immunity* **32**(1), 79–90.

Pitsillidou, C. et al. (2023), 'Identifying age related changes in the human immune system by using polychromatic flow cytometry'.

Polic, B., Kunkel, D., Scheffold, A. & Rajewsky, K. (2001), 'How $\alpha\beta$ t cells deal with induced tcr$\alpha$ ablation', *Proceedings of the National Academy of Sciences* **98**(15), 8744–8749.

Pollard, A. J. & Bijker, E. M. (2021), 'A guide to vaccinology: from basic principles to new developments', *Nature Reviews Immunology* **21**(2), 83–100.

Poloni, C., Schonhofer, C., Ivison, S., Levings, M. K., Steiner, T. S. & Cook, L. (2023), 'T-cell activation–induced marker assays in health and disease', *Immunology and Cell Biology* .

Profaizer, T. & Slev, P. (2020), 'A multiplex, droplet digital pcr assay for the detection of t-cell receptor excision circles and kappa-deleting recombination excision circles', *Clinical Chemistry* **66**(1), 229–238.

Purton, J. F., Sprent, J. & Surh, C. D. (2007), 'Staying alive–naïve cd4+ t cell homeostasis', *European journal of immunology* **37**(9), 2367–2369.

Quah, B. J., Warren, H. S. & Parish, C. R. (2007), 'Monitoring lymphocyte proliferation in vitro and in vivo with the intracellular fluorescent dye carboxyfluorescein diacetate succinimidyl ester', *Nature protocols* **2**(9), 2049–2056.

Quinn, K. M., Hussain, T., Kraus, F., Formosa, L. E., Lam, W. K., Dagley, M. J., Saunders, E. C., Assmus, L. M., Wynne-Jones, E., Loh, L. et al. (2020), 'Metabolic characteristics of cd8+ t cell subsets in young and aged individuals are not predictive of functionality', *Nature Communications* **11**(1), 2857.

Quinn, K. M., Zaloumis, S. G., Cukalac, T., Kan, W.-T., Sng, X. Y., Mirams, M., Watson, K. A., McCaw, J. M., Doherty, P. C., Thomas, P. G. et al. (2016), 'Heightened self-reactivity associated with selective survival, but not expansion, of naïve virus-specific cd8+ t cells in aged mice', *Proceedings of the National Academy of Sciences* **113**(5), 1333–1338.

Ray, S. J., Franki, S. N., Pierce, R. H., Dimitrova, S., Koteliansky, V., Sprague, A. G., Doherty, P. C., de Fougerolles, A. R. & Topham, D. J. (2004), 'The collagen binding $\alpha 1\beta 1$ integrin vla-1 regulates cd8 t cell-mediated immune protection against heterologous influenza infection', *Immunity* **20**(2), 167–179.

Raynor, J. L., Chapman, N. M. & Chi, H. (2021), 'Metabolic control of memory t-cell generation and stemness', *Cold Spring Harbor Perspectives in Biology* **13**(6), a037770.

Reiss, S., Baxter, A. E., Cirelli, K. M., Dan, J. M., Morou, A., Daigneault, A., Brassard, N., Silvestri, G., Routy, J.-P., Havenar-Daughton, C. et al. (2017), 'Comparative analysis of activation induced marker (aim) assays for sensitive identification of antigen-specific cd4 t cells', *PloS one* **12**(10), e0186998.

Remmerswaal, E. B., Hombrink, P., Nota, B., Pircher, H., Ten Berge, I. J., van Lier, R. A. & van Aalderen, M. C. (2019), 'Expression of il-7r$\alpha$ and klrg1 defines functionally distinct cd8+ t-cell populations in humans', *European Journal of Immunology* **49**(5), 694–708.

Restifo, N. P. & Gattinoni, L. (2013), 'Lineage relationship of effector and memory t cells', *Current opinion in immunology* **25**(5), 556–563.

Reuter, M. A., Estrada, P. M. D. R., Buggert, M., Petrovas, C., Ferrando-Martinez, S., Nguyen, S., Japp, A. S., Ablanedo-Terrazas, Y., Rivero-Arrieta, A., Kuri-Cervantes, L. et al. (2017), 'Hiv-specific cd8+ t cells exhibit reduced and differentially regulated cytolytic activity in lymphoid tissue', *Cell reports* **21**(12), 3458–3470.

Richer, M. J., Pewe, L. L., Hancox, L. S., Hartwig, S. M., Varga, S. M., Harty, J. T. et al. (2015), 'Inflammatory il-15 is required for optimal memory t cell responses', *The Journal of clinical investigation* **125**(9), 3477–3490.

Ridge, J. P., Di Rosa, F. & Matzinger, P. (1998), 'A conditioned dendritic cell can be a temporal bridge between a cd4+ t-helper and a t-killer cell', *Nature* **393**(6684), 474–478.

Rodrigues, V., Baudier, J. B. & Chantal, I. (2017), 'Development of a bead-based multiplexed assay for simultaneous quantification of five bovine cytokines by flow cytometry', *Cytometry Part A* **91**(9), 901–907.

Rodriguez, I. J., Lalinde Ruiz, N., Llano León, M., Martínez Enríquez, L., Montilla Velásquez, M. d. P., Ortiz Aguirre, J. P., Rodríguez Bohórquez, O. M., Velandia Vargas, E. A., Hernández, E. D. & Parra López, C. A. (2021), 'Immunosenescence study of t cells: a systematic review', *Frontiers in immunology* **11**, 604591.

Roederer, M., Brenchley, J. M., Betts, M. R. & De Rosa, S. C. (2004), 'Flow cytometric analysis of vaccine responses: how many colors are enough?', *Clinical immunology* **110**(3), 199–205.

Rogers, P. R., Song, J., Gramaglia, I., Killeen, N. & Croft, M. (2001), 'Ox40 promotes bcl-xl and bcl-2 expression and is essential for long-term survival of cd4 t cells', *Immunity* **15**(3), 445–455.

Romero, P., Zippelius, A., Kurth, I., Pittet, M. J., Touvrey, C., Iancu, E. M., Corthesy, P., Devevre, E., Speiser, D. E. & Rufer, N. (2007), 'Four functionally distinct populations of human effector-memory cd8+ t lymphocytes', *The Journal of Immunology* **178**(7), 4112–4119.

Rudolph, M. G., Stanfield, R. L. & Wilson, I. A. (2006), 'How tcrs bind mhcs, peptides, and coreceptors', *Annu. Rev. Immunol.* **24**, 419–466.

Rutishauser, R. L., Martins, G. A., Kalachikov, S., Chandele, A., Parish, I. A., Meffre, E., Jacob, J., Calame, K. & Kaech, S. M. (2009), 'Transcriptional repressor blimp-1 promotes cd8+ t cell terminal differentiation and represses the acquisition of central memory t cell properties', *Immunity* **31**(2), 296–308.

Sabatino, M., Hu, J., Sommariva, M., Gautam, S., Fellowes, V., Hocker, J. D., Dougherty, S., Qin, H., Klebanoff, C. A., Fry, T. J. et al. (2016), 'Generation of

clinical-grade cd19-specific car-modified cd8+ memory stem cells for the treatment of human b-cell malignancies', *Blood, The Journal of the American Society of Hematology* **128**(4), 519–528.

Sachdeva, M., Fischl, M. A., Pahwa, R., Sachdeva, N. & Pahwa, S. (2010), 'Immune exhaustion occurs concomitantly with immune activation and decrease in regulatory t cells in viremic chronically hiv-1 infected patients', *Journal of acquired immune deficiency syndromes (1999)* **54**(5), 447.

Saeed, S., Quintin, J., Kerstens, H. H., Rao, N. A., Aghajanirefah, A., Matarese, F., Cheng, S.-C., Ratter, J., Berentsen, K., van der Ent, M. A. et al. (2014), 'Epigenetic programming of monocyte-to-macrophage differentiation and trained innate immunity', *science* **345**(6204), 1251086.

Sallusto, F., Lanzavecchia, A., Araki, K. & Ahmed, R. (2010), 'From vaccines to memory and back', *Immunity* **33**(4), 451–463.

Sallusto, F., Lenig, D., Förster, R., Lipp, M. & Lanzavecchia, A. (1999), 'Two subsets of memory t lymphocytes with distinct homing potentials and effector functions', *Nature* **401**(6754), 708–712.

Sandgaard, K. S., Lewis, J., Adams, S., Klein, N. & Callard, R. (2014), 'Antiretroviral therapy increases thymic output in children with hiv', *Aids* **28**(2), 209–214.

Schenkel, J. M., Fraser, K. A., Beura, L. K., Pauken, K. E., Vezys, V. & Masopust, D. (2014), 'Resident memory cd8 t cells trigger protective innate and adaptive immune responses', *Science* **346**(6205), 98–101.

Schenkel, J. M., Fraser, K. A., Vezys, V. & Masopust, D. (2013), 'Sensing and alarm function of resident memory cd8+ t cells', *Nature immunology* **14**(5), 509–513.

Schenkel, J. M. & Masopust, D. (2014), 'Tissue-resident memory t cells', *Immunity* **41**(6), 886–897.

Schmitz, I., Krueger, A., Baumann, S., Schulze-Bergkamen, H., Krammer, P. H. & Kirchhoff, S. (2003), 'An il-2-dependent switch between cd95 signaling pathways sensitizes primary human t cells toward cd95-mediated activation-induced cell death', *The Journal of Immunology* **171**(6), 2930–2936.

Scholz, G., Jandus, C., Zhang, L., Grandclément, C., Lopez-Mejia, I. C., Soneson, C., Delorenzi, M., Fajas, L., Held, W., Dormond, O. et al. (2016), 'Modulation of mtor signalling triggers the formation of stem cell-like memory t cells', *EBioMedicine* **4**, 50–61.

Scholzen, T. & Gerdes, J. (2000), 'The ki-67 protein: from the known and the unknown', *Journal of cellular physiology* **182**(3), 311–322.

Schwenk, R., Banania, G., Epstein, J., Kim, Y., Peters, B., Belmonte, M., Ganeshan, H., Huang, J., Reyes, S., Stryhn, A. et al. (2013), 'Ex vivo tetramer staining and cell surface phenotyping for early activation markers cd38 and hla-dr to enumerate and characterize malaria antigen-specific cd8+ t-cells induced in human volunteers immunized with a plasmodium falciparum adenovirus-vectored malaria vaccine expressing ama1', *Malaria Journal* **12**(1), 1–9.

Scott-Browne, J. P., López-Moyado, I. F., Trifari, S., Wong, V., Chavez, L., Rao, A. & Pereira, R. M. (2016), 'Dynamic changes in chromatin accessibility occur in cd8+ t cells responding to viral infection', *Immunity* **45**(6), 1327–1340.

Scott, C. L. & Omilusik, K. D. (2019), 'Zebs: novel players in immune cell development and function', *Trends in immunology* **40**(5), 431–446.

Scudier, G. (2022), 'Characterization of t stem cell memory heterogeneity in humans'.

Sen, D. R., Kaminski, J., Barnitz, R. A., Kurachi, M., Gerdemann, U., Yates, K. B., Tsao, H.-W., Godec, J., LaFleur, M. W., Brown, F. D. et al. (2016), 'The epigenetic landscape of t cell exhaustion', *Science* **354**(6316), 1165–1169.

Sercan, Ö., Stoycheva, D., Hämmerling, G. J., Arnold, B. & Schüler, T. (2010), 'Ifn-$\gamma$ receptor signaling regulates memory cd8+ t cell differentiation', *The Journal of Immunology* **184**(6), 2855–2862.

Sharov, K. S. (2021), 'Hiv/sars-cov-2 co-infection: T cell profile, cytokine dynamics and role of exhausted lymphocytes', *International Journal of Infectious Diseases* **102**, 163–169.

Shaulov, A. & Murali-Krishna, K. (2008), 'Cd8 t cell expansion and memory differentiation are facilitated by simultaneous and sustained exposure to antigenic and inflammatory milieu', *The Journal of Immunology* **180**(2), 1131–1138.

Shedlock, D. J. & Shen, H. (2003), 'Requirement for cd4 t cell help in generating functional cd8 t cell memory', *Science* **300**(5617), 337–339.

Shen, Y., Song, Z., Lu, X., Ma, Z., Lu, C., Zhang, B., Chen, Y., Duan, M., Apetoh, L., Li, X. et al. (2019), 'Fas signaling-mediated th9 cell differentiation favors bowel inflammation and antitumor functions', *Nature Communications* **10**(1), 2924.

Sheridan, B. S., Pham, Q.-M., Lee, Y.-T., Cauley, L. S., Puddington, L. & Lefrançois, L. (2014), 'Oral infection drives a distinct population of intestinal resident memory cd8+ t cells with enhanced protective function', *Immunity* **40**(5), 747–757.

Skon, C. N., Lee, J.-Y., Anderson, K. G., Masopust, D., Hogquist, K. A. & Jameson, S. C. (2013), 'Transcriptional downregulation of s1pr1 is required for the establishment of resident memory cd8+ t cells', *Nature immunology* **14**(12), 1285–1293.

Smith-Garvin, J. E., Burns, J. C., Gohil, M., Zou, T., Kim, J. S., Maltzman, J. S., Wherry, E. J., Koretzky, G. A. & Jordan, M. S. (2010), 'T-cell receptor signals direct the composition and function of the memory cd8+ t-cell pool', *Blood, The Journal of the American Society of Hematology* **116**(25), 5548–5559.

Sok, D. & Burton, D. R. (2018), 'Recent progress in broadly neutralizing antibodies to hiv', *Nature immunology* **19**(11), 1179–1188.

Song, J.-W., Zhang, C., Fan, X., Meng, F.-P., Xu, Z., Xia, P., Cao, W.-J., Yang, T., Dai, X.-P., Wang, S.-Y. et al. (2020), 'Immunological and inflammatory profiles in mild and severe cases of covid-19', *Nature communications* **11**(1), 3410.

Sosinowski, T., White, J. T., Cross, E. W., Haluszczak, C., Marrack, P., Gapin, L. & Kedl, R. M. (2013), 'Cd8$\alpha$+ dendritic cell trans presentation of il-15 to naive cd8+ t cells produces antigen-inexperienced t cells in the periphery with memory phenotype and function', *The Journal of Immunology* **190**(5), 1936–1947.

Sottini, A., Serana, F., Bertoli, D., Chiarini, M., Valotti, M., Tessitore, M. V. & Imberti, L. (2014), 'Simultaneous quantification of t-cell receptor excision circles (trecs) and k-deleting recombination excision circles (krecs) by real-time pcr', *JoVE (Journal of Visualized Experiments)* (94), e52184.

Speiser, D. E., Liénard, D., Rufer, N., Rubio-Godoy, V., Rimoldi, D., Lejeune, F., Krieg, A. M., Cerottini, J.-C., Romero, P. et al. (2005), 'Rapid and strong human cd8+ t cell responses to vaccination with peptide, ifa, and cpg oligodeoxynucleotide 7909', *The Journal of clinical investigation* **115**(3), 739–746.

Steinert, E. M., Schenkel, J. M., Fraser, K. A., Beura, L. K., Manlove, L. S., Igyártó, B. Z., Southern, P. J. & Masopust, D. (2015), 'Quantifying memory cd8 t cells reveals regionalization of immunosurveillance', *Cell* **161**(4), 737–749.

Stempels, F., de Wit, A., Swierstra, M., Maassen, S., Bianchi, F., van den Bogaart, G. & Baranov, M. (2022), 'A sensitive and less cytotoxic assay for identification of proliferating t cells based on bioorthogonally-functionalized uridine analogue', *Journal of immunological methods* **502**, 113228.

Sukumar, M., Liu, J., Mehta, G. U., Patel, S. J., Roychoudhuri, R., Crompton, J. G., Klebanoff, C. A., Ji, Y., Li, P., Yu, Z. et al. (2016), 'Mitochondrial membrane potential identifies cells with enhanced stemness for cellular therapy', *Cell metabolism* **23**(1), 63–76.

Sun, J. C. & Bevan, M. J. (2003), 'Defective cd8 t cell memory following acute infection without cd4 t cell help', *Science* **300**(5617), 339–342.

Surh, C. D., Boyman, O., Purton, J. F. & Sprent, J. (2006), 'Homeostasis of memory t cells', *Immunological reviews* **211**(1), 154–163.

Swain, S. L., Hu, H. & Huston, G. (1999), 'Class ii-independent generation of cd4 memory t cells from effectors', *Science* **286**(5443), 1381–1383.

Szabo, P. A., Miron, M. & Farber, D. L. (2019), 'Location, location, location: Tissue resident memory t cells in mice and humans', *Science immunology* **4**(34), eaas9673.

Takahama, S., Nogimori, T., Higashiguchi, M., Murakami, H., Akita, H. & Yamamoto, T. (2021), 'Simultaneous monitoring assay for t-cell receptor stimulation-dependent activation of cd4 and cd8 t cells using inducible markers on the cell surface', *Biochemical and Biophysical Research Communications* **571**, 53–59.

Tarke, A., Sidney, J., Methot, N., Yu, E. D., Zhang, Y., Dan, J. M., Goodwin, B., Rubiro, P., Sutherland, A., Wang, E. et al. (2021), 'Impact of sars-cov-2 variants on the total cd4+ and cd8+ t cell reactivity in infected or vaccinated individuals', *Cell Reports Medicine* **2**(7).

Tatovic, D., Young, P., Kochba, E., Levin, Y., Wong, F. S. & Dayan, C. M. (2015), 'Fine-needle aspiration biopsy of the lymph node: a novel tool for the monitoring of immune responses after skin antigen delivery', *The Journal of Immunology* **195**(1), 386–392.

Taylor, S. C., Laperriere, G. & Germain, H. (2017), 'Droplet digital pcr versus qpcr for gene expression analysis with low abundant targets: from variable nonsense to publication quality data', *Scientific reports* **7**(1), 2409.

Teixeiro, E., Daniels, M. A., Hamilton, S. E., Schrum, A. G., Bragado, R., Jameson, S. C. & Palmer, E. (2009), 'Different t cell receptor signals determine cd8+ memory versus effector development', *science* **323**(5913), 502–505.

Terrén, I., Orrantia, A., Vitallé, J., Zenarruzabeitia, O. & Borrego, F. (2020), Cfse dilution to study human t and nk cell proliferation in vitro, *in* 'Methods in Enzymology', Vol. 631, Elsevier, pp. 239–255.

Tessitore, M. V., Sottini, A., Roccaro, A. M., Ghidini, C., Bernardi, S., Martellosio, G., Serana, F. & Imberti, L. (2017), 'Detection of newly produced t and b lymphocytes by digital pcr in blood stored dry on nylon flocked swabs', *Journal of Translational Medicine* **15**(1), 1–10.

Thome, J. J., Grinshpun, B., Kumar, B. V., Kubota, M., Ohmura, Y., Lerner, H., Sempowski, G. D., Shen, Y. & Farber, D. L. (2016), 'Long-term maintenance of human naïve t cells through in situ homeostasis in lymphoid tissue sites', *Science immunology* **1**(6), eaah6506.

Thome, J. J., Yudanin, N., Ohmura, Y., Kubota, M., Grinshpun, B., Sathaliyawala, T., Kato, T., Lerner, H., Shen, Y. & Farber, D. L. (2014), 'Spatial map of human t cell compartmentalization and maintenance over decades of life', *Cell* **159**(4), 814–828.

Turner, S. J., Bennett, T. J. & La Gruta, N. L. (2021), 'Cd8+ t-cell memory: The why, the when, and the how', *Cold Dpring Harb Perspect Biol* **13**(5), a038661.

Ulvmar, M. H., Werth, K., Braun, A., Kelay, P., Hub, E., Eller, K., Chan, L., Lucas, B., Novitzky-Basso, I., Nakamura, K. et al. (2014), 'The atypical chemokine receptor ccrl1 shapes functional ccl21 gradients in lymph nodes', *Nature immunology* **15**(7), 623–630.

Utzschneider, D. T., Charmoy, M., Chennupati, V., Pousse, L., Ferreira, D. P., Calderon-Copete, S., Danilo, M., Alfei, F., Hofmann, M., Wieland, D. et al. (2016), 'T cell factor 1-expressing memory-like cd8+ t cells sustain the immune response to chronic viral infections', *Immunity* **45**(2), 415–427.

Vakili, M. E., Faghih, Z., Sarvari, J., Doroudchi, M., Hosseini, S. N., Kabelitz, D. & Kalantar, K. (2022), 'Lower frequency of t stem cell memory (tscm) cells in hepatitis b vaccine nonresponders', *Immunologic Research* **70**(4), 469–480.

Van de Sandt, C. E., Kreijtz, J. H., Geelhoed-Mieras, M. M., Nieuwkoop, N. J., Spronken, M. I., van de Vijver, D. A., Fouchier, R. A., Osterhaus, A. D. & Rimmelzwaan, G. F. (2016), 'Differential recognition of influenza a viruses by m158–66 epitope-specific cd8+ t cells is determined by extraepitopic amino acid residues', *Journal of virology* **90**(2), 1009–1022.

van Heijst, J. W., Gerlach, C., Swart, E., Sie, D., Nunes-Alves, C., Kerkhoven, R. M., Arens, R., Correia-Neves, M., Schepers, K. & Schumacher, T. N. (2009), 'Recruitment of antigen-specific cd8+ t cells in response to infection is markedly efficient', *Science* **325**(5945), 1265–1269.

Van Zelm, M. C., Van Der Burg, M., Langerak, A. W. & Van Dongen, J. J. (2011), 'Pid comes full circle: applications of v (d) j recombination excision circles in research, diagnostics and newborn screening of primary immunodeficiency disorders', *Frontiers in immunology* **2**, 12.

Vasudevan, H. N., Xu, P., Servellita, V., Miller, S., Liu, L., Gopez, A., Chiu, C. Y. & Abate, A. R. (2021), 'Digital droplet pcr accurately quantifies sars-cov-2 viral load from crude lysate without nucleic acid purification', *Scientific reports* **11**(1), 780.

Verstegen, R. H., Aui, P. M., Watson, E., De Jong, S., Bartol, S. J., Bosco, J. J., Cameron, P. U., Stirling, R. G., de Vries, E., van Dongen, J. J. et al. (2019), 'Quantification of t-cell and b-cell replication history in aging, immunodeficiency, and newborn screening', *Frontiers in Immunology* **10**, 2084.

Vidal-Folch, N., Milosevic, D., Majumdar, R., Gavrilov, D., Matern, D., Raymond, K., Rinaldo, P., Tortorelli, S., Abraham, R. S. & Oglesbee, D. (2017), 'A droplet digital pcr method for severe combined immunodeficiency newborn screening', *The Journal of Molecular Diagnostics* **19**(5), 755–765.

Vigano, S., Negron, J., Ouyang, Z., Rosenberg, E. S., Walker, B. D., Lichterfeld, M. & Yu, X. G. (2015), 'Prolonged antiretroviral therapy preserves hiv-1-specific cd8 t cells with stem cell-like properties', *Journal of virology* **89**(15), 7829–7840.

Walker, L. S., Gulbranson-Judge, A., Flynn, S., Brocker, T., Raykundalia, C., Goodall, M., Förster, R., Lipp, M. & Lane, P. (1999), 'Compromised ox40 function in cd28-deficient mice is linked with failure to develop cxc chemokine receptor 5–positive cd4 cells and germinal centers', *The Journal of experimental medicine* **190**(8), 1115–1122.

Waller, E. C., McKinney, N., Hicks, R., Carmichael, A. J., Sissons, J. P. & Wills, M. R. (2007), 'Differential costimulation through cd137 (4–1bb) restores proliferation of human virus-specific "effector memory"(cd28- cd45rahi) cd8+ t cells', *Blood, The Journal of the American Society of Hematology* **110**(13), 4360–4366.

Wang, D., Diao, H., Getzler, A. J., Rogal, W., Frederick, M. A., Milner, J., Yu, B., Crotty, S., Goldrath, A. W. & Pipkin, M. E. (2018), 'The transcription factor runx3 establishes chromatin accessibility of cis-regulatory landscapes that drive memory cytotoxic t lymphocyte formation', *Immunity* **48**(4), 659–674.

Wang, R.-X., Boland, G. J., van Hattum, J. & de Gast, G. C. (2004), 'Long term persistence of t cell memory to hbsag after hepatitis b vaccination', *World journal of gastroenterology* **10**(2), 260.

Weekes, M., Wills, M., Mynard, K., Hicks, R., Sissons, J. & Carmichael, A. (1999), 'Large clonal expansions of human virus-specific memory cytotoxic t lymphocytes within the cd57+ cd28–cd8+ t-cell population', *Immunology* **98**(3), 443–449.

Wehler, T. C., Karg, M., Distler, E., Konur, A., Nonn, M., Meyer, R. G., Huber, C., Hartwig, U. F. & Herr, W. (2008), 'Rapid identification and sorting of viable virus-reactive cd4+ and cd8+ t cells based on antigen-triggered cd137 expression', *Journal of immunological methods* **339**(1), 23–37.

Weng, N.-P., Levine, B. L., June, C. H. & Hodes, R. J. (1995), 'Human naive and memory t lymphocytes differ in telomeric length and replicative potential.', *Proceedings of the National Academy of Sciences* **92**(24), 11091–11094.

Weninger, W., Crowley, M. A., Manjunath, N. & von Andrian, U. H. (2001), 'Migratory properties of naive, effector, and memory cd8+ t cells', *The Journal of experimental medicine* **194**(7), 953–966.

Wherry, E. J. & Ahmed, R. (2004), 'Memory cd8 t-cell differentiation during viral infection', *Journal of virology* **78**(11), 5535–5545.

Wherry, E. J., Ha, S.-J., Kaech, S. M., Haining, W. N., Sarkar, S., Kalia, V., Subramaniam, S., Blattman, J. N., Barber, D. L. & Ahmed, R. (2007), 'Molecular signature of cd8+ t cell exhaustion during chronic viral infection', *Immunity* **27**(4), 670–684.

Wherry, E. J. & Kurachi, M. (2015), 'Molecular and cellular insights into t cell exhaustion', *Nature Reviews Immunology* **15**(8), 486–499.

Wherry, E. J., Teichgräber, V., Becker, T. C., Masopust, D., Kaech, S. M., Antia, R., Von Andrian, U. H. & Ahmed, R. (2003), 'Lineage relationship and protective immunity of memory cd8 t cell subsets', *Nature immunology* **4**(3), 225–234.

Wiesel, M., Crouse, J., Bedenikovic, G., Sutherland, A., Joller, N. & Oxenius, A. (2012), 'Type-i ifn drives the differentiation of short-lived effector cd8+ t cells in vivo', *European journal of immunology* **42**(2), 320–329.

Williams, M. A. & Bevan, M. J. (2007), 'Effector and memory ctl differentiation', *Annu. Rev. Immunol.* **25**, 171–192.

Wölfl, M., Kuball, J., Eyrich, M., Schlegel, P. G. & Greenberg, P. D. (2008), 'Use of cd137 to study the full repertoire of cd8+ t cells without the need to know epitope specificities', *Cytometry Part A* **73**(11), 1043–1049.

Wolfl, M., Kuball, J., Ho, W. Y., Nguyen, H., Manley, T. J., Bleakley, M. & Greenberg, P. D. (2007), 'Activation-induced expression of cd137 permits detection, isolation, and expansion of the full repertoire of cd8+ t cells responding to antigen without requiring knowledge of epitope specificities', *Blood, The Journal of the American Society of Hematology* **110**(1), 201–210.

Woon, S.-T., Mayes, J., Quach, A., Longhurst, H., Ferrante, A. & Ameratunga, R. (2022), 'Droplet digital pcr for identifying copy number variations in patients with primary immunodeficiency disorders', *Clinical and experimental immunology* **207**(3), 329–335.

Wu, H., Witzl, A. & Ueno, H. (2019), 'Assessment of tcr signal strength of antigen-specific memory cd8+ t cells in human blood', *Blood Advances* **3**(14), 2153–2163.

Wu, T., Ji, Y., Moseman, E. A., Xu, H. C., Manglani, M., Kirby, M., Anderson, S. M., Handon, R., Kenyon, E., Elkahloun, A. et al. (2016), 'The tcf1-bcl6 axis counteracts type i interferon to repress exhaustion and maintain t cell stemness', *Science immunology* **1**(6), eaai8593.

Xia, Y., Liu, A., Li, W., Liu, Y., Zhang, G., Ye, S., Zhao, Z., Shi, J., Jia, Y., Liu, X. et al. (2022), 'Reference range of naïve t and t memory lymphocyte subsets in peripheral blood of healthy adult', *Clinical and Experimental Immunology* **207**(2), 208–217.

Xin, A., Masson, F., Liao, Y., Preston, S., Guan, T., Gloury, R., Olshansky, M., Lin, J.-X., Li, P., Speed, T. P. et al. (2016), 'A molecular threshold for effector cd8+ t cell differentiation controlled by transcription factors blimp-1 and t-bet', *Nature immunology* **17**(4), 422–432.

Yang, C. Y., Best, J. A., Knell, J., Yang, E., Sheridan, A. D., Jesionek, A. K., Li, H. S., Rivera, R. R., Lind, K. C., D'cruz, L. M. et al. (2011), 'The transcriptional regulators id2 and id3 control the formation of distinct memory cd8+ t cell subsets', *Nature immunology* **12**(12), 1221–1229.

Yang, J., Liu, M., Hong, D., Zeng, M. & Zhang, X. (2021), 'The paradoxical role of cellular senescence in cancer', *Frontiers in cell and developmental biology* **9**, 722205.

Yewdell, J. W., Norbury, C. C. & Bennink, J. R. (1999), 'Mechanisms of exogenous antigen presentation by mhc class i molecules in vitro and in vivo: implications for generating cd8+ t cell responses to infectious agents, tumors, transplants, and vaccines', *Advances in immunology* **73**, 1–77.

Youngblood, B., Hale, J. S., Kissick, H. T., Ahn, E., Xu, X., Wieland, A., Araki, K., West, E. E., Ghoneim, H. E., Fan, Y. et al. (2017), 'Effector cd8 t cells dedifferentiate into long-lived memory cells', *Nature* **552**(7685), 404–409.

Zajac, A. J., Blattman, J. N., Murali-Krishna, K., Sourdive, D. J., Suresh, M., Altman, J. D. & Ahmed, R. (1998), 'Viral immune evasion due to persistence of activated t cells without effector function', *The Journal of experimental medicine* **188**(12), 2205–2213.

Zaunders, J. J., Munier, M. L., Seddiki, N., Pett, S., Ip, S., Bailey, M., Xu, Y., Brown, K., Dyer, W. B., Kim, M. et al. (2009), 'High levels of human antigen-specific cd4+ t cells in peripheral blood revealed by stimulated coexpression of cd25 and cd134 (ox40)', *The Journal of Immunology* **183**(4), 2827–2836.

Zehn, D., Lee, S. Y. & Bevan, M. J. (2009), 'Complete but curtailed t-cell response to very low-affinity antigen', *Nature* **458**(7235), 211–214.

Zhang, N. & Bevan, M. J. (2011), 'Cd8+ t cells: foot soldiers of the immune system', *Immunity* **35**(2), 161–168.

Zhang, N. & Bevan, M. J. (2013), 'Transforming growth factor-$\beta$ signaling controls the formation and maintenance of gut-resident memory t cells by regulating migration and retention', *Immunity* **39**(4), 687–696.

Zhang, X., Sun, S., Hwang, I., Tough, D. F. & Sprent, J. (1998), 'Potent and selective stimulation of memory-phenotype cd8+ t cells in vivo by il-15', *Immunity* **8**(5), 591–599.

Zhang, Y., Joe, G., Hexner, E., Zhu, J. & Emerson, S. G. (2005), 'Host-reactive cd8+ memory stem cells in graft-versus-host disease', *Nature medicine* **11**(12), 1299–1305.

Zhao, Y., Cai, C., Samir, J., Palgen, J.-L., Keoshkerian, E., Li, H., Bull, R. A., Luciani, F., An, H. & Lloyd, A. R. (2021), 'Human cd8 t-stem cell memory subsets phenotypic and functional characterization are defined by expression of cd122 or cxcr3', *European Journal of Immunology* **51**(7), 1732–1747.

Zheng, L., Fisher, G., Miller, R. E., Peschon, J., Lynch, D. H. & Lenardo, M. J. (1995), 'Induction of apoptosis in mature t cells by tumour necrosis factor', *Nature* **377**(6547), 348–351.

Zhou, X., Yu, S., Zhao, D.-M., Harty, J. T., Badovinac, V. P. & Xue, H.-H. (2010), 'Differentiation and persistence of memory cd8+ t cells depend on t cell factor 1', *Immunity* **33**(2), 229–240.

Zinkernagel, R. M. & Doherty, P. C. (1974), 'Restriction of in vitro t cell-mediated cytotoxicity in lymphocytic choriomeningitis within a syngeneic or semiallogeneic system', *Nature* **248**(5450), 701–702.

Zou, Z., Guo, L., Ahmadi, P., Hartjen, P., Gosau, M., Smeets, R. & Kluwe, L. (2021), 'Two simple and inexpensive methods for preparing dna suitable for digital pcr from a small number of cells in 96-well plates', *Journal of Clinical Laboratory Analysis* **35**(1), e23513.

Zu Horste, G. M., Przybylski, D., Schramm, M. A., Wang, C., Schnell, A., Lee, Y., Sobel, R., Regev, A. & Kuchroo, V. K. (2018), 'Fas promotes t helper 17 cell differentiation and inhibits t helper 1 cell development by binding and sequestering transcription factor stat1', *Immunity* **48**(3), 556–569.